

## Lincoln University Digital Thesis

### Copyright Statement

The digital copy of this thesis is protected by the Copyright Act 1994 (New Zealand).

This thesis may be consulted by you, provided you comply with the provisions of the Act and the following conditions of use:

- you will use the copy only for the purposes of research or private study
- you will recognise the author's right to be identified as the author of the thesis and due acknowledgement will be made to the author where appropriate
- you will obtain the author's permission before publishing any material from the thesis.

**Novel numerical methods for stochastic ordinary and partial  
differential equations in modelling complex systems**

---

A thesis  
submitted in partial fulfilment  
of the requirements for the Degree of  
Doctor of Philosophy  
by  
Parul Tiwari

---

Lincoln University

2023

*This thesis is dedicated to my husband, Mr. Vikas Tiwari, who has been a constant support and encouragement during the challenges and my 'down' moments. I am truly thankful for having him in my life. This work is also dedicated to my parents and brother Mr. Ashvani, who have always loved me unconditionally and whose good examples have taught me to work hard for the things that I have aspire to achieve.*

Abstract of a thesis submitted in partial fulfilment of the requirements for the Degree of Doctor of Philosophy.

**Novel Numerical Methods for Stochastic Ordinary and Partial Differential Equations in Modelling Complex Systems**

by

Parul Tiwari

Many natural and engineered systems are complex due to inherent uncertainty. Stochastic Differential Equations (SDEs) and Stochastic Partial Differential equations (SPDEs) provide a rigorous mathematical foundation for modelling these systems. Understanding the dynamics of complex systems under stochastic influences is crucial for predicting system behaviour. Numerical techniques often struggle to handle the complexity and stochastic nature of these equations. This research focuses on adapting and enhancing numerical methods to provide efficient and reliable solutions. The numerical accuracy and stability of these methods are assessed through simulations and examples. This study introduces the synthesis of stochastic spectral methods to solve complex systems by representing random variables as a sum of orthogonal polynomials. We applied Polynomial Chaos Expansion (PCE) methods to contaminant transport problem and to differential equations with random forcing term. We compute the Wick exponentials and show that Wick product coincides with the ordinary product for deterministic functions. We use Malliavin calculus to find the derivatives of a stochastic quantity and are visualised through graphs. We discuss numerical challenges associated with the PCE methods and their solution strategies. In all examples, our chosen method does better and allows us to lead the way in developing robust and efficient strategies to deal with randomness, ultimately enhancing the reliability and resilience of complex systems across various scientific and engineering domains.

**Keywords:** Stochastic differential and partial differential equations, Itô integral, Cameron-Martin basis, stochastic spectral methods, orthogonal basis function, polynomial chaos expansion, functional spaces, Wick product, and Malliavin calculus.

## Acknowledgements

I stand at the culmination of a long and challenging journey, and I am deeply grateful to the many individuals who have been instrumental in helping me reach this milestone.

First and foremost, I would like to express my profound gratitude to my principle supervisor, *Professor Don Kulasiri*, for his unwavering guidance, expertise, and encouragement throughout this research study. Without his continuous support, care and patience this thesis would not have been possible. I extend my heartfelt appreciation to my co-supervisor, *Professor Sandhya Samarasinghe*, for her insightful thoughts, encouragement, and collaborative spirit. Their mentorship has been invaluable, and I have learned immeasurable lessons under their supervision.

To my colleagues and friends, I owe a debt of gratitude for their camaraderie, stimulating discussions, and shared expertise. Their support and the exchange of ideas have enriched the research and writing process. In particular, I would like to thank Dr. Rahul Kosarwal for their support during initial year of my doctoral study. His expertise in computing space helped me to navigate complex algorithms and ultimately leading to more efficient and accurate results in my research.

I wish to convey my gratitude to Lincoln University, the Health Centre, and the IT Services team for their support and the excellent facilities they provided throughout my academic journey. Also, I want to extend my heartfelt acknowledgment to Lorraine Holmes and Robyn Wilson for their kind-hearted care and generous assistance.

I would like to express my heartfelt appreciation to my parents, Mrs. Kaushal and Mr. Shyamlal and brother Mr. Ashvani for their steadfast love, support, and selfless sacrifices that have formed the bedrock upon which I have built my educational journey. I am deeply grateful for their unconditional love, support, and the values they have instilled in me.

I am deeply grateful to my beloved family and cherished children for their enduring support, boundless patience, and unwavering love. Their understanding during late nights and their encouragement during times of academic stress were the steadfast pillars of my strength.

I am profoundly thankful to my beloved husband, Mr. Vikas Tiwari and cherished children, Ms. Stuti Tiwari and Master Adhrit Tiwari for their enduring support, boundless patience, and love. Their smile is the sunshine that brightens my stressful days and the motivation behind every endeavour I undertake.

Last but not least, I am grateful to the countless authors, researchers, and scholars whose work has shaped my understanding of the subject matter and paved the way for this thesis.

# Table of Contents

<b>Abstract</b> .....	<b>iii</b>
<b>Acknowledgements</b> .....	<b>iv</b>
<b>Table of Contents</b> .....	<b>v</b>
<b>List of Tables</b> .....	<b>viii</b>
<b>List of Figures</b> .....	<b>ix</b>
<b>Chapter 1 Introduction and Motivation</b> .....	<b>1</b>
1.1 Perspective of randomness.....	2
1.2 Stochastic differential and partial differential equations (SDEs and SPDES).....	2
1.2.1 Motivation.....	2
1.2.2 Definition.....	3
1.2.3 Need and importance .....	5
1.3 Stochastic equations and possible research thinking .....	6
1.3.1 Motivational example .....	7
1.4 Objectives for this study .....	8
1.5 Thesis framework.....	9
<b>Chapter 2 Literature Review</b> .....	<b>12</b>
2.1 Stochastic processes .....	12
2.1.1 Microscopic motion of Brownian particles .....	12
2.1.2 Brownian motion as a stochastic process.....	14
2.2 Numerical modelling with complex systems .....	15
2.2.1 Hydrological systems .....	16
2.2.2 Uncertainty quantification.....	19
2.2.3 Control theory.....	20
2.2.4 Chemical master equations (CMEs) .....	21
2.2.5 Financial systems .....	21
2.3 Summary .....	24
<b>Chapter 3 Background Study and Preliminaries</b> .....	<b>26</b>
3.1 Brownian motion (definition and properties).....	26
3.2 Stochastic integration and Itô's formula.....	28
3.3 The Stratonovich integral.....	29
3.4 The Skorohod integral.....	30
3.5 Computational techniques.....	32
3.5.1 Direct integration techniques .....	32
3.5.2 Monte Carlo (MC) methods .....	33
3.5.3 Quasi Monte Carlo (QMC) methods .....	34
3.5.4 Gauss quadrature.....	36
3.5.5 Gauss-Hermite quadrature .....	36
3.6 Numerical analysis of stochastic differential equations .....	36
3.6.1 The Euler-Maruyama (E-M) method.....	36
3.6.2 The Milstein method.....	38

3.6.3	Strong convergence .....	38
3.6.4	Weak convergence.....	38
3.6.5	Numerical example .....	38
3.6.6	A bounded Euler-Maruyama method .....	41
3.6.7	Numerical example .....	42
3.7	Linear stability of the Euler-Maruyama and Milstein methods .....	43
3.8	Summary .....	45
<b>Chapter 4 Stochastic Spectral Methods .....</b>		<b>47</b>
4.1	Motivation.....	47
4.2	Functional space and inner product .....	50
4.2.1	Hilbert space .....	51
4.2.2	Hermite polynomials.....	52
4.2.3	Legendre polynomials .....	53
4.3	Computation of quadrature nodes.....	54
4.4	Framework for input variables and random processes .....	55
4.5	Spectral methods .....	56
4.5.1	Direct spectral methods.....	56
4.5.2	Intrusive stochastic spectral methods .....	56
4.5.3	Non-intrusive Stochastic Spectral Methods.....	58
4.5.4	Polynomial chaos expansion (PCE) methods .....	59
4.6	Need of polynomial chaos methods .....	60
4.7	Generalised polynomial chaos expansion (gPCE) methods .....	63
4.7.1	Formulation of gPCE.....	63
4.7.2	Multi-variate gPCE.....	64
4.8	Evaluating polynomial chaos expansion coefficients .....	67
4.9	Numerical example .....	69
4.9.1	Galerkin's intrusive spectral projection method (ISP) .....	69
4.9.2	Galerkin's non-intrusive spectral projection (NISP).....	70
4.10	Summary .....	71
<b>Chapter 5 Application of Stochastic Spectral Methods .....</b>		<b>73</b>
5.1	Development of a meta model for geometric Brownian motion (gBM) .....	74
5.1.1	Formulation of a random variable in Wiener chaos space .....	74
5.1.2	Computation of coefficients .....	74
5.1.3	Meta model.....	75
5.2	Ordinary differential equation with stochastic input .....	79
5.2.1	Numerical example .....	79
5.3	Stochastic Contaminant Transport .....	84
5.3.1	Polynomial chaos expansion and formulation.....	85
5.3.2	Numerical simulation .....	87
5.3.3	Choice of correct order of PCE expansion .....	90
5.3.4	Effect of boundary conditions on the choice of order of expansion .....	92
5.3.5	Calculation of polynomial chaos coefficients.....	94
5.4	Non-linear dynamical systems .....	96
5.5	Summary .....	99
<b>Chapter 6 Wick Product and Malliavin Calculus .....</b>		<b>101</b>
6.1	Idea behind the Wick product in stochastic analysis.....	102

6.2	Connection between normal ordering (creation and annihilation operator) and the notion of the Wick product in stochastic analysis.....	103
6.3	Relationship between Itô - Skorohod integral and the Wick product .....	103
6.4	Wick product.....	104
6.4.1	Motivation for Wick multiplication (Renormalisation point of view).....	104
6.4.2	The Wick product in Physics .....	105
6.4.3	The Wick product in stochastic analysis .....	106
6.4.4	Properties of the Wick product.....	106
6.4.5	Computation of Wick product .....	107
6.4.6	Comparison between square of Wiener process and Wick exponential of Wiener process .....	109
6.5	Malliavin calculus.....	110
6.5.1	White noise space and Wiener chaos decomposition .....	111
6.5.2	$n$ -dimensional Wiener process .....	113
6.5.3	Important result (Wiener Itô iterated integrals).....	114
6.5.4	Itô representation theorem .....	115
6.5.5	Wiener-Itô chaos expansion theorem .....	115
6.6	Important definitions.....	117
6.6.1	Kondratiev test space.....	117
6.6.2	Hida test space.....	118
6.6.3	Need of the test spaces.....	118
6.7	Stochastic derivative and Malliavin derivative .....	119
6.8	Integration by parts formula and Malliavin derivative .....	120
6.8.1	Chain rule .....	120
6.8.2	Expectation rule .....	120
6.8.3	Malliavin derivative.....	120
6.9	Malliavin derivative and chaos expansion .....	122
6.10	The Skorohod integral and Wiener-Itô chaos expansion.....	123
6.11	Application of the Malliavin derivative .....	124
6.11.1	Contaminant transport .....	126
6.11.2	Numerical simulation .....	129
6.12	Summary .....	132
<b>Chapter 7 Conclusion and Future Directions .....</b>		<b>134</b>
7.1	Discussion.....	134
7.2	Summary of the study and contributions .....	135
7.3	Conclusion.....	136
7.4	Future directions.....	137
<b>References .....</b>		<b>138</b>

## List of Tables

Table 4.1	First six Hermite polynomials and Legendre polynomials.....	53
Table 4.2	Comparative study of Least Square Projection and Regression method. ....	57
Table 4.3	Calculation for multi-indices $\alpha$ and the basis functions. The total number of Hermite polynomials are 3 and the dimension of the random variable is 3. ....	65
Table 5.1	Meta model's input and output parameters.....	78
Table 5.2	Relative error for model validation. ....	78
Table 5.3	Computation time for MC method and PCE method to solve equation (5.1).....	83

## List of Figures

Figure 1.1	Known trajectory of the differential equation (1.1).....	2
Figure 1.2	Probabilistic trajectory of the differential equation (1.6) based on real/complex environment. ....	3
Figure 1.3	Organisation of the thesis and key points in the chapters. ....	11
Figure 2.1	Probability density function $P(\Delta x)$ of Einstein’s Brownian motion model for the displacement $\Delta x$ for a very small time-interval. ....	13
Figure 2.2	Representation of Brownian motion as a random walk process. ....	14
Figure 2.3	Illustration of a smile curve (Soini & Lorentzen, 2019). ....	22
Figure 2.4	Simulation results for price differences between BSM and (Faria & Correia-da-Silva, 2014) model for arbitrary return variance $\lambda^2$ and for negative correlation ( $\rho = -0.5$ ) between shocks in variance and the return. ....	24
Figure 3.1	Generation of a Gaussian random variate (GRV) for different sample sizes and a comparison with MC integration error and the mean. ....	33
Figure 3.2	Quasi Random sequences. Quasi-random sequences are used in variance reduction techniques. The word ‘quasi’ signifies that the values of a low-discrepancy sequence is neither random nor pseudo-random, but share some of the characteristics of both of the random variables. This low-discrepancy property is an added benefit of QMC methods. Using a control variate helps to reduce MC variance (Glasserman, 2003). ....	35
Figure 3.3	Exact solution for population growth model.....	39
Figure 3.4	Euler-Maruyama approximation for population growth model .....	40
Figure 3.5	Simulation results for the Exact and Euler-Maruyama approximation after a number of runs.....	40
Figure 3.6	Strong convergence of a bounded Euler scheme.....	43
Figure 3.7	Mean-square and asymptotic stability for the Euler-Maruyama method. ....	44
Figure 4.1	Convergence of finite difference approximation of the fourth order.....	49
Figure 4.2	Convergence of spectral method approximation of fourth order.....	50
Figure 4.3	Hermite polynomials from order 0 to order 5 for $x \in (-3, 3)$ .....	53
Figure 4.4	Legendre polynomials from order 0 to order 5 for $x \in (-1.5, 1.5)$ .....	54
Figure 4.5	Diagrammatic representation for working process of polynomial chaos expansion methods for SDEs and SPDEs.....	62
Figure 4.6	Equivalence between distributions, basis polynomials, and related input random variables.....	64
Figure 4.7	Product of two Hermite polynomials of second and third order .....	66
Figure 4.8	Product of two Hermite polynomials of second order (left graph) and first order (right graph).....	66
Figure 4.9	Product of two Hermite polynomials of first and second order.....	67
Figure 4.10	Geometrical interpretation of the Stochastic Collocation method for computing polynomial chaos coefficients. ....	68
Figure 4.11	Geometrical interpretation of the Galerkin’s projection method for computing polynomial chaos coefficients. ....	69
Figure 5.1	Spectrum of the PCE coefficients for the meta modelling of geometric Brownian motion using Gaussian quadrature and Least Angle Regression. ....	76
Figure 5.2	Spectrum of the PCE coefficients for the meta modelling of geometric Brownian motion using Subspace and Ordinary Least Squares Regression. ....	77
Figure 5.3	Spectrum of the PCE coefficients for the meta modelling of geometric Brownian motion using Orthogonal Matching Pursuit and Bayesian Compressive Sensing. ....	77
Figure 5.4	Sample response of model output $Y$ against the actual values, based on the validation sample set used for modelling.....	79
Figure 5.5	Deterministic solution of equation (5.18). ....	80
Figure 5.6	Stochastic simulation of equation (5.18) using the stochastic Galerkin method.....	81

Figure 5.7	The MC simulation output for equation (5.18) was obtained by generating $10^5$ samples for the stochastic parameter ' $k$ ' .....	82
Figure 5.8	The PCE simulation for equation (5.18) using Hermite polynomials as an orthogonal basis function and order of polynomial is 5. ....	82
Figure 5.9	Sample response for $y$ , using polynomial chaos expansion, with different order and Hermite polynomials as the orthogonal basis function.....	83
Figure 5.10	Distribution of mean and variance using the PCE method.....	84
Figure 5.11	Simulation of concentration $C$ using the MC method.....	88
Figure 5.12	Simulation of concentration $C$ using the PCE method . ....	88
Figure 5.13	Simulation of concentration $C$ using the MC method.....	89
Figure 5.14	Simulation of concentration $C$ using the PCE method. ....	89
Figure 5.15	Simulation of concentration $C$ using the PCE method with maximum order of polynomial chaos expansion = <b>3</b> .....	90
Figure 5.16	Simulation of concentration $C$ using the PCE method with maximum order of polynomial chaos expansion = <b>4</b> .....	91
Figure 5.17	Simulation of concentration $C$ using the PCE method. ....	91
Figure 5.18	Simulation of concentration $C$ using the PCE method with the Gaussian initial condition and maximum order of polynomial chaos expansion = <b>2</b> .....	92
Figure 5.19	Simulation of concentration $C$ using the PCE method with the Gaussian initial condition and maximum order of polynomial chaos expansion = <b>3</b> .....	92
Figure 5.20	Simulation of concentration $C$ using the PCE method with the Gaussian initial condition and maximum order of polynomial chaos expansion = <b>4</b> .....	93
Figure 5.21	Simulation of concentration $C$ using the PCE method with the Gaussian initial condition and maximum order of polynomial chaos expansion = <b>5</b> .....	93
Figure 5.22	Calculation of the polynomial chaos coefficients of various orders at $x = 0.50$ .....	94
Figure 5.23	Calculation of polynomial chaos coefficients of various orders at $x = 0.25$ .....	94
Figure 5.24	Expectation using the PCE solution and the analytical solution at $x = 0.50$ .....	95
Figure 5.25	Variance using the PCE solution and the analytical solution at $x = 0.50$ . ....	95
Figure 5.26	Expectation using the PCE solution and the analytical solution at $x = 0.50$ . ....	96
Figure 5.27	Variance using the PCE solution and the analytical solution at $x = 0.50$ . ....	96
Figure 5.28	Mean and variance of input state $x$ using the MC method, stochastic collocation method and the PCE method. ....	98
Figure 5.29	Mean and variance of output $u$ using the MC method, the stochastic collocation method, and PCE method.....	99
Figure 6.1	Least square norm of a deterministic second-degree polynomial function. ....	108
Figure 6.2	Realisation of an Itô process.....	108
Figure 6.3	Wick exponential an Itô process.....	109
Figure 6.4	Realisations for squares of Wiener process and squares of Wick exponential of Wiener process.....	110
Figure 6.5	Computation of singular white noise. ....	112
Figure 6.6	Greek (Delta value) under the classical Heston model for a binary call option with a bounded parameter, $K$ , and various parameters defined in Table 2 in existing literature (Zhong & Cass, 2017). ....	125
Figure 6.7	Comparison of simulation errors for Greek (Delta) for a six-dimensional basket type down and out option pricing model under the variance gamma (VG) model using different parameters as defined by Lai and Yao (2016). ....	126
Figure 6.8	Calculation of derivatives of first order (top, magenta, calculated by equation (6.103)), (middle, blue, calculated by equation (6.104)) and of second order (bottom, green, calculated by equation (6.105)). ....	131
Figure 6.9	Derivatives of first order (top, magenta, calculated by equation (6.103)), (middle, blue, calculated by equation (6.104)) and of second order (bottom, green, calculated by equation (6.105)). ....	132

## Notations

$\mathbb{R}$	the real numbers
$\mathbb{R}^n$	$\mathbb{R}^n \times \dots \times \mathbb{R}^n$ ( $n$ -times) = the $n$ -dimensional Euclidean space
$\mathbb{R}^+$	$[0, \infty)$ , the non-negative real numbers
$\mathbb{C}$	the complex numbers
$B(t)$	Brownian motion
$W(t)$	Wiener process
$\xi$	a random variable
$U(t)$	unit step function
$t$	time
$N(0,1)$	Gaussian distribution with mean '0' and standard deviation '1'
$O(h)$	order of size $h$
$\mathcal{H}$	Hilbert space
$H^{-n}(\mathbb{R}^d)$	Sobolov space
$\mathcal{L}^2(\Omega, \mathcal{F}, \wp)$	complete probability space
$X(t)/Y(t)$	stochastic process
$\omega$	realisation of a random variable
$\tilde{f}$	symmetric function of function $f$
$w(x)$	weight function
$H_n(x)$	Hermite polynomial of order $n$
$L_n(x)$	Legendre polynomial of order $n$
$\varphi_\alpha(\xi)$	orthogonal basis function for multi-index $\alpha$ and random variable $\xi$
$\mathcal{J}$	set of multi-indices
$\mathcal{J}_{n,p}$	truncated set of multi-indices with order of orthogonal polynomials ( $n$ ) and number of random variables ( $p$ )
$\mathcal{M}(\mathbb{Y})$	multi-variate function for stochastic input $\mathbb{Y}$
$A_f$	creation operator
$A_f^*$	annihilation operator
$\diamond$	Wick product
$I_n(f)$	$n$ -fold iterated Itô integral
$\ f\ $	norm of the function $f$
$\mathbb{N}_0^{\mathbb{N}}$	set of non-negative integers
$\mathcal{X}_{[0,t]}$	characteristic function defined for $[0, t]$
$\mathcal{D}$	set of all differentiable variables

$\mathbb{D}_t$	Malliavin derivative
$\otimes$	Tensor product
$\in(S \rightarrow S^{\text{new}})$	propagator function from state $S$ to state $S^{\text{new}}$
$p(\xi)$	probability density function of a random variable $\xi$
$\Delta_T^n$	a partition for the interval $(0, T)$
$E(f(\xi))$	Expectation of function $f(\xi)$
$W = (W^{(1)}, W^{(2)}, \dots, W^{(d)})$	$d$ -dimensional Brownian motion
$\odot$	transformation function
$\Omega$	sample space
$F(t, x; \omega)$	random forcing term

# Chapter 1

## Introduction and Motivation

The mathematical modelling of systems is used to understand and analyse the behaviour of a system as a whole and determine the dynamic interactions between the variables present in that system.

Numerical simulation provides a way to solve these mathematical models when an exact solution for the governing system of equations is difficult to achieve or sometimes impossible to obtain.

Differential equations play a major role in defining the models typically used in engineering, physics, economics, finance, and biology. Partial differential equations (PDEs) have been used for several decades to model complex physical systems and capture the effects of the parameters involved in these systems. These equations work on the assumption that the parameters are completely known, a fact which is not true. For example, when modelling the transport mechanism of groundwater contamination, there may be unknown boundaries and initial conditions, along with different geographical locations. In short, the parameter values may vary in terms of time, space, unknown external environments and surroundings, meaning that the system's behaviour is uncertain. These fluctuations are known as "noise". The characterisation of this unknown quantity has to be modelled accurately to ensure the model reflects the reality is attempting to capture.

The mathematical modelling of complex systems has greatly improved in past two decades.

Compared to traditional deterministic approaches where model parameters are assumed to be known, recent techniques are more stable and robust. They have been used in a diverse range of fields; for example, turbulent flow, reaction-diffusion equations, non-linear filtration, reliability engineering, disease diagnostics, and neuroscience. While these random models are influenced by model parameters such as boundaries and initial conditions, they are not pre-assumed and/or predetermined by them.

However, most of the natural interacting systems are too intricate to model completely. Although the power of mathematics shows the ability to generalise the phenomenological aspects, the models are often contractions of real systems, meaning that uncertainties play a significant role in many of the models. Important phenomena in engineering (Xiu & Shen, 2008), physics (R. G. Ghanem et al., 1991) environmental sciences (Venturi et al., 2013), economics (H. Holden et al., 2010) and other sciences are responsible for scientific and technological development; these are developed using mathematical models based on differential equations. However, modelling real life stochastic phenomena is more challenging due to heterogeneity in the parameters or is reliant on having sufficient information, or both. These situations lead a researcher to consider the data as random quantities and to replace deterministic models with random models to better understand the

behaviour of stochastic systems. Stochastic models help a modeller to characterise this randomness in several ways. Suitable mathematical modelling and efficient numerical simulation both play a crucial role in predicting the model's behaviour.

This thesis is by no means exhaustive; instead, it serves as an introduction to this extremely rich theory. It represents only a small portion of the content I learned during my PhD journey. The primary aim of this study is to understand complex physical systems in simple settings and apply numerical methods. The study focuses on two approaches: namely, the Polynomial Chaos Expansion (PCE) theory and Wick product and Malliavin calculus. We are not considering those Complex Physical Systems here for which Manabe, Hasselmann, and Parisi won the Nobel Prize in Physics in year 2021.

## 1.1 Perspective of randomness

We can investigate the random or stochastic phenomena from two perspective. The first is from an optimist's view point: here, the modeller believes in a deterministic universe and thinks that the stochastic parameters are introduced into a model so that a better version of the model can be developed. In contrast, the pessimist thinks that all phenomena are highly stochastic and that nothing is fixed. In a pragmatic sense, each modeller is developing the exact same model but considers the origin of randomness from a different angle.

## 1.2 Stochastic differential and partial differential equations (SDEs and SPDES)

### 1.2.1 Motivation

Let us say  $X(t)$  is the state of a system in  $\mathbb{R}^n$  at time  $t \geq 0$  and consider the ordinary differential equation (ODE):

$$\begin{cases} \frac{dX(t)}{dt} = f(X(t)), t > 0, \\ X(0) = X_0, \end{cases} \quad (1.1)$$

and  $f: \mathbb{R}^n \rightarrow \mathbb{R}^n$  is known. The solution of this ODE is the trajectory  $X(t): t \in [0, \infty) \rightarrow \mathbb{R}^n$  as shown in Figure 1.1.



**Figure 1.1** Known trajectory of the differential equation (1.1).

However, in most of the practical applications, the actual trajectory, or we can say the experimental measures, do not behave the same way as predicted (Figure 1.2). Therefore, it is quite reasonable

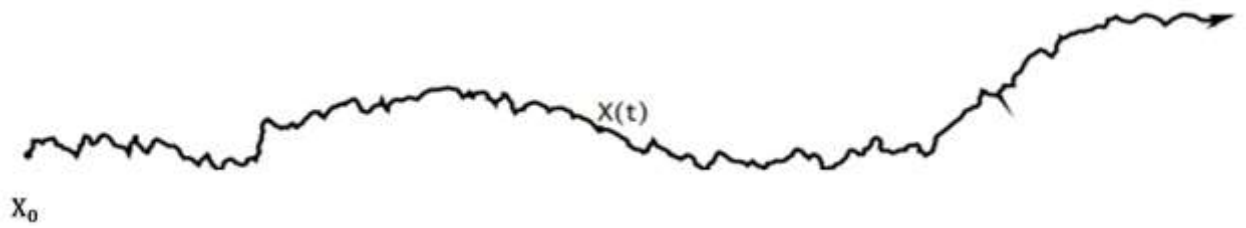


**Figure 1.2 Probabilistic trajectory of the differential equation (1.2) based on real/complex environment.**

to make changes to equation (1.1) and incorporate a random term showing the random effects that disturb the system behaviour. A formal way to do so is to write equation (1.1) as:

$$\begin{cases} \frac{dX(t)}{dt} = f(X(t)) + F(X(t))\xi(t), & t > 0, \\ X(0) = X_0, \end{cases} \quad (1.2)$$

where  $F: \mathbb{R}^n \rightarrow \mathbb{R}^n$  and  $\xi(t) :=$  the random term defining the stochasticity of the system. The representation and modification of the equation (1.2) in this way results in mathematical questions that we need to answer:

1. Define the random term  $\xi(t)$  diligently. It can be the “fluctuations” within the system or can be the “white noise” being used as a stochastic process.
2. Define the meaning of the trajectory/solution  $X(t)$  to solve equation (1.2).
3. Discuss the existence of the solution of equation (1.2) and its dependency upon the initial condition  $X_0$ , function  $f$ , and  $F$ . Also, discuss the uniqueness of the solution.

In this thesis, we consider all of these key concepts and try to provide a detailed explanation for complex physical situations.

### 1.2.2 Definition

It is indefensible to have a fix definition for SDEs and SPDEs. It is better to define a mapping between these equations. Let us consider the origin of the term "noise". Nowadays, the term is generally used as a generic phrase to represent a zero-mean random signal. However, at the time radio signal transmission was developed, noise was considered as an undesired signal which disturbed the broadcast signal due to environmental factors. The noise was considered to originate from flaws in the equipment, either at the sending or receiving end. This issue was caused primarily by the discrete units of charge ( $1.6 \times 10^{19}$  coulombs per electron) that flowed through the valves.

If we consider an electric plate with a leaky capacitor through which a large number of particles (each carrying charge  $q$ ) are passing. The particles are passing in such a way that the  $k^{\text{th}}$  particle is arriving at time  $t_k > 0$ . Let the total number of particles arriving on the plate by time  $t$  be  $N(t)$ :

$$N(t) = \sum_{k=1}^{\infty} U(t - t_k) \quad (1.3)$$

where  $U(t)$  is unit step function.

The irregular arrival of the charged particles results in a specific kind of noise called “shot noise.”

Using Coulomb’s law and the law of conservation, the net charge on the capacitor is:

$$CV(t) = q N(t) - \int_0^t I(\tau) d\tau \quad (1.4)$$

where  $V(t)$  is the voltage across the capacitor and  $I(t)$  is the current in the plate. Applying Ohm’s law, the integral equation for the current  $I(t)$  is:

$$CI(t)R = q N(t) - \int_0^t I(\tau) d\tau \quad (1.5)$$

This equation is easily solvable as  $t_k$  is known, but the behaviour of  $N(t)$  when the time  $t_k$  is not known (except for the inter-arrival time of electrons that follows Poisson’s distribution) with parameter behaviour of the electrons are independent of each other. In this situation, the equation of  $I(t)$  after  $\Delta t$  time, i.e, at time  $t + \Delta t$  is given as:

$$CRI(t + \Delta t) = qN(t + \Delta t) - \int_0^{t+\Delta t} I(\tau) d\tau \quad (1.6)$$

Subtracting equation (1.6) from equation (1.5), we are left with:

$$CRI(t + \Delta t) - CI(t)R = qN(t + \Delta t) - qN(t) - \int_0^{t+\Delta t} I(\tau) d\tau + \int_0^t I(\tau) d\tau \quad (1.7)$$

Or

$$CR[I(t + \Delta t) - I(t)] = q[N(t + \Delta t) - N(t)] - \int_t^{t+\Delta t} I(\tau) d\tau \quad (1.8)$$

Now suppose if:

**Case 1:**  $\Delta t$  is reasonably small, such that there is no notable change in the value of current  $I(t)$  in the interval  $(t, t + \Delta t)$  and thus  $I(t + \Delta t) - I(t) = \Delta I$  and also

$$\int_t^{t+\Delta t} I(\tau) d\tau \approx I(t)\Delta t$$

**Case 2:**  $\Delta t$  is sufficiently large, meaning that the number of electrons reaching the plate will be high during the interval  $(t, t + \Delta t)$ . According to central Limit theorem a better approximation of  $N(t + \Delta t) - N(t)$  in this case is provided by the Gaussian random variable  $W$  with mean rate and variance  $\lambda\Delta t$  instead of the Poisson random deviate. Therefore,

$$N(t + \Delta t) - N(t) \approx \lambda\Delta t + \lambda\Delta W$$

where  $\Delta W$  is a Gaussian random variable with a zero mean value and variance  $\Delta t$ . The sequence of these random variables defines the Gaussian process; say,  $W(t)$  and can be obtained by summing up the increments of  $\Delta W$ . Clearly, the mean value of  $W(t)$  is zero and the variance is  $t$ . The final equation of the current  $I(t)$  can be written as,

$$CR\Delta I = q(\lambda\Delta t + \sqrt{\lambda}\Delta W) - I(t)\Delta t \quad (1.9)$$

This equation assumes that there is no initial current. Rewriting the above equation in a differential form, this equation is an SDE:

$$dI = \frac{q\lambda - I}{CR} dt + \frac{q\sqrt{\lambda}}{CR} dW \quad (1.10)$$

Here  $dW$  is known as Wiener process increment and both  $I$  and  $W$  are the continuous functions everywhere but nowhere differentiable. This equation is an example of an Ornstein Uhlenbeck process. The description above shows that stochastic processes are suitable for capturing the true behaviour of random phenomena.

An SPDE is a partial differential equation (PDE) that has some or all of its coefficients as random terms, such as forcing terms, initial, and boundary conditions. SPDE are now a multidisciplinary field that includes stochastic processes. While this field is seen as a new discipline, it has significant roots dating back to the late 1960s and early 1970s. Now, many specialists from various fields are collaborating to create a sequence of interrelated solutions that define the behaviour of complex systems (Di Nunno et al., 2023; Mata, 2020). A few of the major areas are related to interacting particle systems, fluid dynamics, statistical physics, financial modelling, nonlinear filtering, super-processes, and continuum physics (Bear, 1972; Di Nunno & Øksendal, 2011; Eringen, 2002; Lototsky et al., 1997; Lototsky & Rozovskii, 2006). The researchers interested in quantifying uncertainty are important contributors and are heavy users of the theory and practice of SPDEs.

### 1.2.3 Need and importance

Large-scale computations and numerical methodologies developed in recent decades have improved the applicability of SDEs/SPDEs on a more practical level. Indeed, this advancement has demonstrated the relevance of these equations to a wide range of technological disciplines, including reliability and control theory, data-driven computer prediction and design, decision-making, and risk analysis in the environmental and financial sectors.

In the presence of inherent and extrinsic noise, SDEs/SPDEs are being utilised as a mathematical tool to describe numerous physical, biological, and economic systems. Modelling uncertainties, inbuilt parameters, and aspects of the applied theory such as open-end boundary conditions are all instances of intrinsic noise. In contrast, extrinsic noise can be caused by environmental factors, geographic disparity, or random user input. Another reason for using SPDEs relates to the need to

find a controlled or adjustable solution to complicated physical systems. The advent of noise frequently leads to the emergence of a new phenomenon, both mathematically and phenomenologically.

### **1.3 Stochastic equations and possible research thinking**

We can find a number of reasons and a variety of perspectives on the need to study SDEs/SPDES and their uses in modelling. In financial mathematics, these equations are a central part of modelling; they are used to model the key features such as interest rate, asset prices, risks, and their volatility (Debus, 2013; Faria & Correia-da-Silva, 2014; Heston, 1993; Lund et al., 1991; McComas et al., 2016; J. E. Zhang & Shu, 2003). In applied mathematics these equations are useful for modelling transport equations (Yoshioka et al., 2011), quantum mechanics (Ohsumi, 2019), wave propagation in random media (Millet & Morien, 2000a), neuroscience (J. Ma et al., 2019), population genetics, and mathematical biology (Bellmann, 1979). These equations are also being used in pure mathematics as a natural object to study stochastic processes and dynamical systems and to develop theoretical frameworks, convergence, and stability for the algorithms in the form of lemma and theorems. There is a great need and interest in developing efficient numerical schemes to solve these SDEs: it is essential and profitable too, especially when dealing with randomness. This task may be quite difficult because ingenuous and naïve methods can go wrong when developing and simulating solutions to SDEs.

Given the widespread usage and application of stochastic equations in a diverse range of disciplines, any contribution that improves model performance will have a positive effect on the community and increase the applicability of these models in modelling real life phenomena.

Most of the stochastic models that are developed to capture randomness are known not to fit the data they are supposed to model. For instance, the models developed to study the turbulent flow in a medium based on SDEs may not provide an exact interpretation or truly represent variations which occur in a real setting. These models are based on the mathematical fact of Brownian motion that has infinite variation. Even so, these models represent balanced conjectures to real-world phenomena. Furthermore, as they are mathematically stable, and, to a large extent, also controllable, they can still provide some very useful insights. Researchers argue that the marginal probability distributions of these stochastic equations can report changes in flow captured at discrete points in time.

### 1.3.1 Motivational example

For the sake of simplicity, let us consider an arbitrary 1-dimensional ODE whose parameters are perturbed by a “white noise” term  $W(t)$  and which can be scaled, depending upon the value of function and time:

$$\frac{du_t}{dt} = a(t, u_t) + \sigma(t, u_t)W(t) \quad (1.11)$$

$$u(0) = u_0 \quad (1.12)$$

Before attempting to find a solution for equations (1.11) - (1.12), we need to ask several questions related to the uniqueness and the existence of the solution, stability and its convergence, the dependency of the solution on the initial condition, and most importantly, the conditions and properties of white noise that we need.

$W(t)$  needs to be a random variable, following a specific probability distribution, say “Gaussian” with a mean ‘0’ and a variance of ‘1’; thus,  $W(t) \sim N(0,1)$  and needs to be independent for distinct time instances between the time intervals  $(0, t)$ . In the case of a discrete time system, the existence of  $W(t)$  is such that  $W(t_1)$  and  $W(t_2)$  are independent for  $t_1 \neq t_2$ . However, this condition is presumed in the case of a continuous time system by considering,

$$\frac{dB(t)}{dt} = W(t), \text{ where } B(t) \text{ is the Brownian motion.}$$

The integral form of equation (1.11) is:

$$u(t) = \int_0^t a(\tau, u(\tau))d\tau + \int_0^t \sigma(\tau, u(\tau))W_\tau d\tau \quad (1.13)$$

A more simplified form is,

$$u(t) = \int_0^t a(\tau, u(\tau))d\tau + \int_0^t \sigma(\tau, u(\tau))dB_\tau \quad (1.14)$$

In the above equation, the second integral is the stochastic integral popularly known as the Itô integral (Itô, 1951). We now have a proposition to define the white noise or the random term and can solve the stochastic integral against Brownian motion which will ultimately help in exploring its consequences.

However, the Itô integral is not the only way to characterise this kind of stochasticity: there are more developed and robust frameworks which have been applied during the past few decades and which form a solid base for such SDEs and SPDEs. For instance, let us consider a one-dimensional stochastic wave equation:

$$\frac{\partial^2 u(x, t)}{\partial t^2} = c^2 \frac{\partial^2 u(x, t)}{\partial x^2} + W(x, t), \forall t > 0 \text{ and } x \in \mathbb{R}^d \quad (1.15)$$

with an initial condition,

$$u(x, 0) = \frac{\partial u(x, 0)}{\partial t} = 0 \quad \forall x \in \mathbb{R}^d \quad (1.16)$$

(Walsh, 2006) explained the equation (1.15) as the vibration of one guitar string left outside during a sandstorm. Its solution, when  $c^2 = 1$ , is given as:

$$u(x, t) = \frac{1}{2} \int_0^t \int_{x-(t-\tau)}^{x+(t-\tau)} W(\tau, y) dy d\tau \quad (1.17)$$

$$= \frac{1}{2} \hat{B} \left( \frac{t-x}{\sqrt{2}}, \frac{t+x}{\sqrt{2}} \right) \quad \forall t > 0 \text{ and } x \in \mathbb{R} \quad (1.18)$$

where  $\hat{B}$  is the Brownian sheet whose origin is fixed along the line  $t + x = 0$ . In the case of a higher-dimension ( $d = 2$ ), equation (1.15) represents the motion of a drum skin; however, its solution does not exist in the ordinary sense and some kind of generalised solutions are required to understand the physical meaning and significance of the motions. It is justifiable to believe that while the pressure of wind and the impact of sand particles do not act in the same fashion as the properties of the white noise process, this kind of formulation certainly provides a better approximation of the occurrence of the events. Thus, to obtain generalised solutions, along with their physical interpretations, smoothening procedures are one way of obtaining acceptable solutions capturing real word phenomena.

#### 1.4 Objectives for this study

The research domain of SDEs and SPDEs is extensive and researchers continue to explore these domains, the development and refinement of numerical methods. The list of objectives in the thesis is as follows:

- (i) The first objective in this thesis is to understand how can we constitute these equations.

There is no straight forward answer to this question. The answer mostly depends on type of application for which such equations are being used. It could be based on the roughness of white noise, could be coloured noise or it could be based on some kind of smooth white noise used in place of white noise (Manthey & Mittmann, 2007). Although, there is no need for the smoothening of such solutions as these generalised solutions provide physical interpretations of the system, this approach appears somewhat unpleasant. In contrast, the use of white noise is justified in some mathematical sense. (Holden, 1996) provides a few physical reasons for choosing coloured noise.

- (ii) The second objective is to explore the existing methodology and numerical methods in this research area and identify the research gaps.

By conducting an extensive review of the literature, the research aims to identify gaps in current knowledge and practices. These research gaps serve as opportunities for further advancement in the

field, allowing for the development of innovative computational techniques and numerical strategies that can address the complexities posed by SDEs and SPDEs.

(iii) The third objective for this study is to know how to solve these equations.

SDEs and SPDEs are pervasive in various scientific and engineering domains due to their ability to model systems influenced by random forces and uncertainties. The answer relates to the history of SPDEs; there is a solid mathematical background. For example, the solution of the above wave equation (1.25) is treated as a measurable function (Kallianpur & Sundar, 2014; Walsh, 2006) and depends on a random variable: say  $\omega \in \Omega$  for  $t > 0$  and  $x \in \mathbb{R}^d$  in a higher-order ( $n$ ) Sobolov space  $H^{-n}(\mathbb{R}^d)$  such that,

$$u \in H^{-n}(\mathbb{R}^d)$$

or

$$u: \Omega \times \mathbb{R}_+ \rightarrow H^{-n}(\mathbb{R}^d)$$

The generalised solutions  $(\omega, t)$  are defined pointwise in this space  $H^{-n}(\mathbb{R}^d)$ , a fact which resolves the difficulty of high-dimensionality, to some extent. This approach is based on Itô calculus. The third option is to use a wider space called a Kondratiev space of stochastic distributions which utilises the concept of duality spaces of smooth random variables. (Holden, 1996) uses this approach extensively in his monograph and subsequent research articles.

Indeed, while each method has different axioms, properties, theorems, and repercussions which can be compared, the success and validity of each approach will depend on the strength of the arguments and patrons in favour of that specific approach.

(iv) and (v) The next two objectives are to apply the chosen methodology and numerical methods to certain complex systems and provide hands on examples to show how these techniques work in applied sense.

I will inquire in to the application of spectral stochastic methods and Malliavin calculus to some SDEs and SPDEs and will provide working examples with numerical simulations. I will also discuss the advantages and disadvantages of the methods used.

## 1.5 Thesis framework

The remaining thesis is structured as follows:

This thesis consists of seven chapters. Figure 1.3 illustrates the organisation of the thesis and key points in the chapters.

The current chapter, chapter 1 explains the fundamental concepts, relevance and significance of the research topic, and elucidate the motivation driving the investigation. This chapter offers a

compelling narrative on why SDEs and SPDEs deserve scholarly attention and scrutiny. By providing context and rationale, this chapter establishes a strong foundation upon which the subsequent chapters will build, delving deeper into the intricacies of solving these equations and advancing our understanding of their impact on complex systems.

Chapter 2 explores the existing body of knowledge surrounding stochastic differential equations (SDEs) and stochastic partial differential equations (SPDEs) across various fields and applications. It includes different domains where these equations have found relevance, from physics and engineering to biology, finance, and environmental science.

In Chapter 3 we introduce the preliminary concepts related to SDEs and SPDEs which are necessary for solving complex physical systems. This chapter includes a summary of the numerical methods used to solve these equations along with a brief discussion on the convergence and stability of these solutions.

In chapter 4, we explained the spectral methods especially polynomial chaos expansion methods and their role in stochastic equations.

In chapter 5 we considered the application of polynomial chaos methods to stochastic systems with reference to contaminant transport. This chapter provides examples of hands-on approach working with SDEs/SPDEs. It also includes a comparative study of different methods.

In Chapter 6 we discuss powerful, yet less applied numerical methods in the stochastic space known as Wick calculus and Malliavin calculus.

Chapter 7 provides discussion and numerical challenges, a summary of this research, the key findings, and topics for future exploration.

Computation of examples and simulation are performed in MATLAB/MATHEMATICA software on 11th Gen Intel(R) Core (TM) i5-1135G7. A few programs are also run on Intel(R) Xeon(R) CPU E5-1650 high performance computer of C-fACS (Centre for Advanced Computational Solutions) at Lincoln University.

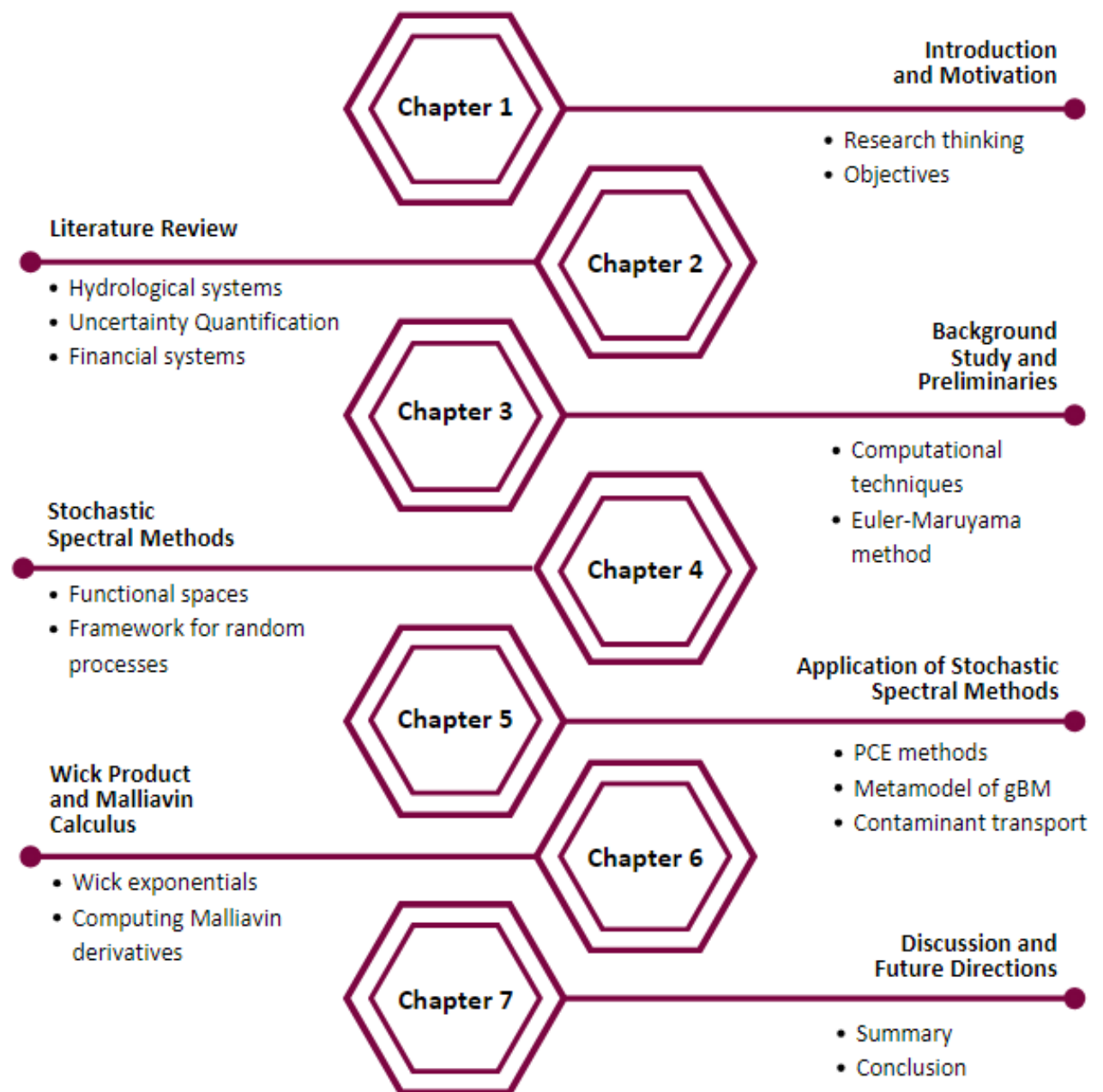


Figure 1.3 Organisation of the thesis and key points in the chapters.

## Chapter 2

### Literature Review

Many physical processes are simulated using mathematical models that lead to partial differential deterministic equations. Due to a lack of data on parameters and initial data, a system's behaviour may differ from the ideal deterministic description. Adding random inputs, such as random variables or stochastic processes, to make a system's explanation more realistic is one way to deal with this issue and compensate for a lack of information. SPDEs are formulated as a result. Computational mathematics, electronics, statistical mechanics, theoretical physics, theoretical psychology, advanced chemical re-action analysis, fluid dynamics, hydrology, and mathematical finance are just a few of the domains where SPDEs are applied. Analytical techniques, such as those proposed by Prato (Istvan Gyongy & Nualart, 1999) can be used in specific types of SPDEs. Several scholars have used finite element approximation for the numerical simulation of SPDEs (Castillo et al., 2002; Elsevier et al., 2001; Walsh, 2006). Boyaval et al. (2022) have solved SPDEs using high-resolution finite volume methods.

PDEs have played a vital role in the development of transport equations (Holden, 1996). When noise in the system dynamics takes place due to the heterogeneity of the media or the randomness of the input variables (such as rainfall and variable boundary conditions), these transport equations can be modelled as SPDEs (Holden, 1996).

#### 2.1 Stochastic processes

In a classic paper from 1905, Einstein (Einstein, 1905) made a mathematical connection between the microscopic random motion of particles and the macroscopic diffusion equation. The current understanding and development of stochastic processes can thus be traced back to Einstein. This was a key result in establishing the atom's existence. Einstein made few observations for stochastic concepts known as the microscopic motion of Brownian particles which is necessary to explain here before we go further.

##### 2.1.1 Microscopic motion of Brownian particles

Let us consider that  $m$  number of particles are suspended in a liquid. Let the change in the displacement of  $x$ - co-ordinate of particle during this time interval  $\Delta t$  be  $\Delta x$ . The number of displaced particles within this duration is,

$$dm = mP(\Delta x)d\Delta x \quad (2.1)$$

where  $P(\Delta x)$  is the probability density (Figure 2.1) of  $d\Delta x$ , and is assumed to be symmetric,  $P(\Delta x) = P(-\Delta x)$

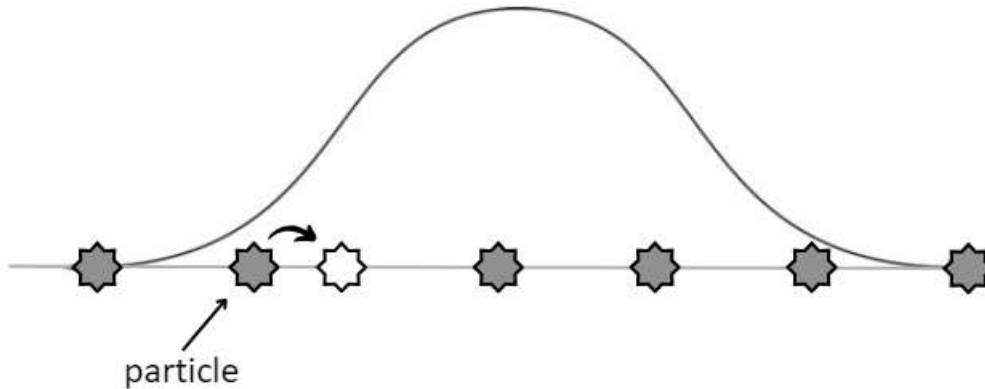


**Figure 2.1** Probability density function  $P(\Delta x)$  of Einstein's Brownian motion model for the displacement  $\Delta x$  for a very small time-interval.

The number of particles per unit volume is denoted as  $N(t, x)$ ; using Taylor's approximation up to second degree terms, the diffusion equation is given by,

$$\frac{\partial N(t, x)}{\partial t} = D \frac{\partial^2 N(t, x)}{\partial x^2} \quad (2.2)$$

where the diffusion coefficient ( $D$ ) is calculated as,

$$D = \frac{1}{\Delta t} \int_{-\infty}^{\infty} \frac{(\Delta x)^2}{2} P(\Delta x) d(\Delta x) \quad (2.3)$$

Einstein (1905) analysed equation (2.2) with macroscopic point of view. Later on, Einstein was able to obtain an expression for mean squared displacement  $\bar{x}(t)$  as a function of time,

$$\bar{x}(t) = \frac{RT}{n} \frac{1}{3\pi\eta d} t \quad (2.4)$$

He also derived a formula for the diffusion coefficient ( $D$ ) in terms of microscopic quantities. Here  $R$ ,  $T$ ,  $n$ ,  $d$  and  $\eta$  denote the gas constant, temperature, Avogadro constant, the diameter of the particles, and viscosity of the fluid, respectively.

So, for a long time, the Brownian motion was used as a stochastic process. For past few decades, Brownian motion provides a representation of a random walk process (Figure 2.2) in which each increment is independent. That is, the direction and magnitude of each change of the process are completely random and independent of the previous changes.

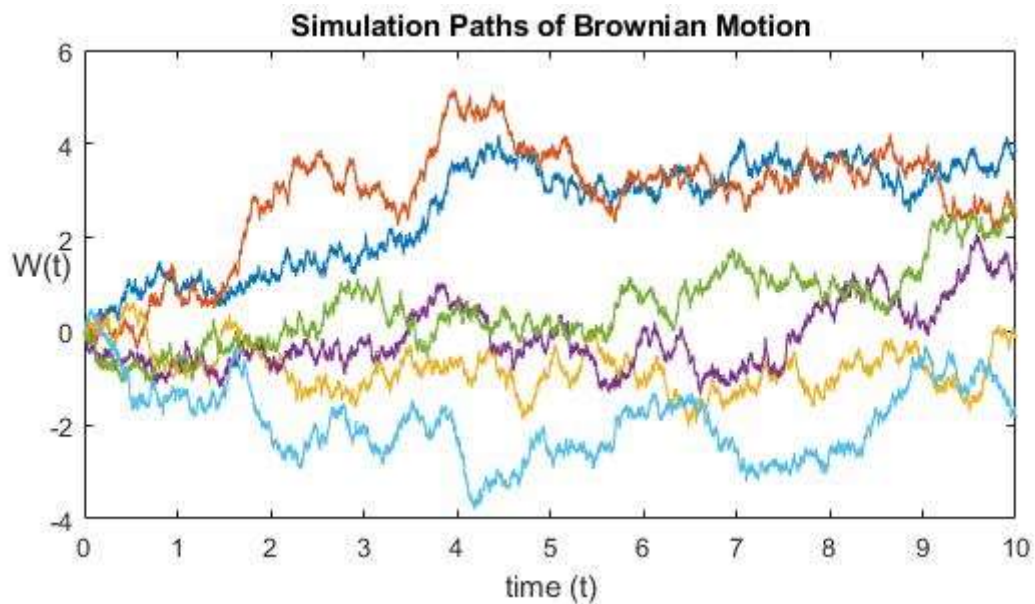


**Figure 2.2 Representation of Brownian motion as a random walk process.**

In other words, Brownian motion provides the solution for the following stochastic differential equation (SDE):

$$\frac{dB(t)}{dt} = W(t) \quad (2.5)$$

where  $W(t)$  is the white noise process or the Wiener process, such that  $W(t)$  and  $W(s)$  are independent for all  $t \neq s$ .

Following Einstein's theory, Langevin (Lemons et al., 1997) developed the mechanistic model for Brownian motion based on friction and random force between the particles.

### 2.1.2 Brownian motion as a stochastic process

Quantum mechanics (QM) is used to provide an accurate description of the system in many-body interactions that capitulate the complex, yet alluring, pattern of Brownian motion. The first-principle model cannot completely define the detailed motion of the molecules. Therefore, probabilistic models are applied to molecular populations to sketch it. This is why Brownian motion is defined as a purely stochastic process in its present form. Wiener, an American mathematician, was the first to examine the mathematical properties of a one-dimensional Brownian motion. The Wiener process is the resulting real-valued continuous-time stochastic formalism.

Stationarity and independent increments are two appealing properties of this well-known stochastic process; that is why it finds frequent use in a wide range of fields, including pure and applied mathematics, quantitative finance, economic model-building, and even evolutionary biology. Modern mathematics, such as stochastic calculus and diffusion processes, rely heavily on the concept of

Brownian motion and mathematical models. In electrical and electronics engineering, a white noise Gaussian process is often used to represent the integral of a Wiener process (K. K. Kim et al., 2013). The same concept is used in filter design to simulate noise and errors (Gustafsson et al., 2018), as well as in control theory to model random/unknown forces (Ata et al., 2005; Harrison, 2011; Velasco, 1985).

Brownian motion is frequently used in quantum physics to study diffusion phenomena related to the Fokker-Planck and Langevin equations (W. Liu et al., 2021; Medved et al., 2020; Paganin & Morgan, 2019). It also serves as the foundation for quantum mechanics' rigorous path integral formulation. For instance, the Wiener process, using the Feynman-Kac formula, provides a solution to the famous Schrodinger's equation (Lisei, 2011; Ohsumi, 2019). Brownian motion dynamics inspired the physical cosmology model of eternal inflation (Koonin, 2007). In the finance and econometric modelling, Brownian motion is a mythical concept; almost all major financial mathematical theories include it (D. Chen & Li, 2022; McComas et al., 2016; Wattanatorn & Sombultawee, 2021). This formalism is especially important in the well-known Black-Scholes option pricing model, for which Myron Scholes was awarded the 1997 Nobel Prize in Economics.

## **2.2 Numerical modelling with complex systems**

Many physical processes are simulated using mathematical models that lead to partial differential deterministic equations. Due to a lack of data on parameters and initial data, a system's behaviour may differ from the ideal deterministic description. Adding random inputs, such as random variables or stochastic processes, to make a system's explanation more realistic is one way to deal with this issue and compensate for a lack of information. SPDEs are formulated as a result. Computational mathematics, electronics, statistical mechanics, theoretical physics, theoretical psychology, advanced chemical re-action analysis, fluid dynamics, hydrology, and mathematical finance are just a few of the domains where SPDEs are applied. Analytical techniques, such as those proposed by Prato (Istvan Gyongy & Nualart, 1999) can be used in specific types of SPDEs. Several scholars have used finite element approximation for the numerical simulation of SPDEs (Castillo et al., 2002; Elsevier et al., 2001; Walsh, 2006). Boyaval et al. (2022) have solved SPDEs using high-resolution finite volume methods.

PDEs have played a vital role in the development of transport equations. When noise in the system dynamics takes place due to the heterogeneity of the media or the randomness of the input variables (such as rainfall and variable boundary conditions), these transport equations can be modelled as SPDEs (Holden, 1996).

### 2.2.1 Hydrological systems

Scholars have modelled water catchment and fluid percolation in porous/fractured structures using SDEs. The application of SDEs in this field help us to understand the physical meaning of an SDE because the underlying mechanism is well-understood. Furthermore, the deterministic mechanism cannot be observed in its entirety, so it must be replaced by a stochastic process that depicts the system's behaviour over a much longer time span.

To account for uncertainties in solute transport, researchers commonly use SDEs for river water quality modelling (Kulasiri, 2015; Yoshioka et al., 2011). The effective behaviour of solute transport in porous media is one of the major points of consideration for hydrogeologists. To understand this behaviour, the modeller needs to understand the average transport dynamics on one side and variations to average behaviour on the other side. The mass transfer processes that affect the motion of solutes under any natural media and the reaction events are influenced by heterogeneity. Solute transport in heterogeneous media requires the quantification of the impact of spatial variability and temporal flow fluctuations. These two parameters affect not only the average transport behaviour but also induce fluctuations in concentration affecting the mean values. Thus, effective modelling of these measurements is essential in real applications including, as has been demonstrated here, in ground water management and water resources management.

Three processes (advection, dispersion, and diffusion) determine solute transport in ground water. Mathematically, these three processes can be defined by an equation known as advection-dispersion equation (ADE) which has been derived and analysed by several authors (Bear, 1972; Fetter, 2001; Freeze & Cherry, 1979). The classical ADE transport equation was developed using the continuum approach and macroscopic mass conservation. Solute advection is defined as the average velocity of solute particle. It defines the centroid of the solute plume at a given time or the average arrival time of solutes at a given depth. A huge collection of research outputs for the solution of advection-dispersion equation is available in literature (Gedeon, 2084; Gelhar et al., 1992; Lemke et al., 2004). Over the two decades, numerical techniques have become more advanced, upgraded, and implemented to locate the effects of parameter uncertainty through transport modelling (Chen et al., 2018; Custodio et al., 2018; Furman, 2008). Further research related to transport in porous media, especially in the groundwater engineering field developed by Ghoraba et al. (2013) and Yadav and Roy (2018) has shown that the average fluid velocity does not describe the actual motion of individual solute particles, and that the advective calculation could, therefore, never provide a full description of solute movement.

Although numerous studies have proved the applicability of solute transport models based on deterministic advection-dispersion equations (Cianci et al., 2011; Deng et al., 2004; Farmer & Vogel,

2016), the success of such deterministic models in describing solute movement in variable field conditions is questionable. The deterministic modelling of solute transport in ground water contamination involves the simulation of hydrodynamic dispersion, advection, and absorption with velocity field. Moreover, these components suffer from significant uncertainty because of scale dependency, even in homogeneous media; their effects are poorer in the case of heterogeneous mediums where micro variations take place in flow parameters. These difficulties have been captured and handled in two ways. One way is to increase the dispersion parameter with distance (Pang & Hunt, 2001) and the other way is to increase it with time (Srivastava et al., 2002).

Another approach to scale dependency and heterogeneity is stochastic modelling in which relevant flow parameters are characterised by a distribution function. Transport in hydrogeological media is essentially stochastic in nature. Stochastic methods are one way to model the associated uncertainties associated with the continuum transport model. In stochastic theories, the mean properties of output variables are considered; this method focuses on the supposition that ensemble means provide a useful description of the larger-scale spatial and temporal trends in practical applications. Although it is not of great importance to know the exact deviation of local fluctuations from the ensemble mean, it is useful to know their likely range. Higher-order moments such as the standard deviation and skewness are used to characterise the random fluctuations. There has been much academic and experimental research conducted on higher-order moments of sub-surface variables (Christakos et al., 1995; Dagan, 1988; Li, Huang, Zeng, Maqsood, & Huang, 2007; Van Rooy, 1986).

The accelerating progress in research on SPDEs has stimulated the involvement of many experts in hydrology (Holden et al., 1993; Serrano & Unny, 1987; Unny, 1989). These SPDEs are driven by space-time Brownian motions or more generally, the space-time Levy process (Ford, 2005; Løkka et al., 2004) and are solved analytically as well as numerically. Curtain and Pritchard (1977) and Ford (2005) have applied the concept of functional analysis in appropriate Sobolov spaces. An integrated and rigorous theory of stochastic PDEs has been used to solve stochastic groundwater flow problems (Márquez-Carreras et al., 2001a; Millet & Morien, 2000b). Balan and Tudor (2010) have implemented the random field approach to prove the necessary and sufficient condition for the existence of the solution of stochastic wave equation with fractional noise. Márquez-Carreras et al. (2001b) used Malliavin calculus to deal with spatially correlated noise.

In addition, more realistic approaches have been applied in stochastic methods to evaluate uncertainties in groundwater flow and transport simulation systems (B. X. Hu et al., 2004). Kaluarachchi (2000), for example, developed a Lagrangian stochastic methodology to represent sub-surface heterogeneity using a spatially correlated random hydraulic conductivity field with a log-

normal distribution. (S. -G Li & McLaughlin, 1991) have explained the importance of statistical ground water modelling and used the non-stationary spectral method to determine the model parameters.

(J. B. Li et al., 2003) proposed a modified fuzzy vertex method for the simulation of petroleum contamination in the sub-surface. (B. X. Hu et al., 2004) applied a numerical moment method to determine the groundwater flow and solute transport in multiscale heterogeneous formations. (K. B. Kim et al., 2018) has attempted quantification of relationships among uncertain hydrogeological parameters and warm-up timings. Other important contributions to stochastic theories in groundwater hydrology can be found in the extant literature (Baalousha & Köngeter, 2006; Croci et al., 2019; Kashyap et al., 2011; Y. P. Li et al., 2008; Yidana et al., 2016) and the references therein. Several martingale techniques have been applied to solve forward and backward porous media equations and Hu et al. (2012) has established gradient approximations for these equations. Forward backward SDEs (FBSDEs), along with finite dimensional noise, are frequently used in mathematical finance and have been studied for a long time (Almada Monter & Budhiraja, 2014). A link from Itô's SDEs to nonlinear Burgers type partial differential equations (PDEs) has been established Wu and Yang (2012). Random walk methods have been applied in diffusion processes for composite porous media (LaBolle et al., 2000). In this article, the authors developed a unique method for ADEs while retaining the computational efficiency of random walk methods. Kloeden and Platen (1992) have made a major contribution in developing numerical solutions for SDEs.

The application of Brownian path is an important factor in a variable step size implementation for SDEs; for example, when a researcher uses a different step size or a different initial value, the integration must follow the same Brownian path. (Burrage & Burrage, 2003) discussed the importance of variable step size implementation over fixed step size. The exit time for numerical algorithms for SDEs to complete the process is a difficult task. (Jansons and Lythe, 2003) have applied a boundary test with exponential time stepping for SDEs. Higham (2001) has provided a detailed algorithmic explanation for simulating an SDE.

Numerous research articles have discussed weak and strong SDEs/SPDEs solutions (Michta, 2004; Siopacha & Teichmann, 2011). Stochastic Runge Kutta methods have been successfully applied to linear SDEs, with various researchers discussing their stability and convergence (Higham et al., 2007; Kloeden & Neuenkirch, 2007; Soheili & Namjoo, 2007; Tian & Burrage, 2002; Yuan & Mao, 2004). Numerical modelling is critical for the management and remediation of groundwater resources. The variability of natural geological formations has a significant impact on pollution migration into groundwater. Stochastic models have been created to account for the restricted understanding of geological properties and natural heterogeneity ((Dagan, 2002).

### 2.2.2 Uncertainty quantification

Uncertainty quantification is a broad topic with many facets that include the identification and representation of uncertainty, uncertainty propagation across different scales, validation for predictive computational models, and the verification and visualisation of uncertainty in higher dimensions. Uncertainty emerges primarily due to stochastic input in the initial and boundary conditions or may be inherent in physical systems. In order to anticipate the performance of complex physical systems precisely, it becomes a necessary part of the analysis to incorporate these uncertainties into the physical model and comprehend how these spreads and affect the end solution.

The uncertainties in complex physical systems can be modelled using SDEs/SPDEs or by reformulating the governing equations of deterministic systems. The groundwater contamination flow is one of the examples that encounter uncertainty. The multi-physics behind contamination issues have captured the interest of many research scholars over the past several decades. Scholars typically use Finite Element (FEM) or Finite Volume (FVM) methods to study the multiphase flow through aquifers and reservoirs. In the case of uncertainty propagation, the simulation times is longer and thus, several cost-effective multiscale methods are applied (Ginting et al., 2014; Henning & Ohlberger, 2009).

Randomness in contaminant flow is not inherent; that is, the permeability of the medium which is a very specific characteristic, responsible for the randomness. Experimentally, we are unable to fully resolve this dynamical physical quantity. So, it is difficult to capture the complete randomness through established hydrological models; they need continuous calibration and upgradation. That is precisely why we must approach contamination issues with caution. Thus, there is a knowledge gap caused by the inbuilt uncertainties. The depiction of randomness in quantities of interest, such as pressure fields or velocity fields, are hampered by three key issues: first of all, it is very expensive to obtain experimental data related to the sub-surface. As a result, there are not enough observations to use and validate.

Second, the nature of the physical quantities is extremely high-dimensional which necessitates the use of dimensionality reduction strategies. The Karhunen-Loeve expansion serves this purpose. Lastly, there are higher chances of discontinuities in the response due to heterogeneity in the media properties.

The real world and its behaviour appear uncertain to humans. Deterministic mathematical models cannot handle such uncertainties. For real and large application scenarios, the random input parameters work as an obstacle for the model output to be accurate. Thus, SDEs and SPDEs are now being used to quantify and propagate uncertainty in most of the physical and dynamical systems.

Over the last few decades, numerous techniques and algorithms have been created to deal with the challenges associated with uncertainty propagation and its quantification. The Monte Carlo (MC) approach is the most conventional technique. It has received wider acceptance among research communities due to its ability to compute the entire solution statistics. The convergence rate of the MC technique is independent of the input dimension. However, for small samples and high-dimensional data, this approach is inefficient.

The spectral Finite Element Method (sFEM) is another popular strategy used to characterise the randomness (R. Ghanem, 1998). Originally, Gaussian random variables (GRV) were used to project the response on a space involving Hermite polynomials. These methods are called Polynomial Chaos (PC) methods. Later on, Xiu and Karniadakis introduced the generalised polynomial chaos expansion (gPCE) approach to quantify uncertainty (Xiu & Karniadakis, 2003). This method reduces the amount of computation while maintaining good accuracy. Since then, a number of improvements (Wan & Karniadakis, 2006; Xiu, 2007, 2009) have been made, particularly in regards to time and computational costs.

These methods can be applied to multi-element cases and can use Legendre's, Chebyshev, and other polynomials rather than just Hermite polynomials. With these approaches, the stochastic space is divided into separate elements; each element is subjected to gPCE. In stochastic collocation methods, the PCE coefficients are approximated using numerical integration and do not require any changes during the simulation process. (Nobile et al., 2008) introduced this method, along with Galerkin approximation, using Gaussian quadrature. Even though these methods can handle higher dimensions, they are nevertheless plagued by the curse of dimensionality. Babuška et al. (2010) resolved this issue using a sparse grid collocation method. The authors succeeded in capturing the discontinuous behaviour of the variables in stochastic space.

(Gramacy & Lee, 2007) applied a local approach for smaller data points and captured the effects of localised features in stochastic space. (Bilionis & Zabarar, 2012) designed a Bayesian experimental technique to train a multi-output Gaussian process which showed better convergence compared to sparse grid methods. D. Zhang et al. (2018) used a physics informed neural network strategy based on arbitrary polynomial chaos and deep learning methods.

### **2.2.3 Control theory**

Stochastic control theory with SDEs can be traced back to the late 19<sup>th</sup> century (Fleming & Lions, 1988). Today, the development of computational models for optimal control strategies are of increasing interest due to industrial requirements to improve productivity (Rippin, 1983). However, randomness in the observed data, model parameters, and implemented inputs can have an adverse

effect on the output (D. L. Ma & Braatz, 2001; Srinivasan et al., 2002). This issue has motivated researchers and engineers to develop more efficient techniques that can quantify the impact of parameters (K. Kim et al., 2013). Numerous researchers have studied stochastic optimal control theory (Dou & Lu, 2019; Dumitrescu et al., 2018; Fabbri et al., 2017; Lü et al., 2022) using SDEs and SPDEs. To control the drift and diffusion term, some researchers have applied the theory of transposition to stochastic evolution equations (Frankowska & Lü, 2020). (B. Øksendal, 2006) has outlined the control theory of a quasilinear stochastic heat equation defining optimal harvesting. (X. Y. Zhou, 2006) has published an important article defining the necessary conditions for the optimal control of SPDEs. (Huschto & Sager, 2013) have applied a Wiener chaos framework to enable the optimal control of a stochastic diffusion equation. Konda et al. (2011) and Li et al. (2014) have used the PCE method to determine the optimal control trajectory in control engineering. Recently, Lü and Zhang (2021) outlined the optimal control theory for SDEs.

#### **2.2.4 Chemical master equations (CMEs)**

Several biological and chemical processes are categorised as Chemical master equations (CMEs). Scholars have proposed different numerical methods for solving CMEs (Gillespie, 1977; Higham, 2008; Munsky & Khammash, 2007; Sidje & Vo, 2015). (Lunz et al., 2021) used augmented CME in the place of classical CME to simulate complex system dynamics. Engblom (2009) used an applied spectral approximation scheme.

The control of a chemical reactor and its operating conditions play an important role in maintaining high quality standards and meeting environmental constraints. Better quality and greater production activities go together. The random behaviour of state variables in modelling is more realistic (Reverberi et al., 2008) than a deterministic model of the chemical reactor. Reverberi et al. (2008) has identified the energy-mass balance of a perturbed chemical reactor using SDE. Kosarwal et al. (2020) and Lunz et al. (2021) have contributed to recent advances in CMEs.

#### **2.2.5 Financial systems**

The role of mathematical skills and modelling in the financial sector is compulsory and a pre-requisite in order to understand market behaviour. Model analysts use advanced probabilistic models to explain unpredictable market movements, derive predictable pricing methods, and analyse the random behaviour of the stock market and financial data. SDEs and SPDEs have been used in financial mathematics for a very long time; for modelling derivatives pricing and hedging. Several financial variables, such as the stock price, asset volatility, interest rate, and option pricing are accurately characterised with the help of these stochastic evolution equations.

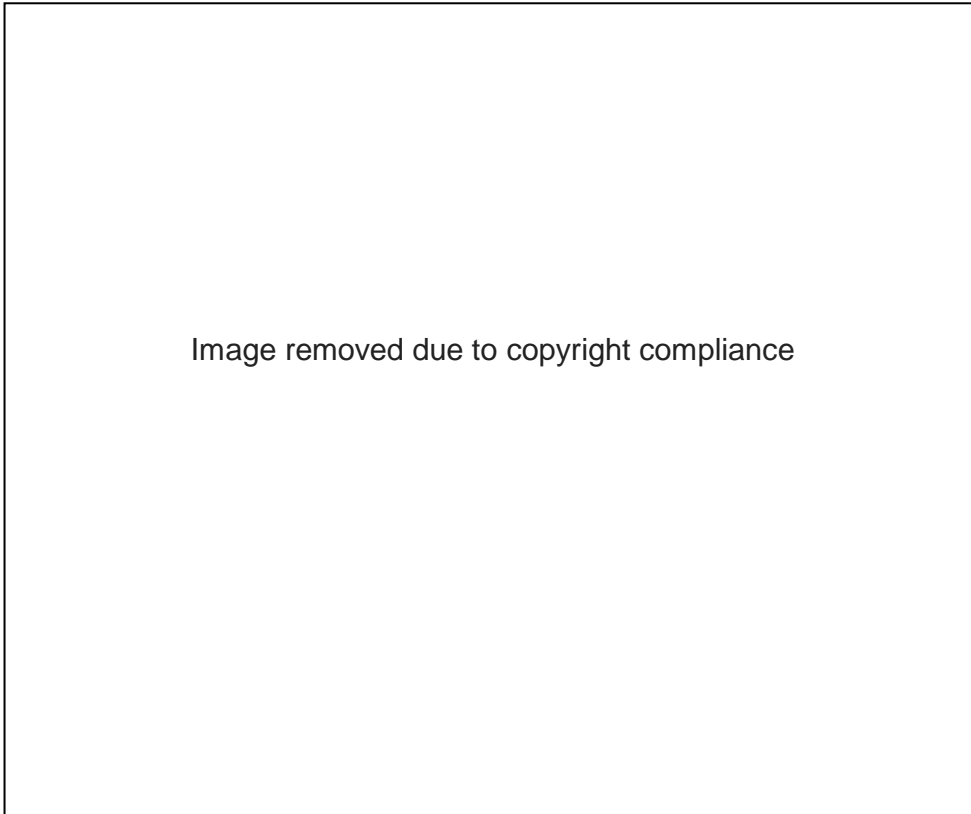


**Figure 2.3** Smile curve for a stock price using classical Black-Scholes model (Soini & Lorentzen, 2019), <https://www.sciencedirect.com/science/article/pii/S0140988319302324>

*Note.* These four graphs show the variation in implied volatility (IV) for options with the same remaining time to expiration. The above smile curve shows that the inclusion of more options will result in a higher IV. It was calculated using the Black-Scholes formula which involves putting the option's market price into it and calculating back the volatility value.

Stochastic volatility models became popular after the existence of a non-flat implied volatility surface which has been noticed in the classical Black-Scholes-Merton (BSM) model. The classical BSM model cannot explain the long-term behaviour of the implied volatility surface such as the smile effect, which indicates that implied volatility tends to vary due to changes in stock price and expiry.

Financial derivatives are being modelled more accurately now using stochasticity in the classical BSM model (Figure 2.3).

The BSM model for a risk-free asset  $A_t$  at time  $t$  with growth rate  $\alpha$  defined by an ODE is given as:

$$d(A_t) = \alpha A_t dt \quad (2.6)$$

which has the classical solution, with an initial investment  $A_0$  as

$$A_t = A_0 e^{at} \quad (2.7)$$

But, for a risky asset, the stock price can be defined more accurately by an SDE

$$d(S_t) = \mu S_t + \sigma S_t dB_t \quad (2.8)$$

where  $\mu$  is the drift,  $B_t$  is a standard Brownian motion, and  $\sigma$  is a risk measure considered to be positive. The larger  $\sigma$  values result in larger fluctuations in  $S_t$ . The drift measure  $\mu$  provides an average rate of growth in asset price. When  $\sigma = 0$ , the above equation is an ODE and the results show that asset price grows exponentially ( $S_t = S_0 e^{\mu t}$ ,  $S_0$  is the initial asset price) with the rate of drift. But, in a real situation, volatility is positive ( $\sigma > 0$ ) and the stock price is given by equation (2.9). The solution of this SDE, using Itô's lemma, is given as a random perturbed exponential function:

$$S_t = S_0 e^{\left(\mu - \frac{\sigma^2}{2}\right)t} + \sigma B_t \quad (2.9)$$

There has been much research on financial modelling using SDEs and SPDEs (Meyer, 2000; Taylor & Princeton, 2005; J. E. Zhang & Shu, 2003).

Such research has sought to answer the following questions:

- How can we mathematically characterise a market without arbitrage?
- How can we determine fair prices for options and derivatives?
- What is the fair value of such financial derivatives?

Heston (1993) has provided a closed-form solution for the European call option price with ambiguous stochastic process. The authors considered the return variance as a stochastic variable  $\lambda(v_t)$  as defined in equation (2.10), and explained the variable behaviour in the variance stochastic process in the following way:

$$\lambda(v_t) = \lambda_1 v_t + \lambda_2 \sqrt{v_t} \quad (2.10)$$

The first term in the right-hand side of the equation (2.10) represents the risk price. The second term defines the ambiguity price. Simulation results for price differences between BSM and the model developed by other authors are plotted as in Figure 2.4.

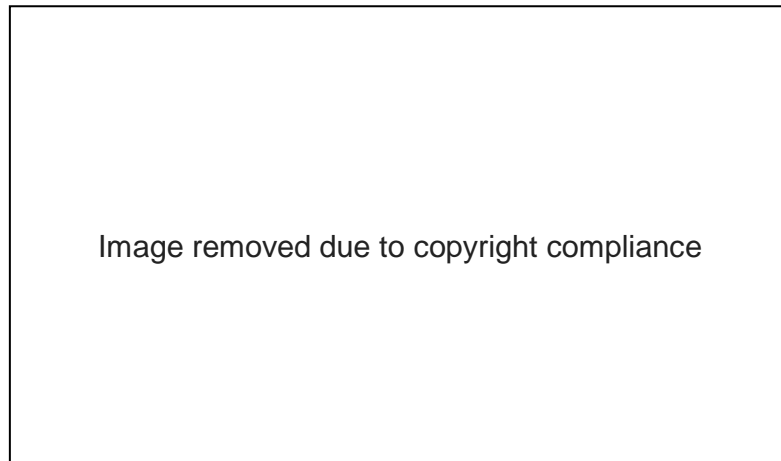


**Figure 2.4** Simulation results for price differences between BSM and (Faria & Correia-da-Silva, 2014) model for arbitrary return variance  $\lambda_2$  and for negative correlation ( $\rho = -0.5$ ) between shocks in variance and the return.

*Note.* In the case of no ambiguity ( $\lambda_2 = 0$ ), the curve matches the output, as in the Heston (1993) model. However, when the correlation coefficient and ambiguity is non-zero, the model displays a “smirk” shape in the implied volatility curve.

The applications of SDEs and SPDEs in the financial sector are not limited to option pricing. (Meyer, 2000) formulated an investment performance SPDE to resolve some of the issues in optimal portfolio selection. These types of SPDEs provide an alternative way to study the evolution of this process beyond the class of Markovian models (Bo & Capponi, 2018; Musiela & Zariphopoulou, 2009). Several scholars have provided detail explanations of basic concepts and the application of stochastic financial models (Di Nunno & Øksendal, 2011; Lund et al., 1991).

In applied mathematics, the modelling of complex systems incorporating randomness are becoming more common. A few examples include the Black-Scholes model (in finance), wireless communications (data transfer in network systems), and brain mapping (in biology). In many of these situations, an exhaustive search and extensive data collection are required to construct an appropriate model. Most of the time, the SDEs/SPDEs that best fit the data fail to provide a simple analytical answer. As a result, a consistent numerical technique is required. The modelling of vibrations and strings, turbulent flows, the motion of fluids (Stochastic Navier-Stokes Equation), the diffusion of heat in a medium (Stochastic Heat Equation), and numerous applications to finance and stock market analysis are all examples of complex physical systems.

### 2.3 Summary

The literature review presented in this chapter provides a comprehensive overview of the extensive research conducted on modelling with SDEs and SPDEs. It is clear from the literature review that

SDEs and SPDEs have found applications in various fields of science and engineering, including finance, physics, biology, and environmental science. These equations provide a powerful framework for capturing and quantifying uncertainty, making them indispensable tools for modelling complex and dynamic systems affected by stochastic processes. Additionally, this chapter also highlights a variety of numerical and analytical techniques that have been developed to solve SDEs and SPDEs.

The discussion arising from the literature review highlights several important aspects. First, the choice of numerical method depends on the specific characteristics of the problem under consideration, including dimensionality, nonlinearity and boundary conditions. Second, there is growing interest in combining stochastic modelling with efficient numerical techniques. Third, the need for uncertainty quantification (UQ) tools is paramount, as SDE and SPDE inherently involve uncertainty and quantifying this uncertainty is essential to make reliable decisions. Finally, SDEs and SPDEs are not only powerful tools for scientific research but also have great potential in solving real-world challenges, such as environmental pollution, financial risk assessment and biological modelling.

Overall, this literature review sets the stage for the following chapter, in which we will dig deeper the foundation for numerical methods for solving SDEs and SPDEs.

## Chapter 3

### Background Study and Preliminaries

The numerical simulation of physical models, underpinned by the increased availability of computational resources, plays a key role in design and decision-making processes of these models resulting in high economic and human impact. In physical systems, the numerical modelling and use of efficient techniques is important for improving response prediction. To obtain reliable predictions, one needs complete control over the conceptual model. Thus, the model has to be built from scratch to ensure that it replicates the data exactly. This chapter summarises the basic concepts and theorems used in the numerical modelling of complex stochastic systems.

#### 3.1 Brownian motion (definition and properties)

Robert Brown, an English physicist, studied what happened when pollen grains were immersed in liquid. He found that they did not stay in a specific position but rather, moved in highly irregular manner, a phenomenon later called Brownian motion. In examining this phenomenon, Einstein (1905) argued that the pollen was kicked by the much smaller fluid molecules, which are in constant thermal motion and continuously collide with molecules travelling at different speeds in different directions, meaning they mostly cancel each other out. The identified motion is related to statistical fluctuations. A mathematical description of this realisation leads to an SDE. The resulting stochastic process  $B(t, \omega)$  for a realisation  $\omega$  is a Wiener process (Wiener, 1938).

Our first task is to build and research Brownian motion. Although there are other ways to accomplish this (Ford, 2005; Biagini et al, 2008), we concentrate on one approach that will be simple to apply to higher-dimension problems that we will explore in later chapters and will use SPDEs.

Let us begin with a definition of white noise as a stochastic process in Borel subsets of  $\mathbb{R}^d$ , not as a time-indexed stochastic process.

##### Definition 3.1

A white noise on  $\mathbb{R}^d$  on a complete probability space  $(\Omega, \mathcal{F}, \mathbb{P})$  is a function  $W$  from Borel subsets to this probability space; i.e.,  $W: \mathcal{B}(\mathbb{R}^d) \rightarrow \mathcal{L}^2(\Omega, \mathcal{F}, \mathbb{P})$  and holds the following properties:

- (i) For all  $x \in \mathcal{B}(\mathbb{R}^d)$ , we have  $W(x) \sim N(0, \lambda(x))$ .
- (ii) For all  $x_1, x_2 \in \mathcal{B}(\mathbb{R}^d)$  and  $x_1 \cap x_2 = \emptyset$ , the random variables  $W(x_1)$  and  $W(x_2)$  are independent, and  $W(x_1 \cup x_2) = W(x_1) + W(x_2)$  holds  $\mathbb{P}$ -almost surely.

From now onwards, we will consider that we can construct a probability space  $(\Omega, \mathcal{F}, \wp)$  and a white noise  $W$  on  $\mathbb{R}^d$ . Although the specifics of this structure are extremely complex, it is not necessary to examine them here. For a fixed probability space  $(\Omega, \mathcal{F}, \wp)$  and a white noise function  $W$ , let us focus on subset  $[0, T] \subseteq \mathbb{R}$  for some fixed  $T > 0$ . We now define Brownian motion, from a white noise, in the following manner:

**Definition 3.2**

For any given white noise  $W(t)$ , Brownian motion is considered a stochastic process  $\{B(t)\}_{t \in [0, T]}$  defined from the white noise as  $\{B(t)\} = W((0, t])$ . It satisfies the following properties:

- a)  $B(t, \omega) = 0$  at  $t = 0$ ; defines the position of the particle at the arbitrarily chosen initial time ( $t = 0$ ) and are continuous and non-differentiable function of  $t$  for  $t \geq 0$ .
- b) The increments of Brownian motion are independent and are normally distributed with mean zero and variance  $(t_{i+1} - t_i)$ , i.e.;  
 $B(t_1, \omega), \{B(t_2, \omega) - B(t_1, \omega)\}, \dots \dots \dots \{B(t_n, \omega) - B(t_{n-1}, \omega)\}$  are independent for all  $0 \leq t_1 < t_2 < \dots \dots \dots < t_n$  and  $E\{B(t_i, \omega)\} = 0$ , and  
 $Var\{B(t_{i+1}, \omega) - B(t_i, \omega)\} = t_{i+1} - t_i$
- c) The stochastic variation of  $B(t, \omega)$  at time  $t$  is determined by Gaussian probability distribution which has a zero mean for all values of  $t$ .
- d) The co-variance of the Brownian motion is given by,  
 $E\{B(t_i, \omega)B(t_j, \omega)\} = \min(t_i, t_j)$
- e) The generalised Wiener process is given by  $E\{B(t_i, \omega)B(t_j, \omega)\} = \int_0^{\min(t_i, t_j)} q(\tau) d\tau$ ; where  $q(\tau)$  is the covariance kernel that determines the correlation between the stochastic process values at different times. In the case of a perfectly positive correlation  $q(\tau) = 1$ , the process is a standard Wiener process.

**Remark 3.1**

A few other important properties of Brownian motion are tricky and elude us:

- Are the sample paths of Brownian motion  $B(t)$  continuous? Generally, the answer is no, but, a stochastic process with continuous sample paths can be constructed by matching the finite-dimensional distributions of the stochastic process with those of Brownian motion. Durrett (2010) provides detailed proof and explains the Kolmogorov-Chentsov theorem in his textbook on random and stochastic processes.

- Is there any relationship between Brownian motion and a random walk? The answer is, yes. Donsker theorem (van der Vaart & Wellner, 1996) states that Brownian motion is the limiting case of a sequence of suitably scaled random walks.
- Ordinary calculus differs from stochastic calculus.

### Lemma 3.1

Brownian motion  $B(t)$  has a quadratic variation equal to  $t$  up to time  $t \in [0, T]$  and a total variation equal to  $\infty$ , both holding  $\mathcal{P}$ -almost surely. Using this lemma, we know that  $\int_0^t \{dB(t)\}^2 = t$ .

On differentiation, we have  $\{dB(t)\}^2 = dt$ . While there is no clear significance to this equation mathematically, it is an important equation for stochastic calculus. For example, while smoothening the functions in ordinary calculus, for a very small step size  $h$ , the term  $h^n \rightarrow 0$  is important for some fixed degree of interest  $d$  and for some integer  $n \leq d$ . Also, the same term  $h^n \rightarrow 0$  is negligible for  $n > d$ .

This process is easy in ordinary calculus as  $n$  is integer valued. However, in stochastic calculus there could be the terms involving half-integer values such as  $dB(t) = dt^{1/2}$ .

Thus, one important conclusion about Brownian motion is that its non-zero quadratic variation compels us to adopt a completely different viewpoint while deciding between negligible and important terms.

## 3.2 Stochastic integration and Itô's formula

To deal with stochastic processes, it is necessary to understand the appropriate stochastic integration and its existence conditions. As long as the functions are of finite variation, the classical Lebesgue-Stieltjes integrals serve the best. In the case of randomness, the statistical behaviour of the functions like noise cannot be precisely predicted and none of its path is differentiable at any instant. In such situations, the Itô definition of integration helps to define such integrals. Itô introduced the concept of a stochastic integral based on a standard Brownian motion (Klebaner, 2005). It follows the martingale property. Later on, it was generalised to local martingale and semi-martingale. When the future expected value of the process  $\{X(t)\}$  is equal to  $X(t)$ , the stochastic process  $\{X(t)\}$  is martingale – that is,

$$E\{X(t + \Delta t)/I_t\} = X(t) \text{ converges almost surely;}$$

where  $I_t$  is the information about  $\{X(t)\}$  up to the time  $t$ .

Let  $\{X(t)\}$  be a continuous adapted random process for  $0 \leq t \leq T$ .

For any partition  $\Delta_T^n = \{0 = t_0 < t_1 < \dots < t_n = T\}$ ,

The Itô integral of the process for a realisation  $\omega$  is defined as,

$$\begin{aligned} I\{X(t, \omega)\} &= \int_0^T X(t, \omega) dB(t, \omega) \\ &= \sum_0^{n-1} C_i (B(t_{i+1}) - B(t_i)) \end{aligned}$$

where  $X(t, \omega) = C_i$ , for  $t_i < t < t_{i+1}$ ,  $i = 0, 1, \dots, n-1$ .

In a more general way,

$$\begin{aligned} I\{X(t, \omega)\} &= \int_0^T X(t, \omega) dB(t, \omega) \\ &= \sum_0^{n-1} X(t_i^n, \omega) (B(t_{i+1}^n, \omega) - B(t_i^n, \omega)); \end{aligned} \quad (3.1)$$

and this sum converges in probability.

Let us denote  $I\{X(t, \omega)\}$  as  $I_T(X)$  in short notation to define a few properties of the Itô integral.

### Lemma 3.2

Let  $X$  and  $Y$  be any elementary processes and  $\alpha, \beta \in \mathbb{R}$  be any reals. The Itô integral  $I_T$  satisfies the following properties:

- (3.2.1)  $I_T(\alpha X + \beta Y) = \alpha I_T(X) + \beta I_T(Y)$  (Linearity)
- (3.2.2)  $E[I_T(X)] = 0$  (Mean Zero)
- (3.2.3)  $\|I_T(X)\|_{\mathcal{L}^2(\Omega)} = \|X\|_{\mathcal{L}^2([0, T] \times \Omega)}$  (Itô Isometry)
- (3.2.4)  $\{I_t(X)\}_t$  is a martingale with respect to the filtration  $\{\mathcal{F}_t^B\}_t$  (martingale)
- (3.2.5)  $\{I_t(X)\}_t$  is  $\mathcal{P}$ -almost surely continuous in  $t$ . (Continuity)

In order to Itô integrate we must also place some restrictions on the measurability of the stochastic processes. While (Jacka & Oksendal, 1987) resolved this issue by considering  $f$  to be adapted, we still need to be able to integrate  $f$  on the space  $([0, T] \times \Omega \otimes \mathcal{F})$ . When (Lalley, 2012) modified it, in his proof, the collection of stochastic processes became cumbersome.

### 3.3 The Stratonovich integral

The Stratonovich integral of two Itô processes  $X(t)$  and  $Y(t)$  is defined as:

$$\int_{t_1}^{t_2} X(t) \circ dY(t) = \int_{t_1}^{t_2} X(t) dY(t) + \frac{1}{2} \int_{t_1}^{t_2} dX(t) dY(t) \quad (3.2)$$

In stochastic differential form, this integral can be written as:

$$X(t) \circ dY(t) = X(t) dY(t) + \frac{1}{2} dX(t) dY(t) \quad (3.3)$$

For a test function  $f(x, t)$ , having continuous partial derivatives  $\frac{\partial f}{\partial x}$ ,  $\frac{\partial f}{\partial t}$  and  $\frac{\partial^2 f}{\partial x^2}$ , the Stratonovich integral can also be defined using Hida's white noise theory (Accardi et al., 2001).

### 3.4 The Skorohod integral

For non-adapted processes, Anatoliy Skorohod introduced the Skorohod integral ("The Skorohod Integral," 2009) as an extension of the Itô integral. Let us consider a measurable stochastic process  $Z(t)$ ,  $t \in [0, T]$ , such that the expectation of the random variable  $Z(t)$  is  $E[Z^2(t)] < \infty$  and  $Z(t)$  is  $\mathcal{F}_t$ -measurable. Let Wiener-Itô chaos expansion of  $Z(t)$  be,

$$Z(t) = \sum_{j=0}^{\infty} I_j(f_j, t) = \sum_{j=0}^{\infty} I_j(f_j(\cdot, t)) \quad (3.4)$$

Then, the Skorohod integral of  $Z(t)$  is defined as,

$$\delta(Z) := \int_0^t Z(t) \delta W(t) := \sum_{j=0}^{\infty} I_{j+1}(\tilde{f}_j) \quad (3.5)$$

where  $\tilde{f}_j$  are the symmetric functions for all  $j = 1, 2, \dots$  derived from  $f_j(\cdot, t)$  for all  $j = 1, 2, \dots$  and is convergent in  $\mathcal{L}^2(\emptyset)$ . This integral is related to the Malliavin derivative that is the backbone of the stochastic calculus of variations ("Malliavin Calculus for Lévy Processes with Applications to Finance," 2009).

#### Definition 3.3

An Itô SDE similar to an integral equation. The integral equation form of an Itô SDE for a stochastic process  $X(t)$  on the interval  $[0, T]$  is given as,

$$X(t) = X_0 + \int_0^t \mu(\tau, X(\tau)) d\tau + \int_0^t \sigma(\tau, X(\tau)) dB(\tau) \quad (3.6)$$

Here, the first term of the integral is the drift term, the second term is the diffusion, and  $X_0 \in \mathbb{R}$  is the initial condition. Feasible conditions on  $\mu$ ,  $\sigma$  and  $X_0$  will help in determining the solution for the above SDE. Now we will explain what we mean for a stochastic process to be a solution to stochastic ordinary differential (SODE) equation (3.6).

Let us recall our motivating example from Chapter 1 (Section 1.3.1). We are interested in finding the conditions for parameters  $\mu$ ,  $\sigma$  and  $\mu_0$  for which equation (1.11) has a solution, probably unique.

Also, for a stochastic process, it is crucial to know what it means to have a solution and/or the kind of solution the modeller is interested in.

### Definition 3.4 Strong solution

An SODE solution is said to be strong if an explicit map from Brownian motion to the stochastic process exists. However, this may not be possible for some complex physical systems and the modeller needs to find weak solutions which satisfy the conditions of the system under study. The following theorem is helpful in setting up the conditions for the existence and uniqueness of strong solutions.

### Theorem 3.1

An SDE defined by equation (1.11) in Chapter 1 has a strong solution over the interval  $[0, T]$  if  $\mu(t, x)$  and  $\sigma(t, x)$  satisfies the following conditions:

- (i)  $|\mu(t, x_1) - \mu(t, x_2)| + |\sigma(t, x_1) - \sigma(t, x_2)| \leq C_1|x_1 - x_2|$
- (ii)  $|\mu(t, x)| + |\sigma(t, x)| \leq C_2(1 + |x|)$

where  $\mu(t, x): [0, T] \times \mathbb{R}, \sigma(t, x): [0, T] \times \mathbb{R}, \mu_0 \in \mathbb{R}$  and is deterministic. For a SPDE given by,

$$dX + (-\Delta)(X)dt = f(X)dt + g(X)dW$$

with Hilbert-valued (H-valued) stochastic Wiener process  $W$ , a predictable H-valued process  $X(t): t \in [0, T]$  is considered strong solution if,

$$X(t) = x_0 + \int_0^t [\Delta X(\tau) + f(X(\tau))]d\tau + \int_0^t g(X(\tau)) dW\tau, \forall t \in [0, T] \quad (3.7)$$

### Definition 3.5 Weak solution

For equation (3.8), a predictable H-valued process  $X(t): t \in [0, T]$  is considered a weak solution if,

$$\begin{aligned} \langle X(t), Y \rangle &= \langle x_0, Y \rangle + \int_0^t [-\langle X(\tau), -\Delta Y \rangle + \langle f(X(\tau)), Y \rangle] d\tau + \\ &\int_0^t \langle g(X(\tau)) dW\tau, Y \rangle, \forall t \in [0, T], Y \in H_0^1 \cap H^2 \end{aligned} \quad (3.8)$$

### 3.5 Computational techniques

#### 3.5.1 Direct integration techniques

In stochastic analysis, quantities of interest can be represented by the expected value of certain functionals of the dependent variable; say,  $y$  and is denoted as  $E(f(y(\xi); \xi))$ . The value of this expectation is defined in the form of integrals and the need to compute certain integrals, with respect to the probability measure  $P_\xi$  as –

$$E(f) = \int_{\mathbb{R}} f(y(x); x) dP_\xi(x) = \int_{\mathbb{R}} f(y(x); x) p_\xi(x) dx \quad (3.9)$$

where  $p(\xi)$  is the probability density function of  $\xi$ . There are several numerical integration techniques available. More specifically, these integration strategies have the formulation that leads to the following estimation:

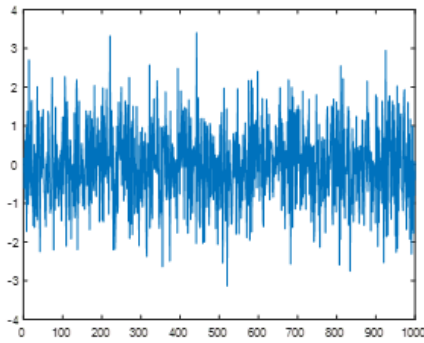
$$E(f) \approx Q_i(f) = \sum_{i=1}^n f(y(x_i); x_i) w_i \quad (3.10)$$

where the  $x_i$  are the points and  $w_i \in \mathbb{R}$  are the weights of integration. The model response is then evaluated for possible outcomes  $\xi = x_i$  of the selected random variables. Finally, it requires the solution of a system having  $n$  uncoupled deterministic equations

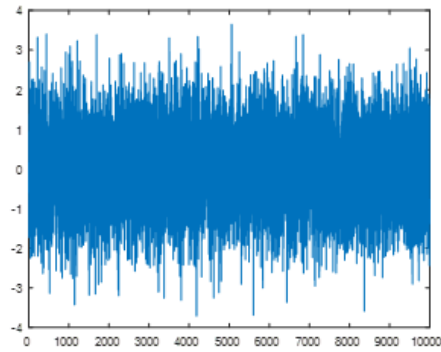
$$\mathcal{L}(y(x_i); x_i) = b(x_i), i = 1, 2, \dots, \dots, n \quad (3.11)$$

### 3.5.2 Monte Carlo (MC) methods

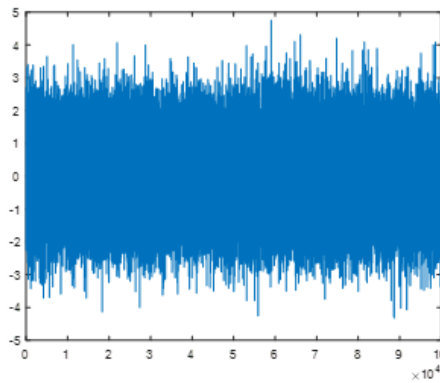
MC methods approximate the outcomes based on random sampling and the law of inertia of large numbers.



(a) For 1000 sample points: mean = 1.006,  
MC integration error = 0.0883,  
statistical error = 0.0271



(b) For  $10^4$  sample points, mean = 0.985,  
MC integration error = 0.0271,  
statistical error = 0.0271



(c) For  $10^5$  sample points: mean = 0.9976, MC integration error = 0.0088,  
statistical error = 0.027

**Figure 3.1 Generation of a Gaussian random variate (GRV) for different sample sizes and a comparison with MC integration error and the mean.**

Practically, these random samples are pseudo random samples of the basic random variable  $\xi$ . As shown in Figure 3.1, an integration error is defined by a Gaussian Random Variable (GRV).

A basic MC estimator of an integral of a quantity of interest (expectation), say  $\mu$ , is given by,

$$\text{Mean } (\mu) = \int_{\mathbb{R}} f(x) p(x) dx = E[f(x)] \approx \frac{1}{n} \sum_{i=1}^n f(x_i), \quad (3.12)$$

the variance of the estimator is,

$$\text{var}(\mu) = \frac{\text{var}[f(x)]}{n},$$

The MC estimator does not work accurately for large variance. Statistical errors in the confidence interval can be too large to believe that the interval is valid.

**Remark 3.2 Variance reduction**

Standard deviation of the estimator equals  $\frac{\sigma_t}{\sqrt{n}}$ . For small confidence interval we can reduce the variance. For example:  $\text{var}[f(x)] = 1$ , and a smaller confidence interval is required say  $10^{-2}$ ,

Thus,

$$\text{var}[f(x)] = 10^{-4}(n) \quad (3.13)$$

Thus, we need  $n = 10^4$  sample points. Numerous techniques based on the control variate such as importance sampling, stratified sampling, and anthetic variates are available in literature. Zhang and Karniadakis (2017) used different reduction methods to avoid generating a large number of sample points.

**Remark 3.3**

The convergence rate of the basic MC estimator for a one-dimensional integral is,  $O\left(\frac{1}{\sqrt{n}}\right)$ . While this convergence is free from stochastic dimensions, it is slow. The positive side of this independence confirms the applicability of MC methods in problems with high-stochastic dimensions.

**3.5.3 Quasi Monte Carlo (QMC) methods**

Computing mathematical models using MC methods is expensive due to the requirement of a large number of sample points. One solution is to use variance reduction techniques. An error in these approaches is proportional to  $\frac{1}{n}$  as compared to  $\frac{1}{\sqrt{n}}$  as in the MC methods. Kroese et al. (2011) have provided a detailed study of these techniques.

**Remark 3.4 Low discrepancy sequence**

Consider an arbitrary set. If the proportion of points in a sequence of this set is near to the proportion to the measures of this set, the discrepancy of the sequence is low. Some of these sequences are shown in Figure 3.2.

Let us say we want to estimate  $E(f_1)$  and we have a control variate  $f_2$  with known expectation. It is highly correlated with  $f_1$ . In this situation, the following unbiased estimator for  $E(f_1)$ , based on  $n$  independent samples  $\xi^{(i)}, i = 1, 2, \dots, n$ , can be applied:

$$\frac{1}{n} \sum_{i=1}^n \{f_1(\xi^{(i)}) - \lambda(f_2(\xi^{(i)}) - E[f_2])\} \quad (3.14)$$

where  $\rho$  is the correlation coefficient between  $f_1$  and  $f_2$  and  $\lambda = \rho \sqrt{\frac{\text{var}(f_1)}{\text{var}(f_2)}}$ . Computing mathematical models using MC methods is expensive due to the requirement of a large number of sample points.

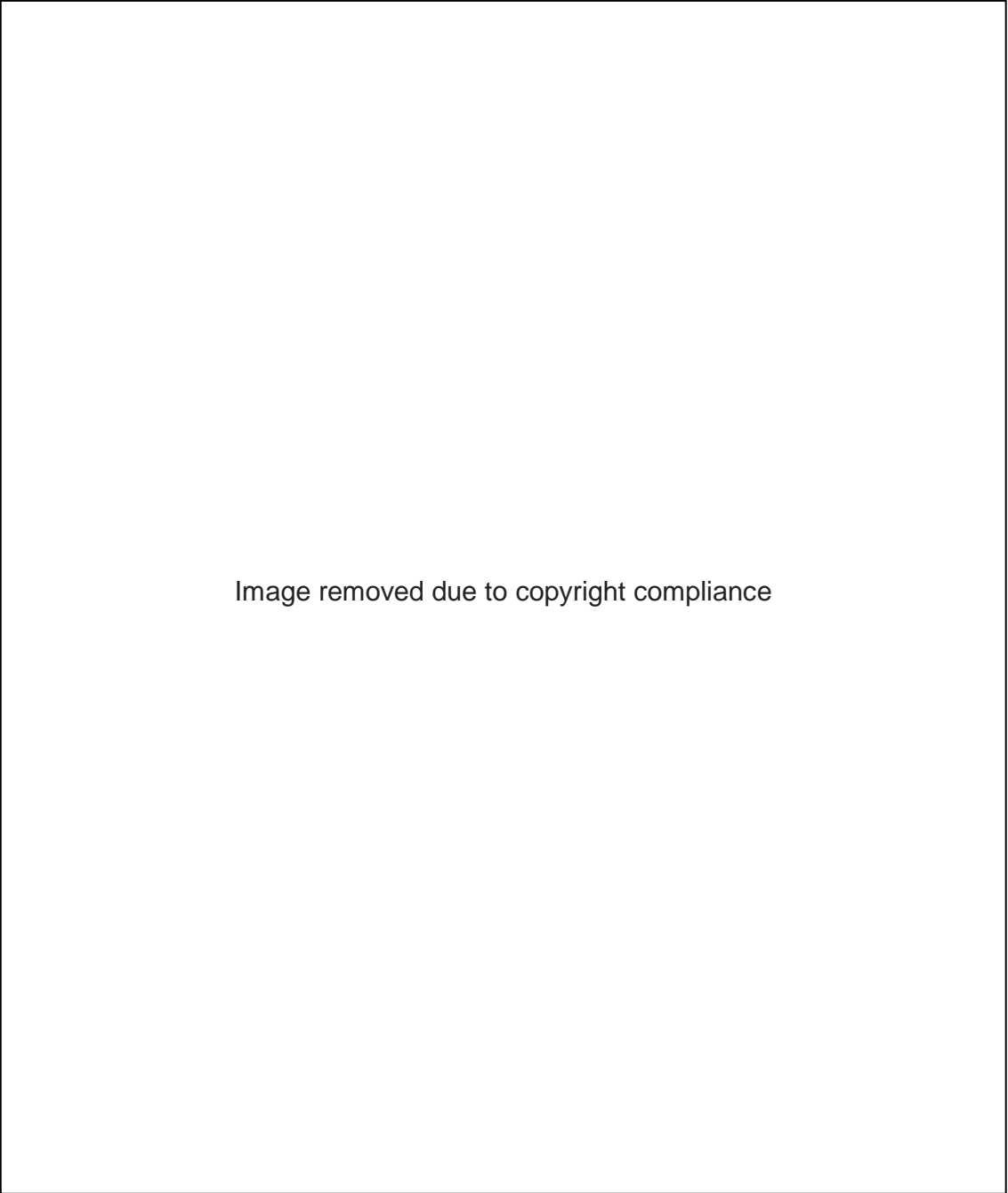


Image removed due to copyright compliance

**Figure 3.2** Quasi Random sequences. Quasi-random sequences are used in variance reduction techniques. The word ‘quasi’ signifies that the values of a low-discrepancy sequence is neither random nor pseudo-random, but share some of the characteristics of both of the random variables. This low-discrepancy property is an added benefit of QMC methods. Using a control variate helps to reduce MC variance (Glasserman, 2003), <https://link.springer.com/book/10.1007/978-0-387-21617-1>

The classical quadrature rule can also be used to evaluate integrals. Some common rules are the Gauss quadrature, Gauss-Hermite quadrature, and Clenshaw Curtis (Elvira et al., 2019; Pütz et al., 2022).

### 3.5.4 Gauss quadrature

For a function  $f(x)$  which has continuous derivatives (smooth enough) in an interval  $[a, b]$ , the Gauss quadrature rule for  $f(x)$  with weight function  $w(x)$  is given as:

$$\int_a^b f(x) w(x) dx \approx \sum_{k=0}^n c_k f(x_k) \quad (3.15)$$

The weight function  $w(x)$  possesses the following conditions:

- (i)  $w(x) \geq 0, \forall x \in (a, b)$
- (ii)  $\int_a^b w(x) dx > 0$
- (iii)  $\int_a^b x^k w(x) dx$  is well-defined for  $k = 0, 1, 2, \dots$

If the polynomial exactness of equation (3.15) is  $(2n + 1)$ , then the quadrature rule is called a Gauss quadrature.

### 3.5.5 Gauss-Hermite quadrature

For a sufficiently smooth function  $f(x), x \in \mathbb{R}$ , the Gauss Hermite quadrature is,

$$E(f(\xi)) = \frac{1}{\sqrt{2\pi}} \int_{\mathbb{R}} f(x) e^{-x^2/2} dx \approx \sum_{i=1}^n f(x_i) w_i \quad (3.16)$$

where  $\xi_i$  is a stochastic Gaussian random variable,  $w_i$ 's are the assign weights given by,

$$w_i = \frac{n!}{n^2 [H_{n-1}(x_i)]^2}$$

and  $x_i$  is the  $n$ th Hermite polynomial given by,

$$H_n(x) = (-1)^n e^{x^2/2} \frac{d^n}{dx^n} (e^{-x^2/2}) \quad (3.17)$$

## 3.6 Numerical analysis of stochastic differential equations

The concepts of the numerical analysis of SDEs help us to understand how the solution to a particular SDE can be simulated on a computer while ensuring that the results are somewhat similar to the real answer. We focus on one-step approximations for a discrete, fixed time, 1-dimensional SDE in order to keep things simple. There are two main numerical schemes for solving SDEs: the Euler-Maruyama scheme and the Milstein scheme.

### 3.6.1 The Euler-Maruyama (E-M) method

This numerical scheme is the generalisation of Euler's method for ODEs to solve SODEs. Consider an Itô SDE (Kloeden & Platen, 1992) of the form,

$$dS_t = \mu(t, S_t)dt + \sigma(t, S_t)dW_t \quad (3.18)$$

where  $W_t$  is a standard Wiener process on the interval  $[0, T]$ . To solve this equation numerically, we discretise the time interval with an  $h$  (a sufficiently small) step size. Symbolically, equation (3.18) can be written as,

$$S_t = S_{t_0} + \int_{t_0}^t \mu(t, S_t)dt + \int_{t_0}^t \sigma(t, S_t)dW_t \quad (3.19)$$

the E-M approximation is calculated using the Itô-Taylor expansion.

The first integral on the right-hand side of equation (3.19), using an Itô-Taylor expansion, is,

$$\int_{t_0}^t \mu(t, S_t)dt = \int_{t_0}^t \mu(t_0 + (t - t_0), S_0 + S(t) - S_0)dt \quad (3.20)$$

$$= h\mu(t_0, S_0) + O(h^{3/2}) \quad (3.22)$$

or simply,

$$S_{n+1} = S_n + \mu(t_n, S_n) \int_{t_n}^{t_{n+1}} d\tau + \sigma(t_n, S_n) \int_{t_n}^{t_{n+1}} dW_\tau \quad (3.22)$$

where  $n = 0, 1, \dots, N - 1$  for  $t_0 < t_1 < \dots < t = T$  and  $N \in \mathbb{N}$ .

Thus, for an  $m$ -dimensional SDE,  $S^h = (S_1^h, S_2^h, \dots, S_m^h)$  defined by Mackevičius (2011), is written as follows:

$$S_{t_{n+1}}^h = S_{t_n}^h + h \mu(t_n, S_{t_n}^h) + \sigma(t_n, S_{t_n}^h) \Delta B_n \quad (3.23)$$

with

$$\Delta B_n = B_{t_{n+1}} - B_{t_n}, t_n = nh$$

$\Delta B_n$  is the sequence of identically independent Gaussian random variables having a zero mean and standard deviation,  $h$ .

Equation (3.23) can be rewritten as,

$$S_{t_{n+1}} - S_{t_n} = h \mu(t_n, S_{t_n}^h) + \sqrt{h} \sigma(t_n, S_{t_n}^h) B_n + O(h) \quad (3.24)$$

The order condition for  $h$  judges the quality of the numerical scheme. Consequently, the variation in step size  $h$  defines the convergence rate of the numerical scheme. In numerical approximation, based on model requirements, the two most-commonly-used definitions of convergence are strong and weak convergence.

### 3.6.2 The Milstein method

This scheme was developed by Milstein. The order of convergence for this method is different from the E-M scheme. For equation (3.18), this scheme has a strong and weak convergence of order 1. The Milstein scheme for equation (3.18), given by Kloeden and Platen (1992), is given as follows:

$$\begin{aligned} S_{t_{n+1}} - S_{t_n} &= h \mu(t_n, S_{t_n}^h) + \sqrt{h} \sigma(t_n, S_{t_n}^h) B_n \\ &+ \sigma(t_n, S_{t_n}^h) \frac{\partial \sigma(t_n, S_{t_n}^h)}{\partial S} \left(\frac{1}{2} h\right) (B_n^2 - 1) + O(h^{3/2}) \end{aligned} \quad (3.25)$$

### 3.6.3 Strong convergence

For an SDE, given by equation (3.18), a numerical scheme is said to be strongly convergent of order  $p$  at time  $T = nh$  if,

$$\sup_{t \leq T} E |S_t^h - S_n| = O(h^p) \quad (3.26)$$

where  $S_t^h$  and  $S_n$  are the solutions to the different SDE obtained using the same Wiener process.

Hence, a pathwise convergence of solutions is required for a numerical scheme to have strong convergence.

### 3.6.4 Weak convergence

The notion of weak convergence comes up with the voluntarily requirement of pathwise convergence. Weak convergence eases some of the regularity conditions on solution and is helpful in those models where the modeller is only interested in calculating the statistical moments such as mean, variance, and kurtosis.

A numerical scheme is said to be weakly convergent of order  $q$  at time  $T = nh$  if,

$$\sup_{t \leq T} E [f(S_t^h)] - E[f(S_n)] = O(h^q) \quad (3.27)$$

Thus, for SDE equation (3.18), an E-M scheme is strongly convergent to the order of  $\frac{1}{2}$  and weakly convergent to the order of 1.

### 3.6.5 Numerical example

We shall apply the E-M method to a simple population growth model which has an exact solution. Similar to equation (3.18), the population growth model equation of a species ( $S$ ) in time  $t$  years is written as:

$$dS_t = \alpha S_t dt + \beta S_t dW_t \quad (3.28)$$

where  $\alpha$  and  $\beta$  are the model parameters. The exact solution of this equation, using Itô's formula, is given by:

$$S_t = S_0 e^{\left(\left(\alpha - \frac{\beta^2}{2}\right)t + \beta W_t\right)} \quad (3.29)$$

Simulation (three runs) of the population growth model for an exact solution, with parameter values  $\alpha = 0.35$  and  $\beta = 0.25$  is shown in Figure 3.3.

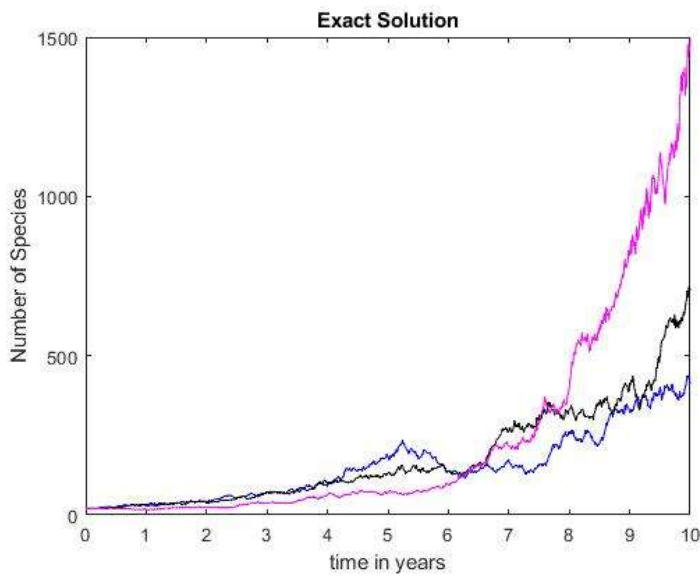


**Figure 3.3** Exact solution for population growth model

*Note.*  $\alpha = 0.35$ ,  $\beta = 0.25$ . Initial population is assumed to be  $S_0 = 20$  and  $\Delta t = 0.01$  with the same parameter values for all computations, the E-M approximation is also plotted for the three runs for comparison in Figure 3.4.

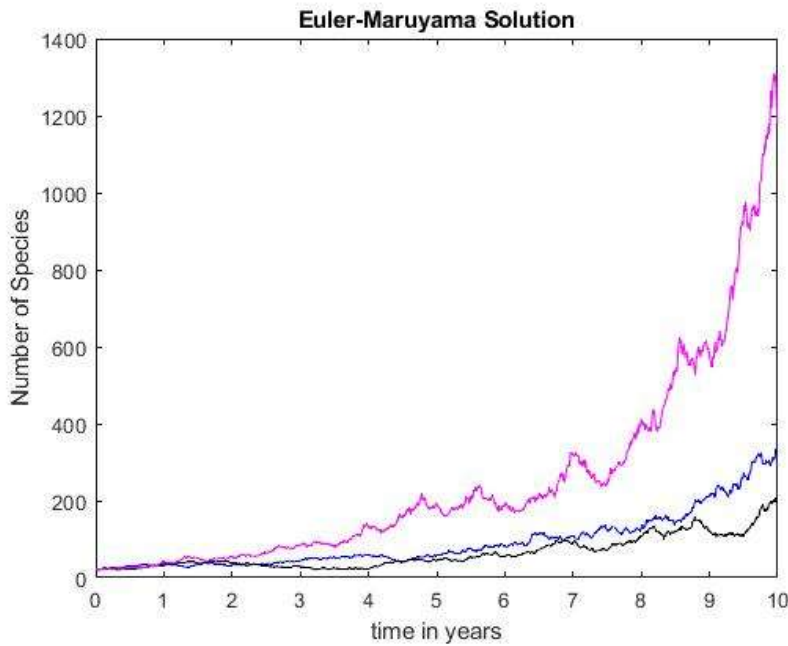


**Figure 3.4 Euler-Maruyama approximation for population growth model**

Note.  $\alpha = 0.35, \beta = 0.25$ . The initial population is assumed to be  $S_0 = 20$  and  $\Delta t = 0.01$

The simulation results are different for the same parameter values because of the stochastic nature of the model. Thus, it is a good idea to run the simulation numerous times and choose an average value to see how the given system behaves (Figure 3.5).

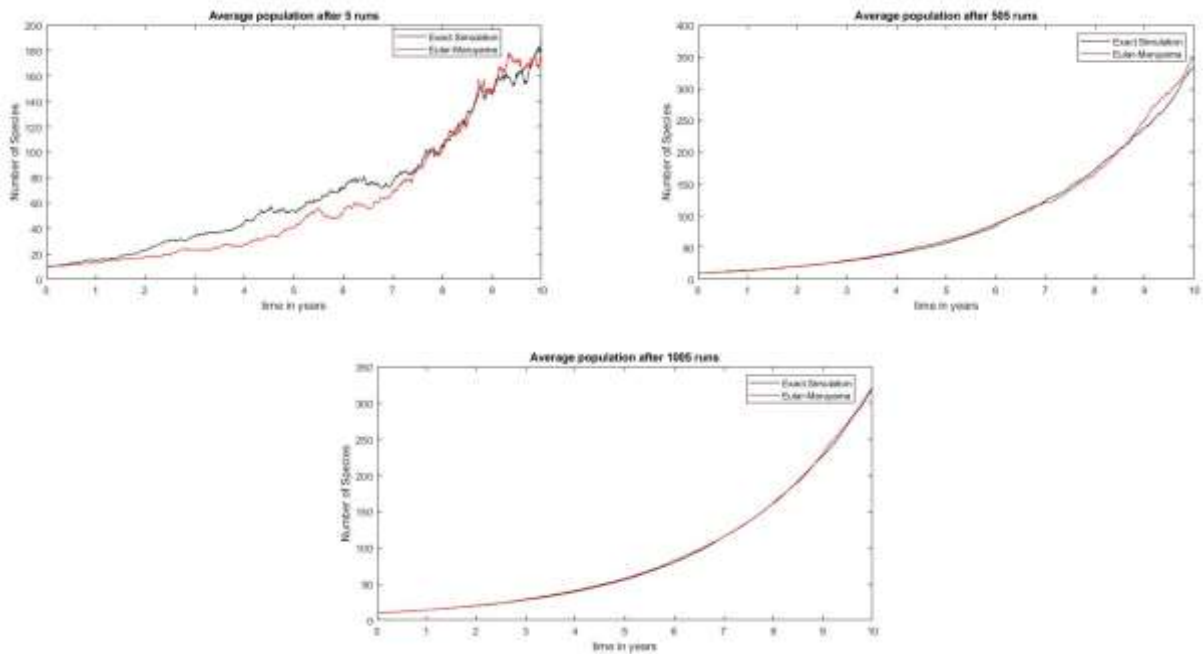


**Figure 3.5 Simulation results for the Exact and Euler-Maruyama approximation after a number of runs.**

*Note.* The first graph on the top left corner is the average population growth after five simulations. The results from the E-M scheme differ from the exact solution. However, as the simulation runs are increased, the E-M approximations coincide with the actual solution.

### 3.6.6 A bounded Euler-Maruyama method

We shall consider the same SDE defined in equation (3.28)

$$dX(t) = \alpha X(t)dt + \beta X(t)dW(t), X(0) = x_0 \quad (3.30)$$

where  $X(t) \in \mathbb{R}^n$  for all  $t \in (0, T)$ . Also,  $W(t)$  is a  $d$ - dimensional Brownian motion starting at 0,  $\alpha: \mathbb{R}^n \rightarrow \mathbb{R}^{n \times d}$ ,  $x_0$  is an  $\mathcal{F}_0$  – measurable and independent of  $W(t)$ .

In this section, we assume that first- and higher-order moments of  $x_0$  are finite and that the solution is to be approximated under the local Lipschitz condition.

#### The Local Lipschitz condition

For some finite  $R$ , there exists a positive constant  $k$ , such that for all  $x, y \in \mathbb{R}^n$  with  $\|x\|, \|y\| \leq R$ ,

$$\|\alpha(x) - \alpha(y)\| + \|\beta(x) - \beta(y)\| \leq k(R)\|x - y\| \quad (3.31)$$

Approximating equation (3.31) in continuous time domain, we have

$$Y(t) = Y_0 + \int_0^t \alpha(Y(\tau))d\tau + \int_0^t \beta(Y(\tau))dW(\tau) \quad (3.32)$$

where  $Y(t) = Y_i$  for  $t \in (t_i, t_{i+1})$ . In discrete time domain, we have

$$Y(t) = Y_k + \alpha(Y_i)(t - t_i) + \beta(Y_i)(W(t) - W(t_i)), \forall t \in (t_i, t_{i+1}). \quad (3.33)$$

#### Theorem 3.2 (Higham et al., 2007)

If  $\alpha$  and  $\beta$ , as defined in equation (3.30), satisfy the local Lipschitz condition, and for some

$c \geq 3$ , there exists a constant  $C$  such that,

$$E\left[\sup_{0 \leq t \leq T} \|Y(t)\|^c\right] \leq C E\left[\sup_{0 \leq t \leq T} \|X(t)\|^c\right] \leq C \quad (3.34)$$

then equation (3.32) satisfies the relation,

$$\lim_{\Delta t \rightarrow 0} E\left[\sup_{0 \leq t \leq T} \|Y(t) - X(t)\|^2\right] = 0 \quad (3.35)$$

We consider  $\beta = (\beta_1, \beta_2, \dots, \beta_d)$  as a column vector of the matrix  $\beta$ , i.e.,  $\beta_i$ 's,  $1 \leq i \leq d$ .

Also,  $W = (W^{(1)}, W^{(2)}, \dots, W^{(d)})$  is the  $d$  – dimensional Brownian motion. Then, equation (3.30) can be written as,

$$X(t) = x_0 + \int_0^t \alpha(x(\tau))d\tau + \sum_{i=1}^d \int_0^t \beta_i(x(\tau))dW^{(i)}(\tau), \forall t \in (0, T) \quad (3.36)$$

We are interested to see, “what happens if the derivative of drift coefficient  $\alpha$  grows continuously (assuming by polynomial order at least)”?

We still assume that  $\beta$  is globally Lipschitz continuous and  $\alpha$  is one-sided globally Lipschitz continuous. Thus, for a real number  $K > 0$ ,

$$\left. \begin{aligned} \|\alpha'(x)\| &\leq K(1 + \|x\|^K), \\ \|\beta(x) - \beta(y)\| &\leq K\|x - y\|, \\ \langle x - y, \alpha(x) - \alpha(y) \rangle &\leq K\|x - y\|^2 \end{aligned} \right\} \quad (3.37)$$

Hence, by mean value theorem for derivatives  $\alpha$  will also satisfy Theorem 3.2 and the numerical scheme converges strongly as long as all the conditions of equation (3.37) are satisfied.

However, the difficulty of finding the zeros of a nonlinear equation at each time step is computationally expensive. To resolve this problem, (Kloeden & Platen, 1992) proposed the bounded Euler scheme by defining some  $P_0 = x_0$  and binding the drift coefficient by a factor:  $1 + \|\alpha(P_m)\|\Delta t$ . Therefore, a bounded or a Tamed Euler approximation is given by,

$$P_{m+1} = P_m + \frac{\alpha(P_m)}{1 + \|\alpha(P_m)\|\Delta t} + \beta(P_m)\Delta W_m, 0 \leq m \leq N - 1 \quad (3.38)$$

Hence, the drift term will not generate large excursions and will be bounded by 1. Also, the numerical scheme will not explode because  $\beta$  is still globally Lipschitz continuous.

### 3.6.7 Numerical example

Let us solve equation (3.30) with a drift term, as locally Lipschitz continuous function  $\alpha(x) = x^3 - x^5$  and the diffusion term is  $\beta(x) = x$  and  $t \in (0,1)$ .  $\alpha(x)$  satisfies the condition of one-sided Lipschitz continuous function and grows with the polynomial Order. It can be seen from the graph (Figure 3.6) that the bounded Euler’s approximation has a strong convergence of order  $\frac{1}{2}$ .

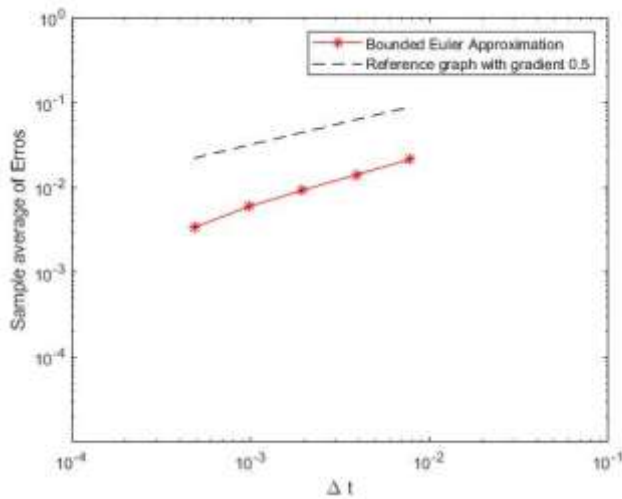


**Figure 3.6 Strong convergence of a bounded Euler scheme.**

*Note.* Graph is plotted for a total of five-time discretisation  $\Delta t = 2^{-8}, 2^{-9}, 2^{-10}, 2^{-11}$  and  $2^{-12}$ . We also stimulate  $1E4$  realisations for each discretisation. A log-log plot is used to show the error convergence with respect to the reference gradient 0.5, which shows that the Tamed/Bounded Euler scheme has a strong convergence (order  $\frac{1}{2}$ ) when the drift coefficient is growing linearly.

### 3.7 Linear stability of the Euler-Maruyama and Milstein methods

Several stability theories for deterministic ODEs have been established in the literature with a small step size,  $\Delta t$ , and over a finite interval. The long-term behaviour of the stochastic models, when  $t \rightarrow \infty$ , is also of great interest. The idea here is to apply a numerical method for a specific problem with some qualitative characteristics. The model must be capable of reproducing this feature for other types of problems.

Here we consider equation (3.30) again with same parameters,  $\alpha$  and  $\beta$ , but with  $\alpha, \beta \in \mathbb{C}$ . When  $\beta = 0$  and  $x_0$  is a constant, equation (3.30) is a deterministic linear equation  $\frac{dX(t)}{dt} = \alpha X(t)$ ,  $\alpha \in \mathbb{C}$  and has an exact solution  $x_0 e^{\alpha t}$ .

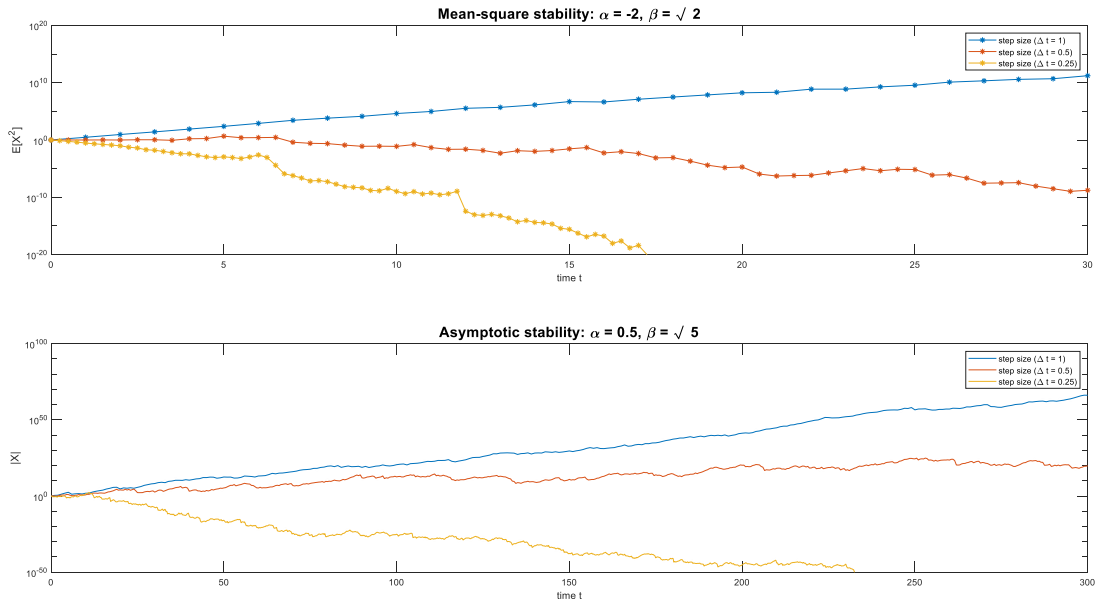


**Figure 3.7 Mean-square and asymptotic stability for the Euler-Maruyama method.**

*Note.* For mean-square stability, the parameter set values are  $x_0 = 1, \alpha = -2, \beta = \sqrt{2}$ . These parameter values satisfy equation (3.39), so the solution is mean-square stable. For numerical approximation using the E-M method,  $5 \times 10^4$  discrete Brownian paths are used for three different time-intervals:  $\Delta t = 1, 0.5, 0.25$ . Only the simulation for smaller step size,  $\Delta t = 0.25$ , satisfies equation (3.39) for which the curve converges to zero. The graph is plotted on a logarithmic scale on a vertical axis. To analyse the behaviour of the solution completely, the sample size of the Brownian motion can be increased. For asymptotic stability, the parameter set has the following values:  $x_0 = 1, \alpha = 0.5, \beta = \sqrt{5}$ . These values show that while the solution set is asymptotically stable (equation (3.40)), it is not stable in the mean-square sense (equation (3.39)). A single Brownian path is used for E-M approximation so we computed over  $[0, 300]$ . In this case also, only for small step size,  $\Delta t = 0.25$ , the solution converges to zero. For  $\Delta t = 0.5$  and  $\Delta t = 1$ , the solution curve increases.

For an initial value  $x_0$ , if  $\lim_{t \rightarrow \infty} X(t) = 0$ , we consider it as a stability condition. However, to apply this idea in the case of stochastic equations, we need to define the stability term because randomness can be in several directions. Furthermore, their norms are not typically identical. In the stochastic sense, we can rely on two measures of stability known as mean-square stability and asymptotic stability (here the assumption is that  $x_0 \neq 0$  with 100% certainty, i.e.,  $P(X) = 1$ ).

Thus, the solution of equation (3.30), as given by equation (3.36), satisfies the following conditions of stability:

$$\lim E [X(t)^2] = 0 \Leftrightarrow R\{\alpha\} + \frac{1}{2}|\beta|^2 < 0 \quad (3.39)$$

$$\lim_{t \rightarrow \infty} X(t) = 0, \text{ with probability } 1 \Leftrightarrow R\left\{\alpha - \frac{1}{2}|\beta|^2\right\} < 0 \quad (3.40)$$

The left-hand sides of equation (3.39) and equation (3.40) characterise the mean-square and asymptotic stability in terms of parameters  $\alpha$  and  $\beta$  and shown in Figure 3.7. It is also clear from the two equations above that if equation (3.30) is mean-square stable, then asymptotic stability is obvious. However, the reverse is not true.

### Remark 3.5

Suppose equation (3.30) has mean-square stable and asymptotic stable solutions for a chosen set of parameters. Now we need to figure out what the appropriate step size ( $\Delta t$ ) is, so that the Euler-Maruyama solution is stable

We answered this question by using the property of expectation for the mean-square stable solution using E-M approximation as,

$$\lim_{t \rightarrow \infty} E (X_i^2) = 0 \Leftrightarrow |1 + \Delta t \alpha|^2 + \Delta t |\beta|^2 < 1 \quad (3.41)$$

For an asymptotic stable solution, applying the strong law of large numbers and an iterated logarithm,

$$\lim_{t \rightarrow \infty} X_i = 0, \text{ with } P(X_i)=1 \Leftrightarrow E \log |1 + \Delta t \alpha + \sqrt{\Delta t} \beta N(0,1)| \quad (3.42)$$

Figure 3.7 shows the mean-square and asymptotic stable solutions for different step sizes.

## 3.8 Summary

This chapter provides a basic introduction to stochastic differential equations (SDE) and stochastic partial differential equations (SPDE), which serve as the foundation for the following chapters. In this chapter, we have provided a comprehensive summary of the preliminary concepts related to SDEs and SPDEs. We begin by elucidating the basic definitions and characteristics of these stochastic equations, highlighting their importance in modelling systems influenced by stochastic processes.

This chapter provides an overview of the numerical methods used to solve these equations. We discussed several numerical aspects and strategies including Monte Carlo simulation, quadrature rules and Euler-Maruyama method.

In addition, the concept of convergence and stability in numerical solutions is also introduced. Convergence analysis is necessary to evaluate the accuracy of numerical methods, ensuring that the solutions approximate the real solutions of the underlying equations as the grid size or sample size

increases. On the other hand, considering stability is important to avoid quantitative instability that can make solutions unreliable.

Although these methods have been used for decades, these techniques have certain limitations (such as non-linear equations, sparsity in input variables, and the heterogeneity of the medium). Also, due to the stochastic nature of the model, the computational cost is likely to be quite high.

A convenient and alternative approach is to use spectral representation (Kim et al., 2007) such as the polynomial chaos expansion (PCE) methods (Wiener 1938; Cameron & Martin 1947), stochastic collocation (SC) methods (Kamrani 2016), and stochastic reduced order models (SROMs) (Ie Matre et al. 2002). Of all the spectral expansion techniques, PCE methods have received the most attention from the research community for three key reasons: i) these methods are fast and efficient, ii) these methods can handle different types of systems involving random variables of different distributions, iii) the estimation of second and higher-order moments, along with the ease of integration via non-intrusive approaches. PCE methods have a strong mathematical basis and functional relationships for statistical quantities such as mean, variance and density functions can be obtained from these representations.

In this following chapter, we explained the landscape of stochastic spectral methods, uncovering their central role in overcoming the challenges of uncertainty and chance in complex systems. We have explored the foundations of polynomial chaos expansion methods, recognizing their unique ability to quantify and exploit the dynamics of stochastic processes.

# Chapter 4

## Stochastic Spectral Methods

Stochastic spectral methods are at the forefront of contemporary scientific research due to their central role in solving complex problems characterized by uncertainty and randomness. In the fields of applied mathematics and computer science, these methods provide a powerful arsenal for modelling, simulating and analysing systems influenced by stochastic processes, thus ensure more robust and reliable decision making. These methods are not limited to any particular area. What sets stochastic spectral methods apart is their unique ability to analyse the complex interactions between deterministic and stochastic components in a given system, thereby paving the way for unprecedented insights into the behaviour of complex phenomena.

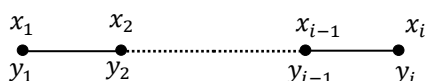
Spectral expansion theory is based on the principle of Weierstrass theorem which states that any continuous function within a finite closed interval can be approximated uniformly using polynomials. However, the existence of solutions must exist within the linear space of those polynomials of a specified degree. Stochastic spectral methods are at the forefront of contemporary scientific research due to their central role in solving complex problems characterized by uncertainty and randomness. In the fields of applied mathematics and computer science, these methods provide a powerful arsenal for modelling, simulating and analysing systems influenced by stochastic processes, thus ensure more robust and reliable decision making. These methods are not limited to any particular area. What sets stochastic spectral methods apart is their unique ability to analyse the complex interactions between deterministic and stochastic components in a given system, thereby paving the way for unprecedented insights into the behaviour of complex phenomena. In this context, it becomes increasingly important to deepen the principles and applications of stochastic spectral methods to exploit their full potential to solve real-world challenges.

### 4.1 Motivation

Our motivation for choosing spectral stochastic methods relates to the convergence rate and efficiency of these methods in working with differentiation formulae of higher orders.

We shall start with a simple example, by considering a uniform mesh  $\{x_1, x_2, \dots, x_n\}$  with the interval  $h$  such that  $x_{i+1} - x_i = h$ .

The  $n$ -data values corresponding to these  $x_i$ -values,  $1 \leq i \leq n$ , are  $y_i$ ,  $1 \leq i \leq n$ .



Now the question that needs an answer is, how can this data be used to approximate the derivatives (let us say of the first order)?

The obvious answer is using finite differences. If  $y_i$  denotes the approximate value of  $y$  at  $x_i$ , using Taylor's series expansion up to second order finite differences, we have

$$y(x+h) = y(x) + hy'(x) + \frac{h^2}{2!}y''(x) \quad (4.1)$$

and,

$$y(x-h) = y(x) - hy'(x) + \frac{h^2}{2!}y''(x) \quad (3.2)$$

Using these two equations, we get,

$$y'(x) = \frac{y(x+h) - y(x-h)}{2h} \quad (4.3)$$

at  $x = x_i$ ,

$$y'_i = \frac{y_{i+1} - y_{i-1}}{2h} \quad (4.4)$$

where  $y'_i = y'(x_i)$ ,  $y_{i+1} = y(x_{i+1})$  and  $y_{i-1} = y(x_{i-1})$

Now we can show that this approximation can also be achieved by interpolation using polynomials which will lead us to spectral methods:

For a unique polynomial  $P_i$  of degree  $\leq 2$ ,  $i = 1, 2, \dots, n$ , let  $P_i(x_{i-1}) = y_{i-1}$ ,  $P_i(x_i) = y_i$

and  $P_i(x_{i+1}) = y_{i+1}$ .

Set  $y_i = P'_i(x_i)$ . For a fixed  $i$ , the interpolant  $P_i$  can be written as-

$$P_i(x) = y_{i-1}C_{-1}(x) + y_iC_0(x) + y_{i+1}C_1(x) \quad (4.5)$$

where  $C_{-1}(x) = \frac{(x-x_i)(x-x_{i+1})}{2h^2}$ ,  $C_0(x) = \frac{-(x-x_{i-1})(x-x_{i+1})}{h^2}$  and  $C_1(x) = \frac{(x-x_{i-1})(x-x_i)}{2h^2}$

An approximation similar to equation (4.4), i.e.,  $y'_i$  is obtained by differentiating and evaluating equation (4.5) at  $x = x_i$ . The same concept can be implemented to approximate higher order derivatives.

This brief explanation shows that we can achieve finite order differences of a higher order using interpolation. This is the basis of spectral methods.

To make it clear, we plotted the 4<sup>th</sup> order finite differences for the function  $f(x) = e^{-\cos x}$  for the domain  $(-\pi, \pi)$ . Assuming the periodicity of the data, Figure 4.1 is plotted for the maximum error against the number of points  $n$ .

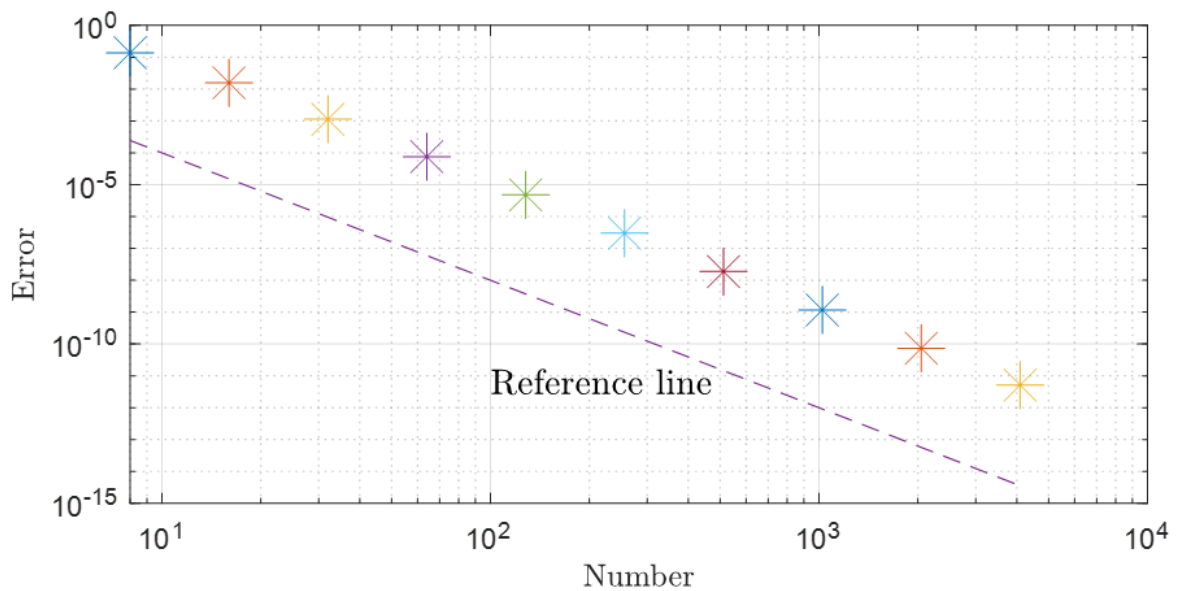


**Figure 4.1** Convergence of finite difference approximation of the fourth order.

*Note.* The possible use of large data points is due to the implementation of sparse matrices for  $f(x) = e^{-\cos x}$ . However, the use of more higher order differences will result in circulant matrices. Therefore, we use spectral methods to utilise the differentiation of infinite order.

In order to apply spectral methods in the place of finite differences, we chose orthogonal polynomials to fit. Trigonometric functions are the obvious choice for the above periodic domain. However, for non-periodic problems, algebraic polynomials represent a better choice. This is explained in Section 4.3.4 and Section 4.3.5. Figure 4.2 illustrates the convergence of the polynomial spectral method using trigonometric functions for the function  $f(x) = e^{-\cos x}$  on the domain  $(-\pi, \pi)$ . In this case, the matrix is denser and a smaller number of data points are needed to achieve the same level of accuracy.

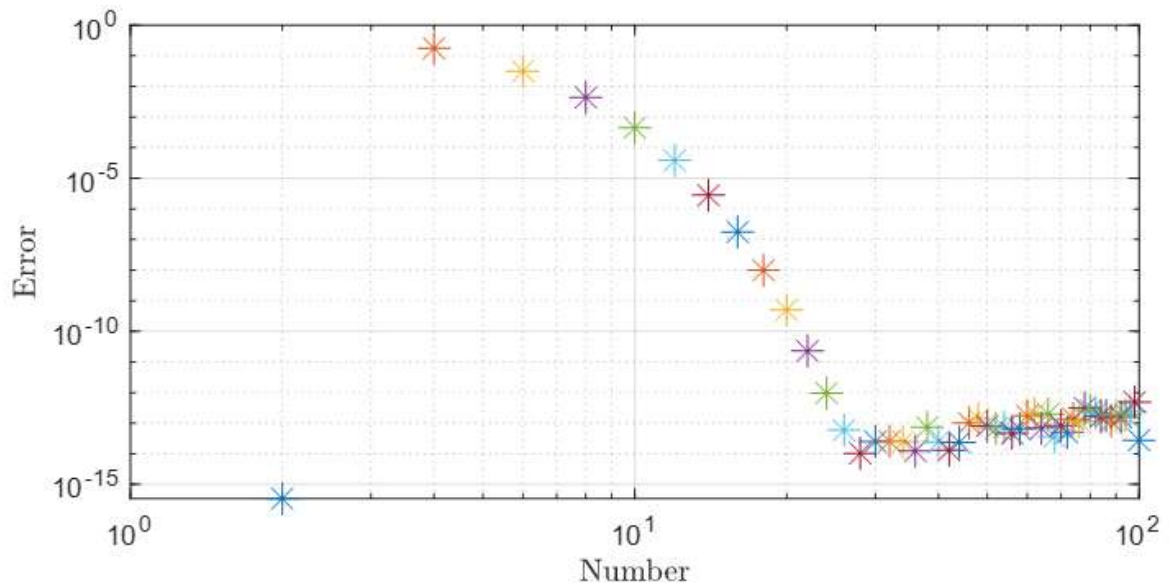


**Figure 4.2 Convergence of spectral method approximation of fourth order.**

*Note.* Using the spectral method, the error for  $f(x) = e^{-\cos x}$  decreases very quickly, eventually reaching a precision so high that computer rounding errors prevent further improvement. The key point here is to determine whether the convergence rate of spectral methods is faster than the Finite Difference (FDM) and the Finite Element method (FEM). The error decreases with  $O(N^{-c})$  in the FDM and the FEM methods where  $N$  is the number of data points and  $c$  is a constant that depends on the smoothness of the solution and order of the approximation. However, in spectral methods, the convergence rate is faster with  $O(c^N)$ ,  $0 < c < 1$  provided that the solution is infinitely differentiable.

Efforts in the development of spectral methods, along with other computational schemes, have been increasing over time. This objective of this chapter is to introduce these methods and implement at least one of them to reduce computational efforts. This thesis focuses on advanced computational settings rather than solving advanced SPDEs.

The theory of stochastic spectral methods revolves around the basis functions, orthogonal polynomials, random variables, and probability distributions. This thesis does not cover the theory of random variables and probability distributions (see (Cramer, 1970) for more information in probability theories).

## 4.2 Functional space and inner product

Spectral methods search for a functional representation of the solution of the model or the quantity of interest. These spaces consist of sets of functions that share certain properties or characteristics, making them invaluable tools for understanding, analysing, and solving complex

mathematical problems. An important functional space; Hilbert space is explained in next section, Kondratiev test space and Hida test space are explained in chapter 5.

#### 4.2.1 Hilbert space

A Hilbert space  $\mathcal{L}^2$  equipped with an inner product  $\langle \cdot, \cdot \rangle$  for a Lebesgue measure  $\mu$  within the domain  $D$  is such that,

$$\|x\|_2 = \left( \int_D |x|^2 d\mu \right)^{1/2} < \infty \quad (4.6)$$

Also, for a Lebesgue measure,

$$\int_D f(x) d\mu(x) = \int_D f(x) w(x) dx \quad (4.7)$$

where the integral on the right-hand side of equation (4.7) is the weighted integral and is defined as,

$$\int_{-\infty}^{\infty} w(x) dx = \mu(\mathbb{R}) \quad (4.8)$$

Also, the inner product for  $p, q \in \mathcal{L}^2$  is defined as,

$$\langle p, q \rangle = \int_D p(x) q(x) d\mu(x) = \int_D p(x) q(x) w(x) dx \quad (4.9)$$

The inner product  $\langle \cdot, \cdot \rangle$  is always defined for a weighted function. A weighted Hilbert space  $\mathcal{L}_w^2[x_1, x_2]$  can be defined as,

$$\mathcal{L}_w^2[x_1, x_2] = \{p: [x_1, x_2] \rightarrow \mathbb{R} \mid \int_{C_1}^{C_2} p^2(x) d\mu(x)\} = \int_{C_1}^{C_2} p^2(x) w(x) < \infty \quad (4.10)$$

Also, a stochastic Hilbert space for a stochastic variable  $\xi$  can be formulated as:

$$\mathcal{L}_{dF_\xi}^2(I_\xi) = \left\{ f: I_\xi \rightarrow \mathbb{R} \mid E[f^2(\xi)] = \int_{I_\xi} f^2(\xi) dF_\xi < \infty \right\} \quad (4.11)$$

Recurrence relations and orthogonal polynomials

A system of polynomials  $\{P_n(x), n \in \mathbb{N}\}$  is said to be orthogonal if for some positive real measure  $\lambda$

$$\int_D P_n(x) P_m(x) d\lambda(x) = C_n \delta_{mn} \quad \forall m, n \in \mathbb{N} \quad (4.12)$$

where  $C_n$  is the normalisation constant and  $\delta_{mn}$  is the Kronecker delta function, defined as,

$$\delta_{mn} = \begin{cases} 1, & \text{when } m = n \\ 0, & \text{otherwise} \end{cases} \quad (4.13)$$

The system is orthonormal for  $C_n = 1$ . Orthogonal polynomials are defined by a three-term recurrence relation,

$$P_{n+1}(x) = (x - a_n)P_n(x) - b_nP_{n-1}(x), \forall n > 0 \quad (4.14)$$

where

$$a_n = \frac{\langle x P_n(x), P_n(x) \rangle}{\langle P_n(x), P_n(x) \rangle}$$

and

$$b = \frac{\langle P_n(x), P_n(x) \rangle}{\langle P_{n-1}(x), P_{n-1}(x) \rangle} \geq 0$$

More details on orthogonal polynomials and three-term recurrence relations can be found in Gubner (2020) and Xiu (2009).

#### 4.2.2 Hermite polynomials

There are two definition used in the literature for Hermite polynomials: one used by physicists  $H_n(x)$ . The other one, called probabilistic Hermite polynomials, is used mostly by mathematicians.

The three-term recurrence relation for Hermite polynomials is,

$$H_{n+1}(x) = x H_n(x) - n H_{n-1}(x) \quad (4.15)$$

with  $H_0(x) = 1$  and  $H_1(x) = x$

The normalisation constant,  $C_n$  in this case, is given by the norm of  $H_n(x)$ , i.e.,

$$C_n = \langle H_n(x), H_n(x) \rangle = \int_{-\infty}^{\infty} H_n^2(x) w(x) dx \quad (4.16)$$

where  $w(x)$  is the Gaussian weight function defined as  $w(x) = \frac{1}{\sqrt{2\pi}} e^{-x^2/2}$ .

Hence,  $C_n = \frac{1}{2^n} n!$

However, the three-term recurrence relation for probabilistic Hermite polynomials is given by,

$$H_{n+1}(x) = 2x H_n(x) - 2n H_{n-1}(x) \quad (4.17)$$

with  $H_0(x) = 1$ ,  $H_1(x) = 2x$  and  $C_n = 2^n n!$

### 4.2.3 Legendre polynomials

Legendre Polynomials are a special sub-set of Jacobi polynomials and the three-term recurrence relation for Legendre polynomials is given by,

$$L_{n+1}(x) = \frac{2n+1}{n+1}x L_n(x) - \frac{n}{n+1}L_{n-1}(x) \quad (4.18)$$

with  $L_0(x) = 1$ ,  $L_1(x) = x$  and  $n > 0$

For the normalisation constant  $C_n = \frac{1}{2^{n+1}}$  and for the given weight function  $w(x)$ , Legendre polynomials form an orthogonal basis for  $\mathcal{L}^2[-1,1]$ . The first six physicist's Hermite polynomials and Legendre polynomials are summarised in Table 4.1 and are plotted in Figures 4.3 and Figure 4.4 respectively.

**Table 4.1 First six Hermite polynomials and Legendre polynomials.**

Hermite Polynomials $H_n(x)$	Legendre Polynomials $L_n(x)$
$H_0(x) = 1$	$L_0(x) = 1$
$H_1(x) = x$	$L_1(x) = x$
$H_2(x) = x^2 - 1$	$L_2(x) = \frac{1}{2}(3x^2 - 1)$
$H_3(x) = x^3 - 3x$	$L_3(x) = \frac{1}{2}(5x^3 - 3x)$
$H_4(x) = x^4 - 6x^2 + 3$	$L_4(x) = \frac{1}{8}(35x^4 - 30x^2 + 3)$
$H_5(x) = x^5 - 10x^3 + 15x$	$L_5(x) = \frac{1}{8}x(63x^4 - 70x^3 + 15)$

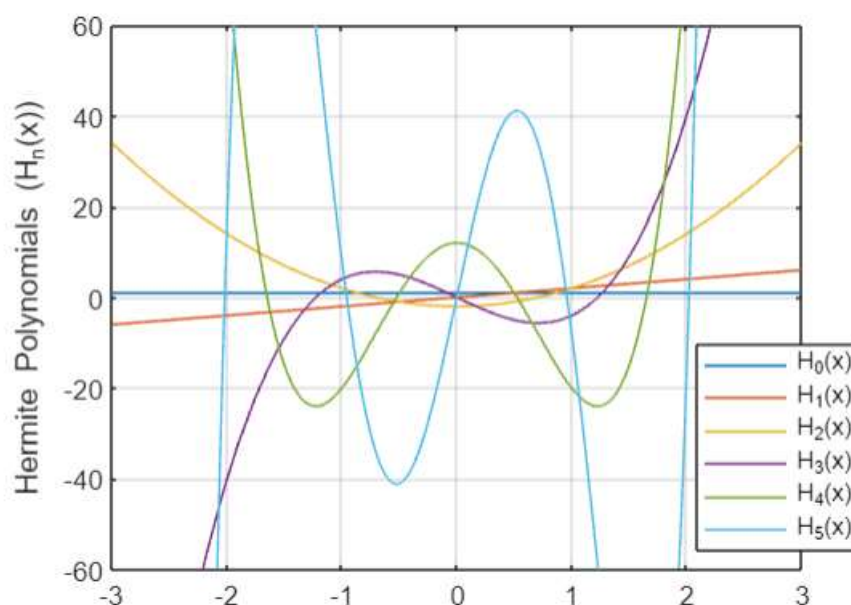


**Figure 4.3 Hermite polynomials from order 0 to order 5 for  $x \in (-3, 3)$**

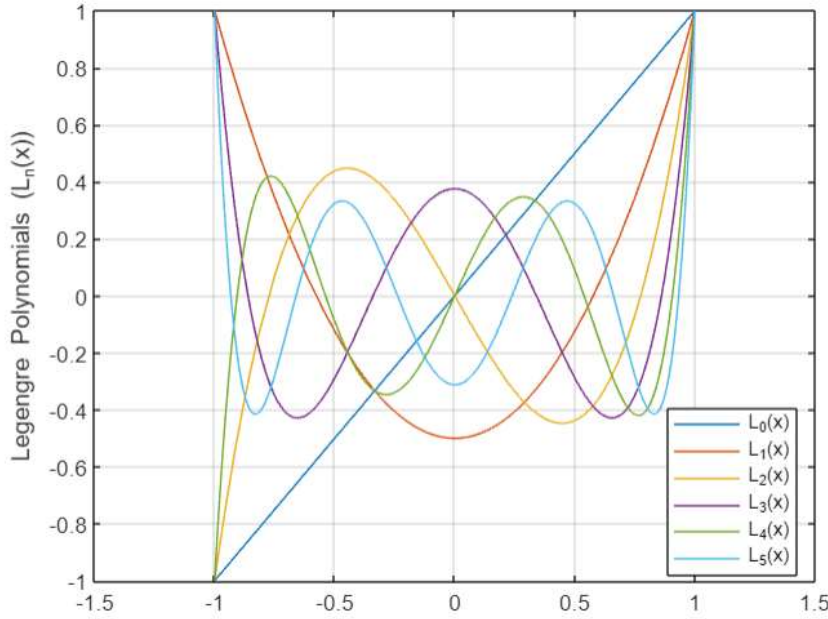


**Figure 4.4** Legendre polynomials from order 0 to order 5 for  $x \in (-1.5, 1.5)$ .

Several other orthogonal polynomials that are used in spectral methods are Laguerre polynomials (Abell & Braselton, 2014), Jacobi polynomials and Charlier polynomials (Abdul-Hadi et al., 2020).

### 4.3 Computation of quadrature nodes

As explained in Chapter 3, Section 3.6, nodes are computed to find numerical integration. An alternative way of computing an integral  $\int_D f(x)d\mu(x)$  involves computation of another integral  $\int_D g(x)w_\mu(x)dx$ , where function  $g(x)$  is analogous to  $f(x)$  and its integral is known. This integral can be computed as,

$$\int_D g(x)w_\mu(x)dx = \sum_{i=1}^n w_i g(x_i) \quad (4.19)$$

here  $x_i$  is the  $i$ th node for the range of integration and  $w_i$  is the weight associated with  $i$ th node. The orthogonal polynomials defined in the previous section will serve the purpose of  $g(x)$  and the weights  $w_i$  are chosen as close to  $w_\mu(x)$  as possible.

In order to evaluate the Gauss Hermite quadrature (see equation 3.16, Chapter 3),

$d\mu(x) = e^{-x^2/2}$  and the measure  $\mu(\mathbb{R}) = \sqrt{2\pi}$ . The weights and nodes can be computed using the eigen-value decomposition of the Jacobi matrix and is given by  $w_i = \frac{n!}{n^2[H_{n-1}(x_i)]^2}$ .

## 4.4 Framework for input variables and random processes

Although it is true that fast computation with stochastic numerical methods is an important step for modelling stochastic processes, the most crucial step is to deal with random inputs and to characterise their randomness. So, the key idea is to reduce the infinite dimensional random probability space into a space which is finite and suitable for computation. This task is not easy, but can be achieved using a set of finite dimensional random variables. In addition, the independency of chosen random variables is necessary and is often a requirement for most (if not all) of the numerical schemes. The two main components that need parameterisation before the simulation process are random variables and stochastic processes. The following algorithm is used to parameterise the random variables:

---

Algorithm 1: when the input variables are stochastic

---

In the case of system parameters as a random input, we need to ensure that the parameters are independent. This aim can be achieved using the following steps:

- Consider the system parameter as  $X = (X_1, X_2, \dots, X_d)$ ,  $d \geq 1$  with PDF  $F_X(x) = P(X \leq x), \forall x \in \mathbb{R}^d$ .
- Define a suitable mapping known as a transformation map  $T$ , such that  $X = T(\xi)$  for  $\xi = (\xi_1, \xi_2, \dots, \xi_d) \in \mathbb{R}^d$ , where  $\xi_i, i = 1, 2, \dots, d$  are mutually independent.

---

There are several physical systems in which input variables are considered a stochastic process, such as the conductivity of a material which is random in space, a random forcing term in the modelling system that is time dependent. In such situations, the approach is to consider a finite dimensional discretisation of the actual random process and then study the process by discretising the region into a set of finite indices. Algorithm 2 is applicable for this type of system.

---

Algorithm 2: when input parameters are random processes

---

When input parameters are random processes

- Consider the stochastic process  $X_k, k \in D$ , which models the random input.  $K$  belongs to the index set  $D_k$  or domain (time/space) and then discretise.
-

- 
- Find a suitable map known as transformation map  $T$ , such that  $X = T(\xi)$  for  $\xi = (\xi_1, \xi_2, \dots, \xi_d) \in \mathbb{R}^d$ , where  $\xi_i, i = 1, 2, \dots, d$  are mutually independent random variables.
- 

The accuracy of the solution will depend on finer discretisation; however, this process will lead to high computation cost due to larger dimensions. Thus, a balance between approximation accuracy and dimensionality reduction techniques is required.

## 4.5 Spectral methods

In spectral methods, the idea is to search for a functional representation of the quantity of interest, say,  $Q(u(\xi)) \approx \sum_{\alpha \in \mathfrak{S}_p} Q_\alpha \vartheta_\alpha(\xi)$ , where  $Q_\alpha$ 's are the coefficients that need to be determined.  $\mathfrak{S}_p$  is the index set and  $\vartheta_\alpha(\xi)$  is a known basis of functions such as Hermite or Legendre polynomials. This approach serves as a response surface of the model. Once this functional relationship has been established, it is easy and quick to evaluate the model to obtain statistical moments and perform sensitivity analysis.

Several stochastic spectral methods have been developed after the work by Ghanem (R. G. Ghanem et al., 1991). These methods are categorised based on the choice of basis functions.

### 4.5.1 Direct spectral methods

No specific implementation is required for these methods to determine the coefficients, except for solving uncoupled deterministic equations. Table 4.2 provides a brief introduction to some of the Least square projection and regression methods and the advantages and disadvantages associated with each method.

### 4.5.2 Intrusive stochastic spectral methods

Intrusive stochastic spectral methods are a class of numerical methods used to solve SDEs and SPDEs with random inputs. These methods are "intrusive" in the sense that they require modification of the original deterministic solver to handle the stochastic inputs directly. This modification typically involves adding terms to the deterministic equations to account for the random inputs.

The basic idea of intrusive stochastic spectral methods is to represent the solution to the SDE or SPDE as a sum of orthogonal basis functions, such as polynomials or trigonometric functions, as in non-intrusive methods. However, instead of using a surrogate model, the stochastic expansion is incorporated directly into the deterministic solver.

**Table 4.2 Comparative study of Least Square Projection and Regression method.**

Least Square Projection method	Regression method
<ul style="list-style-type: none"> <li>This method projects the approximate solution of <math>Q</math> on space <math>\mathcal{L}^2(\xi, dP_\xi)</math> spanned by orthonormal basis functions (especially Hermite polynomials) <math>\{H_\alpha\}_{\alpha \in \mathfrak{S}_p}</math>.</li> <li>Projection with respect to inner product is given as           <math display="block">\langle v, w \rangle_{\mathcal{L}^2(\xi, dP_\xi)} = E[v(x), w(x)] = \int v(x)w(x)dP_\xi(x)</math> </li> <li>The coefficients <math>Q_\alpha</math> using <math>\{H_\alpha\}</math> <math display="block">Q_\alpha = \langle Q, H_\alpha \rangle_{\mathcal{L}^2(\xi, dP_\xi)} = E(Q(u(\xi); \xi)H_\alpha(\xi))</math> </li> <li>Any of the integration technique (chapter 2 section 2.5) can be applied to calculate <math>Q_\alpha</math> given by           <math display="block">Q_\alpha = \sum_{m=1}^M w_m Q(u(x_m); x_m) H_\alpha(x_m)</math> </li> </ul> <p>This will result in <math>M</math> uncoupled equations and a deterministic numerical code will solve these equations such as Runge Kutta method or Euler's method.</p> <p><b>Pros and Cons:</b></p> <p>This approach is quite comprehensive and a specific integration method is to be chosen for almost accurate projection. For instance, if MC method is applied, larger sample cost (Le Matre et al., 2002).</p>	<ul style="list-style-type: none"> <li>These methods are based on optimisation of the coefficients <math>Q_\alpha</math> and work on the principle of response surface methods.</li> <li>The coefficient <math>Q_\alpha</math> is optimised by           <math display="block">\min_{\{Q_\alpha\}_{\alpha \in \mathfrak{S}_p}} \sum_{m=1}^M w_m (Q(u(x_k); x_k) - \sum_{\alpha \in \mathfrak{S}_p} Q_\alpha H_\alpha(x_k))^2</math> </li> </ul> <p>with <math>w_m</math> as weights and <math>x_k</math> as regression points.</p> <ul style="list-style-type: none"> <li>The set of decomposition coefficient <math>Q_\alpha</math> is obtained by solving the set of linear equations given by           <math display="block">C Q_{\alpha\beta} = S_\alpha, \text{ where } C = \{\dots \dots \dots, Q_\alpha, \dots\} \in \mathbb{R}</math> <math display="block">Q_{\alpha\beta} = \sum_{m=1}^M w_m H_\alpha(x_m) H_\beta(x_m)</math> </li> </ul> <p>and</p> $S_\alpha = \sum_{m=1}^M w_m H_\alpha(x_m) Q(u(x_m); x_m)$ <p><b>Pros and Cons:</b></p> <p>The appropriate value of <math>w_m</math> and <math>x_m</math> is difficult to determine. A number of choices for these values are suggested in (Blatman &amp; Sudret, 2008). Some of these choices are QMC sampling with <math>w_m = x_m = \frac{1}{M}</math> or Gaussian quadrature nodes and weights as <math>w_m</math> and <math>x_m</math>.</p>

<p><b>Suggestion:</b></p> <p>Function (<math>QH_\alpha</math>) needs to satisfy regularity condition that is known a priori, so adaptive quadrature rule would be preferable as compared to classical ones. However, defining a specific error formula for these quadrature rules is still a challenge.</p>	<p><b>Suggestion:</b></p> <p>These methods are similar to <math>\mathcal{L}^2</math>-projection methods because the coefficient matrix of <math>Q_\alpha</math> is <math>Q_{\alpha\beta} = \langle H_\alpha, H_\beta \rangle_M</math>.</p> <p>Also, if chosen values provide exact integration values, regression methods are equivalent to least square projection methods.</p>
---	--

One popular intrusive stochastic spectral method is the stochastic Galerkin method (Matthies & Keese, 2005; Pettersson et al., 2014; Xiu & Shen, 2008; T. Zhou & Tang, 2012). This method involves representing the solution as a sum of orthogonal basis functions, and then using these basis functions to approximate the solution to the SDE or SPDE. The coefficients of the expansion are determined by solving a system of equations derived from the original problem, typically using techniques such as Galerkin projection or least-squares regression.

Another popular intrusive stochastic spectral method is the stochastic finite element method (SFEM). SFEM involves representing the solution as a sum of finite element basis functions, and then using these basis functions to approximate the solution for the SDE (Blatman & Sudret, 2008; Frauenfelder et al., 2005; R. G. Ghanem & Spanos, 1991; Keese, 2003).

Intrusive stochastic spectral methods have several advantages over non-intrusive methods, including higher accuracy and greater efficiency for problems with highly nonlinear or non-smooth solutions. However, they require modification of the original deterministic solver, which can be more challenging to implement and may limit the flexibility of the method. The choice of method will depend on the specific characteristics of the problem being solved, the desired accuracy, and computational efficiency.

### 4.5.3 Non-intrusive stochastic spectral methods

Non-intrusive spectral methods approximate the solution to the SPDE using a series of basis functions. The coefficients of the basis functions are determined by solving a system of equations derived from the original SPDE. Spectral methods are often used when the solution is expected to be smooth and when the forcing term is known.

These methods are "non-intrusive" in the sense that they do not require the original deterministic solver to be modified in order to handle stochastic inputs. Instead, they use a surrogate model to represent the solution in terms of a spectral expansion.

The basic idea of non-intrusive stochastic spectral methods is to represent the solution to the SDE/SPDE as a sum of orthogonal basis functions, such as polynomials or trigonometric functions. The coefficients of the expansion are determined using numerical techniques such as regression or interpolation.

One popular non-intrusive stochastic spectral method is the stochastic collocation method (SCM). SCM involves evaluating the solution at a set of deterministic collocation points and using these evaluations to construct a surrogate model. The surrogate model can then be used to estimate the solution at any point in the domain, including those with stochastic inputs (Babuška et al., 2010; Eldred & Burkardt, 2009; Kamrani, 2016; Nobile et al., 2008; Z. Zhang et al., 2015).

Another popular approach in this category is the polynomial chaos expansion (PCE) method. PCE involves representing the solution as a sum of orthogonal polynomials, such as Legendre or Hermite polynomials. The coefficients of the expansion are determined by projecting the original problem onto the polynomial basis, which can be done using techniques such as Galerkin projection or least-squares regression (Blatman & Sudret, 2008; Kaintura et al., 2018; S. & S., 2006; Villegas et al., 2012; Wan & Karniadakis, 2006; Xiu et al., 2002).

The main advantage of non-intrusive stochastic spectral methods is that they are non-intrusive, meaning that they do not require modifications to the underlying deterministic solver or the PDE itself. Instead, they rely on sampling the solution at specific points and using this information to compute the coefficients of the spectral expansion.

Another advantage of non-intrusive stochastic spectral methods is their ability to handle high-dimensional problems with a relatively small number of samples. This is because the spectral expansion can capture the global behaviour of the solution, allowing for accurate approximation of the solution using only a few terms.

However, non-intrusive stochastic spectral methods can be computationally expensive for certain types of problems, especially when the number of stochastic dimension is large. In these cases, it may be necessary to use intrusive methods, which require modifications to the deterministic solver or the PDE itself.

#### **4.5.4 Polynomial chaos expansion (PCE) methods**

PCE methods are a class of numerical methods used to solve SDEs and SPDEs with random inputs. PCE methods involve representing the solution to the SDE or SPDE as a series of orthogonal polynomials, such as Legendre or Hermite polynomials, that are functions of the random inputs. The basic idea of PCE methods is to approximate the solution as a sum of polynomial functions that are orthogonal, with respect to the probability distribution of the random inputs (Kaintura et al.,

2018). The coefficients of the expansion are determined by solving a system of equations derived from the original problem, typically using techniques such as Galerkin projection or least-squares regression. The resulting PCE can then be used to estimate the solution at any point in the domain, including those with stochastic inputs.

One advantage of PCE methods is that they can be used to efficiently propagate uncertainty through the system, allowing for the efficient estimation of statistics such as mean and variance (Huschto & Sager, 2013; Najm, 2008). PCE methods can also be used to efficiently quantify the effect of input uncertainties on the system response, such as in sensitivity analysis.

PCE methods can be used in both intrusive and non-intrusive implementations. While intrusive PCE methods modify the original deterministic solver to handle the stochastic inputs directly, non-intrusive PCE methods use a surrogate model to represent the solution in terms of the PCE.

Overall, PCE methods are a powerful tool for solving SDE and PDE with random inputs. They offer accuracy and efficiency, and have wide application: for example, they have been used in engineering, physics, and finance. However, their accuracy and efficiency depend on the choice of polynomial basis and the complexity of the problem being solved.

## 4.6 Need of polynomial chaos methods

Here are some reasons why polynomial chaos methods have a wider acceptance rate:

- **Efficient representation of stochastic processes:** polynomial chaos methods allow for an efficient representation of stochastic processes in terms of a finite number of basis functions. This can greatly reduce the computational cost of simulating or analysing these processes.
- **Accurate representation of moments:** polynomial chaos methods have been shown to accurately represent the moments of stochastic processes with Gaussian and non-Gaussian inputs. This means that they can be used to estimate statistics such as mean and variance with higher accuracy.
- **Versatility:** these methods can be applied to a wide range of problems, including those involving random fields, SDEs, and random dynamical systems.
- **Flexibility:** these methods allow for the use of different types of orthogonal polynomials as basis functions, which can be chosen based on the properties of the input distribution. This allows for greater flexibility in modelling a variety of stochastic processes.
- **Robustness:** polynomial chaos methods are robust to small perturbations in the input distribution, making them suitable for modelling processes with slightly non-Gaussian inputs.

A typical diagrammatic representation (Figure 4.5) for working of polynomial chaos methods shows the following steps:

- (i) Input: the input needed for the polynomial chaos method is an SDE or SPDE with random inputs.
- (ii) Basis functions: the next step involves selecting a set of orthogonal basis functions, such as Legendre or Hermite polynomials, to represent the solution as a series expansion.
- (iii) Expansion coefficients: the coefficients of the expansion are determined by projecting the original problem onto the polynomial basis, using techniques such as Galerkin projection or least-squares regression.
- (iv) Surrogate model (non-intrusive only): in non-intrusive PCE methods, a surrogate model is constructed to represent the solution in terms of the polynomial expansion. This surrogate model can be used to efficiently estimate the solution at any point in the domain.
- (v) Solve: the resulting polynomial chaos expansion can be used to solve the original problem, including propagating uncertainty through the system and estimating statistics such as mean and variance.
- (vi) Output: the output of the method is the solution to the SDE or PDE, represented in terms of the polynomial chaos expansion.

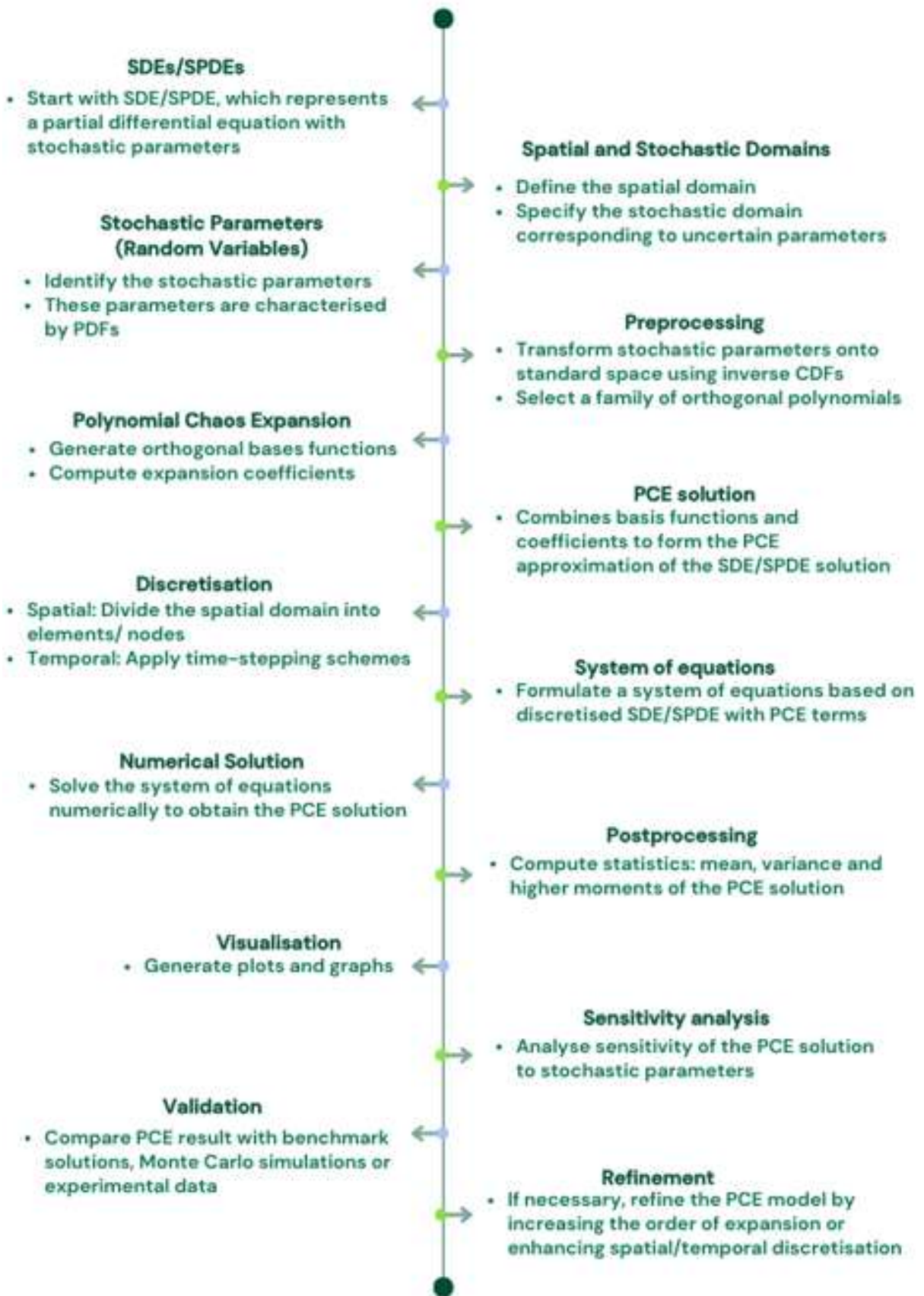


Figure 4.5 Diagrammatic representation for working process of polynomial chaos expansion methods for SDEs and SPDEs.

## 4.7 Generalised polynomial chaos expansion (gPCE) methods

Wiener PCE methods use Hermite polynomials and express the solution of random differential equations in terms of these smoothed orthogonal polynomials. Although these homogeneous Wiener polynomial chaos is quite useful and satisfy certain universal polynomial characteristics, more useful for Gaussian distributed random input parameters. For non-Gaussian random variables, Hermite polynomial based chaos expansion is slow. (Xiu et al., 2002) introduced gPCE with the help of the Askey scheme for orthogonal polynomials. It involves mapping the stochastic solution onto a set of polynomials that are orthogonal to the probability distribution of the input parameter (Xiu, 2010a).

Thus, instead of finding the random solution of the SDE, the problem is reduced to evaluating the expansion coefficients. The basis functions are selected based on the distribution of random parameters. The correspondence between the basis functions and their known distributions is available in the extant literature (Xiu, 2009) and is summarised in Figure 4.6.

### 4.7.1 Formulation of gPCE

Let us consider a complex stochastic system modelled by the equation,

$$\mathfrak{S}(t, \omega; y) = 0 \quad (4.20)$$

with the initial condition  $y(t_0) = y_0$ . This system is defined on a probability space  $(\Omega, \mathcal{F}, \mathcal{P})$  with

$\omega \in \Omega$  and  $t \in [0, T]$ .

Let the solution of the equation (4.20) within the Hilbert space  $\mathcal{L}^2([0, T] \times \Omega)$  is given by  $y(t, \omega)$  after reducing infinite dimensional probability space  $(\Omega, \mathcal{F}, \mathcal{P})$  to finite dimensional probability space as defined in section 4.4.

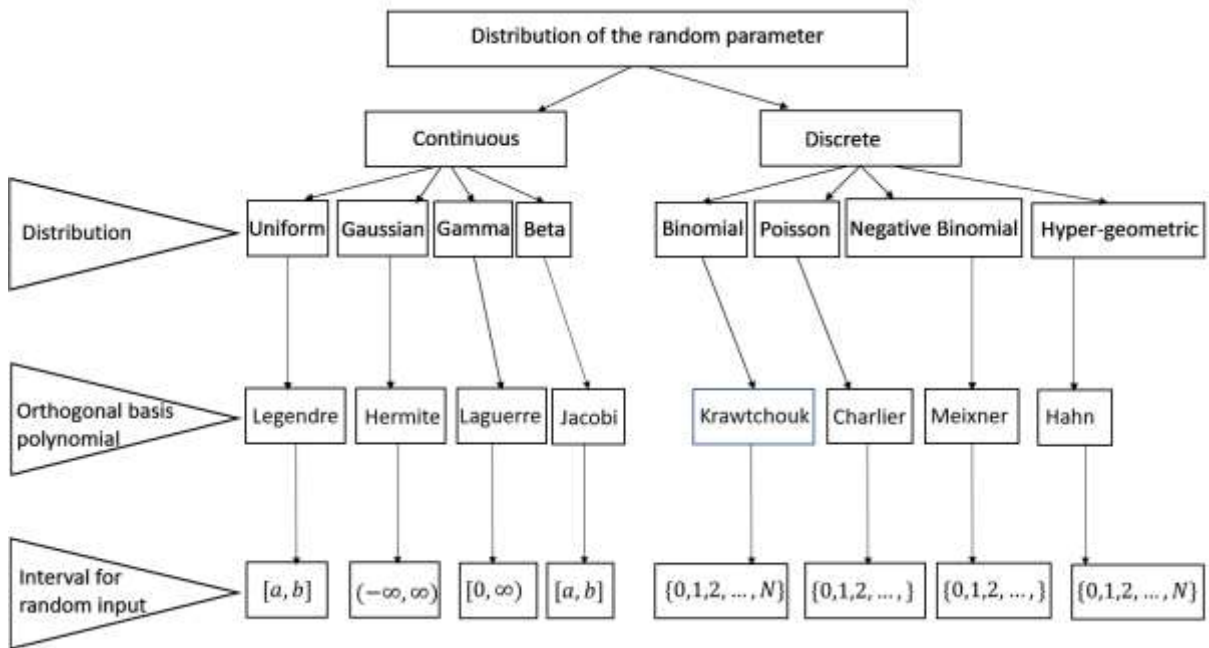


**Figure 4.6 Equivalence between distributions, basis polynomials, and related input random variables.**

The finite dimensional probability space of random variable  $\xi$  is defined as

$\xi = (\xi_1, \xi_2, \dots, \xi_d) \in \mathbb{R}^d$ . The random input is represented as  $\omega \in \Omega$ . Equation (4.20) is then reduced to,

$$\mathfrak{S}(t, \xi; y) = 0, \text{ with } y(t_0, \xi) = y_0(\xi) \quad (4.21)$$

In order to find number of solutions for equation (4.21), numerous realisations of the random variable have to be used for a fixed temporal variable.

#### 4.7.2 Multi-variate gPCE

Generalised PCE (gPCE) is very straightforward and easily expanded for multi-dimensional uncertainty description. The key point here is that instead of having univariate polynomials we will have multivariate polynomials (again, a function of the random variables  $\xi$  of the uncertainty).

In the case of a high-dimensional variable, the solution of equation (4.21) using gPCE is written as,

$$y(\xi) = \sum_{|\alpha|=0}^{\infty} y_{\alpha} \varphi_{\alpha}(\xi) \quad (4.22)$$

where  $y_{\alpha}$  are the basis coefficients and are calculated as,

$$y_{\alpha} = \frac{1}{\gamma_{\alpha}} E[y(\xi) \varphi_{\alpha}(\xi)] \quad (4.23)$$

Where  $\gamma_\alpha = E[\varphi_\alpha^2]$  and  $\alpha$  is the ordered set of multi-indices defined as  $|\alpha| = \alpha_1 + \alpha_2 + \dots + \alpha_d$  for a  $d$ -dimensional random variable.

For computation, the expansion order has to be truncated (say up to  $M$  terms). The expansion order  $M$  is a function of the number of uncertainties as well as the user specified order of the polynomials (say  $P$ ). Thus, the larger the number of uncertainties and the higher the order of polynomials (which is basically the user's choice), the larger the expansion order which typically results in more computational efforts and greater complexity.

A truncated gPCE is,

$$y(\xi) = \sum_{|\alpha|=0}^M y_\alpha \varphi_\alpha(\xi) \quad (4.24)$$

The total number of terms in truncated expansion is  $M + 1$  and is evaluated as-

$$\text{total number of terms} = M + 1 = \frac{(d+P)!}{d! P!}$$

**Table 4.3 Calculation for multi-indices  $\alpha$  and the basis functions. The total number of Hermite polynomials are 3 and the dimension of the random variable is 3.**

$ \alpha $	$\alpha$	$\varphi_\alpha(\xi)$	$ \alpha $	$\alpha$	$\varphi_\alpha(\xi)$
0	(0,0,0)	$\varphi_0(\xi) = 1$	3	(3,0,0)	$\varphi_3(\xi) = H_3(\xi_1) = \xi_1^3 - 3\xi_1$
1	(1,0,0)	$\varphi_1(\xi) = H_1(\xi_1) = \xi_1$	3	(0,3,0)	$\varphi_3(\xi) = H_3(\xi_2) = \xi_2^3 - 3\xi_2$
1	(0,1,0)	$\varphi_1(\xi) = H_1(\xi_2) = \xi_2$	3	(0,0,3)	$\varphi_3(\xi) = H_3(\xi_3) = \xi_3^3 - 3\xi_3$
1	(0,0,1)	$\varphi_1(\xi) = H_1(\xi_3) = \xi_3$	3	(1,2,0)	$\varphi_3(\xi) = H_1(\xi_1)H_2(\xi_2) = \xi_1(\xi_2^2 - 1)$
2	(2,0,0)	$\varphi_2(\xi) = H_2(\xi_1) = \xi_1^2 - 1$	3	(2,1,0)	$\varphi_3(\xi) = H_2(\xi_1)H_1(\xi_2) = (\xi_1^2 - 1)\xi_2$
2	(0,2,0)	$\varphi_2(\xi) = H_2(\xi_2) = \xi_2^2 - 1$	3	(1,0,2)	$\varphi_3(\xi) = H_1(\xi_1)H_2(\xi_3) = \xi_1(\xi_3^2 - 1)$
2	(0,0,2)	$\varphi_2(\xi) = H_2(\xi_3) = \xi_3^2 - 1$	3	(2,0,1)	$\varphi_3(\xi) = H_2(\xi_1)H_1(\xi_3) = (\xi_1^2 - 1)\xi_3$
2	(1,1,0)	$\varphi_2(\xi) = H_1(\xi_1)H_1(\xi_2) = \xi_1\xi_2$	3	(0,1,2)	$\varphi_3(\xi) = H_1(\xi_2)H_2(\xi_3) = \xi_2(\xi_3^2 - 1)$
2	(1,0,1)	$\varphi_2(\xi) = H_1(\xi_1)H_1(\xi_3) = \xi_1\xi_3$	3	(0,2,1)	$\varphi_3(\xi) = H_2(\xi_2)H_1(\xi_3) = (\xi_2^2 - 1)\xi_3$
2	(0,1,1)	$\varphi_2(\xi) = H_1(\xi_2)H_1(\xi_3) = \xi_2\xi_3$	3	(1,1,1)	$\varphi_3(\xi) = H_1(\xi_1)H_1(\xi_2)H_1(\xi_3) = \xi_1\xi_2\xi_3$

The orthogonal basis function  $\varphi_\alpha(\xi)$  is calculated by the tensor product of the orthogonal polynomial basis function for a single variable.

Therefore,

$$\varphi_\alpha(\xi) = \prod_{i=1}^d \varphi_{\alpha_i}(\xi_i), 0 \leq |\alpha| \leq N \quad (4.25)$$

The calculations for finding a few  $\alpha$  values and  $\varphi_\alpha(\xi)$  are shown in Table 4.3.

Figure 4.7 to Figure 4.9 shows the product of two dimensional Hermite polynomials of different orders. The horizontal and vertical axes are considered axis of first and second Hermite polynomials. The surface plot shows the product of these Hermite polynomials. Other orthogonal polynomials can be used in the place of Hermite polynomials (Xiu, 2010b; Xiu & Karniadakis, 2006) based on the Askey scheme.

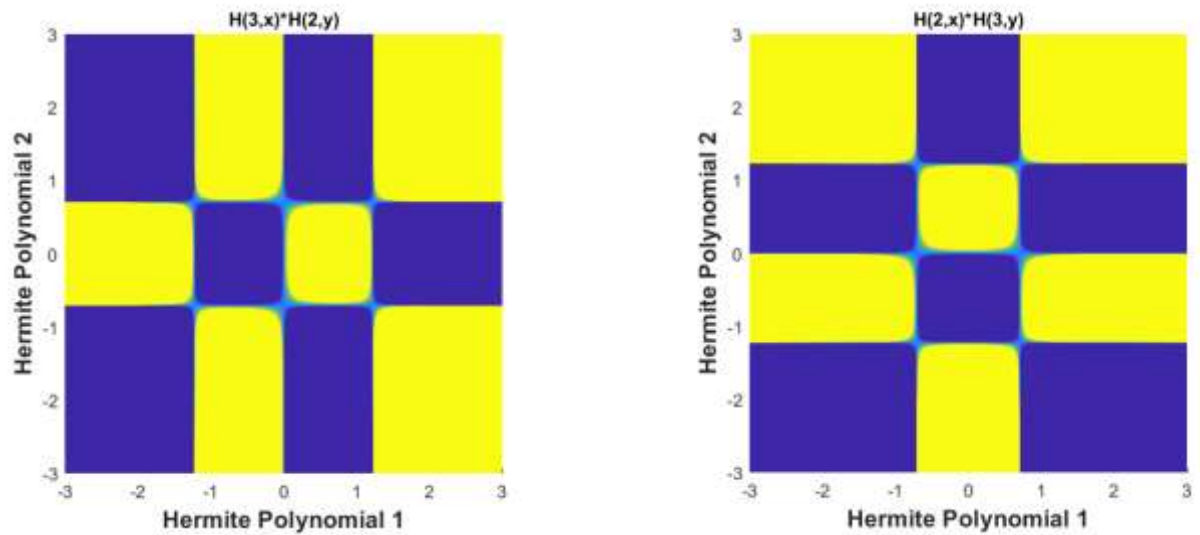


Figure 4.7 Product of two Hermite polynomials of second and third order

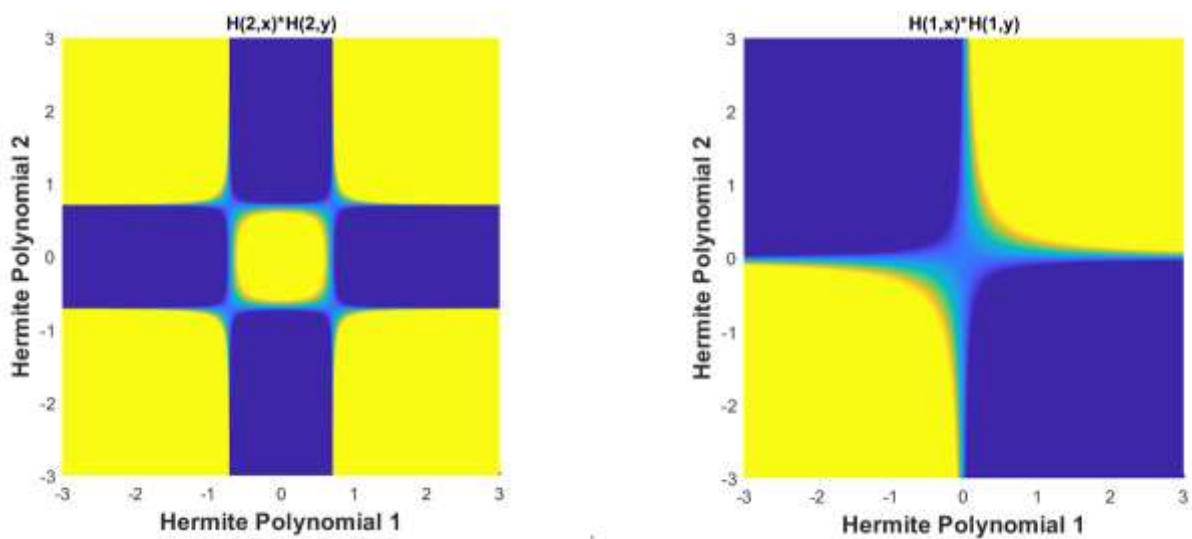


Figure 4.8 Product of two Hermite polynomials of second order (left graph) and first order (right graph).

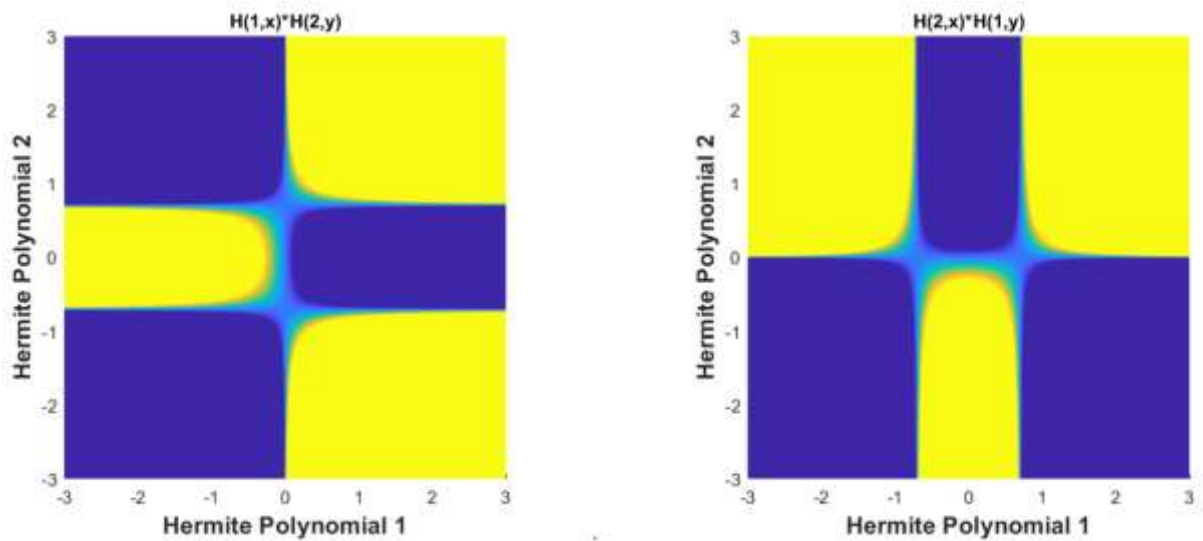


Figure 4.9 Product of two Hermite polynomials of first and second order.

#### 4.8 Evaluating polynomial chaos expansion coefficients

There are two general methods for calculating these polynomial chaos expansion coefficients. The first one is called the stochastic collocation method. Basically, it involves sampling the uncertainties and then evaluating the response of the system to those uncertainties samples and essentially treating the expansion coefficients so this method takes the polynomial expansions as a fitting function. The response of the evaluated system is to be fit to that those samples to the gPCE expansion in a regression sense essentially. Using the stochastic collocation method (Figure 4.10), the chaos coefficients  $y_\alpha$ , as defined in equation (4.24), are calculated by,

$$\sum_{\alpha=0}^M y_\alpha \varphi_\alpha(\xi_j), j = 1, 2, \dots, S, \quad (4.26)$$

where  $S$  is the number of samples chosen.

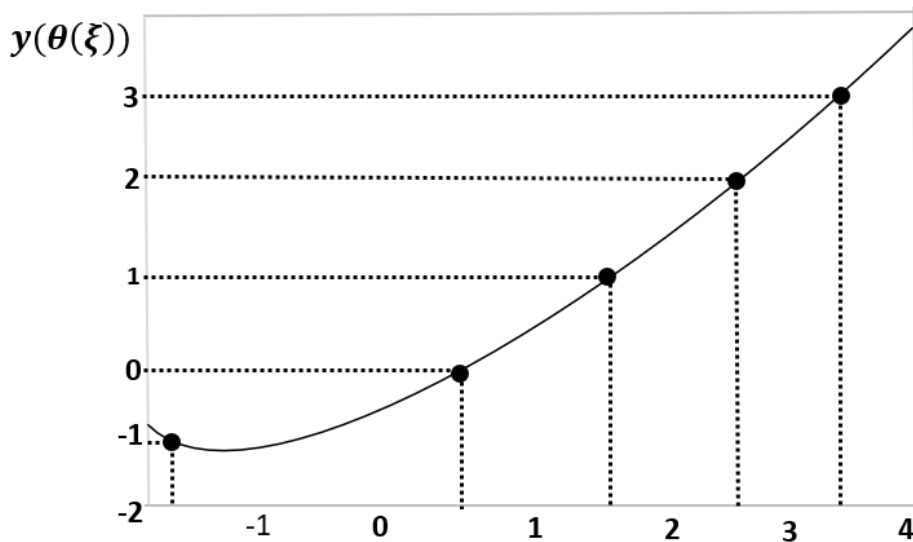


**Figure 4.10 Geometrical interpretation of the Stochastic Collocation method for computing polynomial chaos coefficients.**

Another method is the Galerkin's projection method (Figure 4.11) which essentially uses the orthogonal property of the polynomials. This method essentially projects the error that is  $(y - \hat{y})$  (approximation error) associated with the gPCE expansion onto the subspace spanned by the multivariate polynomial basis of the expansion.

The chaos coefficients  $y_\alpha$ , as defined in equation (4.24), are calculated by,

$$y_\alpha = \frac{\langle y, \varphi_\alpha \rangle}{\langle \varphi_\alpha^2 \rangle}, \alpha = 0, 1, \dots, M \quad (4.27)$$

The two versions of this method are the intrusive projection method (which relies on projecting the governing equations of the model onto the polynomial basis functions) and the non-intrusive projection method (in this method the response of the system is projected instead of projecting the full governing equations).

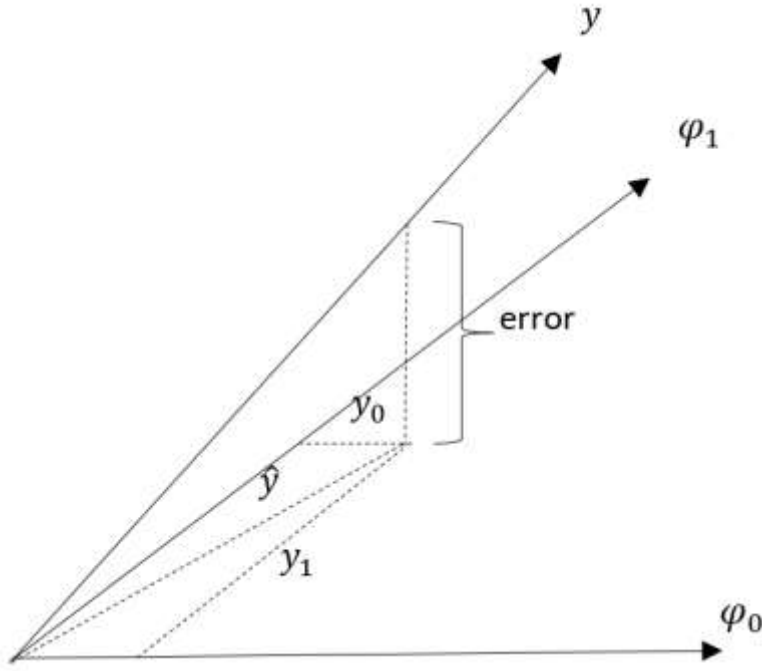


**Figure 4.11 Geometrical interpretation of the Galerkin's projection method for computing polynomial chaos coefficients.**

The non-intrusive method is similar to the collocation method. However, there is a fundamental difference in that the samples are chosen systematically to evaluate this inner product (Galerkin integrals).

## 4.9 Numerical example

Let us consider a very simple example to evaluate  $y$  with one stochastic parameter  $\zeta$  defined by the stochastic equation

$$\dot{y}(t) = \zeta y(t) \quad (4.28)$$

### 4.9.1 Galerkin's intrusive spectral projection method (ISP)

**Step 1:** The quantity of interest  $y$  is stochastic and the parameter  $\zeta$  is uncertain. The first step is to write these variables in terms of polynomial expansion. Therefore, the truncated expansion of  $y$  and  $\zeta$  are,

$$y(t) = \sum_{\alpha=0}^M y_{\alpha}(t) \varphi_{\alpha}(\xi) \quad (4.29)$$

and

$$\zeta = \sum_{\beta=0}^M \zeta_{\beta}(t) \varphi_{\beta}(\xi) \quad (4.30)$$

**Step 2:** Now substituting these expansions into the equation (25), we get,

$$\frac{d}{dt} \left( \sum_{\alpha=0}^M y_{\alpha}(t) \varphi_{\alpha}(\xi) \right) = \left( \sum_{\beta=0}^M \zeta_{\beta}(t) \varphi_{\beta}(\xi) \right) \left( \sum_{\alpha=0}^M y_{\alpha}(t) \varphi_{\alpha}(\xi) \right) \quad (4.31)$$

Since the polynomials are independent of time, we essentially only need to take the derivatives of the coefficients.

$$\left( \sum_{\alpha=0}^M \frac{dy_{\alpha}(t)}{dt} \varphi_{\alpha}(\xi) \right) = \left( \sum_{\alpha=0}^M \sum_{\beta=0}^M y_{\alpha}(t) \zeta_{\beta}(t) \varphi_{\alpha}(\xi) \varphi_{\beta}(\xi) \right) \quad (4.32)$$

**Step 3:** Projecting equation (4.32) on to the basis function  $\varphi_{\gamma}(\xi)$ ,

$$\left\langle \sum_{\alpha=0}^M \frac{dy_{\alpha}(t)}{dt} \varphi_{\alpha}(\xi) \varphi_{\gamma}(\xi) \right\rangle = \left\langle \sum_{\alpha=0}^M \sum_{\beta=0}^M y_{\alpha}(t) \zeta_{\beta}(t) \varphi_{\alpha}(\xi) \varphi_{\beta}(\xi) \varphi_{\gamma}(\xi) \right\rangle \quad (4.33)$$

**Step 4:** Applying the orthogonal property of basis functions, equation (4.33) is reduced to

$$\langle \varphi_{\gamma}^2 \rangle \frac{dy_{\alpha}}{dt} = \sum_{\alpha=0}^M \sum_{\beta=0}^M y_{\alpha}(t) \zeta_{\beta}(t) \langle \varphi_{\alpha}(\xi) \varphi_{\beta}(\xi) \varphi_{\gamma}(\xi) \rangle \quad (4.34)$$

Now, we can solve the above equation (4.34) for the coefficients. Although this is a very rigorous way of computing the coefficients, every time when we change the model the whole code has to be rewritten and tailored for every case for every model. These inner products are not straightforward for highly nonlinear systems. Furthermore, while solving equation (4.34), we get a set of  $(M + 1)$  ODEs per state variable and there are also errors associated with the time derivative. The approximations of the time derivative would lead to long time integration problems. The non-intrusive spectral projection method helps to resolve these issues.

#### 4.9.2 Galerkin's non-intrusive spectral projection (NISP)

This method is straightforward. It also relies on numerical integration to obtain the coefficients. However, computing the inner products relies on the sampled response of the system. There are essentially two ways to do this:

- One way is to conduct random sampling like Monte Carlo or Quasi Monte Carlo samples in which samples are drawn and the integral is evaluated. This approach is particularly effective when dealing with discontinuous functions and also high-dimensional systems in the sense of uncertainties; however, this form of approximation has a relatively very slow convergence rate. The chaos coefficients are calculated as,

$$y_\alpha = \frac{\langle y, \varphi_\alpha \rangle}{\langle \varphi_\alpha^2 \rangle} = \frac{1}{\langle \varphi_\alpha^2 \rangle} \int y(\theta(\xi)) \varphi_\alpha(\xi) p_\xi(\xi) d\xi \quad (4.35)$$

Using random sampling the integral is evaluated as,

$$\int y(\theta(\xi)) \varphi_\alpha(\xi) p_\xi(\xi) d\xi = \frac{1}{S} \sum_{j=1}^S y(\theta(\xi_j)) \varphi_\alpha(\xi_j) \quad (4.36)$$

- Another approach for computing the projected integral involves applying the quadrature rules where the integral can be approximated as a weighted integrand evaluated at the different quadrature nodes. This is a particularly effective method for 1-dimensional case where we have a univariate uncertainty; these integrals can be computed exactly. However, the problem in this approach is that as we go to higher uncertainty dimensions then we would have to evaluate the tensor product which scales exponentially with the number of function evaluations. Using this approach, the integral in equation (4.35) is evaluated as,

$$\int y(\theta(\xi)) \varphi_\alpha(\xi) p_\xi(\xi) d\xi = \sum_{j=1}^Q q_j y(\theta(\xi_j)) \varphi_\alpha(\xi_j) \quad (4.37)$$

where  $q_j$  is the  $j$ th quadrature node.

## 4.10 Summary

In this exploration of stochastic spectral methods, a multitude of strategies and techniques are discussed that allow us to solve complex problems full of uncertainty. From Monte Carlo simulations to polynomial chaos expansions and from spectral methods to Galerkin formulae, this chapter have dissected the toolbox that allows us to confront stochastic phenomena. Each approach has its own strengths and nuances, satisfying a wide range of applications spanning many different fields. Each of these strategies has their distinct advantages and limitations. Monte Carlo methods, through their simplicity and flexibility, offer a common language for stochastic processes. Polynomial chaos expansion provides an elegant route to capturing nonlinearity and uncertainty through orthogonal basis functions. Spectral methods exploit the ability to transform problems into spectral domains, thereby allowing for efficient, higher-order approximations. Galerkin's formulations, with their variational foundations, provide robust frameworks for deterministic and stochastic systems.

At the end of this chapter, we turn our focus to the practical applications of these methods. In the next chapter, we will delve deeper into the field of polynomial chaos methods, using them as excellent tools to solve real-world challenges in complex systems. This transition from theory to practice will highlight the power of these methods and their transformative impact on the ability to model, understand, and design wider range of systems.

In the next chapter, we discussed various domains of science and engineering to apply these methods and solved complex problems such as contaminant transport and stochastic advection-diffusion equations, addressing linear and nonlinear systems. Furthermore, we also develop a metamodel using geometric Brownian motion that has venture into the world of finance, exploring option pricing where the ability to model uncertainty is paramount.

This next chapter is the bridge between theory and practice, where our understanding of stochastic spectral methods will be put to the test against tangible and complex scenarios. Our aim is not only to demonstrate the versatility of these methods but also to provide valuable insights and solutions that can impact industries, research, and decision-making processes.

## Chapter 5

### Application of Stochastic Spectral Methods

Stochastic Partial Differential Equations (SPDEs) are powerful mathematical tools used to describe complex physical, biological, and engineering systems subjected to uncertainty and randomness. These equations capture the interplay between deterministic evolution and stochastic fluctuations, making them indispensable for modelling real-world phenomena such as heat transfer in random media, fluid flow in porous media, and financial derivatives pricing under uncertain market conditions. However, solving SPDEs analytically or numerically can be highly challenging due to the intrinsic randomness involved. This is where stochastic spectral methods come into play; they offer a versatile and efficient framework for tackling SPDEs by representing the solution in a spectral expansion, based on orthogonal polynomial chaos, or another stochastic basis. These methods provide researchers with a systematic approach to quantifying uncertainties, enabling researchers to propagate them using simulations, and gain deeper insights into the underlying stochastic processes. In this context, the importance of stochastic spectral methods cannot be overstated; they empower researchers and practitioners to address real-world problems that involve both deterministic dynamics and inherent randomness with accuracy and efficiency.

Stochastic spectral methods have extensive applications in various scientific and engineering fields (El-Amrani et al., 2012; Matthies et al., 1997; Tryoen et al., 2010) where the presence of uncertainty plays an important role. These methods use spectral representations to model and analyse random processes. These methods comment on statistical properties of the model under study and provide valuable insights. A prominent application of these methods is in finance. Here, stochastic spectrum techniques enable the pricing and risk assessment of complex derivatives that consider the inherent uncertainties of the underlying assets. Furthermore, in computational physics, these methods provide efficient techniques for simulating and studying stochastic systems such as molecular dynamics and quantum mechanics by incorporating randomness into the governing equations. Probabilistic spectral methods can also be applied to data science and machine learning, enabling probabilistic modelling, uncertainty quantification, and Bayesian inference. The application of probabilistic spectral methods spans a wide range of fields, contributing to improved decision-making, a deeper understanding of complex systems, and more robust statistical analysis in the face of uncertainty. This chapter examines some of these applications using stochastic spectral methods.

## 5.1 Development of a meta model for geometric Brownian motion (gBM)

### 5.1.1 Formulation of a random variable in Wiener chaos space

A sequence of random variables  $W = \{W(t)\}_{t \geq 0} \in \mathbb{R}$  in a time domain on a probability space  $(\Omega, \mathcal{F}, \mathbb{P})$  is known as a standard Brownian motion and satisfies all the properties defined in Chapter 3 (Definition 3.2).

For a fixed  $T \in (0, \infty)$  and a filtration, let  $\mathcal{F}_t^W$  be the sigma-algebra generated by these random variables for  $0 \leq t \leq T$ .

Using Cameron-Martin basis (Cameron & Martin, 1947) for a countable multi-index set,

$$\mathcal{J} = \{(\alpha_i^j, i, j \geq 1), \alpha_i^j \in \{0, 1, \dots\}\} \text{ with } \alpha! = \prod_{i,j} \alpha_i^j! \quad (5.1)$$

here  $i$  and  $j$  are the number of Gaussian random variables and the Wiener processes respectively.

According to the Cameron-Martin theorem, there exists an orthonormal basis  $m_i, i \geq 1$  of square integrable space  $\mathcal{L}^2([0, T])$ , such that a set of independent random variables  $\xi_{ij}$  is defined as,

$$\xi_{ij} = \int_0^T m_i(\tau) dW_\tau^j \quad (5.2)$$

Now, the set of random variables known as Cameron-Martin basis are defined as,

$$\mathfrak{X} = \{\xi_\alpha, \alpha \in \mathcal{J}\} \quad (5.3)$$

A space generated by this basis is the Wiener chaos space  $\mathfrak{w}$  and a random variable

$f(\omega) \in \mathfrak{w}$ , for some realisation  $\omega$  is written in terms of Wiener chaos expansion as,

$$f = \sum_{\alpha \in \mathcal{J}} a_\alpha \xi_\alpha \quad (5.4)$$

An orthogonal basis for multi-indices is calculated using the definition provided in Table 4.3 in Chapter 4.

### 5.1.2 Computation of coefficients

For a random variable  $f(\mathbb{X})$ , where  $\mathbb{X} = (\xi_{1j}, \xi_{2j}, \dots)$ ,

$$f(\mathbb{X}) = \sum_{\alpha \in \mathcal{J}} a_\alpha \xi_\alpha(\mathbb{X}) \quad (5.5)$$

and,

$$a_\alpha = \frac{\langle f, \xi_\alpha \rangle}{\|\xi_\alpha\|^2} \quad (5.6)$$

also,

$$E(f(\mathbb{X})) = a_{\alpha_0}, \alpha_0 = (0, 0, \dots) \quad (5.7)$$

$$\text{var}(f(\mathbb{X})) = \sum_{\alpha \in \mathcal{J}} a_{\alpha}^2 \|\xi_{\alpha}\|^2 \quad (5.8)$$

For computation purpose, the truncation scheme is,

$$\mathcal{J}_{n,p} = \{\alpha = (\alpha_1, \alpha_2, \dots, \alpha_p), |\alpha| \leq n\} \quad (5.9)$$

where  $n$  and  $p$  are the higher order Hermite polynomials and the maximum number of Gaussian random variables used in the expansion.

With this truncation scheme, we have

$$f(\mathbb{X}) \approx \sum_{\alpha \in \mathcal{J}_{n,p}} a_{\alpha} \xi_{\alpha}(\mathbb{X}) \quad (5.10)$$

### 5.1.3 Meta model

With the above set up defined, we now develop a meta model for geometric Brownian motion (Jacka & Oksendal, 1987) given by the solution of SDE, as defined in Section 3.7.1.

Again,

$$dY_t = \mu(t, Y_t)dt + \sigma(t, Y_t)dW_t \quad (5.11)$$

gBM is the solution of equation (5.11).

Applying the Euler-Maruyama method and using independent increments of the Wiener process and for each increment  $m = \{0, 1, \dots, M - 1\}$ , we have,

$$Y_{t_{m+1}} = Y_{t_m} (1 + \mu(t_m, Y_{t_m})\Delta t_m + \sigma(t_m, Y_{t_m})\sqrt{\Delta t_m}N(0,1)) \quad (5.12)$$

for  $0 = t_1 < t_2 < \dots < t_{M-1} < t_M = T$  and  $\Delta t_m = t_{m+1} - t_m$

For meta modelling, we input this multivariate function in the form,

$$Y_{t_m} = \mathcal{M}(\mathbb{Y}) \quad (5.13)$$

$$\mathbb{Y} = (\xi_1, \xi_2, \dots, \xi_{m-1}), \xi_i \sim N(0,1)$$

and, for the Euler-Maruyama scheme,

$$W(t) \sim N(0, t), t \in [0, T]$$

This model automatically chooses Hermite polynomials as the basis functions since the random variables are Gaussian. More conveniently, equation (5.13) is written as

$$Y_t = Y_{t_m} = Y_0 \prod_{m=0}^{M-1} (1 + \mu(t_m, Y_{t_m})\Delta t_m + \sigma(t_m, Y_{t_m})\sqrt{\Delta t_m} \xi_m) \quad (5.14)$$

Using a suitable transformation, gBM converts the SDE (5.11) into the form (5.13).

Using Itô's lemma and defining  $X_t = \ln S_t$ , we get

$$dX_t = \left(\mu - \frac{1}{2}\right)\sigma^2 dt + \sigma(t, X_t)dW_t \quad (5.15)$$

Now for any computed value of  $X_t$ , we have,

$$S_t = e^{X_t} \quad (5.16)$$

and this output is of the form

$$S_T = \mathcal{M}(\mathbb{Y}, \odot) \quad (5.17)$$

where  $\odot$  is the transformation.

Using a UQLab framework (Marelli & Sudret, 2014) and feeding input  $\mathbb{Y}$  as gBM, we develop a meta model. Figure 5.1 to Figure 5.3 represent the PCE coefficients spectrum based on different methods. The output of the model is summarised in Table 5.1.

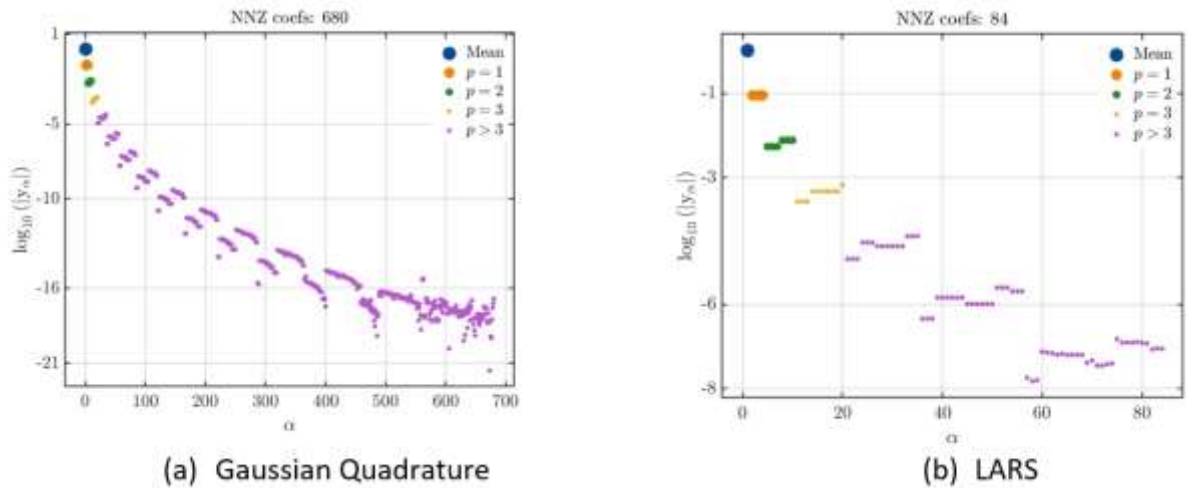


**Figure 5.1** Spectrum of the PCE coefficients for the meta modelling of geometric Brownian motion using Gaussian quadrature and Least Angle Regression.

*Note.* NNZ represents the number of non-zero coefficients in the chaos expansion.

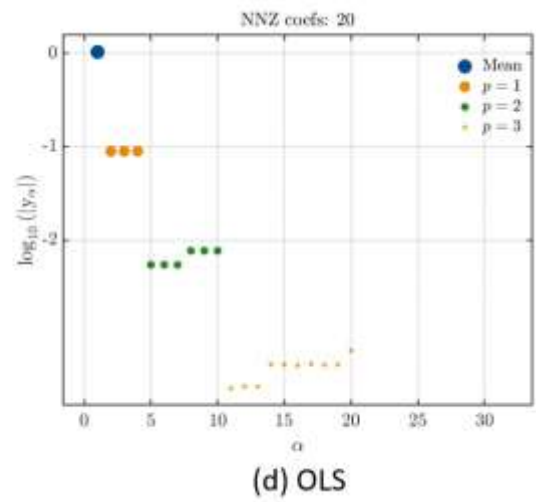
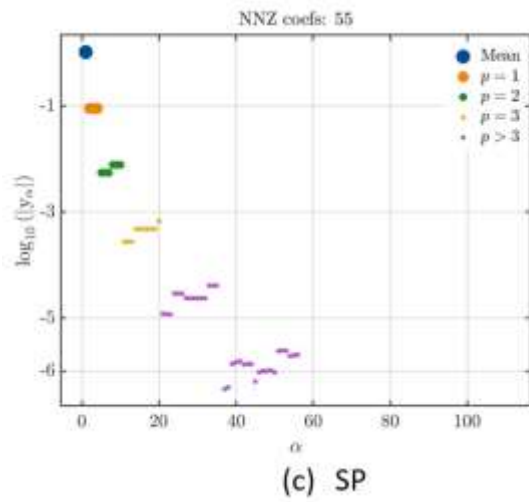


**Figure 5.2** Spectrum of the PCE coefficients for the meta modelling of geometric Brownian motion using Subspace and Ordinary Least Squares Regression.

*Note.* NNZ represents the number of non-zero coefficients in the chaos expansion.

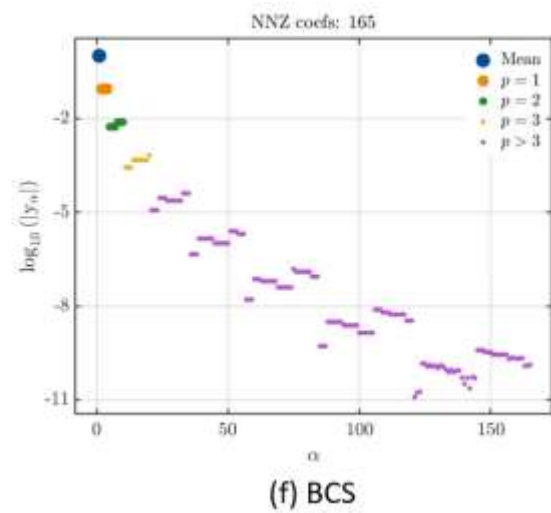
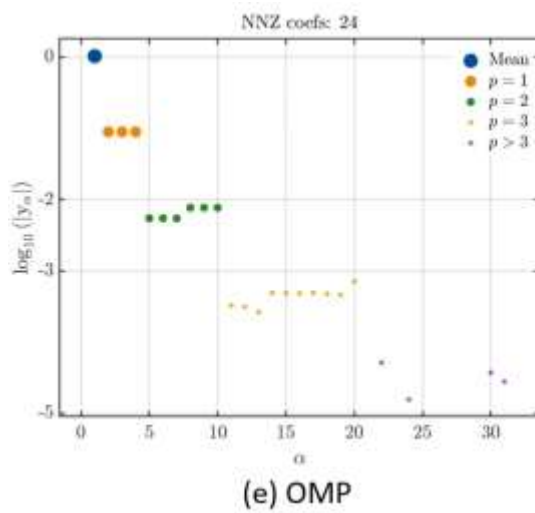


**Figure 5.3** Spectrum of the PCE coefficients for the meta modelling of geometric Brownian motion using Orthogonal Matching Pursuit and Bayesian Compressive Sensing.

*Note.* NNZ represents the number of non-zero coefficients in the chaos expansion.

**Table 5.1 Meta model's input and output parameters.**

Parameters	Method					
	Gaussian Quadrature	BCS	LARS	SP	OMP	OLS
Number of input variables	3	3	3	3	3	3
Maximal degree	14	8	6	9	5	5
q-norm	1	1	1	0.75	0.75	0.75
Size of full basis	680	165	84	111	32	32
Size of sparse basis	680	165	84	55	24	20
Full model evaluations	3375	500	150	150	150	150
Quadrature error	2.24E-29	2.54E-19	1.04E-13	8.13E-12	3.52E-07	1.43E-07
Mean value	1.0305	1.0305	1.0305	1.0305	1.0305	1.0305
Standard deviation	0.1554	0.1554	0.1554	0.1554	0.1554	0.1554
Coefficient of variation	15.09%	15.09%	15.09%	15.09%	15.09%	15.09%

*Note.* These methods are Gaussian quadrature, Ordinary Least Squares Regression (OLS), Least Angle Regression (LARS), Orthogonal Matching Pursuit (OMP), Subspace (SP), and Bayesian Compressive Sensing (BCS). The hyperbolic truncation scheme is used with q-norm in the range  $0 \leq q\text{-norm} \leq 1$ . The Sobol sequence sampling strategy is used for all methods. The graphs show that the number of PCE coefficients can be reduced using a suitable evaluation method and the sparse sampling technique.

This model is also validated with a set of 1E4 samples. The results for the validation error using different approaches are provided in Table 2.

**Table 5.2 Relative error for model validation.**

Validation Parameter	Gaussian Quadrature	BCS	LARS	SP	OMP	OLS
Relative error	4.59E-28	1.56E-18	1.27E-13	1.10E-06	7.54E-11	6.92E-07

Figure 5.4 plots the actual and PCE evaluated output  $y$ .

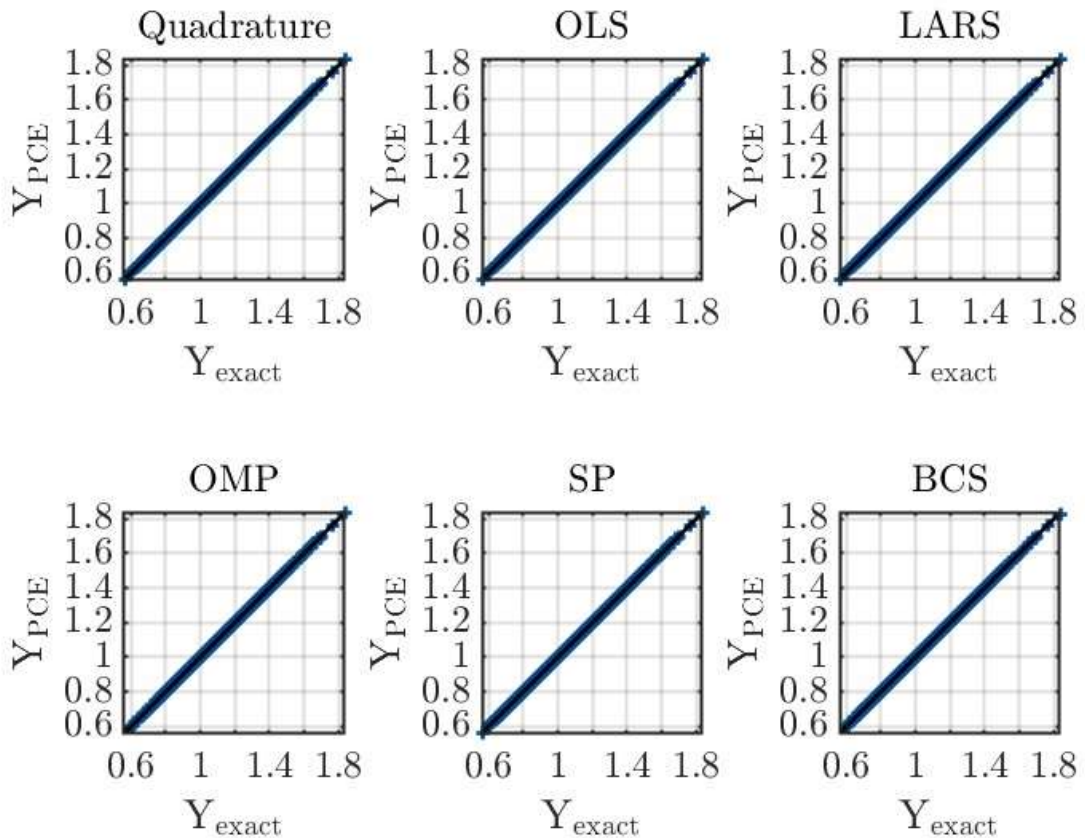


**Figure 5.4** Sample response of model output  $Y$  against the actual values, based on the validation sample set used for modelling.

## 5.2 Ordinary differential equation with stochastic input

One-dimensional first-order differential equations with stochastic inputs form an attractive research area, located at the boundary between differential equations and stochastic processes. Here, the rate of change of the variable depends not only on the determinant factor, but also on random influences. Stochastic inputs introduce a degree of unpredictability and uncertainty to the system, challenging traditional deterministic modelling approaches. For example, in physics, they can be used to model the behaviour of particles under the influence of random forces, or to describe the diffusion of matter in media with random fluctuations. In finance, these inputs can be used to model the movement of stock prices under the influence of random market forces. Moreover, in biological systems, these equations can capture the effects of stochastic variations in gene expression and biochemical reactions.

### 5.2.1 Numerical example

Let us consider a simple differential equation with input parameter ' $k$ ' defined as,

$$\frac{dy}{dt} = -ky \quad (5.18)$$

with initial condition  $y(0) = y_0$

The exact solution of this ODE is  $y = y_0 e^{-kt}$ . The expected value of this stochastic equation is  $y = y_0 \exp\left(-\frac{t^2}{2}\right)$ .

We first plot the solution of equation (5.18) when  $k$  is deterministic (Figure 5.5) with initial condition  $y(0) = 1$ .

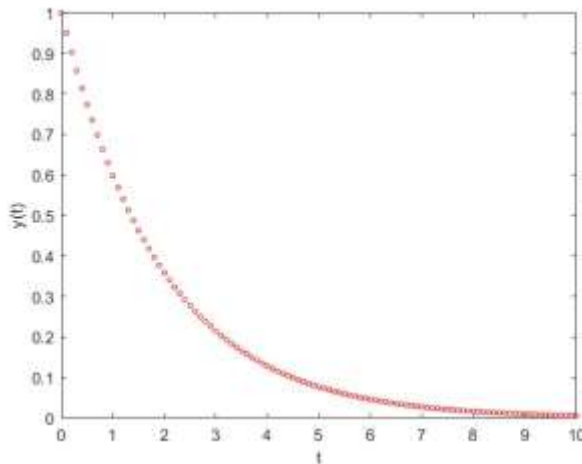


**Figure 5.5** Deterministic solution of equation (5.18).

However, most of the parameters in real-life phenomena and complex systems do not show deterministic behaviour; that is why we now encounter stochasticity in input parameters.

Now, let us consider ' $k$ ' as a stochastic input, varying uniformly between the interval [2,4].

As explained in Chapter 4, we applied the stochastic Galerkin method to characterise the variability in ' $k$ ' (Figure 5.6).

While applying this method, stochastic collocation is sampled at the collocation nodes

[0.2254 1 1.7746] with weights [0.4444 0.2778 0.2778] as described in Chapter 3 (Section 3.5.5).

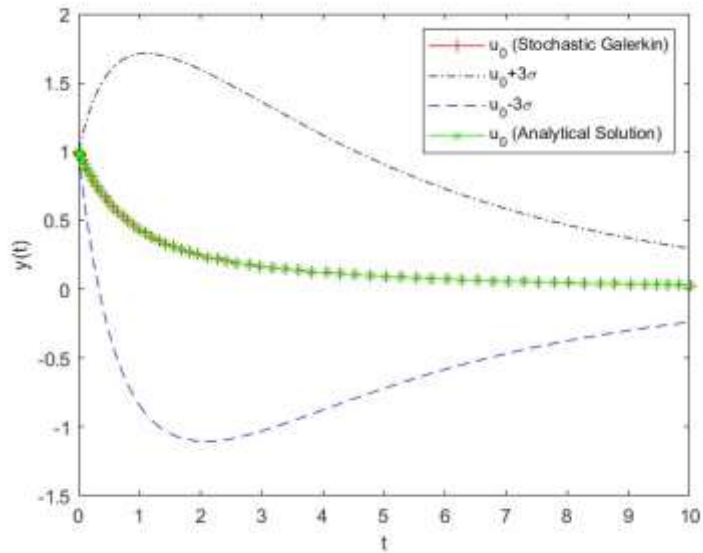


**Figure 5.6 Stochastic simulation of equation (5.18) using the stochastic Galerkin method.**

It is clear from the graph; discretising the randomness through nodes only means that the stochastic nature of the parameter, such as random fluctuations in chemical reactions due to factors like temperature variations or the presence of impurities, is not visible. Biological processes often involve random factors, such as genetic mutations, cellular interactions, and population fluctuations. Equations similar to equation (5.18) are being used to model these processes at the single-cell level.

We solve this equation using Polynomial chaos expansion and Monte Carlo (MC) simulation using 10000 samples. For MC simulation, random samples for  $k(t)$  are generated, assuming a Gaussian distribution for each time step using the pseudo random number generator (Dunn & Shultis, 2023) in MATLAB. Performing the integral for each time step, storing the solutions for each sample in the solutions array, sample results for 5 outputs are plotted in Figure 5.7 and Figure 5.8 to visualise the stochastic behaviour of the solution.

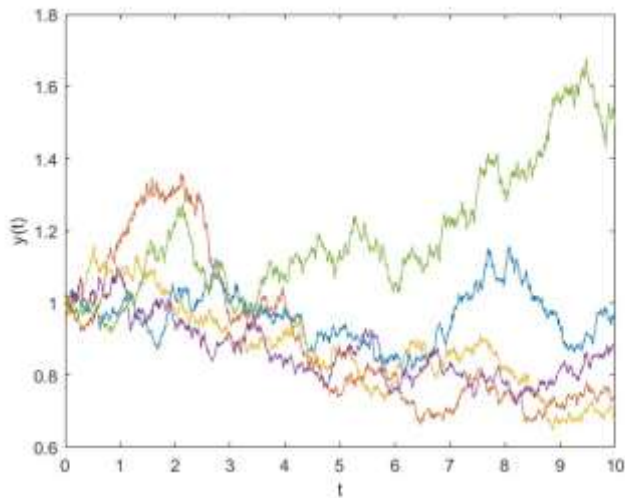


**Figure 5.7** The MC simulation output for equation (5.18) was obtained by generating  $10^5$  samples for the stochastic parameter ' $k$ '.

*Note.* Initial condition  $y(0) = 1$  with time step  $\Delta t = 10^3$ .

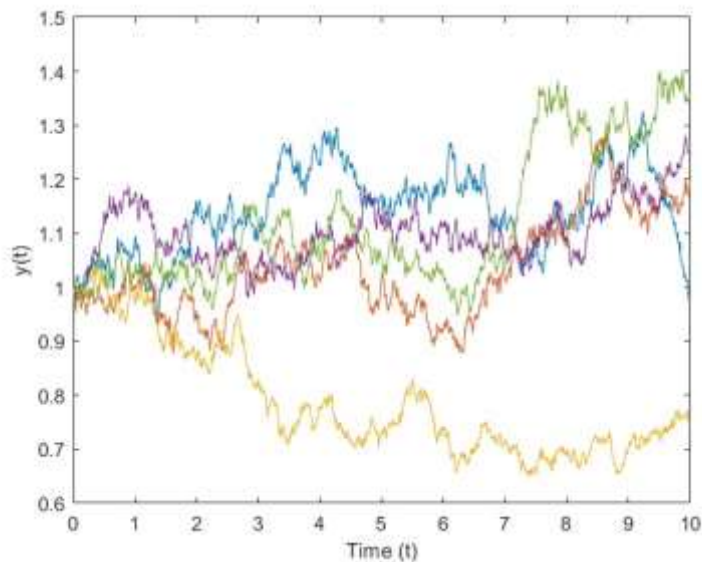


**Figure 5.8** The PCE simulation for equation (5.18) using Hermite polynomials as an orthogonal basis function and order of polynomial is 5.

*Note.* Initial condition  $y(0) = 1$  with a time step  $\Delta t = 10^3$ .

While the results obtained using the MC method and the PCE method are almost similar, we observed differences in the computational efficiency of both methods. Table 5.3 shows the difference in computing times for both of the methods. Although this difference is not so significant (because the governing equation (5.18) is simple and does not involve much complexity. For complex systems involving a large number of parameters, this difference is quite significant. Some efforts have been made to resolve this problem using quasi-MC methods and variance reduction methods.

**Table 5.3 Computation time for MC method and PCE method to solve equation (5.1).**

Statistics	MC Simulation	PCE Simulation
Mean	0.000100	0.701900
Variance	0.000000	0.023199
Execution Time (in seconds)	2.906200	0.332824

Figure 5.9 illustrates the individual response for output  $y$  based on various polynomial orders.

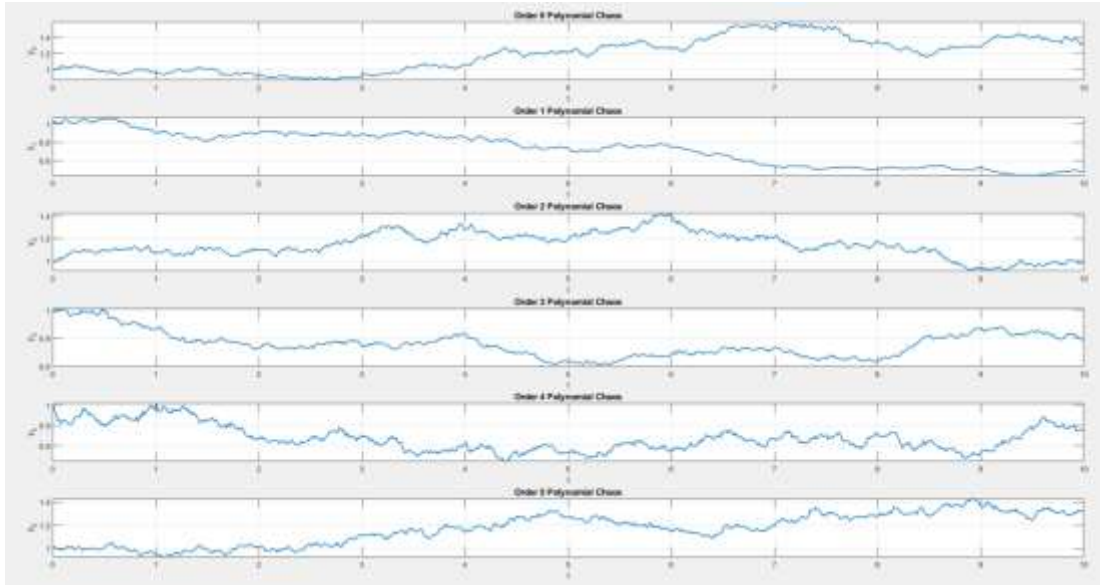


**Figure 5.9 Sample response for  $y$ , using polynomial chaos expansion, with different order and Hermite polynomials as the orthogonal basis function.**

*Note.* Initial condition  $y(0) = 1$  with time step  $\Delta t = 10^3$ .

The mean response and variance of the output for the time-interval  $(0,10)$  is plotted in Figure 5.10.

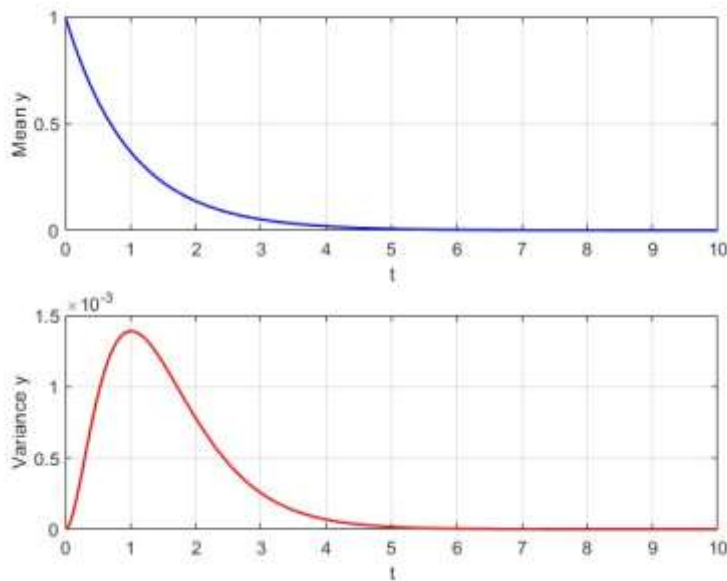


**Figure 5.10** Distribution of mean and variance using the PCE method.

### 5.3 Stochastic contaminant transport

Hydrological models have been used to understand the movement and distribution of water, pollutants, and pollutants in natural systems, such as rivers, lakes, groundwater, and watersheds. These models provide valuable tools for assessing water quality, managing water resources, and minimising the impact of contaminants on aquatic ecosystems and human health. One of the key elements of hydrological modelling is the advection dispersion equation (ADE), a basic mathematical framework used to describe the transport and dispersion of solutes in bodies of water.

The advection-dispersion equation represents the interaction between two essential mechanisms that govern contaminant transport: advection and dispersion. Advection refers to the mass movement of water and dissolved substances, driven by factors such as velocity and hydraulic gradient. In contrast, dispersion represents the spreading and mixing of contaminants due to molecular diffusion and turbulent flow. Together, these phenomena influence the fate and transport of contaminants, making ADE a cornerstone of hydrogeology, environmental engineering, and water resource management. A detailed literature review has been provided in Section 2.2.1 of Chapter 2.

This study explores the integration of the advection dispersion equation in relation to the dynamics of contaminant transport. By analysing how contaminants disperse and move in aquatic systems, researchers and water resource managers can obtain important information about contaminant behaviour, evaluate environmental risks, and design effective control and mitigation strategies. This involves modelling the transport of contaminants, such as chemicals or pollutants, while considering the uncertainties inherent in parameters such as hydraulic conductivity and source release rate.

The Polynomial Chaos Expansion (PCE) method has proven to be a powerful tool in addressing this challenge. PCE exploits orthogonal polynomial basis, such as Hermite or Legendre polynomials, to represent uncertain parameters as random variables in a probabilistic framework. By scaling the solution along these polynomials, the PCE method effectively quantifies the propagation of uncertainty, thereby providing insight into the probabilistic behaviour of contaminant transport. This approach enables decision makers and scientists to better assess risks, design remediation strategies, and make informed choices in complex environmental situations. The stochastic transport of contaminants using PCE illustrates the intersection of advanced mathematics and environmental science, providing a robust framework for managing environmental risks and uncertainties.

### 5.3.1 Polynomial chaos expansion and formulation

The stochastic ADE for contaminant transport (El-Amrani et al., 2012) is given below:

$$\frac{\partial C}{\partial t} + \mu \cdot \nabla C = \nabla \cdot [\kappa(x; \omega) \nabla C] + F(t, x; \omega), \quad (t, x; \omega) \in \mathbb{R}^+ \times \mathbb{D} \times \Omega \quad (5.19)$$

with the initial condition  $C(0, x; \omega) = C_0(x; \omega)$ .

Where  $C$  is the concentration of the contaminant within the bounded domain  $\mathbb{D} \in \mathbb{R}^d (d = 1, 2)$ ,  $\mathbb{R}^+$  is the time domain  $(0, T]$  and  $\Omega$  is the sample space.  $F(t, x; \omega)$  is the random forcing term.

We consider  $F(t, x; \omega) = \sigma \frac{\partial W}{\partial t}$ , where  $\sigma$  is the standard deviation of the stochastic term, and  $\frac{\partial W}{\partial t}$  represents the time derivative of a Wiener process which introduces stochastic variability.

$\mu$  is the mean advection velocity representing the bulk flow of the fluid,  $\kappa(x; \omega)$  is the dispersion coefficient characterising the rate of diffusion, and  $C_0(x; \omega)$  is the initial condition.

$\kappa(x; \omega)$  and  $C_0(x; \omega)$  are both real valued functions in  $D$  and  $\Omega$  for all random inputs.

MC simulation is the most popular approach for solving equation (5.19), based on random number generation, in which the response of each sample is stored and the problem becomes deterministic. Taking all responses in to account, an ensemble of the final solution is obtained. While this is a straightforward approach, the computational effort is high in order to obtain a convergent solution. PCE considers this issue using the Wiener-Askey chaos theory (explained in Section 4.7 of Chapter 4) suggested by (Xiu & Karniadakis, 2006).

In gPCE, random numbers are chosen based on the probability distribution of input variables and corresponding orthogonal basis functions. A correspondence between the two are shown in Figure 4.6 in Chapter 4.

As explained in Section 4.7.2 of Chapter 4, choosing  $\{\varphi_n\}, n = 0, 1, \dots$  as orthogonal polynomials for random variable  $\xi$  satisfies the orthogonality condition given.

Applying gPCE to equation (5.19), we have

$$\kappa(x; \omega) = \sum_{i=0}^N \kappa_i(x, t) \varphi_i(\xi) \quad (5.20)$$

$$C(t, x; \xi) = \sum_{j=0}^N C_j(t, x) \varphi_j(\xi) \quad (5.21)$$

and

$$F(t, x; \xi) = \sum_{j=0}^N F_j(t, x) \varphi_j(\xi) \quad (5.22)$$

The value of  $N$  (the total number of expansion terms) is based on the order of polynomials ( $n$ ) used and the dimension of the random space ( $p$ ). It is given by,

$$N + 1 = \frac{(n + p)!}{n! p!} \quad (5.23)$$

Substituting equation (5.20) to equation (5.22) in the governing equation (5.19), we get

$$\begin{aligned} & \sum_{j=0}^N \frac{\partial C_j(t, x)}{\partial t} \varphi_j(\xi) + \mu \sum_{j=0}^N \nabla C_j(t, x) \varphi_j(\xi) \\ &= \nabla \cdot \left[ \sum_{i=0}^N \kappa_i(x) \varphi_i(\xi) \nabla \left( \sum_{j=0}^N C_j(t, x) \varphi_j(\xi) \right) \right] + \sum_{j=0}^N F_j(t, x) \varphi_j(\xi) \end{aligned} \quad (5.24)$$

Rewriting the above equation,

$$\sum_{j=0}^N \frac{\partial C_j(t, x)}{\partial t} \varphi_j + \mu \sum_{j=0}^N \nabla C_j(t, x) \varphi_j = \left[ \sum_{i=0}^N \sum_{j=0}^N \nabla \cdot [\kappa_i(x) \nabla C_j(t, x)] \right] \varphi_i \varphi_j + \sum_{j=0}^N F_j(t, x) \varphi_j \quad (5.25)$$

Next, applying the Galerkin projection onto each polynomial basis to ensure that the induced error is orthogonal to functional space spanned by truncated finite dimensional basis functions  $\varphi_n$ . Projecting  $\varphi_m$  for each  $m = \{0, 1, \dots, N\}$  and applying the orthogonality conditions, we get

$$\frac{\partial C_m}{\partial t} + \mu \nabla C_m = \sum_{i=0}^N \sum_{j=0}^N \nabla \cdot [\kappa_i(x) \nabla C_j] \mathbf{E}_{imj} + F_m \quad (5.26)$$

where  $\mathbf{E}_{imj} = \langle \varphi_i \varphi_k \varphi_j \rangle$  and is calculated as  $\mathbf{E}_{imj} := \frac{\langle \varphi_i \varphi_j \varphi_m \rangle}{\langle \varphi_m, \varphi_m \rangle}$  by setting up the definition of  $\varphi_n$ .

The above equation can be written as,

$$\frac{\partial C_m}{\partial t} + \mu \nabla C_m = \sum_{j=0}^N \nabla \cdot [a_{mj}(x) \nabla C_j] + F_m \quad (5.27)$$

or

$$\frac{\partial C_m}{\partial t} = \sum_{j=0}^N [a_{mj}(x) \nabla^2 C_j + b_{mj}(x) \cdot \nabla C_m] - \mu \cdot \nabla C_m + F_m, \quad m = 0, 1, \dots, N \quad (5.28)$$

where,

$$a_{mj}(x) = \sum_{i=0}^N \kappa_i(x) \mathbf{E}_{imj} \quad (5.29)$$

and,

$$b_{mj}(x) = \sum_{i=0}^N \nabla \kappa_i(x) \mathbf{E}_{imj} = \nabla a_{mj}(x) \quad (5.30)$$

Equation (5.28) is a set of (N+1) coupled deterministic equations with an initial condition,

$$C(0, x; \omega) = \sum_{j=0}^N C_j(0, x) \varphi(\xi) = C_0(x; \omega)$$

where the coefficients  $C_j(0, x) = C_0(x)$  in the expansion are deterministic and we are able to obtain the initial and boundary conditions for each expanded equation in (5.28).

### 5.3.2 Numerical simulation

For numerical simulation, we considered a one-dimensional case and the equation,

$$\frac{dC(t, x; \omega)}{dt} + \mu \frac{dC(t, x; \omega)}{dx} = \frac{d}{dt} \left[ \kappa(x; \omega) \frac{dC(t, x; \omega)}{dx} \right] + F(t, x; \omega) \quad (5.31)$$

with the deterministic initial condition  $C(0, x; \omega) = 1$  and boundary conditions  $x \in [0, 1)$ . Without a loss of generality, randomness in transport is characterised by considering the random forcing term as  $F(t, x; \omega) = \sigma \frac{\partial W}{\partial t}$  with the Wiener process term and  $\kappa(x; \omega)$  is characterised with  $\kappa(x; \omega) = \xi$ .

While completing MC simulation,  $10^5$  random numbers are generated. For Polynomial chaos expansion the randomness in  $\sigma$  is captured through the polynomial basis functions and the Wiener process. Figure 5.11 and Figure 5.12 shows the concentration profile using the MC method with  $10^4$  samples and the PCE method of polynomial order 3 for  $C(0, x; \omega) = 1$ .

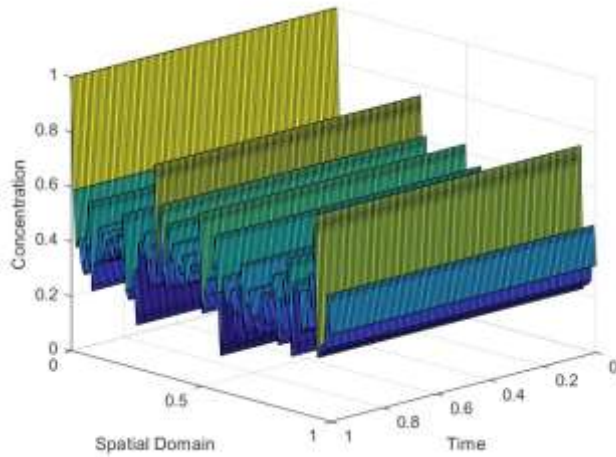


**Figure 5.11 Simulation of concentration  $C$  using the MC method.**

*Note.* Time domain  $\mathbb{R}^+$  is  $(0,1]$  with time step  $\Delta t = 0.01$ ,  $C(0, x; \omega) = 1$ , space domain  $x \in [0,1]$  and number of random samples = 10000.

The Figure 5.12 shows that PCE method is better in capturing the randomness in  $C(t, x; \omega)$  compared to MC simulation.

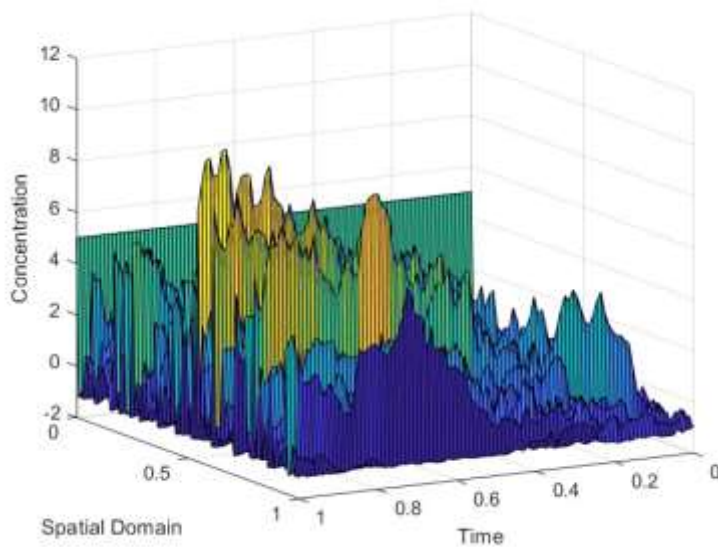


**Figure 5.12 Simulation of concentration  $C$  using the PCE method .**

*Note.* Time domain  $\mathbb{R}^+$  is  $(0,1]$  with time step  $\Delta t = 0.01$ ,  $C(0, x; \omega) = 1$ , using Hermite polynomials of order 3 and maximum order of polynomial chaos expansion = 5. The mean and standard deviation of the Gaussian distribution are 0 and 1, respectively.

Figure 5.13 which show the MC simulation and Figure 5.14 using PCE are plotted with periodic boundary conditions  $C(0, x; \omega) = \sin \pi x$  and for the same initial condition  $C(0, x; \omega) = 1$ .

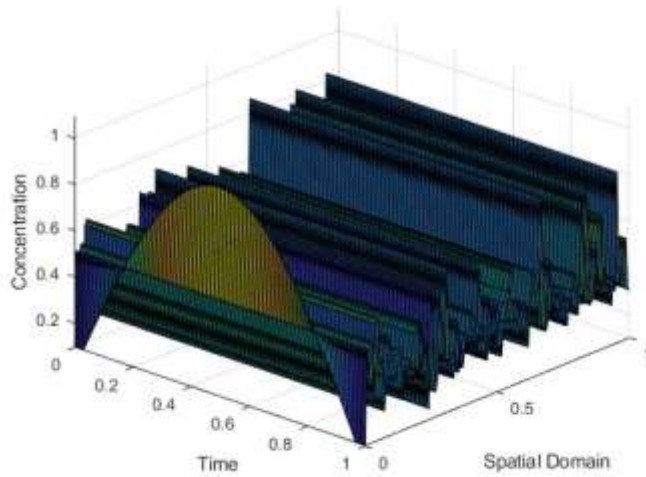


**Figure 5.13 Simulation of concentration  $C$  using the MC method.**

*Note.* Time domain  $\mathbb{R}^+$  is  $(0,1]$  with time step  $\Delta t = 0.01$ ,  $C(0, x; \omega) = \sin \pi x$ , the number of random samples = 1000000 and space domain  $x \in [0,1)$ . The total elapsed time for the simulation is 6.065921 seconds.

When the number of random samples for MC are increased to  $10^6$  for the periodic boundary condition, the randomness is captured, but the computational time is higher (6.065921 seconds) when compared to the PCE method (0.314977 seconds).

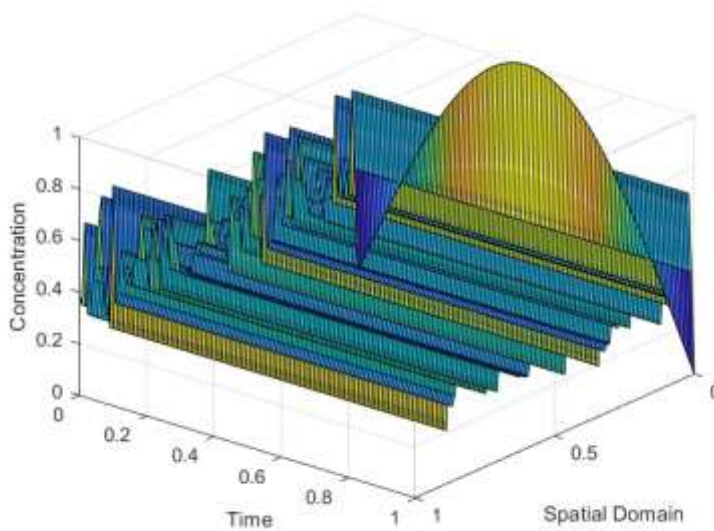


**Figure 5.14 Simulation of concentration  $C$  using the PCE method.**

*Note.* The time domain  $\mathbb{R}^+$  is  $(0,1]$  with time step  $\Delta t = 0.01$ ,  $C(0, x; \omega) = \sin \pi x$ , using Hermite polynomials of order 3 and maximum order of polynomial chaos expansion = 5. The mean and standard deviation of Gaussian distribution are 0 and 1, respectively. The total elapsed time for the simulation is 0.314977 seconds.

### 5.3.3 Choice of correct order of PCE expansion

The Polynomial chaos expansion (PCE) order plays a central role in determining the accuracy and computational efficiency of simulations. The higher order expansion includes more polynomial basis functions, capturing more complex interactions and dependencies between random variables. In short, increasing the order of PCE can improve the accuracy of the approximations, thereby allowing a more accurate representation of the underlying stochastic processes (see Figure 5.15, Figure 5.16 and Figure 5.17).

However, the polynomial chaotic order effect is not without its trade-offs. Higher-order PCE requires the evaluation of an increasing number of basis functions, resulting in a significant computational burden, especially when dealing with a large number of uncertain parameters. This computational cost can quickly become prohibitive, making it difficult to apply high-order PCE to real-world problems.

In contrast, the use of low-order PCE can introduce errors in stochastic simulations, mainly because it may not accurately capture complex, higher-order interactions between random variables. While lower-order PCE is computationally efficient, it provides limited accuracy in representing complex stochastic processes. As a result, estimated statistics, such as mean, variance, and moments, may deviate from their true values, leading to errors in forecasting and decision-making.

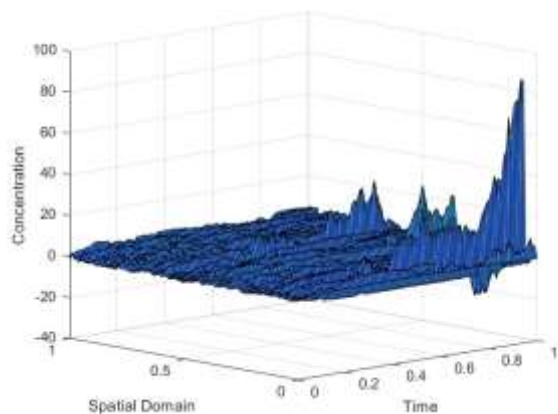


**Figure 5.15 Simulation of concentration  $C$  using the PCE method with maximum order of polynomial chaos expansion = 3.**

*Note.*  $C(0, x; \omega) = 1$ , Time domain  $\mathbb{R}^+$  is  $(0,1]$ , time step  $\Delta t = 0.01$ , using Hermite polynomials of order 3. The mean and standard deviation of Gaussian distribution are 0 and 1, respectively. The elapsed time is 6.062707 seconds.

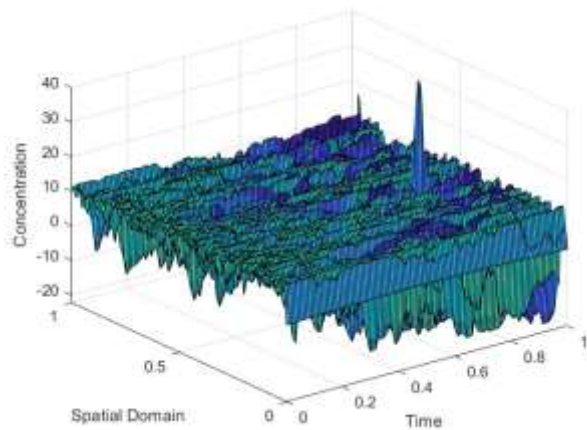


**Figure 5.16 Simulation of concentration  $C$  using the PCE method with maximum order of polynomial chaos expansion = 4.**

*Note.*  $C(0, x; \omega) = 1$ , Time domain  $\mathbb{R}^+$  is  $(0,1]$ , time step  $\Delta t = 0.01$ , using Hermite polynomials of order 4 and maximum order of polynomial chaos expansion = 4. The mean and standard deviation of Gaussian distribution are 0 and 1, respectively. The elapsed time is 8.840493 seconds.

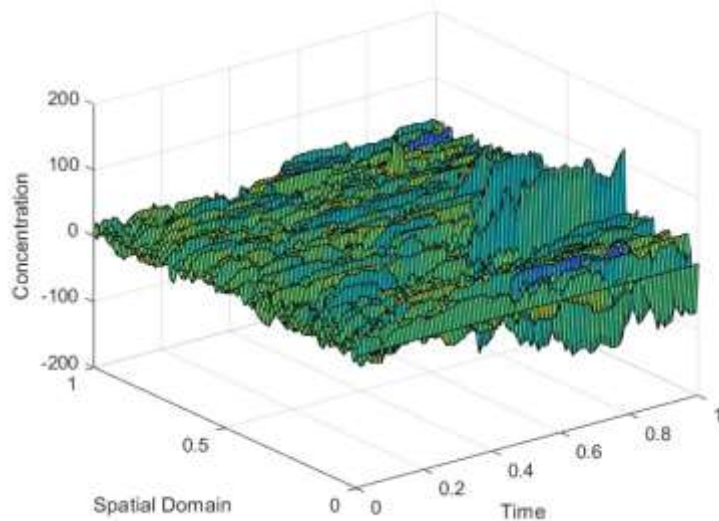


**Figure 5.17 Simulation of concentration  $C$  using the PCE method.**

*Note.*  $C(0, x; \omega) = 1$ , Time domain  $\mathbb{R}^+$  is  $(0,1]$ , time step  $\Delta t = 0.01$ , using Hermite polynomials of order 4 and maximum order of polynomial chaos expansion = 5. The mean and standard deviation of Gaussian distribution are 0 and 1, respectively. The elapsed time is 10.137710 seconds.

In the above graphs, (Figure 5.15 to Figure 5.17) PCE with order 5 provides a more realistic solution with given boundary condition for  $C(t, x; \omega)$  throughout the domain. The choice of polynomial chaos ordering in computation involves a delicate balance between accuracy and computational efficiency. We should consider the complexity of the particular problem, the available computational resources, and the desired level of accuracy when determining the appropriate ordering for PCE.

### 5.3.4 Effect of boundary conditions on the choice of order of expansion

The choice of boundary conditions plays an important role in determining the appropriate order of polynomial chaos expansion (PCE) for computer simulations. Graphs for the Gaussian initial condition  $C(0, x; \omega) = \frac{1}{\sigma_G \sqrt{2\pi}} \exp(-(x - \mu)^2 / 2\sigma_G^2)$  for different order of Hermite polynomials are shown in Figures 5.18 to Figure 5.21.

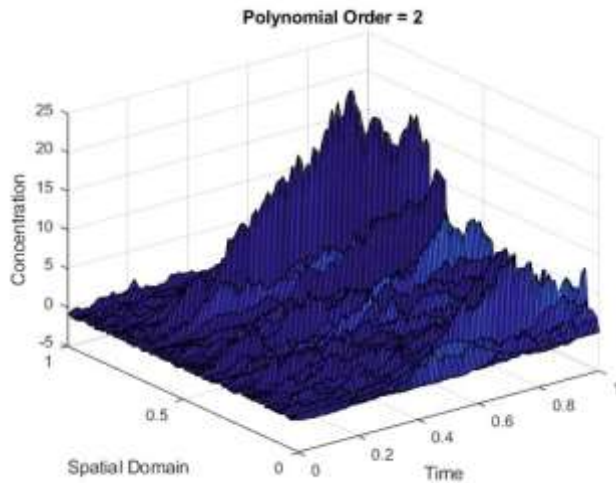


**Figure 5.18** Simulation of concentration  $C$  using the PCE method with the Gaussian initial condition and maximum order of polynomial chaos expansion = 2.

*Note.* Time domain  $\mathbb{R}^+$  is  $(0,1)$ , time step  $\Delta t = 0.01$ , Hermite polynomials of order 3. The mean and standard deviation of Gaussian distribution is  $\mu = 0.5$  and standard deviation  $\sigma_G = 0.1$ .

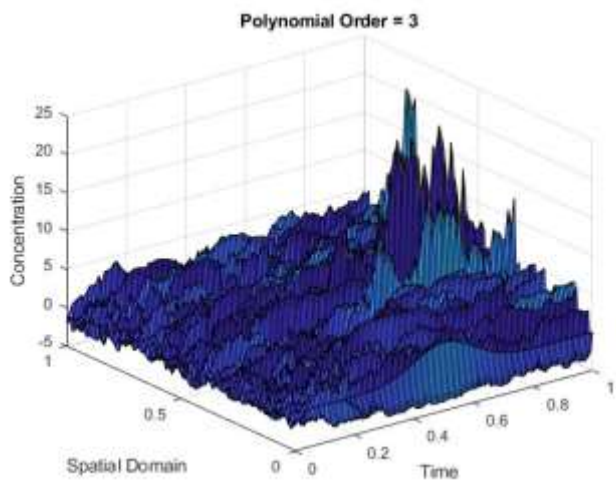


**Figure 5.19** Simulation of concentration  $C$  using the PCE method with the Gaussian initial condition and maximum order of polynomial chaos expansion = 3.

*Note.* Time domain  $\mathbb{R}^+$  is  $(0,1)$ , time step  $\Delta t = 0.01$ , Hermite polynomials of order 3. The mean and standard deviation of Gaussian distribution is  $\mu = 0.5$  and standard deviation  $\sigma_G = 0.1$ .

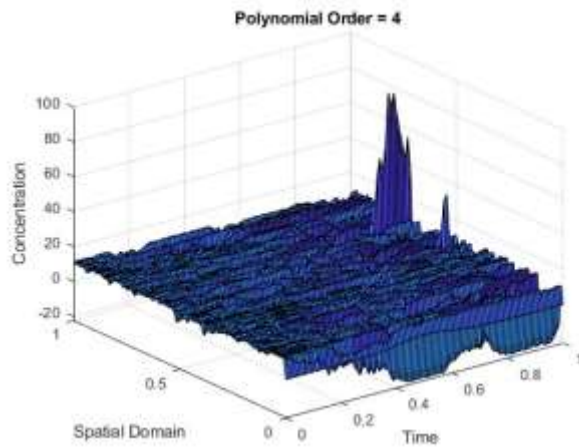


**Figure 5.20** Simulation of concentration  $C$  using the PCE method with the Gaussian initial condition and maximum order of polynomial chaos expansion = 4.

*Note.* Time domain  $\mathbb{R}^+$  is  $(0,1]$ , time step  $\Delta t = 0.01$ , Hermite polynomials of order 3. The mean and standard deviation of Gaussian distribution is  $\mu = 0.5$  and standard deviation  $\sigma_G = 0.1$

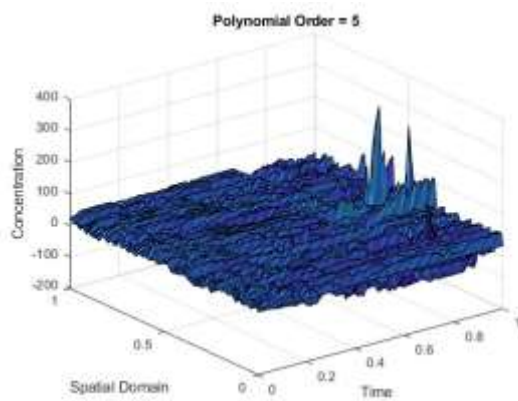


**Figure 5.21** Simulation of concentration  $C$  using the PCE method with the Gaussian initial condition and maximum order of polynomial chaos expansion = 5.

*Note.* Time domain  $\mathbb{R}^+$  is  $(0,1]$ , time step  $\Delta t = 0.01$ , Hermite polynomials of order 3. The mean and standard deviation of Gaussian distribution is  $\mu = 0.5$  and standard deviation  $\sigma_G = 0.1$

Boundary conditions determine the behaviour of a random process at the boundaries of the domain of interest. For example, imposing periodic or reflection boundary conditions can have a significant impact on the statistical properties of the random field. In cases where the boundary conditions introduce additional sources of randomness or nonlinearity, higher order PCE may be needed to accurately capture these effects.

In contrast, simpler boundary conditions, such as Dirichlet or Neumann conditions, can lead to smoother responses, allowing lower-order PCEs to provide accurate approximations. Therefore, choosing the appropriate PCE order is closely related to understanding the boundary conditions and

their influence on the stochastic behaviour of the system, thereby ensuring that the computational model faithfully represents the physical reality of the problem.

The graphs (Figure 5.18 to Figure 5.21) show that lower order polynomials are capable of capturing the Gaussian distribution more accurately than higher order polynomials.

### 5.3.5 Calculation of polynomial chaos coefficients

Polynomial chaos coefficients are calculated by adopting the strategy explained in Section 4.7.2 of Chapter 4. The number of gPCE coefficients are 4, starting from order '0' to order '3'. Figure 5.22 and Figure 5.23 plot the PCE coefficients at time domain  $x = 0.50$  and  $x = 0.25$ , respectively.

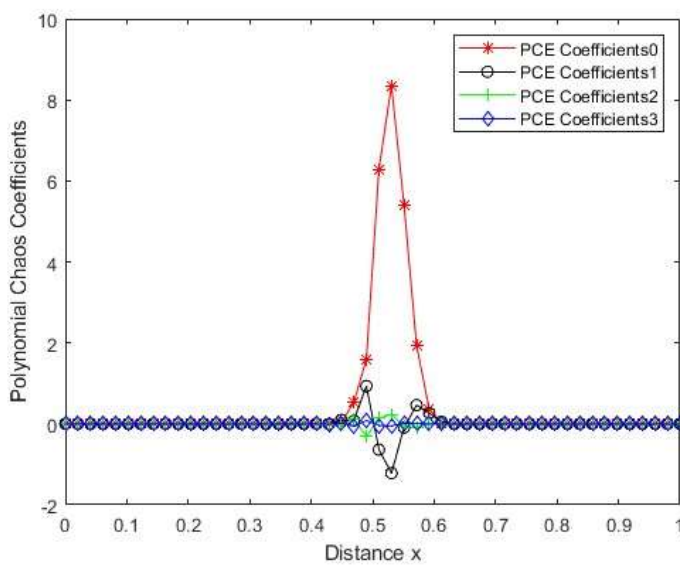


Figure 5.22 Calculation of the polynomial chaos coefficients of various orders at  $x = 0.50$ .

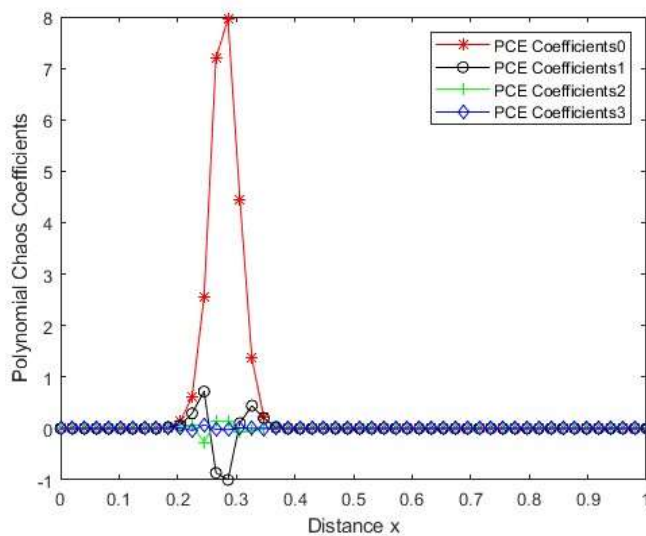


Figure 5.23 Calculation of polynomial chaos coefficients of various orders at  $x = 0.25$ .

Figure 5.24 and Figure 5.25 compare the mean values and variances of PCE solution with the exact solution at  $x = 0.50$ .

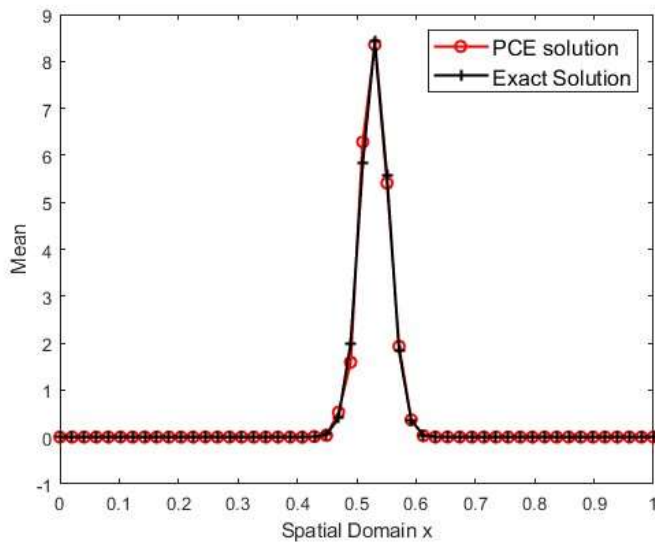


Figure 5.24 Expectation using the PCE solution and the analytical solution at  $x = 0.50$ .

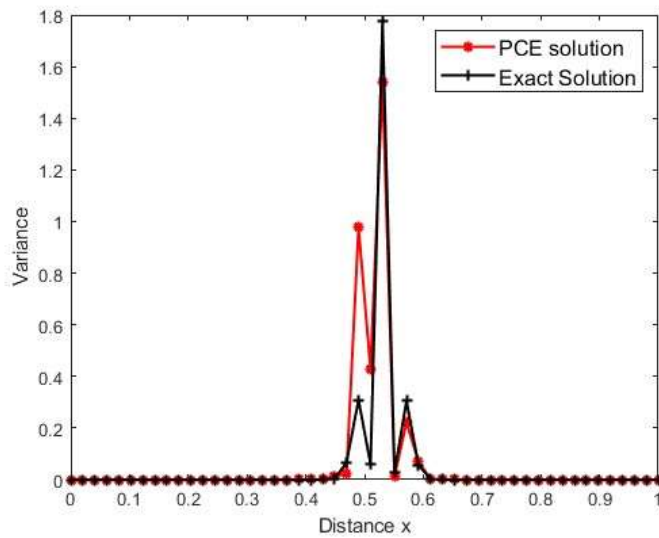


Figure 5.25 Variance using the PCE solution and the analytical solution at  $x = 0.50$ .

A comparative study of mean and variances for the exact and the PCE methods are provided in Figure 5.26 and Figure 5.27 at  $x = 0.25$ .

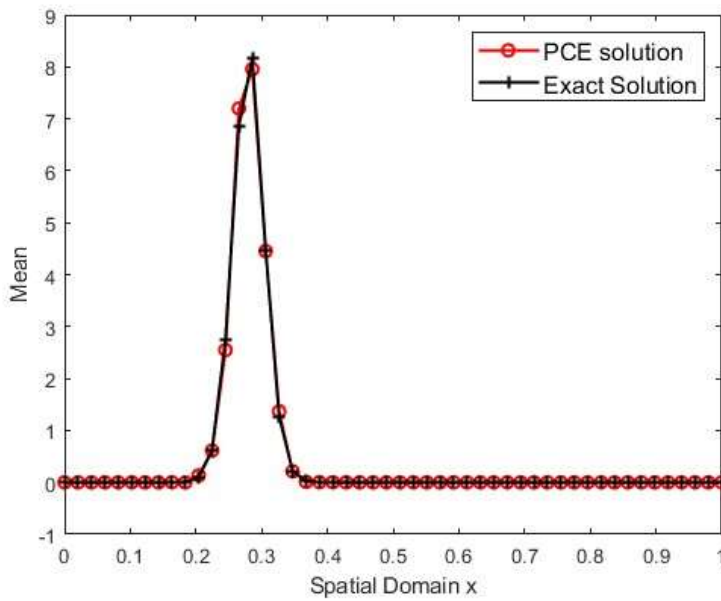


Figure 5.26 Expectation using the PCE solution and the analytical solution at  $x = 0.50$ .

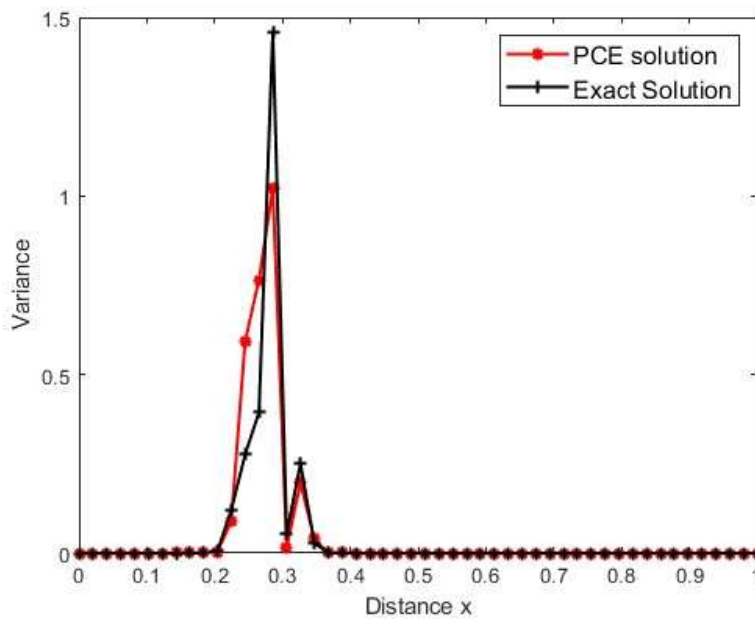


Figure 5.27 Variance using the PCE solution and the analytical solution at  $x = 0.50$ .

## 5.4 Non-linear dynamical systems

Managing nonlinear dynamical systems constitutes a formidable challenge that spans many different fields like science and engineering. Unlike linear systems, which often admit elegant closed-form solutions, nonlinear systems exhibit complex behaviours that defy simple analysis. These systems, characterised by complex interactions, feedback loops, and nonlinearities, appear frequently in fields such as physics, biology, economics, and engineering, making it difficult to understand; controlling them becomes a vital effort. The study of nonlinear dynamical systems seeks to understand how

small changes in the initial conditions or system parameters can lead to profoundly different outcomes.

To navigate this complex landscape, researchers and engineers have developed countless mathematical and computational techniques, including the polynomial chaos expansion (PCE) method. This method provides a powerful way to understand the complexity of nonlinear systems, enabling accurate modelling, analysis, and prediction, while accounting for uncertainties, variability, and randomness. In this context, PCE emerges as a flexible tool that allows us to address the multifaceted challenges posed by nonlinear dynamic systems, paving the way for improved decision-making, system design, and risk assessment.

PCE provides a systematic way to address these challenges by representing system responses as polynomial expansions based on orthogonal basis functions, such as Hermite, Legendre, or Chebyshev polynomials. The key to solving nonlinear problems lies in the underlying functions and their interactions. PCE allows us to express system variables as a weighted sum of these basis functions, where the coefficients can be efficiently determined using techniques such as regression or Galerkin projection. By choosing appropriate basis functions and scaling orders, we can accurately approximate the behaviour of the system under many input conditions, including nonlinear regimes. Additionally, PCE enables the quantification of uncertainty by incorporating random inputs, making it a powerful tool for modelling and analysing complex systems subject to random variation.

We shall consider a non-linear system defined by the stochastic equation,

$$\frac{du}{dt} = k(\xi)u^3(t) \quad (5.32)$$

We can deal with this non-linear system similar to equation (4.28) using the PCE method with Galerkin projection. Although multiplication does not affect the orthogonality of the base polynomial, the total number of integrals involved are significantly increased.

$k(\xi)$  is stochastic but time invariant. PCE expansion is given by,

$$\sum_{i=0}^N \dot{u}_j \langle \varphi_i, \varphi_i \rangle = \sum_{j,k,l,m=0}^N k_j u_{k,l,m} \langle \varphi_j \varphi_k \varphi_l \varphi_m, \varphi_i \rangle \quad (5.33)$$

Using orthogonality of the basis functions,

$$\dot{u}_j = \frac{1}{\langle \varphi_i, \varphi_i \rangle} \sum_{j,k=0}^N k_j u_k \langle \varphi_j \varphi_k, \varphi_i \rangle = \sum_{k=0}^N \mathbf{E} k_j u \quad (5.34)$$

Here,  $\mathbf{E}$  is given similar to equation (5.26), but the dimensions of the coefficient matrix  $\tilde{\mathbf{E}}$  is

$\tilde{\mathbf{E}} \in \mathbb{R}^{(N+1) \times (N+1)^3}$ ; that is,  $(N + 1)^4$  integrals are evaluated. This is the reason why PCE suffers with the curse of dimensionality and can only provide good results for low-dimensional non-linear systems as it adds an additional state space in expansion. One of the main advantages of PCE is the low computational effort involved in system simulation compared to sampling-based methods. This makes it ideally suitable for tasks that require a lot of simulation. The graph below in Figure 5.28 and Figure 5.29 shows comparative results for mean and variance using the MC method, the stochastic collocation method, and the PCE method with different initial conditions.

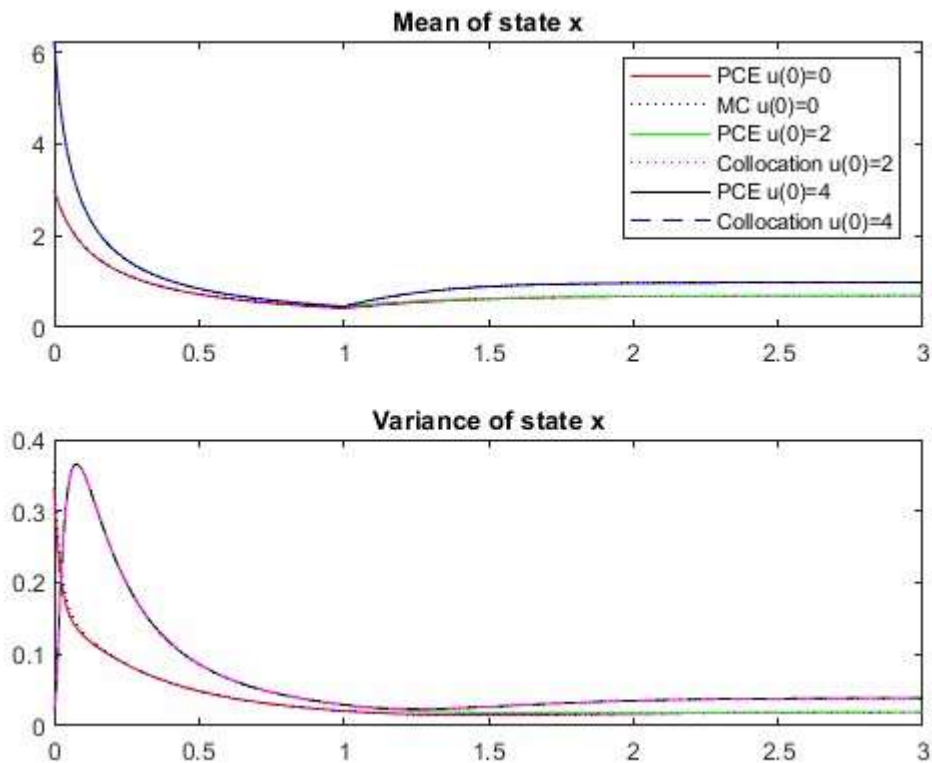


**Figure 5.28 Mean and variance of input state  $x$  using the MC method, stochastic collocation method and the PCE method.**

*Note.* Stochastic input parameter is  $k(\xi)$  defined by two input parameters,  $a$  and  $b$ . Parameter  $a$  is uniformly distributed in  $[1, 2]$  and parameter  $b$  is normally distributed with mean = 1 and standard deviation = 0.01.

While the graphs show that the PCE methods are able to handle non-linear systems, if the non-linearity is high, the PCE methods do not work very well because the convergence of polynomial chaos methods can be very slow in highly nonlinear systems. To accurately represent the system's behaviour, a large number of polynomial terms may be needed, making scaling computationally expensive.

In addition, highly nonlinear systems often exhibit discontinuities or singularities in their response. The parameter range for such systems is very wide; PCE methods may find it difficult to represent system's behaviour accurately.

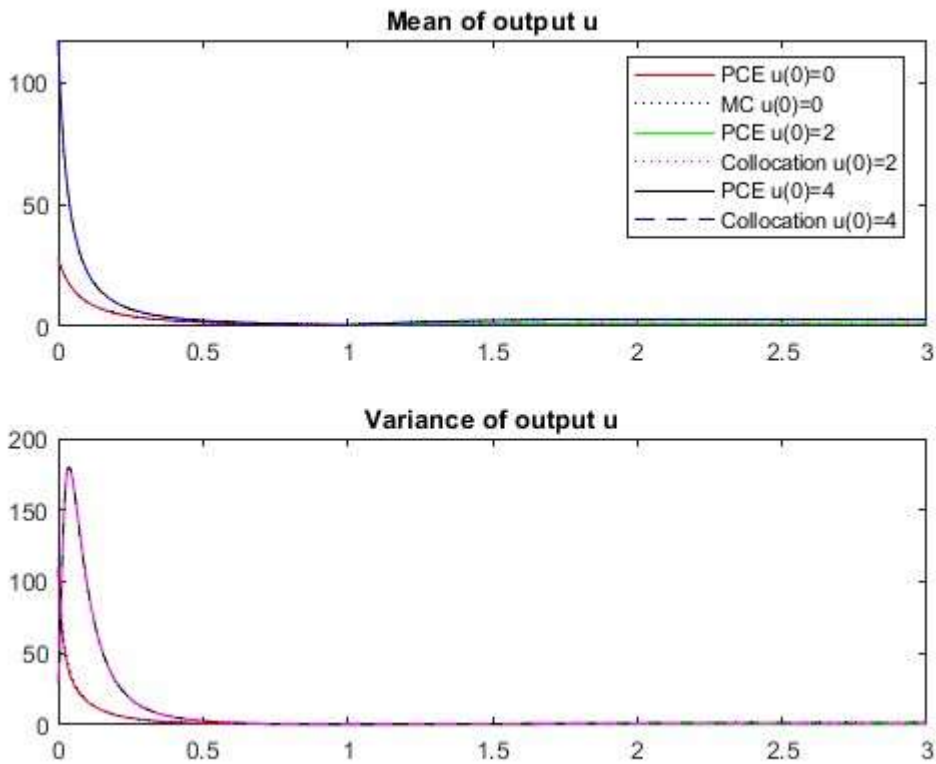


**Figure 5.29 Mean and variance of output  $u$  using the MC method, the stochastic collocation method, and PCE method.**

*Note.* Stochastic input parameter is  $k(\xi)$  defined by two input parameters,  $a$  and  $b$ . Parameter  $a$  is uniformly distributed in  $[1, 2]$  and parameter  $b$  is normally distributed with mean = 1 and standard deviation = 0.01.

## 5.5 Summary

As we conclude this chapter, it is evident that the toolbox of stochastic spectral methods is vast and versatile. While stochastic spectral methods offer a remarkable set of tools for handling uncertainty, they are not without their limitations. One of the primary challenges lies in their computational intensity, especially when dealing with high-dimensional problems. Monte Carlo simulations, for instance, may need an extensive number of samples to achieve convergence, rendering them computationally expensive. Likewise, polynomial chaos expansions face challenges in capturing highly nonlinear dynamics effectively, often necessitating an increased number of terms or advanced techniques to approximate the solution accurately. As a result, these methods may struggle to

provide real-time solutions for complex systems, restricting their applicability in scenarios where rapid decision-making is crucial.

Another limitation arises from the inherent assumptions made during the modelling process. Stochastic spectral methods often assume certain statistical properties of the underlying uncertainties, such as square integrable spaces, specific probability distributions, or correlations. These assumptions, while simplifying the problem, may not always align with the true nature of the system, leading to model inaccuracies. Moreover, the curse of dimensionality remains a formidable obstacle, particularly in high-dimensional problems, as it can exponentially increase the computational burden. Consequently, stochastic spectral methods may encounter practical difficulties when applied to real-world situations with vast parameter spaces. Addressing these limitations requires ongoing research into more efficient algorithms, adaptive strategies, and novel techniques to enhance the versatility and reliability of stochastic spectral methods in handling complex, high-dimensional, and nonlinear systems.

In the next chapter, we take a step into a less-used but powerful tool; Wick and Malliavin calculus. This sophisticated approach offers unique insights and capabilities in handling stochastic systems. In this chapter, we deepen our understanding and enhance our problem-solving prowess in the dynamic landscape of uncertainty.

## Chapter 6

### Wick Product and Malliavin Calculus

In the realm of stochastic analysis, Wick and Malliavin calculus stand as powerful and sophisticated mathematical tools that have revolutionized our understanding of stochastic processes and their applications across various domains. These specialized branches of calculus offer innovative techniques to probe, manipulate, and derive properties of random variables and stochastic systems, providing invaluable insights into the behaviour of complex and uncertain phenomena.

Wick calculus, rooted in quantum field theory and statistical mechanics, offers a unique approach to compute moments and cumulants of stochastic processes efficiently. It unveils the hidden structure of stochastic functionals, allowing researchers to explore higher-order statistics and gain a deeper understanding of the inherent randomness in various systems. By simplifying complex statistical calculations, Wick calculus has found applications in diverse fields, from quantum physics to financial modelling, where precise statistical descriptions are essential.

On the other hand, Malliavin calculus introduces a powerful method for differentiating through stochastic processes. This technique facilitates the estimation of gradients, sensitivities, and higher-order derivatives of random variables with respect to underlying stochastic processes. Malliavin calculus has wide-ranging applications, particularly in finance, where risk management, option pricing, and portfolio optimization demand accurate assessments of uncertainties.

In quantum field theory, infinite quantities have been discovered that emerged (mathematically) from the product of generalised functions. In order to extract meaningful information from these infinite quantities, the Italian theoretical physicist Gian Carlo Wick (1909-1992) suggested a renormalisation process (Wick, 1950) and created the concept of the Wick product.

Wick's idea of Gaussian Wick calculus is based on the following definition:

*An operator  $A$  acting on the bosonic Fock space (The Fock space is the (Hilbert) direct sum of tensor products of copies of a single-particle Hilbert space) is said to be normally ordered if in its representation in terms of annihilation and creation operators all the creation operators appear to the left of all annihilation operators.*

The basic building component in this framework is the concept of Wick product (also known as an  $S$ -product by Wick), which is a multiplication for functions defined on potentially infinite dimension Gaussian spaces. This idea of Wick's can be traced back from the notion of creation and an annihilation operator.

We know that the normally ordered powers of the position operator naturally generate a new idea of multiplication for Hermite polynomials, and therefore for certain classes of functions constructed on Gaussian spaces (Kadison & Ringrose, 1992).

## 6.1 Idea behind the Wick product in stochastic analysis

Let us consider a creation operator  $\mathbb{A}_f$  and an annihilation operator  $\mathbb{A}_f^*$  related to  $f \in \mathcal{L}^2([0, T])$  and the positive operator  $\mathbb{A}_f + \mathbb{A}_f^*$ .

Let us consider

$$(\mathbb{A}_f + \mathbb{A}_f^*)^2 = \mathbb{A}_f^2 + \mathbb{A}_f \mathbb{A}_f^* + \mathbb{A}_f^* \mathbb{A}_f + (\mathbb{A}_f^*)^2 \quad (6.1)$$

We know that the creation and the annihilation operator satisfy the canonical commutation rule,

$$[\mathbb{A}_f, \mathbb{A}_f^*] = \mathbb{A}_f \mathbb{A}_f^* - \mathbb{A}_f^* \mathbb{A}_f = |f|^2 I \quad (6.24)$$

where  $I$  is the identity operator, replacing the term  $\mathbb{A}_f \mathbb{A}_f^*$  with  $|f|^2 I + \mathbb{A}_f^* \mathbb{A}_f$  from (6.2) in (6.1), we have,

$$(\mathbb{A}_f + \mathbb{A}_f^*)^2 = \mathbb{A}_f^2 + \mathbb{A}_f \mathbb{A}_f^* + \mathbb{A}_f^* \mathbb{A}_f + |f|^2 I + (\mathbb{A}_f^*)^2 \quad (6.3)$$

$$=: (\mathbb{A}_f + \mathbb{A}_f^*)^2 : + |f|^2 I \quad (6.4)$$

equivalently,

$$\begin{aligned} : (\mathbb{A}_f + \mathbb{A}_f^*)^2 : &= (\mathbb{A}_f + \mathbb{A}_f^*)^2 - |f|^2 I \\ &= H_{2,|f|^2}(\mathbb{A}_f + \mathbb{A}_f^*) \end{aligned} \quad (6.5)$$

where  $H_{2,|f|^2}$  denotes the Hermite polynomial of degree 2 and the parameter  $|f|^2$ .

Using mathematical induction ( $\forall n \in \mathbb{N}$ ), we can show that,

$$: (\mathbb{A}_f + \mathbb{A}_f^*)^n : = H_{n,|f|^2}(\mathbb{A}_f + \mathbb{A}_f^*) \quad (6.6)$$

The Wick product first appeared as a renormalisation operator in quantum physics (Wick, 1950). In probability theory, the condition of ordinary multiplication with the Itô differentiation rule is imitated by the Wick product with the ordinary differentiation rule (H. (Helge) Holden, 2010). The primary issue with using the Wick product with random variables is that it does not perform operations in points. Despite the computing challenges, its good analytical features make it a natural tool to use in stochastic analysis.

## 6.2 Connection between normal ordering (creation and annihilation operator) and the notion of the Wick product in stochastic analysis

Let  $(\Omega, \mathcal{F}, \wp)$  be a probability space called a classical Wiener space over the interval  $[0, T]$ . According to the Wiener Itô chaos expansion theorem explained in Chapter 4, this space is isomorphic to the Hilbert space  $H_s(\mathcal{L}^2[0, T])$ .

In short, if  $\psi$  is an isomorphism from a Wiener space to the Hilbert space, i.e.,

$$\psi: \mathcal{L}^2(\Omega, \mathcal{F}, \wp) \rightarrow H_s(\mathcal{L}^2[0, T])$$

and  $X$  is a random variable, such that  $X \in \mathcal{L}^2(\Omega, \mathcal{F}, \wp)$ , the working of the operator

$(\mathbb{A}_f + \mathbb{A}_f^*)$  on  $H_s(\mathcal{L}^2[0, T])$  corresponds via this isomorphism and is given by,

$$\int_0^T X \cdot f(s) dB_s = \psi^{-1}((\mathbb{A}_f + \mathbb{A}_f^*)\psi(X)) \quad (6.7)$$

This property of isomorphism helps us to identify the operator  $(\mathbb{A}_f + \mathbb{A}_f^*)$  with the help of the random variable  $\int_0^T f(s) dB_s$  and can be defined as,

$$:\left(\int_0^T f(s) dB_s\right)^2 := :(\mathbb{A}_f + \mathbb{A}_f^*)^2: \quad (6.8)$$

$$= H_{2,|f|^2}(\mathbb{A}_f + \mathbb{A}_f^*) \quad (6.9)$$

$$= H_{2,|f|^2}\left(\int_0^T f(s) dB_s\right) \quad (6.10)$$

A Wick product can be formulated analogously by considering Wiener integrals and their analogues to the SDEs in terms of Wick calculus. This notion is called a Wick square and is written as,

$$:\left(\int_0^T f(s) dB_s\right)^2 := \int_0^T f(s) dB_s \diamond \int_0^T f(s) dB_s \quad (6.11)$$

From now onwards, we use this symbol ' $\diamond$ ' to denote the Wick product.

## 6.3 Relationship between Itô - Skorohod integral and the Wick product

Equation (6.3) describes the role of the Wick product in stochastic analysis and also shows the relationship between the Itô-Skorohod integral and the Wick product. Consider an Itô-Skorohod integrable process  $\{X_t\}_{t \in [0, T]}$ , such that,

$$\int_0^T X_t dB_t = \int_0^T X_t \diamond W(t) dt \quad (6.12)$$

where  $W(t) = \frac{dB_t}{dt}$  is the white noise and represents the distribution behaviour of Brownian motion that follows Hida's distribution.

## 6.4 Wick product

The Wick product was initially used as a renormalisation process. T. Hida and N. Ikeda (HIDA & IKEDA, 2001) proposed the Wick product for stochastic analysis. Later on, this concept was expanded H. (Helge) Holden (1996) to include white noise in the Wick products of stochastic distributions and applied Gaussian Wick calculus. A detailed and clear overview of the Wick product. Wick renormalisation is explained in Hu and Yan (2009).

### 6.4.1 Motivation for Wick multiplication (Renormalisation point of view)

White noise  $W(t)$  can be represented as an element of Hida dual space  $(\mathcal{L}^2)^{-1}$  as,

$$W(t) = \lim_{\Delta t \rightarrow 0} \frac{1}{\Delta t} \int_t^{t+\Delta t} dB_u \quad (6.13)$$

$$= \int_{\mathbb{R}} \delta_t dB_u \quad (6.14)$$

where  $\delta_t$  is the Dirac measure of  $t$  that belongs to the dual Sobolov space. Using Itô's formula,

$$(W_t)^2 \approx \left( \frac{1}{\Delta t} \int_t^{t+\Delta t} dB_u \right)^2 \quad (6.15)$$

$$(W_t)^2 \approx \left( \frac{1}{\Delta t} \int_t^{t+\Delta t} dB_u \right)^2 \quad (6.16)$$

$$= \frac{2}{(\Delta t)^2} \int_t^{t+\Delta t} \left( \left( \int_t^v dB_u \right) dB_v + \frac{1}{\Delta t} \right) \quad (6.17)$$

The additive re-normalisation of the above term is,

$$= \frac{2}{(\Delta t)^2} \int_t^{t+\Delta t} \left( \left( \int_t^v dB_u \right) dB_v \right)$$

$$\begin{aligned}
&= 2 \int_t^{t+\Delta t} \left( \left( \int_t^v dB_u \right) \frac{dB_v}{\Delta t} \right) \\
&\rightarrow \int \int \delta_t(u) \delta_t(v) dB_u dB_v \text{ as } \Delta t \rightarrow 0
\end{aligned}$$

This motivates the definition of,

$$\int \delta_t dB \diamond \delta_t dB = \int \delta_t \otimes \delta_t dB^{\otimes 2} \quad (6.18)$$

Here  $\otimes$  is the symmetrized tensor product.

The generalised structure of the solutions is transferred to the stochastic component, and the SPDEs are interpreted in the typical strong sense with respect to the time parameter  $t$  and the spatial parameter  $x \in \mathbb{R}^d$ . Thus, generalised random variable spaces must be introduced. A particularly appealing aspect of using the Wick product is the ability to define a unique white noise process as a rigorous mathematical object, such as the time derivative of the Brownian motion. SDEs can therefore be solved as true differential equations, which is how they are typically understood, rather than just as integral equations.

The Wick product is used in the context of white noise analysis to solve the issue of pointwise multiplication of generalised functions. It is clearly specified in the test and generalised stochastic function of Kondratiev spaces (Definition 6.6.1).

It is tempting to replace all products with Wick products and all non-linear functions with their Wick equivalents in order to solve the multiplicative noise and non-linear equations problems because the Wick product is a product in the algebraic sense. Although the Wick product performs very smoothly as a mathematical object, care should be taken when using it. The stochastic and PDE components are somewhat separate, which is a nice feature, especially for Wick-type equations.

#### 6.4.2 The Wick product in Physics

The representation of the Wick product in physics is based on Gjessing's explanation (Gjessing et al., 1992). If  $(\Omega, \mathcal{F}, \rho)$  is a probability space,  $X$  is a random variable. Let us define a formal derivative of  $X$  by considering a formal power series in  $X$  as,

$$\frac{\partial}{\partial X} \left( \sum_{n=0}^{\infty} a_n X^n \right) = \sum_{n=0}^{\infty} (n+1) a_{n+1} X^n \quad (6.19)$$

The recursive formula to find the Wick product of  $X^m$  is denoted as  $:X^m:$  and is defined as,

$$\frac{\partial}{\partial X} (:X^m:) = m(:X^{m-1}:) \quad (6.20)$$

with

$$:X^0:= 1 \text{ and } E[:X^m:] = 0, \quad m = 1,2, \dots \dots \dots \quad (6.21)$$

Hence,

$$\begin{cases} :X := X - E(X) \\ :X^2 := X^2 - 2XE(X) - E(X^2) + 2(E(X))^2 \\ :X^3 := X^3 - 3X^2E(X) - 3XE(X)^2 + 6XE(X)^2 - E(X)^3 + 6E(X)E(X^2) - 6E(X^3) \end{cases} \quad (6.22)$$

### 6.4.3 The Wick product in stochastic analysis

If  $(\mathbf{S})^*$  is a Hida distribution space and  $f(\omega)$  and  $g(\omega)$  are two elements of  $(\mathbf{S})^*$  defined as,

$$f(\omega) = \sum_{\alpha} a_{\alpha} H_{\alpha} \quad (6.23)$$

and

$$g(\omega) = \sum_{\beta} b_{\beta} H_{\beta} \quad (6.24)$$

where  $\alpha$  and  $\beta$  are the multi-indices, then the Wick product of  $f(\omega)$  and  $g(\omega)$  is defined as,

$$f(\omega) \diamond g(\omega) = \sum_{\alpha, \beta} a_{\alpha} b_{\beta} H_{\alpha+\beta} \quad (6.25)$$

Also,  $f(\omega) \diamond g(\omega) \in (\mathbf{S})^*$ . A detailed explanation and application of the Wick product can be found in the extant literature (H. Holden et al., 1991; Y. Hu & Yan, 2009; Venturi et al., 2013b).

### 6.4.4 Properties of the Wick product

The following are some of the properties of the Wick product used in stochastic analysis:

- $W^{\diamond 2}(t) = W^2(t) - t, \quad t \geq 0$
- For a random process  $X, E[\exp^{\diamond}(X)] = \exp E[X]$
- $E[X \diamond Y] = E[X]E[Y]$
- Chain rule: for an analytic function  $g: \mathbb{C} \rightarrow \mathbb{C}, i. e., g(\mathbb{R}) \subseteq \mathbb{R},$

$$\frac{d}{dt} [g^{\diamond}(X(t))] = (g')^{\diamond}(X(t))^{\diamond} X'(t) \quad (6.26)$$

also,

$$\begin{aligned} & \left( \int_{\mathbb{R}} g(x) dW(x) \right) \diamond \left( \int_{\mathbb{R}} h(y) dW(y) \right) \\ &= \left( \int_{\mathbb{R}} g(x) dW(x) \right) \left( \int_{\mathbb{R}} h(y) dW(y) \right) - \int_{\mathbb{R}} g(t)h(t)dt, \end{aligned}$$

$$(6.27)$$

$\forall g, h \in \mathcal{L}^2(\mathbb{R})$  and are deterministic.

e) In general, the  $n$ th Wick exponential of  $\vartheta$  is defined as

$$\vartheta^{\diamond n} = \|f\|^n H_n\left(\frac{\vartheta}{\|f\|}\right) \quad (6.28)$$

where  $\vartheta = \int_{\mathbb{R}} f dW$

and hence,

$$W^{\diamond n}(t) = t^{\frac{n}{2}} H_n\left(\frac{W(t)}{t^{\frac{1}{2}}}\right), n = 0, 1, 2, \dots \dots \dots \quad (6.29)$$

$$\exp^{\diamond} \left\{ \int_{\mathbb{R}} f dW \right\} = \exp \left\{ \int_{\mathbb{R}} f dW - \frac{1}{2} \|f\|^2 \right\}, f \in \mathcal{L}^2(\mathbb{R}) \quad (6.30)$$

and,

$$\exp^{\diamond} W(t) = \exp \left\{ W(t) - \frac{1}{2} t \right\}, \forall t \geq 0 \quad (6.31)$$

Equation (6.28) to equation (6.31) are very important from computational point of view. These equations help us to understand the basic building block of smoothed white noise process and need of Wick product. It is explained in next Section 6.4.5 and Section 6.4.6.

### 6.4.5 Computation of Wick product

The objective of this section is to compute the Wick product and Wick exponential given by equation 6.30. First we will compute least square norm of a deterministic function  $f(t)$ , i.e.,  $f \in \mathcal{L}^2(\mathbb{R})$  and is given by a second-degree polynomial.

Let

$$f(t) = a + bt + ct^2 \quad (6.32)$$

$\mathcal{L}^2$ -norm of  $f(t)$  is

$$\|f\| = \left( \int_0^t (f(t))^2 dt \right)^{1/2} \quad (6.335)$$

When  $f(t) = 1$ ,  $\|f\| = \left( \int_0^t dt \right)^{1/2} = \sqrt{t}$ ,

when  $a = 0, b = 1, c = 0$ ;  $\|f\| = \left( \int_0^t (f(t))^2 dt \right)^{1/2} = \sqrt{\frac{t^3}{3}}$  and

when  $a = 1, b = 2, c = 0.001$ ;  $\|f\| = \sqrt{2 \times 10^{-7} t^5 + 0.001 t^4 + 1.334 t^3 + 2 t^2 + t}$  and is plotted in Figure 6.1.

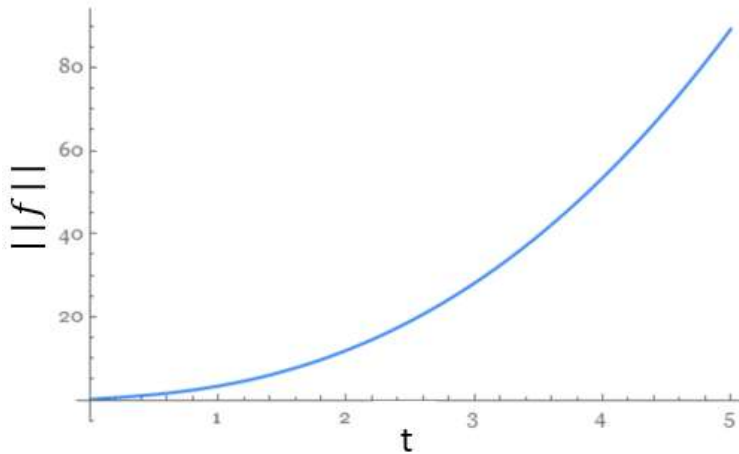


**Figure 6.1** Least square norm of a deterministic second-degree polynomial function.

Now, let  $\vartheta(t) = \int_{\mathbb{R}} f(t)dW$ , this is an Itô process and a realisation of  $\vartheta$  for the interval  $[0,1]$  is shown in Figure 6.2.

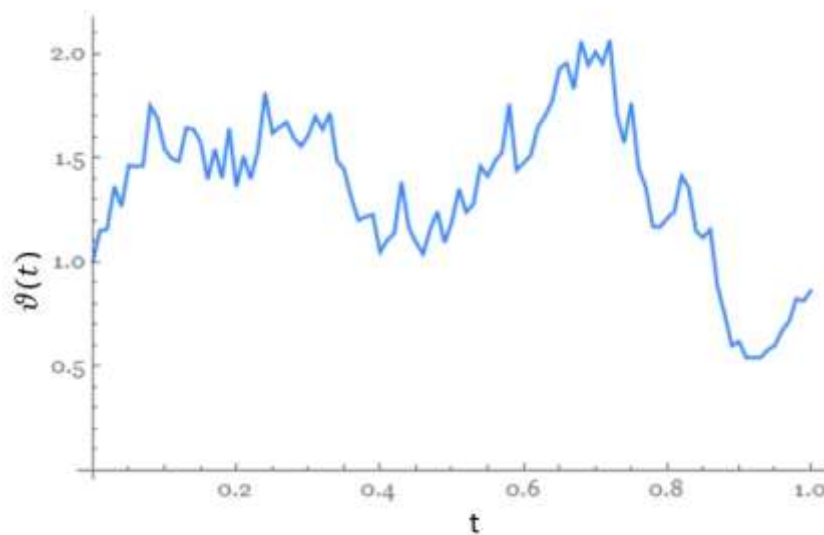


**Figure 6.2** Realisation of an Itô process.

Let  $\Psi(t) = \frac{\vartheta}{\|f\|}$  so that using equation 6.28,

$$\vartheta^{\diamond n} = \|f\|^n H_n(\Psi(t)) \quad (6.34)$$

we have,

$$\Psi(t) = \frac{\int_0^t f(t)dW(t)}{\|f\|} \quad (6.35)$$

As we have already computed the numerator  $\int_0^t f(t)dW(t)$  and denominator  $\|f\|$ , we can compute  $\Psi(t)$  and then incorporating this  $\Psi(t)$  into equation 6.28, we can compute  $\vartheta^{\diamond n}$  as

$$\vartheta^{\diamond n} = \|f\|^n H_n(\Psi(t))$$

Further, using equation 6.30, we have

$$\exp^{\diamond} \left\{ \int_{\mathbb{R}} f(t) dW(t) \right\} = \exp^{\diamond} \{ \vartheta(t) \} = \exp \left\{ \vartheta(t) - \frac{1}{2} \|f\|^2 \right\} \quad (6.36)$$

also, if  $f(t) = 1$ ,

$$\exp^{\diamond} \left\{ \int_{\mathbb{R}} f(t) dW(t) \right\} = \exp^{\diamond} \{ W(t) \} = \exp \left\{ W(t) - \frac{1}{2} t \right\} \quad (6.37)$$

for  $f(t) = 1 + 2t + 0.001t^2$ , the graph for Wick exponential as given by equation 6.36 is plotted in Figure 6.3.

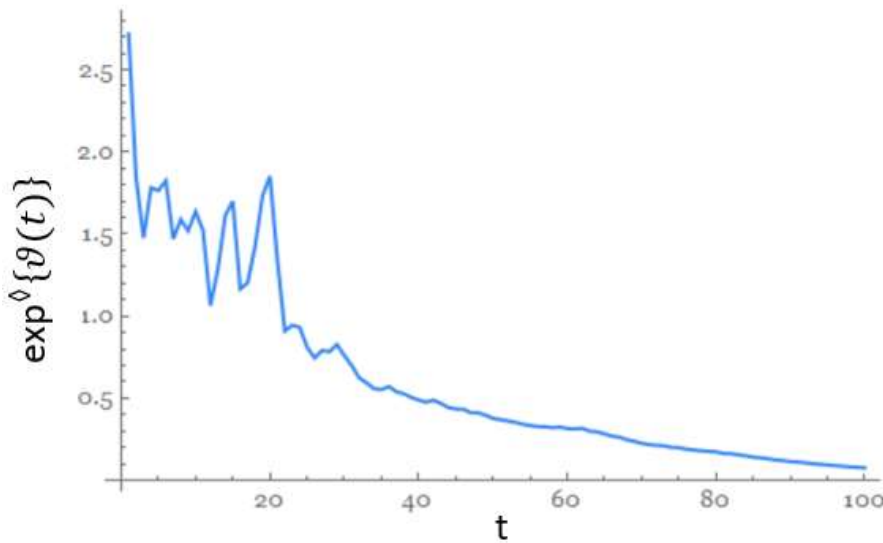


**Figure 6.3** Wick exponential an Itô process.

Note. For Figure 6.3, an Itô process is  $\vartheta(t) = \int_{\mathbb{R}} f(t) dW(t)$ ,  $f(t) = a + bt + ct^2$  with  $a = 1, b = 2$ , and  $c = 0.001$ .

#### 6.4.6 Comparison between square of Wiener process and Wick exponential of Wiener process

This section shows the significance of choosing Wick exponential which are obtained by smoothed white noise i.e., wiener process  $W(t)$ . There are certain situations in which the input random parameter cannot be negative. For example, the concentration of a chemical in transport processes. If we use the realisations of sample paths of Wiener process as input random parameter, there are chances of negative values in those sample paths. Using Wick exponentials of Wiener process as input random parameter resolve this problem as the realisations of wick exponentials are always positive.

Let us understand it by computing  $W^2(t)$  and  $W^{\diamond 2}(t)$ . Using equation 6.34

$$W^{\diamond n}(t) = t^{\frac{n}{2}} H_n \left( \frac{W(t)}{t^{\frac{1}{2}}} \right)$$

$$W^{\diamond 2}(t) = t H_2 \left( \frac{W(t)}{\sqrt{t}} \right) \quad (6.38)$$

We know that  $H_2(x) = x^2 - 1$ , thus,

$$H_2 \left( \frac{W(t)}{\sqrt{t}} \right) = \frac{W^2(t)}{t} - 1$$

and

$$W^{\diamond 2}(t) = t \left( \frac{W^2(t)}{t} - 1 \right) = W^2(t) - t \quad (6.39)$$

Computation of  $W^2(t)$  and  $W^{\diamond 2}(t)$  are shown in Figure 6.4 for  $10^3$  time steps.

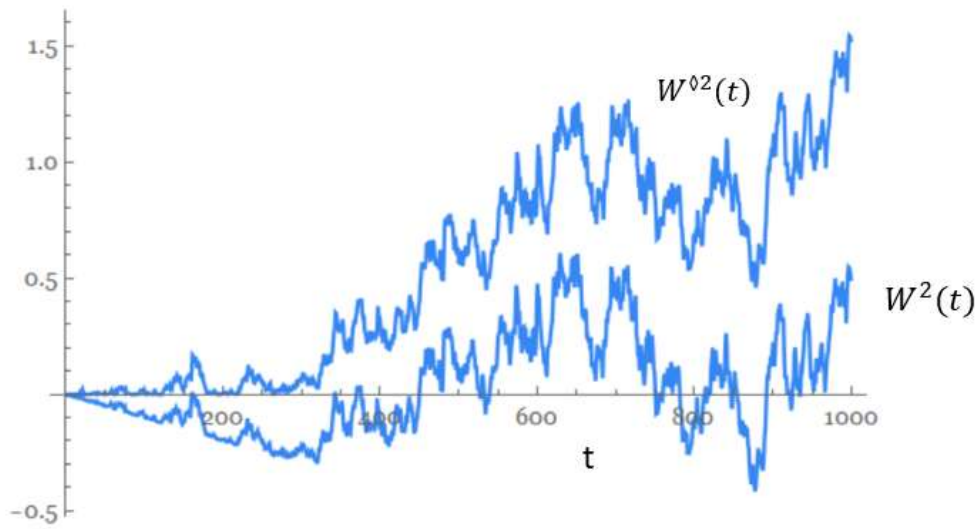


**Figure 6.4** Realisations for squares of Wiener process and squares of Wick exponential of Wiener process.

Thus, we conclude from Figure 6.4, Wick exponential can resolve the issue of random input parameter to be negative.

## 6.5 Malliavin calculus

In his renowned 1976 paper "Stochastic calculus of variation and hypoelliptic operators," Paul Malliavin (Malliavin et al., 1978) introduced Malliavin calculus. Malliavin calculus was originally developed to study the regularity of the law of functionals of the Brownian motion, especially the solution of SDEs driven by Brownian noise. This extends the conventional differentiation notions to deal with random variables and stochastic processes. It is a calculus with infinite dimensions that is defined in the Wiener space. Malliavin calculus introduces the idea of a derivative with regard to a Wiener process, which enables us to examine complex random functionals and investigate their

sensitivity to modifications in the underlying probability measures (Bueno-Guerrero et al., 2017; K. Liu et al., 2022; Nualart & Saussereau, 2009).

The initial use of Malliavin calculus was to demonstrate the correctness of conclusions regarding the smoothness of density of the SDE solutions driven by Brownian motion (Y. Hu et al., 2019). For many years, this was the only known use of Malliavin calculus. Later on, the findings of Malliavin derivative have been extended to finance (Kohatsu-Higa & Montero, 2001).

The authors demonstrate how explicit equations for replicating portfolios of contingent claims in markets driven by Brownian motion can be obtained using the Malliavin derivative. This greatly increased both mathematicians' and finance researchers' interest in the Malliavin calculus. (Fournié et al., 1999) compute Greeks using Malliavin calculus. As a result of their work, substantial focus has been placed on improving and generalising the Monte Carlo methods for computing the Greeks as well as expanding the computations to a larger class of alternatives and models (Biagini et al., 2008; Petrou, 2008; "Stochastic Calculus of Variations in Mathematical Finance," 2006).

The modelling of stochastic finance using jump type diffusion models has gained popularity during the last three decades (B. K. (Bernt K. Øksendal & Sulem, 2007; Schoutens, 2003). This is due to mounting data suggesting that Jump processes are able to capture abrupt, discontinuous changes or "jumps" in the underlying process, which is why they are sometimes thought of as more realistic when simulating specific real-world occurrences. Jump processes enable more flexible and precise description of many dynamic systems than continuous processes (such as Brownian motion). The statistics indicate that the log returns of stocks and indexes are not normally distributed, in contrast to the continuous time models that employ the normal distribution to fit the log returns of the underlying asset prices. Most financial assets' log returns are skewed, with higher kurtosis than in a normal distribution (Solé et al., 2007).

A cornerstone of cutting-edge research in probability and finance, Malliavin calculus has become a vital tool for understanding and solving challenging problems due to its elegant methodology and significant ramifications. More applications using Malliavin calculus include (Cosentino et al., 2021; Lanconelli, 2022; Levajković et al., 2015; K. Liu et al., 2022; Venturi et al., 2013b).

### **6.5.1 White noise space and Wiener chaos decomposition**

White noise is often used as a mathematical model for random disturbances. In probability theory, a white noise probability space refers to a particular type of stochastic process or sequence of random variables.

For a real separable Hilbert space  $\mathcal{H} \in \mathcal{L}^2(\Omega, \mathcal{F}, \wp)$ , the white noise is a linear isometry  $W: \mathcal{H} \rightarrow \mathcal{L}^2(\Omega, \mathcal{F}, \wp)$  such that for all  $a$ , each  $W(\zeta)$  is a real valued Gaussian random variable. Alternatively, for all  $a, b \in \mathcal{H}$ ,

$$E[W(a)] = 0, E[W(a)W(b)] = \langle a, b \rangle \quad (6.40)$$

To prove this, we take a sequence  $\{\xi_i\}_{i \geq 0}$  of i.i.d normal random variables and an orthonormal basis  $\{e_i\}_{i \geq 0}$  of Hilbert space  $\mathcal{H}$ .

For  $a = \sum_{i \geq 0} a_i e_i$ , it is sufficient to set,

$$W(a) = \sum_{i \geq 0} a_i \xi_i \quad (6.41)$$

along with the convergence in  $\mathcal{L}^2(\Omega, \mathcal{F}, \wp)$ .

The orthonormal basis function  $e_i(x)$  for a Hermite polynomial function

$H_n(x) = (-1)^n e^{x^2/2} \frac{d^n}{dx^n} (e^{-x^2/2})$  is obtained by substituting  $x = z/\sqrt{2}$  and is given by,

$$e_i(x) = (\pi)^{-1/4} ((i-1)!)^{-1/2} e^{-z^2/4} H_{i-1}(z) \quad (6.42)$$

and  $e_i \in S(\mathbb{R})$ , Schwartz space for all  $i$ .

Now, define an inner product of  $e_i$  and a random variable  $\omega$  as

$$\vartheta_i(\omega) = \langle \omega, e_i \rangle = \int_{\mathbb{R}} e_i(x) dW(x, \omega), \omega \in \Omega \quad (6.43)$$

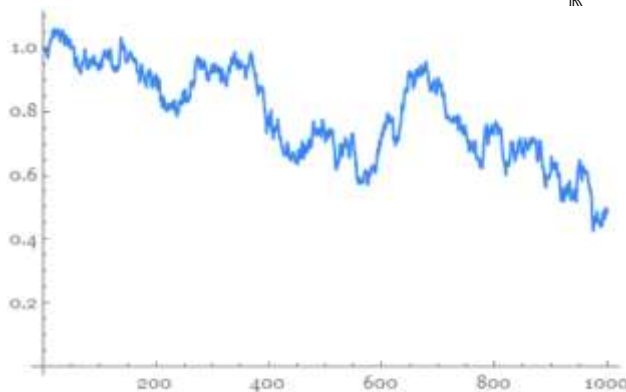


**Figure 6.5** Computation of singular white noise.

For some multi-indices  $\alpha = (\alpha_1, \alpha_1, \dots, \alpha_n), n = 1, 2, \dots, \alpha \neq 0$

$$H_\alpha(\omega) = \prod_{i=1}^n H_{\alpha_i}(\vartheta_i(\omega)), \omega \in \Omega$$

Thus, singular white noise  $W(t)$ ,  $t \in \mathbb{R}$  is defined as,

$$W(t) = \sum_i \int_0^t e_i(z) dz H_{\alpha_i}(\omega) \quad (6.44)$$

It is shown in Figure 6.5.

For  $H_1(1) = x$ ,  $H_{\alpha_i}(\omega) = \vartheta_i(\omega)$ , Thus,  $H_1(\vartheta_i(\omega)) = \vartheta_i(\omega)$ .

Finally, white noise can be expressed as,

$$W(t) = \sum_i e_i(t) \vartheta_i(\omega)$$

$$W(t) = e_1(t) \vartheta_1(\omega) + e_2(t) \vartheta_2(\omega) + \dots \dots \dots \quad (6.45)$$

It is defined as the chaos decomposition of Wiener process.

### 6.5.2 $n$ -dimensional Wiener process

An  $n$ -dimensional Wiener process is determined by a white noise as follows:

The elements of the Hilbert space  $\mathcal{H}$  are written as  $(\mathbf{1}_{(0,t]}^i)$ ,  $i = 1, \dots, m$  such that,

$$(\mathbf{1}_{(0,t]}^i)_j(\tau) = \begin{cases} 1, & \tau \in (0, t] \\ 0, & \text{otherwise} \end{cases} \quad (6.46)$$

and set  $W_i(\tau) = W(\mathbf{1}_{(0,t]}^i)$

Thus  $E[W_i(\tau)W_j(s)] = \delta_{ij}(\tau \wedge s)$ , which is a standard Wiener process. Therefore, we can write,

$$W(a) = \sum_{i=1}^n a_i(\tau) dW_i(\tau) \quad (6.47)$$

or more precisely,

$$\int_0^T f(t) dW_t := W(\mathbf{1}_{(0,t]} f) \quad (6.48)$$

This is also called Wiener integral of  $f$  over  $(0, T)$ .

Now, let  $\mathcal{S}$  be the space of all the polynomial  $f$  of degree  $n$  whose elements belongs to

$$W \in \mathcal{L}^2(\Omega, \mathcal{F}, \mathcal{P}), p \in \mathcal{H} \in \mathcal{L}^2_{(0,t]}(\Omega, \mathcal{F}, \mathcal{P}) \text{ and } W(p) = \int_0^T p dW \mid p \in \mathcal{H}.$$

If  $f \in \mathcal{F} \in \mathfrak{s}$ , there exists  $n \in \mathbb{N}$ , a polynomial  $f$  of degree  $n$  and  $p_1, p_2, \dots, p_n \in \mathcal{L}^2(\Omega, \mathcal{F}, \mathfrak{P})$  such that,

$$F(\omega) = f(W(p_1), \dots, W(p_n))$$

where  $W(p) = \int_0^T p(t) dW$  and  $\omega$  is a realisation of the Wiener process.

**Definition 6.5.1**

For a real symmetric function  $g$ , the symmetrisation  $\tilde{g}$  of  $g$  is defined as,

$$\sum g(x_{\sigma_1}, \dots, x_{\sigma_n}) = n! \tilde{g}(x_1, \dots, x_n) \quad (6.49)$$

for all possible permutations  $\sigma_1, \dots, \sigma_n$ .

**Definition 6.5.2**

If  $g$  is a deterministic- function on  $\mathcal{L}^2([0, T])$ , for all  $n \geq 1$ , the  $n$ -fold iterated Itô integral is defined as,

$$I_n(g) := \int_0^T \int_0^{t_n} \dots \int_0^{t_3} \left( \int_0^{t_2} g(t_1, \dots, t_n) dW(t_1) dW(t_2) \dots dW(t_{n-1}) dW(t_n) \right) \quad (6.50)$$

Also, applying Itô's isometry

$$E[I_n^2(f)] = \|f\|_{\mathcal{L}^2([0, T])}^2$$

**Definition 6.5.3**

For two iterated Itô integrals,

$$E[I_m(f)I_n(f)] = \begin{cases} \langle f, g \rangle_{\mathcal{L}^2([0, T])}, & n = m \\ 0, & n \neq m \end{cases} \quad (6.51)$$

Also, if  $f \in \tilde{\mathcal{L}}^2_{([0, T]^n)}$

$$J_n(f) = n! I_n(f)$$

and

$$E[J_n^2(f)] = n! \|f\|_{\mathcal{L}^2([0, T]^n)}^2 \quad (6.52)$$

**6.5.3 Important result (Wiener Itô iterated integrals)**

In the special case of Hermite polynomials  $h_n$ , when the integrand is the tensor power of a function  $f \in \mathcal{L}^2([0, T])$ , the Wiener Itô iterated integral is defined as,

$$\begin{aligned} n! \int_0^T \int_0^{\tau_n} \dots \int_0^{\tau_3} \left( \int_0^{\tau_2} f(t_1) f(t_2) \dots, f(t_n) dW(\tau_1) dW(\tau_2) \dots dW(\tau_{n-1}) dW(\tau_n) \right) \\ = \|f\|^n h_n \left( \frac{\zeta}{\|f\|} \right) \end{aligned} \quad (6.53)$$

where  $\|f\| = \|f\|_{\mathcal{L}^2([0, T])}$  and

$$\zeta = \int_0^T f(t) dW(t) \quad (6.54)$$

#### 6.5.4 Itô representation theorem

For  $f \in \mathcal{L}^2(\Omega, \mathcal{F}, \wp)$  and  $T > 0$ , there exists a unique process, say  $X$ , in the square integrable space such that,

$$f = E(f) + \int_0^T X_\tau dW_\tau \quad (6.55)$$

#### 6.5.5 Wiener-Itô chaos expansion theorem

Let us define a sequence of non-negative integers  $\mathbb{N}_0^{\mathbb{N}}$  and let the set of these integers be defined as,

$$I = \mathbb{N}_0^{\mathbb{N}}$$

in which the sequence has only finitely many non-zero components. These sequences have the following characteristics:

- (i) A sequence defined as  $\alpha = (\alpha_1, \alpha_2, \dots, \alpha_p, 0, 0, \dots)$ ,  $\alpha_j \in \mathbb{N}_0$ ,  $j = 1, 2, \dots, p \in \mathbb{N}$ .
- (ii) A sequence of zero with only entry '1' at the  $i$ th component given as,  $\varepsilon^{(i)} = (0, \dots, 0, 1, 0, \dots)$ ,  $i \in \mathbb{N}$  is called the  $i$ th unit vector.
- (iii) If any sequence has all components with '0' entry is defined as multi-index  $\mathbf{0}$ .
- (iv) The length of a multi-index  $\alpha$  is given as,

$$|\alpha| = \sum_{i=1}^{\infty} \alpha_i$$

- (v) Component-wise operations with multi-indices are carried as,

$$\alpha + \gamma = (\alpha_1 + \gamma_1, \alpha_2 + \gamma_2, \dots)$$

$$\alpha! = \alpha_1! \alpha_2! \alpha_3! \dots$$

$$\text{and } \binom{\alpha}{\gamma} = \frac{\alpha!}{\gamma! (\alpha - \gamma)!}$$

For a square integrable Hilbert space of random variables  $\xi_i$ ,  $1 = 1, 2, \dots$ , the orthogonal basis using Hermite polynomials is defined as,

$$H_\alpha(\omega) = \prod_{i=1}^{\infty} h_{\alpha_i}(\langle \omega, \xi_i \rangle), \alpha \in I$$

such that  $\|H_\alpha\|_{\mathcal{L}^2}^2 = \alpha!$

and any element  $f(\omega) \in \mathcal{L}^2(\Omega, \mathcal{F}, \wp)$  can be represented using the Wiener chaos expansion theorem as

$$f(\omega) = \sum_{\alpha \in I} C_\alpha H_\alpha(\omega) \quad (6.56)$$

where  $\omega$  belongs to the Gaussian white noise probability space,  $C_\alpha \in \mathbb{R}$ ,  $\alpha \in I$  and

$$\|f\|_{L^2}^2 = \sum_{\alpha \in I} C_\alpha^2 \alpha! < \infty$$

### Example 6.5.1

To find the Wiener-Itô chaos expansion of the random variable  $\xi(\omega) = W^2(\tau, \omega)$ .

We know that,

$$\begin{aligned} \int_0^\tau \int_0^{\tau_2} 1 dW(\tau_1) dW(\tau_2) &= \int_0^\tau W(\tau_2) dW(\tau_2) \\ &= \frac{1}{2} W^2(\tau) - \frac{1}{2} \tau \end{aligned}$$

Re-writing,

$$\begin{aligned} W^2(\tau) &= \tau + 2 \int_0^\tau \int_0^{\tau_2} dW(\tau_1) dW(\tau_2) \\ &= \tau + 2 \int_0^\tau \int_0^{\tau_2} \chi_{[0,t]}(\tau_1) \chi_{[0,t]}(\tau_2) dW(\tau_1) dW(\tau_2) \\ &= \tau + I_2[f_2] \end{aligned} \quad (6.57)$$

with  $f_2(\tau_1, \tau_2) = \chi_{[0,t]}(\tau_1) \chi_{[0,t]}(\tau_2)$

### Example 6.5.2

To find the chaos expansion to the solution of the SDE,

$$dY(t) = \mu Y(t) dt + \sigma Y(t) dW(t), \text{ with } Y_0 = y, t > 0 \quad (6.58)$$

Also, using chaos expansion to calculate  $E[Y(t)]$  and  $E[Y^2(t)]$ .

The solution of equation (6.58) is the geometric Brownian motion given as,

$$Y(t) = y \exp \left[ \left( \mu - \frac{\sigma^2}{2} \right) t + \sigma W(t) \right]$$

or,

$$Y(t) = y \exp(\mu t) \exp \left( \sigma W(t) - \frac{1}{2} \sigma^2 t \right) \quad (6.59)$$

using  $f(\tau) = \sigma \mathbf{1}_{[0,t]}(\tau)$  and the result of the Wiener Itô iterated integral

$$\exp\left(\sigma W(t) - \frac{1}{2}\sigma^2 t\right) = \sum_{n=0}^{\infty} \frac{\|f\|^n}{n!} h_n\left(\frac{\sigma W(t)}{\|f\|}\right) \quad (6.60)$$

but  $\|f\| = \left(\int_0^t \sigma^2 d\tau\right)^{\frac{1}{2}} = \sigma\sqrt{t}$

Hence,

$$\begin{aligned} Y(t) &= y \exp(\mu t) \sum_{n=0}^{\infty} \frac{\sigma^n t^{n/2}}{n!} h_n\left(\frac{W(t)}{\sqrt{t}}\right) \\ &= y \exp(\mu t) \sum_{n=0}^{\infty} \sigma^n I_n \left( \frac{\mathbf{1}_{[0,t]}(\tau_1) \mathbf{1}_{[0,t]}(\tau_2) \dots \dots \mathbf{1}_{[0,t]}(n)}{n!} \right) \\ Y(t) &= \sum_{n=0}^{\infty} I_n \left( y \exp(\mu t) \frac{\sigma^n}{n!} \mathbf{1}_{[0,T]}^{\otimes n} \right) \end{aligned} \quad (6.61)$$

Now,

$$\begin{aligned} EY(t) &= I_0(y \exp(\mu t)) \\ EY(t) &= y \exp(\mu t) \end{aligned} \quad (6.62)$$

since

$$I_n = \begin{cases} 0, & n \neq 0 \\ 1, & n = 0 \end{cases}$$

therefore

$$EY(t) = y \exp(\mu t)$$

now,

$$\begin{aligned} EY^2(t) &= \|Y(t)\|_{\mathcal{L}^2([0,T])}^2 \\ &= \sum_{n=0}^{\infty} n! \left\| y \exp(\mu t) \frac{\sigma^n}{n!} \mathbf{1}_{[0,T]}^{\otimes n} \right\|_{\mathcal{L}^2([0,T]^n)}^2 \\ &= \sum_{n=0}^{\infty} n! \frac{y^2 \exp(2\mu t)}{(n!)^2} \sigma^{2n} t^n \\ &= y^2 \exp(2\mu t) \sum_{n=0}^{\infty} \frac{(\sigma^2 t)^n}{n!} \\ EY^2(t) &= y^2 \exp(2\mu t + \sigma^2 t) \end{aligned} \quad (6.63)$$

## 6.6 Important definitions

### 6.6.1 Kondratiev test space

The random variables of the Kondratiev test space  $(S)_1$  contains the elements of function  $F$  defined by Wiener chaos expansion as,

$$F = \sum_{\alpha \in I} a_{\alpha} H_{\alpha} \in \mathcal{L}^2([0, T]), a_{\alpha} \in \mathbb{R}, \alpha \in I$$

such that,

$$\|F\|_{1,r}^2 = \sum_{\alpha \in I} a_\alpha^2 (\alpha!)^2 (2\mathbb{N})^{r\alpha} < \infty, \text{ for all } r \in \mathbb{N}_0$$

Also, the generalised random variable  $f$  of the Kondratiev test space  $(S)_{-1}$  of the form

$$f = \sum_{\alpha \in I} b_\alpha H_\alpha \in \mathcal{L}^2([0, T]), b_\alpha \in \mathbb{R}, \alpha \in I$$

are such that,

$$\|f\|_{-1,-r}^2 = \sum_{\alpha \in I} b_\alpha^2 (\alpha!)^2 (2\mathbb{N})^{-r\alpha} < \infty, \text{ for some } r \in \mathbb{N}_0$$

### 6.6.2 Hida test space

Random variables of the Hida test space  $(S)_0$  contains the elements of function  $F$  defined by Wiener chaos expansion as,

$$F = \sum_{\alpha \in I} a_\alpha H_\alpha \in \mathcal{L}^2([0, T]), a_\alpha \in \mathbb{R}, \alpha \in I$$

such that,

$$\|F\|_{0,r}^2 = \sum_{\alpha \in I} a_\alpha^2 (\alpha!)^2 (2\mathbb{N})^{r\alpha} < \infty, \text{ for all } r \in \mathbb{N}_0$$

Also, the generalised random variable  $f$  of the Hida test space  $(S)_{-0}$  of the form

$$f = \sum_{\alpha \in I} b_\alpha H_\alpha \in \mathcal{L}^2([0, T]), b_\alpha \in \mathbb{R}, \alpha \in I$$

are such that,

$$\|f\|_{0,-r}^2 = \sum_{\alpha \in I} b_\alpha^2 (\alpha!)^2 (2\mathbb{N})^{-r\alpha} < \infty, \text{ for some } r \in \mathbb{N}_0$$

### 6.6.3 Need of the test spaces

We know that the Wick product of the two test functions, say,  $f(\omega), g(\omega) \in (S)_{-1}$ , satisfying chaos expansion theorem  $f(\omega) = \sum_{\alpha \in \Omega} a_\alpha H_\alpha(\omega) \in$  and  $g(\omega) = \sum_{\beta \in \Omega} b_\beta H_\beta(\omega)$  for unique

$a_\alpha, b_\beta \in \mathbb{R}$  is given as

$$\begin{aligned} f(\omega) \diamond g(\omega) &= \sum_{\gamma} \left( \sum_{\alpha+\beta=\gamma} a_\alpha b_\beta \right) H_\gamma(\omega) \\ &= \sum_{\alpha} \sum_{\beta} a_\alpha b_\beta H_{\alpha+\beta}(\omega) \end{aligned}$$

It is important to note that the Kondratiev spaces are closed under Wick multiplication whereas  $\mathcal{L}^2(\Omega, \mathcal{F}, \wp)$  is not.

#### Example 6.6.1

To prove this, let us take a random variable  $f(\omega) \in \mathcal{L}^2$  such that,

$$f(\omega) = \sum_{n=1}^{\infty} \frac{1}{n\sqrt{n!}} H_n(\omega)$$

We have,

$$\|f\|_{\mathcal{L}^2}^2 = \sum_{n=1}^{\infty} \frac{1}{n^2} < \infty$$

thus  $f(\omega) \in \mathcal{L}^2$ ,

but,

$$\begin{aligned} \|f \diamond f(\omega)\|_{\mathcal{L}^2}^2 &= \sum_{n=1}^{\infty} \left( \sum_{p=1}^{\infty} \frac{1}{p(n-p)\sqrt{p!(n-p)!}} \right)^2 n! \\ &\geq \sum_{n=1}^{\infty} \left( \sum_{p=1}^{\infty} \frac{1}{p(n-p)} \right)^2 = \infty \end{aligned}$$

Hence,  $f \diamond f(\omega) \notin \mathcal{L}^2$ .

## 6.7 Stochastic derivative and Malliavin derivative

Let the directional derivative of a function  $F: \Omega \rightarrow \mathbb{R}$  in the direction of  $v$  exists in strong sense, where  $v = \int_0^t g(\tau) d\tau \in \Omega$  (Cameron Martin space). Then,

$$\mathbb{D}_v F(\omega) := \frac{\lim_{\Delta \rightarrow 0} F(\omega + \Delta v) - F(\omega)}{\Delta}$$

exists in  $\mathcal{L}^2(\mathcal{F})$ . Also, there exists,

$$\phi(t, \omega) \in \mathcal{L}^2(\mathcal{F} \times v)$$

such that,

$$\mathbb{D}_v F(\omega) = \int_0^T \phi(t, \omega) g(t) dt, \forall v \in \Omega \quad (6.64)$$

then we say  $\mathbb{D}_t F(\omega)$  is the stochastic derivative of  $F(\omega)$  and set  $\mathbb{D}_t F(\omega) := \phi(t, \omega)$ . The set of all differentiable variables are denoted by  $\mathfrak{D}$ .

**Example 6.7.1:** Suppose  $F(\omega) = \int_0^T f(\tau) d\omega(\tau)$  and  $f(\tau) \in \mathcal{L}^2([0, T])$ ,

Then if  $v \in \mathcal{L}^2([0, T])$ ,

$$\begin{aligned} F(\omega + \Delta v) &= \int_0^T f(\tau) (d\omega(\tau) + \Delta dv(\tau)) \\ &= \int_0^T f(\tau) d\omega(\tau) + \Delta \int_0^T f(\tau) g(\tau) d(\tau) \\ \frac{F(\omega + \Delta v) - F(\omega)}{\Delta} &= \int_0^T f(\tau) g(\tau) d(\tau), \forall \Delta > 0 \end{aligned}$$

From equation (6.64),

$$F \in \mathfrak{D} \text{ and } \mathbb{D}_t F(\omega) = f(t) \forall t \in [0, T], \omega \in \Omega,$$

If we choose  $f(t) = \mathcal{X}_{[0, t_1]}(t)$ ,

we have,

$$F(\omega) = \int_0^T \mathcal{X}_{[0, t_1]}(\tau) d\omega(\tau) = W(t_1)$$

Therefore,

$$\mathbb{D}_t W(t_1) = \mathcal{X}_{[0, t]}(t) \quad (6.65)$$

## 6.8 Integration by parts formula and Malliavin derivative

### 6.8.1 Chain rule

Let  $\mathfrak{s}$  denotes the set of all random variables  $F := \phi(\theta_1, \theta_2, \dots, \theta_n)$  such that,

$$\phi(x_1, x_2, \dots, x_n) = \sum_{\alpha} C_{\alpha} x_{\alpha} \quad (6.66)$$

is a polynomial known as the Wiener polynomial with  $x^{\alpha} = x_1^{\alpha_1} \dots \dots x_n^{\alpha_n}$ ,  $\alpha = (\alpha_1, \dots \dots \alpha_n)$  and

$$\theta_j = \int_0^T g_j(t) dW(t) \text{ for some } g_j \in \mathcal{L}^2([0, T]), j = 1, \dots \dots, n$$

Now,

$$F = \phi(x_1, x_2, \dots, x_n) \in \mathfrak{s}$$

i.e.,

$$F \in \mathfrak{D}$$

then

$$\mathbb{D}_t F = \sum_{j=1}^n \frac{\partial \phi}{\partial \theta_j}(\theta_1, \theta_2, \dots, \theta_n) f_j(t) \quad (6.67)$$

### 6.8.2 Expectation rule

For  $F, \phi \in \mathfrak{D}$  and  $v \in \Omega$  with  $g \in \mathcal{L}^2([0, T])$ ,

$$E[\mathbb{D}_v, F, \phi] = E \left[ F \cdot \phi \int_0^T g(\tau) dW(\tau) \right] - E[F \cdot \mathbb{D}_v \phi]$$

Proof of this formula can be found in the extant literature (Di Nunno & Øksendal, 2011).

### 6.8.3 Malliavin derivative

The core mathematical object in Malliavin calculus is the Malliavin derivative, denoted by  $\mathbb{D}_t$ , which acts on random variables to produce functionals that encode the sensitivity of these variables to changes in the underlying probability measure. This derivative is defined as an infinite-dimensional operator on a suitable space of smooth random variables.

For  $F \in \mathfrak{D}$ , there exists  $\{F_n\}_{n=1}^{\infty} \in \mathfrak{S}$  so that  $F_n \rightarrow F$  in  $\mathcal{L}^2([0, T])$ .

The Malliavin derivative of  $F$  is defined as,

$$\mathbb{D}_t F = \lim_{n \rightarrow \infty} \mathbb{D}_t F_n \text{ in } \mathcal{L}^2([0, T] \times \nu) \quad (6.68)$$

and  $\{\mathbb{D}_t F_n\}_{n=1}^{\infty}$  is convergent in  $\mathcal{L}^2([0, T] \times \nu)$ .

**Note:** If  $F \in \mathbb{D} \cap \mathfrak{D}$ , both stochastic and Malliavin derivative coincide.

### Example 6.8.1

Suppose  $F(\omega) = e^{\omega(t_0)}$ ,  $t_0 \in [0, T]$ . To find the Malliavin derivative of  $F(\omega)$ .

Using equation (6.65)

$$\mathbb{D}_t W(t) = \mathcal{X}_{[0, T]}(t), \forall t \in [0, T]$$

where  $\mathcal{X}_{[0, T]}(t)$  is the characteristic function and is given by

$$\mathcal{X}_{[0, T]}(t) = \begin{cases} 1, & \tau \leq t \\ 0, & \tau \geq t \end{cases}$$

Now using equation (6.67), the Malliavin derivative of  $F(\omega) = e^{\omega(t_0)}$  is,

$$\mathbb{D}_t [e^{\omega(t_0)}] = \exp(W(t_0)) \cdot \mathcal{X}_{[0, t_0]}(t)$$

### Example 6.8.2

To find the Malliavin derivative of  $Y(t)$  given by the SDE,

$$dY(t) = \mu Y(t)dt + \sigma Y(t)dW(t), \text{ with } Y_0 = y \quad (6.69)$$

The solution of equation (6.69) is the equation of geometric Brownian motion given as,

$$Y(t) = y \exp\left[\left(\mu - \frac{\sigma^2}{2}\right)t + \sigma W(t)\right]$$

Taking the Malliavin derivative  $\mathbb{D}_\tau$  to  $Y(t)$ ,

$$\begin{aligned} \mathbb{D}_\tau Y(t) &= y \exp\left(\left(\mu - \frac{\sigma^2}{2}\right)t\right) \mathbb{D}_\tau \exp(\sigma W(t)) \\ &= y \exp\left(\left(\mu - \frac{\sigma^2}{2}\right)t\right) \exp(\sigma W(t)) \sigma \mathbb{D}_\tau W(t) \\ &= \sigma Y(t) \mathbf{1}_{[0, t]}(\tau) \end{aligned}$$

Thus, we have

$$\mathbb{D}_\tau Y(t) = \begin{cases} \sigma Y(t), & \tau \leq t \\ 0, & \tau \geq t \end{cases}$$

### Example 6.8.3

To find the Malliavin derivative of  $Y(t)$  given by the SDE

$$dY(t) = \mu Y(t)dt + \sigma dW(t), \text{ with } Y_0 = y \quad (6.70)$$

The solution of equation (6.70) is the Ornstein-Uhlenbeck (OU) process and is given by,

$$Y(t) = \exp(\mu t) \left[ y + \sigma \int_0^t \exp(-\mu s) dW(s) \right] \quad (6.71)$$

Re-writing equation (6.71),

$$Y(t) = \exp(\mu t) \left[ y + \sigma \int_0^T \mathbf{1}_{[0,t]}(s) \exp(-\mu s) dW(s) \right] \quad (6.72)$$

now applying the Malliavin derivative  $\mathbb{D}_\tau$  to both sides of the equation (6.72).

Since the Malliavin derivative is deterministic for the Ornstein-Uhlenbeck (OU) process, we get,

$$\begin{aligned} \mathbb{D}_\tau Y(t) &= \exp(\mu t) \left[ \sigma \mathbb{D}_\tau \int_0^T \mathbf{1}_{[0,t]}(s) \exp(-\mu s) dW(s) \right] \\ &= \exp(\mu t) \sigma \mathbf{1}_{[0,t]}(\tau) \exp(-\mu \tau) \\ &= \sigma \exp(\mu(t-\tau)) \mathbf{1}_{[0,t]}(\tau) \end{aligned}$$

## 6.9 Malliavin derivative and chaos expansion

The Malliavin derivative can also be defined via the Wiener-Itô chaos expansion theorem. As we have already defined the Malliavin derivative  $\mathbb{D}_\tau$  for smooth random variables, the result is obvious. The Malliavin derivative for multiple Itô iterated integrals defined as  $I_n(f^{\otimes n})(\omega) = h_n(\langle \omega, \varphi \rangle)$

is given as,

$$\mathbb{D}_\tau I_n(f^{\otimes n}) = h_n'(\langle \omega, \varphi \rangle) \varphi(t) \quad (6.73)$$

applying the property of Hermite polynomials,

$$\begin{aligned} \mathbb{D}_\tau I_n(f^{\otimes n}) &= n h_{n-1}(\langle \omega, \varphi \rangle) \varphi(t) \\ &= n I_{n-1}(\varphi^{\otimes(n-1)} \cdot \varphi(t)) \end{aligned}$$

for  $F = \sum_{n=0}^{\infty} I_n(f_n)$ ,  $f_n \in \tilde{\mathcal{L}}^2([0, T]^n)$

$$\mathbb{D}_\tau(F) = \sum_{n=1}^{\infty} n I_{n-1} f_n(\odot, t) \quad (6.74)$$

where  $\odot$  denotes the multiple integration taken over  $(n-1)$  variables and does not depend on which variable is set free as  $t$  because  $f_n$  is considered as symmetric.

## 6.10 The Skorohod integral and Wiener-Itô chaos expansion

The Skorohod integral is an extension of the Itô integral when the integrands are not necessarily  $\mathcal{F}_t$ -adapted.

Let a stochastic process  $X(t, \omega)$  be such that  $t \in [0, T]$ ,  $\omega \in \Omega$ ,  $X(t, \cdot)$  is  $\mathcal{F}_t$ -measurable and  $E[X^2(t, \omega)] < \infty, \forall t \in [0, T]$ .

We get functions  $g_{n,t}(t_1, t_2, \dots, t_n) \in \tilde{\mathcal{L}}^2(\mathbb{R}^n)$  such that,

$$X(t, \omega) = \sum_{n=0}^{\infty} I_n(g_{n,t}(\cdot))$$

where  $g_{n,t}(t_1, t_2, \dots, t_n) = g_n(t_{1,t}, \dots, t_{n,t})$ . As  $g_{n,t}(\cdot)$  depends on the parameter  $t$ , it will be a function of  $(n + 1)$  parameters.

Now we can define the Skorohod integral of  $X$  as,

$$\delta X := \int_0^T X(t, \omega) \delta W(t) := \sum_0^{\infty} I_{n+1}(\tilde{X}_n) \quad (6.75)$$

### Example 6.10.1

To evaluate the Skorohod integral,

$$\int_0^T W^2(\tau) \delta W(\tau), \quad \tau \in [0, T] \text{ and fixed}$$

Using the Wiener-Itô representation theorem given in equation (6.55), we have

$$\int_0^T W^2(\tau_0) \delta W(\tau) = \int_0^T (\tau_0 + I_2(f_2)) \delta W(\tau)$$

where  $f_2(\tau_1, \tau_2, \tau) = \mathcal{X}_{[0, \tau_0]}(\tau_1) \mathcal{X}_{[0, \tau_0]}(\tau_2)$

and,

$$\tilde{f}_2(\tau_1, \tau_2, \tau) = \frac{1}{3} [f_2(\tau_1, \tau_2, \tau) + f_2(\tau, \tau_2, \tau_1) + f_2(\tau_1, \tau, \tau_2)]$$

$$= \frac{1}{3} [\mathcal{X}_{[0, \tau_0]}(\tau_1) \mathcal{X}_{[0, \tau_0]}(\tau_2) + \mathcal{X}_{[0, \tau_0]}(\tau) \mathcal{X}_{[0, \tau_0]}(\tau_2) + \mathcal{X}_{[0, \tau_0]}(\tau_1) \mathcal{X}_{[0, \tau_0]}(\tau)]$$

$$= \frac{1}{3} [\mathcal{X}_{\{\tau_1, \tau_2 < \tau_0\}} + \mathcal{X}_{\{\tau, \tau_2 < \tau_0\}} + \mathcal{X}_{\{\tau_1, \tau < \tau_0\}}]$$

$$= \mathcal{X}_{\{\tau_1, \tau_2 < \tau_0\}} + \frac{1}{3} \mathcal{X}_{\{\tau_1, \tau_2 < \tau_0 < \tau\}} + \frac{1}{3} \mathcal{X}_{\{\tau, \tau_2 < \tau_0 < \tau_1\}} + \frac{1}{3} \mathcal{X}_{\{\tau_1, \tau < \tau_0 < \tau_2\}}$$

Thus,

$$\begin{aligned}
\int_0^T W^2(\tau_0) \delta W(\tau) &= \tau_0 W(T) + \int_0^T I_2(f_2) \delta W(\tau) \\
&= \tau_0 W(T) + I_3(\tilde{f}_2) \\
&= \tau_0 W(T) + 6J_3(\tilde{f}_2) \\
&= \tau_0 W(T) + 6 \int_0^T \int_0^{\tau_3} \int_0^{\tau_2} \mathbf{X}_{[0, \tau_0]}^{\otimes 3}(\tau_1, \tau_2, \tau_3) dW(\tau_1) dW(\tau_2) dW(\tau_3) \\
&\quad + 6 \int_0^T \int_0^{\tau_3} \int_0^{\tau_2} \frac{1}{3} \mathbf{X}_{\{\tau_1, \tau_2 < \tau_0 < \tau_3\}} dW(\tau_1) dW(\tau_2) dW(\tau_3) \\
&= \tau_0 W(T) + \tau_0^{3/2} h_3 \left( \frac{W(\tau_0)}{\sqrt{\tau_0}} \right) + 2 \int_{\tau_0}^T \int_0^{\tau_0} \int_0^{\tau_2} dW(\tau_1) dW(\tau_2) dW(\tau_3) \\
&= \tau_0 W(T) + \tau_0^{3/2} \left( \frac{W^3(\tau_0)}{\tau_0^{3/2}} - 3 \frac{W(\tau_0)}{\sqrt{\tau_0}} \right) + 2 \int_{\tau_0}^T \left( \frac{W^3(\tau_0)}{2} - \frac{\tau_0}{2} \right) dW(\tau_3)
\end{aligned}$$

using  $dW(\tau_3) = W(T) - W(\tau_0)$ , we get,

$$\int_0^T W^2(\tau_0) \delta W(\tau) = W^2(\tau_0)W(T) - 2\tau_0 W(\tau_0)$$

## 6.11 Application of the Malliavin derivative

Malliavin derivatives are primarily applied to simulate the Greeks in option pricing models and to reduce the variance of Greeks. The uncertainty in option pricing are modelled by a complete probability space  $(\Omega, \mathcal{F}, \mathcal{P})$  according to a filtration  $\{\mathcal{F}_t, t \in [0, T]\}$  generated by the standard Wiener process  $W(t)_{t \in [0, T]}$ .

Here  $T$  denotes the expiry date of the price  $P(x)$ , defined as the expectation of discounted payoff function,

$$P(x) = E^{\mathbf{P}} \left[ f(X_T) \exp \left( - \int_0^T r_\tau d\tau \right) \right] \text{ for } \sigma\text{-algebra } \mathcal{F}_0,$$

With a risk neutral measure  $\mathbf{P}$ , risk free rate  $r_\tau$  and the price,  $X_T$ , given by the diffusion equation (6.69)

$$dX_t = rX_t dt + \sigma X_t dW_t, \text{ with initial condition } X_0 = X$$

For a strong unique solution  $X_t$  of the above equation taking the PDF,  $P(x)$  can be written as,

$$P(x) = \int_{-\infty}^{\infty} e^{-rT} f\left(x \exp\left(rT + \sigma\sqrt{T}z - \frac{1}{2}\sigma^2T\right)\right) \frac{1}{\sqrt{2\pi}} e^{-z^2/2} dz$$

Using the finite difference method for the two shifted prices (Nunno, 2009), the expectation of discounted prices can be written as,

$$\frac{\partial P}{\partial x} = E^P\left(\frac{e^{-rT}}{x\sigma T}\right) \mathcal{W}_T f(X_T) \quad (6.76)$$

This payoff function is smoothed using the process with a weight function  $\mathcal{W}_T$  which does not depend on the payoff. It is also useful in the case of discontinuous payoffs.

Now, this stochastic weight function can be determined using the Malliavin derivative according to Theorem 2.3.1 in Nualart and Saussereau (2009) as follows,

$$\mathbb{D}_\tau X_T = Y_t Y_\tau^{-1} \sigma(\tau, X_\tau) \mathbf{1}_{\{\tau \leq t\}} \text{ a. s.}$$

Assuming that the payoff depends on a finite set of payment dates:  $t_1, t_2, \dots, t_n$  with  $t_0$  and  $t_n = T$ .

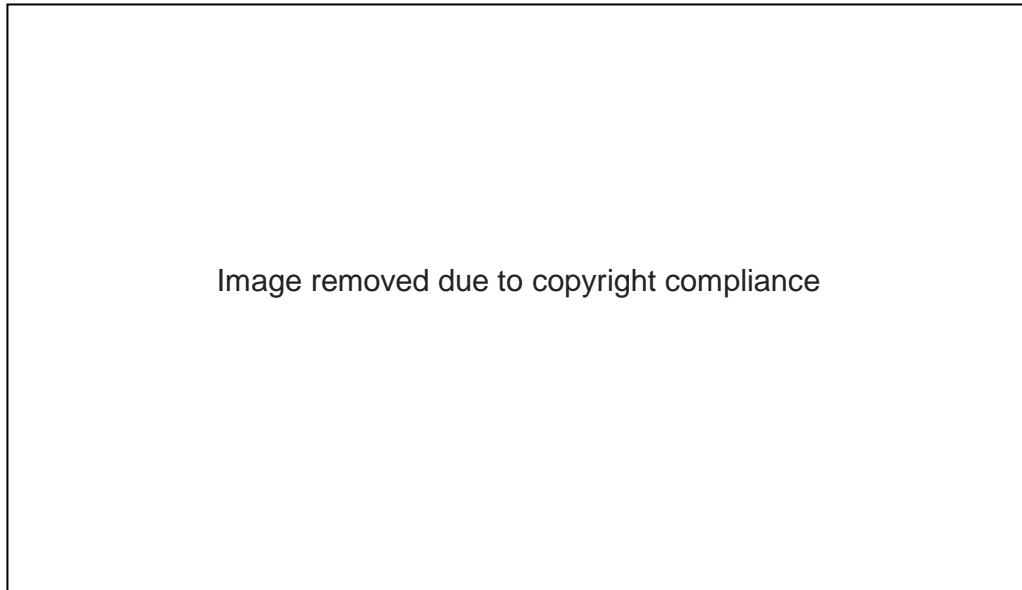


**Figure 6.6** Greek (Delta value) under the classical Heston model for a binary call option with a bounded parameter,  $K$ , and various parameters defined in Table 2 in existing literature (Zhong & Cass, 2017).

*Note.* Function used for Figure 6.6 is the payoff function defined as  $f(x) = 1_{x>K}$

For a classical Heston model, (Zhong & Cass, 2017) obtained the closed form, finite difference and the Malliavin calculus solutions for Greeks (Delta, Gamma, Vega) for the European and binary call

options and compared the delta values (Figure 6.6). The Malliavin Calculus Monte Carlo (MC) results are closer to exact solution.

Lai and Yao (2016) derived the Greek formula for the European-style multi-asset options using dependent Brownian motion. The numerical results show that Malliavin calculus is a more efficient computational method than the finite difference method and Monte Carlo methods for non-smooth payoffs. Accuracy and efficiency can be improved using variance reduction techniques and by using Sobol sequences. The authors claimed ten thousand times more efficiency for six asset options (see Figure 6.7).

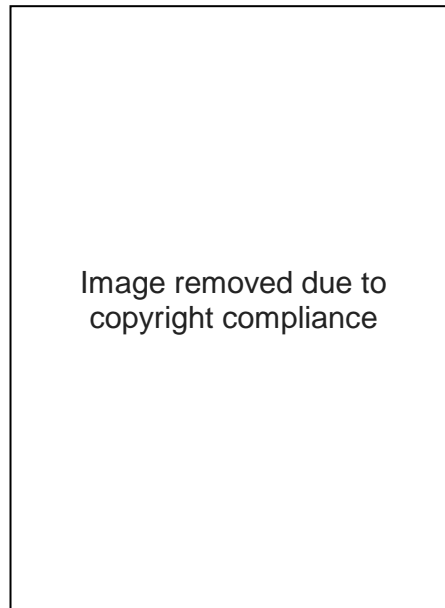


**Figure 6.7 Comparison of simulation errors for Greek (Delta) for a six-dimensional basket type down and out option pricing model under the variance gamma (VG) model using different parameters as defined by Lai and Yao (2016).**

### 6.11.1 Contaminant transport

We assume that the system evolves in some state space  $S$  and is stochastic. The state of the simulation changes at each simulation, from  $S$  to  $S^{\text{new}}$ , and is defined by a propagator  $\epsilon(S \rightarrow S^{\text{new}})$ , having probability distribution  $P(S)$  and satisfies the following property,

$$P^{\text{new}}(S^{\text{new}}) = \int_S \epsilon(S \rightarrow S^{\text{new}}) P(S) dS \quad (6.77)$$

In short,

$$P^{\text{new}} = \int \epsilon P \quad (6.78)$$

In this approach, at each state, the particle position is changing with the trajectory of the particle movement. Also, the product  $\epsilon(S_1 \rightarrow S_2) \times \dots \times \epsilon(S_{n-1} \rightarrow S_n)$  is proportional to probability of occurrence of states,  $\{S_1, \dots, S_n\}$ . Let,

$$\mathbb{w}(S_1, \dots, S_n) = \epsilon(S_1 \rightarrow S_2) \times \dots \times \epsilon(S_{n-1} \rightarrow S_n) \quad (6.79)$$

Consider an average quantity  $Q$ . It could be chemical concentration of various species in water flow or in a biochemical network. It could be the average of permeabilities in a heterogenous medium).  $Q$  can be defined as,

$$\langle Q \rangle = \int Q P \quad (6.80)$$

where  $P$  is the probability distribution function. We are interested in capturing the sensitivity of  $\langle Q \rangle$  with respect to variations in parameter  $v$  for a stochastic force field  $F$ .

We have,

$$\frac{\partial \langle Q \rangle}{\partial v} = \int Q P A_v \quad (6.81)$$

Where  $A_v = \frac{\partial \ln P}{\partial v}$ .

We start tracking our system with an additional stochastic variable  $p_v$  along with state space. It is such that it does not change system's dynamics. Thus, the extended state space is  $\{S, p_v\}$ .

We now calculate the average  $p_v$  in the extended state space and set the rule for updating  $p_v$ , such that  $\langle p_v \rangle_S = p_v$ .

This means that the average value of  $p_v$  at a particular point measures the derivative of probability distribution with respect to the parameter of interest  $v$ .

Using equation (6.81),

$$\frac{\partial Q}{\partial v} = \langle Q, p_v \rangle \quad (6.82)$$

$p_v$  is the Malliavin weight and the updating rule after each simulation is derived from the system's stochastic equation of motion.

Differentiating (6.77) and using short hand notation,

$$p_v^{\text{new}}(p_v^{\text{new}}) = \int \epsilon P \left( p_v + \frac{\partial \ln \epsilon}{\partial v} \right) \quad (6.83)$$

Using the above equation. The updating rule is,

$$p_v^{\text{new}} = p_v + \frac{\partial \ln \epsilon}{\partial v} \quad (6.84)$$

**Remark 6.11.1**

For the purpose of simulation,

- The initial Malliavin weight is assumed to be zero, i.e.,  $p_v = 0$ .
- Quantity  $\langle Q \rangle$  and  $\frac{\partial \langle Q \rangle}{\partial v}$  are time-dependent. Therefore,

$$\langle Q \rangle \approx \frac{1}{N} \sum_{i=1}^N Q_i(t) \quad (6.85)$$

and,

$$\frac{\partial \langle Q \rangle}{\partial v} \approx \frac{1}{N} \sum_{i=1}^N Q_i(t) p_{v,i}(t) \quad (6.86)$$

where  $N$  is the total number of simulations.

From equation (6.84),

$$p_v = \frac{\partial \ln w}{\partial v} \quad (6.87)$$

$w$  is given by equation (6.79).

Let us capture the movement of a particle (contaminant) in a force field characterised by 1-dimensional Brownian motion. Also, let the particle position set out by ' $x$ ' as,

$$\frac{dx}{dt} = F(x) + \xi \quad (6.88)$$

where  $F(x)$  is the force field and  $\xi$  is the Gaussian white noise. Discretising the new position for particle as,

$$x^{\text{new}} = x + F(x)\Delta t + \zeta \quad (6.89)$$

in which  $\Delta t$  is the time step and  $\zeta$  is the Gaussian random variate with zero mean and variance  $\Delta t$ .

The propagator function is given by,

$$\epsilon(x \rightarrow x^{\text{new}}) = \frac{1}{\sqrt{2\pi\Delta t}} \exp\left(-\frac{(x^{\text{new}} - x - F(x)\Delta t)^2}{2\Delta t}\right)$$

The force field is stochastic. It is characterised by the parameter  $v$ , we have

$$\frac{\partial \ln \epsilon(x \rightarrow x^{\text{new}})}{\partial v} = \frac{x^{\text{new}} - x - F(x)\Delta t}{\Delta t} \frac{\partial F}{\partial v} \quad (6.90)$$

using  $x^{\text{new}} - x - F(x) = \zeta$ , we get,

$$p_v^{\text{new}} = p_v + \zeta \frac{\partial F}{\partial v} \quad (6.91)$$

**Remark 6.11.2**

$\zeta$  in equation (6.91) is the same as updating the position in equation (6.89). Hence the change in the Malliavin weight is completely determined by the end points  $x$  and  $x^{\text{new}}$ .

- Since  $\zeta$  is an uncorrelated random variate, the average weight is  $\langle p_v^{\text{new}} \rangle = \langle p_v \rangle$  with initial condition  $\langle p_v \rangle = 0$ .

- Actually, the average weight  $\langle p_{\nu}^{\text{new}} \rangle$  over the space  $S$  for a specific point due to different trajectories is the expected value of the Malliavin weight.

Differentiating again equation (6.90) with respect to another parameter say ' $\lambda$ ',

$$\frac{\partial^2 \ln \mathbb{E}(x \rightarrow x^{\text{new}})}{\partial \nu \partial \lambda} = (x^{\text{new}} - x - F(x)\Delta t) \frac{\partial^2 F}{\partial \nu \partial \lambda} - \Delta t \frac{\partial F}{\partial \lambda}$$

Therefore, the updating rule for Malliavin weight is,

$$p_{\nu\lambda}^{\text{new}} = p_{\nu\lambda} + \zeta \frac{\partial^2 F}{\partial \nu \partial \lambda} - \Delta t \frac{\partial F}{\partial \nu} \frac{\partial F}{\partial \lambda} \quad (6.92)$$

The average value over replicate simulation is,

$$\langle p_{\nu\lambda}^{\text{new}} \rangle = \langle p_{\nu\lambda} \rangle - \Delta t \frac{\partial F}{\partial \nu} \frac{\partial F}{\partial \lambda} \quad (6.93)$$

Hence, we can say that the average value drifts in time.

### 6.11.2 Numerical simulation

Suppose the stochastic force field is linear and is taken as,

$$F = -\xi_1 x + \xi_2 \quad (6.94)$$

Equation (6.94) is a Langevin equation and is a random process (Zwanzig, 2001) whose mean position is given by,

$$\langle x(t) \rangle = x_0 e^{-\xi_1 t} + \frac{\xi_2}{\xi_1} (1 - e^{-\xi_1 t}) \quad (6.95)$$

Our aim is to find the derivative of  $\langle x(t) \rangle$  with respect to  $\xi_1$  and  $\xi_2$  by setting up the initial value of  $\xi_1$  as finite and take  $\xi_2 = 0$ . We get,

$$\frac{\partial \langle x(t) \rangle}{\partial \xi_1} = -x_0 t e^{-\xi_1 t} \quad (6.96)$$

$$\frac{\partial \langle x(t) \rangle}{\partial \xi_2} = \frac{1 - e^{-\xi_1 t}}{\xi_1} \quad (6.97)$$

and,

$$\frac{\partial^2 \langle x(t) \rangle}{\partial \xi_1 \partial \xi_2} = \frac{t e^{-\xi_1 t}}{\xi_1} - \frac{1 - e^{-\xi_1 t}}{\xi_1^2} \quad (6.98)$$

To calculate the derivatives, the computation of the Malliavin weight using equations (6.91) and (6.93) are given as,

$$p_{\xi_1}^{\text{new}} = p_{\xi_1} + \zeta \frac{\partial F}{\partial \xi_1}$$

or,

$$p_{\xi_1}^{\text{new}} = p_{\xi_1} - \zeta x \quad (6.99)$$

similarly,

$$p_{\xi_2}^{\text{new}} = p_{\xi_2} + \zeta, \quad (6.100)$$

$$p_{\xi_1 \xi_2}^{\text{new}} = p_{\xi_1 \xi_2} + x \Delta t \quad (6.101)$$

and the position update rule is,

$$x^{\text{new}} = x - \xi_1 x \Delta t + \zeta \quad (6.102)$$

Hence, the derivatives using equation (6.99) to equation (6.102),

$$\frac{\partial \langle x(t) \rangle}{\partial \xi_1} = \langle x(t) p_{\xi_1}(t) \rangle \quad (6.103)$$

$$\frac{\partial \langle x(t) \rangle}{\partial \xi_2} = \langle x(t) p_{\xi_2}(t) \rangle \quad (6.104)$$

And

$$\frac{\partial^2 \langle x(t) \rangle}{\partial \xi_1 \partial \xi_2} = \langle x(t) (p_{\xi_1 \xi_2}(t) + p_{\xi_1}(t) p_{\xi_2}(t)) \rangle \quad (6.105)$$

Figure 6.8 illustrates the derivatives using Malliavin weight for different time steps and choosing the same sample size.

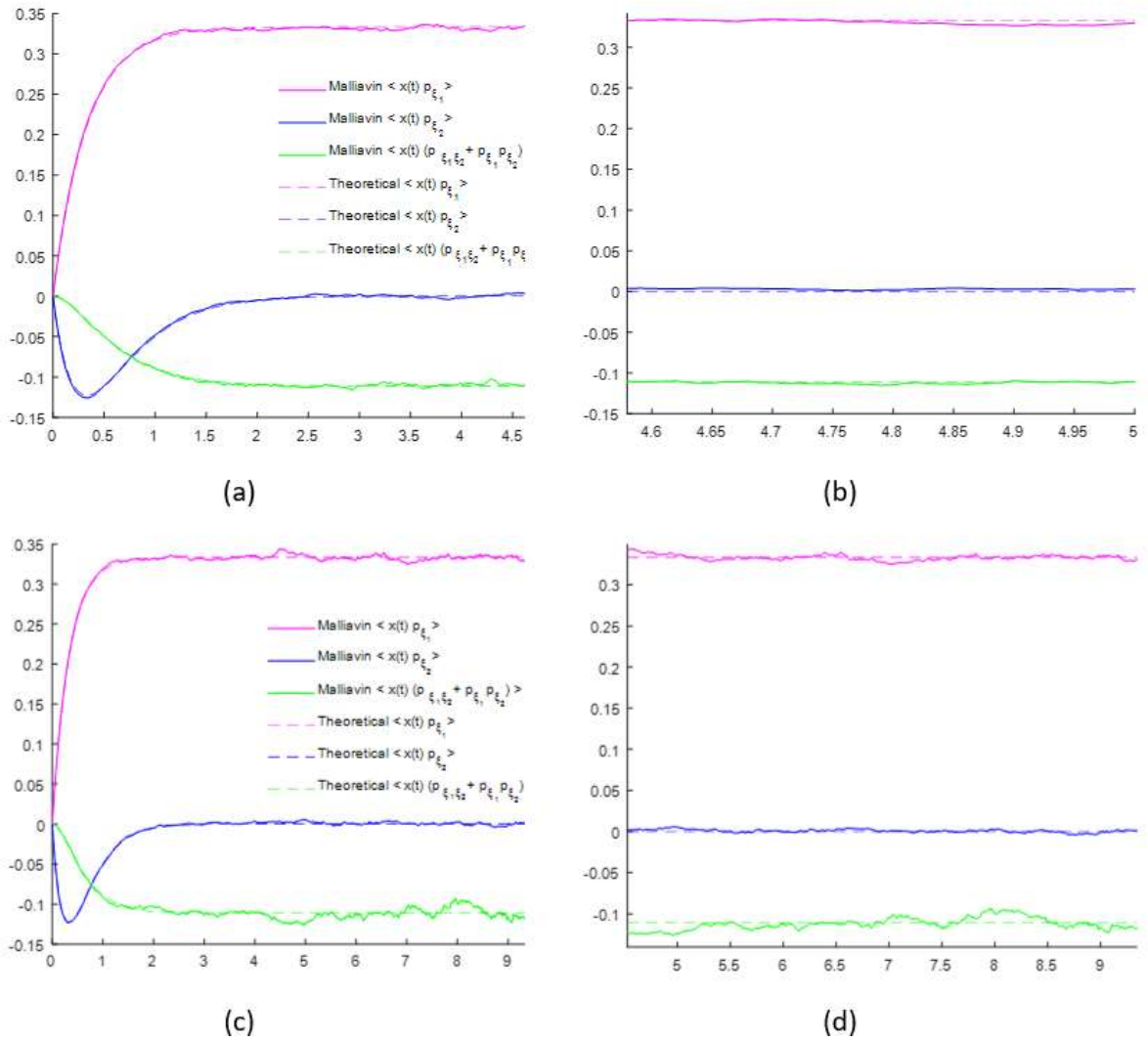


**Figure 6.8** Calculation of derivatives of first order (top, magenta, calculated by equation (6.103)), (middle, blue, calculated by equation (6.104)) and of second order (bottom, green, calculated by equation (6.105)).

*Note.* Figure 6.8 (a) is for  $t = 5$ ,  $\Delta t = 0.01$ ,  $N = 10^5$  samples, finite value of  $\xi_1 = 3$  and starting position of particle as  $x_0 = 1$ . Dashed lines shows the computation of theoretical derivatives given by equations (6.96) to (6.98) and solid lines show the value of these derivatives using Malliavin weights, as given in equation (6.103) to equation (6.105). All the derivatives are time-dependent. When we change the value of  $t = 10$ , the graph in (c) shows that these derivatives fluctuate as  $t$  increases. Figure 6.8 (b) and Figure 6.8 (d) are the zoom in graphs of (a) and (c) respectively. The graphs show that fluctuation is higher for larger  $t$  values and almost negligible for smaller  $t$  values.

Figure 6.9 shows the computation of derivatives using Malliavin weight for different time steps and choosing the large sample size as compared to Figure 6.8. With larger sample size and smaller time steps, we observed that fluctuations in first and second order derivatives are reduced.

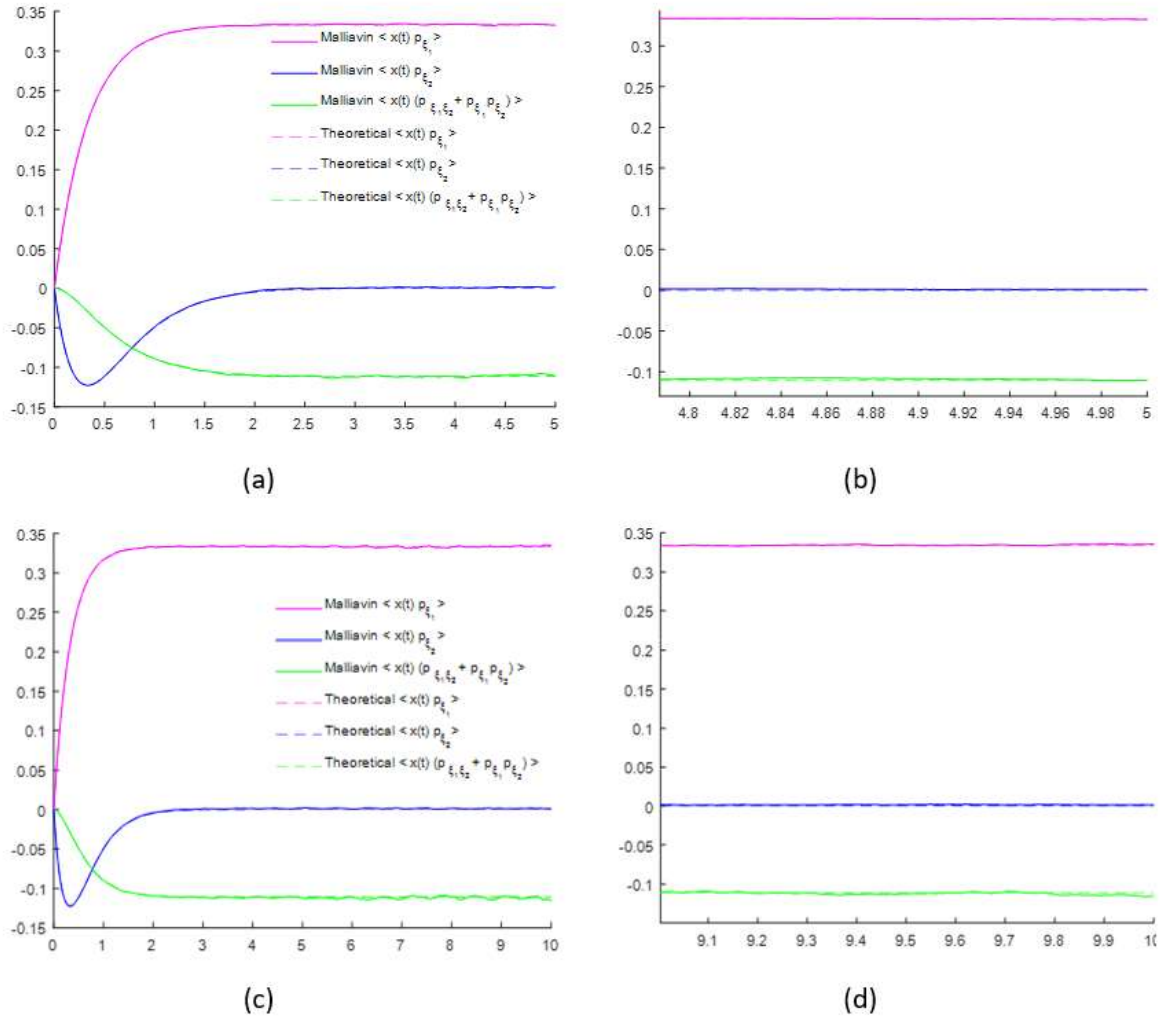


**Figure 6.9** Derivatives of first order (top, magenta, calculated by equation (6.103)), (middle, blue, calculated by equation (6.104)) and of second order (bottom, green, calculated by equation (6.105)).

*Note.* Figure 6.9 (a) is plotted for  $t = 5$ ,  $\Delta t = 0.001$ ,  $N = 10^6$  samples, finite value of  $\xi_1 = 3$  and  $x_0 = 1$  and in Figure (d)  $t = 10$ ,  $\Delta t = 0.001$ ,  $N = 10^6$  samples and  $x_0 = 1$ . The dashed lines represent the theoretical derivatives. The solid lines are the values using Malliavin weights. Graphs (b) and (d) are the zoom in graph of (a) and (c) respectively. These plots show that the fluctuation in derivatives is less compared to the variations in Figure 6.8 in which we used small sample size and large step size. The fluctuation is less even for larger  $t$  values.

## 6.12 Summary

The Wick and Malliavin calculus constitute a powerful and advanced mathematical framework used to probe the complexity of stochastic processes. The Wick calculus, an extension of the Itô calculus, offers an ingenious approach to calculating the expected values of functions of random processes, a task that can be extremely difficult. By introducing the concept of stochastic Wick products, this calculus allows the practitioner to efficiently evaluate complex expressions, thereby allowing the

analysis of higher order and cumulative moments in stochastic models. It also serves as a bridge between quantum physics and stochastic analysis, demonstrating its interdisciplinary importance.

On the other hand, Malliavin's calculus delves into functional differentiation of random processes. It provides a set of tools for computing gradient-like objects involving fundamental stochastic processes, a fundamental activity in many different fields including finance, physics, and engineering. This calculation has found many applications in sensitivity estimation, risk management, and option pricing in financial mathematics. Additionally, the Malliavin calculus plays a central role in solving partial differential equations governed by stochastic processes, providing a deep understanding of stochastic phenomena in mathematical modelling. In essence, these two complementary calculations, Wick and Malliavin, open new avenues for studying the statistical and analytical properties of stochastic processes, revealing hidden subtleties and facilitating conditions for a deeper understanding of an uncertain world.

In conclusion, Wick and Malliavin's derivative emerge as indispensable tools for navigating the complex terrain of stochastic processes. However, these powerful tools are not without limitations. Wick calculations can be computationally demanding, especially when dealing with high-dimensional systems, which limits its applicability in complex situations. Additionally, the complexity of the Malliavin calculus requires a solid mathematical foundation, making it difficult for practitioners in non-mathematical fields to access. Additionally, both calculations may not be suitable for highly nonlinear systems, where analytical solutions remain elusive. However, recognizing these limitations does not prevent us from grasping the remarkable possibilities of Wick and Malliavin's calculus. Instead, it requires continued research and development to expand their applicability and accessibility, ensuring that they remain valuable assets in the effort to understand and harness the power of random processes.

## Chapter 7 Conclusion and Future Directions

This study has delved deep into the numerical aspects of stochastic differential equations (SDEs) and stochastic partial differential equations (SPDEs) with a focus on leveraging stochastic spectral methods. We have embarked on a journey through the realm of mathematical modelling, where uncertainty and randomness are ubiquitous, and have explored techniques to effectively synthesize the numerical solutions to these complex equations.

### 7.1 Discussion

Numerical methods for solving complex systems face several challenges, given the inherent complexities of the governing equations and the presence of stochastic terms. One of the main obstacles is the explosion of complexity as the dimensionality of the problem increases. Polynomial chaos expansion (PCE) is based on the construction of a basis of orthogonal polynomials depending on the random variables of the system. When dealing with high-dimensional systems or a large number of uncertain parameters, the computational cost involved in generating and evaluating these polynomials becomes prohibitive. PCE methods also suffer with this since the number of PCE coefficients increases exponentially with higher dimension and require a large number of simulations to estimate statistical properties accurately. We could use sparse PCE, to mitigate the exponential growth in computational demand.

Another key aspect lies in the need to accurately approach random processes that exhibit non-smooth or discontinuous behaviour. PCE methods inherently assume a certain degree of flexibility in stochastic processes, which may not be the case in real situations. Discontinuous or irregular stochastic processes can lead to poor convergence of PCE approximations, making them less effective in capturing the true dynamics of the system. In such cases, specialized techniques, such as generalized polynomial chaos (gPCE), are needed in order to effectively handle these non-smooth stochastic processes.

Additionally, the accuracy of chaos expansion depends on the choice of quadrature rule and the number of quadrature points used. Finding the optimal balance between accuracy and computational efficiency is not a simple task. Advanced sampling techniques such as quasi-Monte Carlo and sparse grid methods have been developed to address these problems, allowing researchers to approach complex systems with greater precision in while still managing computational costs.

Another challenge is to choose appropriate discretization methods. Different equations may require different spatial and temporal discretisation strategy. Also, complex systems often This can be computationally expensive. However, we observed PCE methods shows better performance as

compared to MC methods, but, this could be for the systems we chose and so, cannot be generalised for all complex systems.

Overall, although polynomial chaos methods provide a powerful framework for managing randomness in complex systems governed by SDEs and SPDEs, it is essential to carefully consider the specific numerical challenges posed by the problem and is necessary for successful implementation of the method.

## **7.2 Summary of the study and contributions**

This study contributes by synthesizing and consolidating existing computational and numerical methods to solve complex systems governed by SDEs SPDEs. This synthesis provides a comprehensive understanding of the tools and techniques available to researchers and practitioners working in fields where uncertainty and opportunity play a central role. By providing a systematic and coherent overview of these methods, the thesis equips the reader with the knowledge and skills to effectively solve real-world problems.

The first objective was to understand formulation of these equations. To achieve this target, we discuss the basic requirements to constitute these equations in chapter 1 and Chapter 3 and also provided few motivational examples to support these concepts. We also did an exhaustive literature review in Chapter 2 to understand the application areas of different models governed by SDEs and SPDEs.

The second objective is accomplished in chapter 3 and Chapter 4 where we explored several methodology and numerical techniques to characterise the stochastic nature of the system and also studied the stability of these methods. We identified that in certain settings PCE methods provide insightful results and computational efficiency is better as compared to other popular methods. However, we also identified that PCE methods are not free from curse of dimensionality.

The third objective is achieved through hunting the methodologies, numerical techniques, and computational tools employed for solving SDEs and SPDEs and is mostly accomplished in chapter 4. We explained from basic concepts to how to solve stochastic integration, orthogonal basis functions and other important tools required to use PCE methods for random terms. Achieving this objective led us to next two objectives where we applied the chosen stochastic spectral method (PCE method) to some complex systems.

To achieve the fourth and fifth objective, we considered some examples from environmental modelling, non-linear systems and financial systems. The governing equations are chosen in a way so that they represent the general system not specifically belong to a particular field.

For instance, the stochastic advection dispersion equation is not limited to environmental sciences but also being used in Geological sciences (to understand the advection and dispersion of groundwater in complex geological structures), in Atmospheric sciences (to study the dispersion of air pollutants in the atmosphere, considering wind patterns and turbulence), and in Biological sciences (to analyse how populations spread and interact in heterogeneous habitats). We also provided a comparative study of the methods used and pros and cons of each method. Since the domain of this research is extensive, one method applied may not be applicable or may need some assumptions to apply it to other SDEs and SPDEs. Chapter 5 includes Wick product analysis and Malliavin derivative example where we computed some Wick exponentials. We anticipated the formulation and numerical simulation for a stochastic quantity to show how Malliavin derivatives can be computed. This is an important concept for the SDEs and SPDEs because simulating the derivative of a stochastic quantity bears a lot of challenges.

### **7.3 Conclusion**

This study centres around comprehensive discussion and application of stochastic spectral methods to tackle a range of problems. We have shown how these methods can be employed to solve contaminant transport models and other stochastic differential equations with random forcing term. Through our analysis, we have provided insight into the benefits and limitations of these methods, shedding light on their applicability and areas where they excel.

Furthermore, we have ventured into the realm of Wick products and Malliavin calculus, highlighting their significance in handling stochastic processes. Our specific example involving Malliavin weights for differential equations with random forcing terms has demonstrated the power of this calculus in finding derivatives of stochastic term.

Throughout our exploration, we have scrutinized the utility of polynomial chaos expansion (PCE) methods. We have not only discussed the advantages of PCE, such as its ability to handle uncertainty and provide insights into sensitivity analysis, but have also acknowledged its limitations when dealing with highly nonlinear dynamical systems.

To illustrate the practical aspects of our discussions, we have provided specific examples showcasing when PCE methods are particularly useful. From solving stochastic advection-diffusion equations to addressing complex physical systems, we have shown how PCE can outperform other methods but only in specific examples.

In summary, this thesis has journeyed through the fascinating landscape of stochastic spectral methods and Malliavin calculus, offering valuable insights into their application in solving SDEs and SPDEs involved in complex systems. We have delved into the intricacies of Wick products and Malliavin calculus, and we have provided a critical examination of the strengths and weaknesses of polynomial chaos expansion. This work represents a stepping stone for further research and applications in the ever-evolving field of stochastic analysis and modelling.

## 7.4 Future directions

This study suggests several future directions to follow the current work:

- We can use sparse PCE, surrogate modelling techniques, and adaptive sampling strategies to extend PCE to systems with a large number of random variables.
- To extend this research, we can combine the strengths of PCE in handling uncertainty with the power of deep learning and neural networks that can lead to more accurate and efficient predictive models for complex systems.
- Data-driven gPCE methods can be developed that can capture the inherent variability in the data due to various factors such as environmental conditions, sensor noise, or manufacturing variations. Data-driven PCE models can account for this variability, allowing for more robust predictions and design considerations and can provide a true picture of the complex system. Data-driven PCE models will be adaptive and can learn through data making them suitable for highly complex systems.
- By developing data-centric PCE models, we can uncover hidden patterns and relationships in the data that might be challenging for experts to identify manually and particularly useful in situations where limited prior knowledge exists.
- We can develop more adaptable, and scalable PCE models that integrate with big data and make them indispensable tools in the era of data-driven decision-making.

## References

- Abdul-Hadi, A. M., Abdulhussain, S. H., & Mahmmod, B. M. (2020). On the computational aspects of Charlier polynomials. *Http://Www.Editorialmanager.Com/Cogenteng*, 7(1), 1763553. <https://doi.org/10.1080/23311916.2020.1763553>
- Abell, M. L., & Braselton, J. P. (2014). Higher Order Equations. *Introductory Differential Equations*, 131–225. <https://doi.org/10.1016/B978-0-12-417219-7.00004-1>
- Accardi, L., Kuo, H. H., Obata, N., Saitô, K., Si, S., Streit, L., HIDA, T., & IKEDA, N. (2001). ANALYSIS ON HILBERT SPACE WITH REPRODUCING KERNEL ARISING FROM MULTIPLE WIENER INTEGRAL. In *Selected Papers of Takeyuki Hida* (pp. 142–168). WORLD SCIENTIFIC. [https://doi.org/10.1142/9789812794611\\_0009](https://doi.org/10.1142/9789812794611_0009)
- Almada Monter, S. A., & Budhiraja, A. (2014). Infinite dimensional forward-backward stochastic differential equations and the KPZ equation. *Electronic Journal of Probability*, 19. <https://doi.org/10.1214/EJP.V19-2709>
- Ata, B., Harrison, J. M., & Shepp, L. A. (2005). Drift rate control of a Brownian processing system. *Https://Doi.Org/10.1214/105051604000000855*, 15(2), 1145–1160. <https://doi.org/10.1214/105051604000000855>
- Baalousha, H., & Köngeter, J. (2006). Stochastic modelling and risk analysis of groundwater pollution using FORM coupled with automatic differentiation. *Advances in Water Resources*, 29(12), 1815–1832. <https://doi.org/10.1016/J.ADVWATRES.2006.01.006>
- Babuška, I., Nobile, F., & Tempone, R. (2010). A Stochastic Collocation Method for Elliptic Partial Differential Equations with Random Input Data. *Https://Doi.Org/10.1137/100786356*, 52(2), 317–355. <https://doi.org/10.1137/100786356>
- Balan, R. M., & Tudor, C. A. (2010). The stochastic wave equation with fractional noise: A random field approach. *Stochastic Processes and Their Applications*, 120(12), 2468–2494. <https://doi.org/10.1016/J.SPA.2010.08.006>
- Bear, J. (1972). *Dynamics of Fluids in Porous Media* (Dover Civil and Mechanical Engineering). Published in 1972 Reprint in 1988 in New York NY) by Dover, 784. [https://books.google.com/books/about/Dynamics\\_of\\_Fluids\\_in\\_Porous\\_Media.html?hl=iw&id=lurmlFGhTEC](https://books.google.com/books/about/Dynamics_of_Fluids_in_Porous_Media.html?hl=iw&id=lurmlFGhTEC)
- Bellmann, K. (1979). Li, Wen-Hsiung: Stochastic models in population genetics. Benchmark Papers in Genetics Vol. 7. Dowden, Hutchinson & Ross, Stroudsburg, Pennsylvania 1977. 484 S. *Biometrical Journal*, 21(3), 297–297. <https://doi.org/10.1002/bimj.4710210311>
- Biagini, F., Hu, Y., Øksendal, B., & Zhang, T. (2008). *Stochastic Calculus for Fractional Brownian Motion and Applications*. <https://doi.org/10.1007/978-1-84628-797-8>
- Bilionis, I., & Zabarav, N. (2012). Multi-output local Gaussian process regression: Applications to uncertainty quantification. *Journal of Computational Physics*, 231(17), 5718–5746. <https://doi.org/10.1016/J.JCP.2012.04.047>
- Blatman, G., & Sudret, B. (2008). Sparse polynomial chaos expansions and adaptive stochastic finite elements using a regression approach. *Comptes Rendus Mécanique*, 336(6), 518–523. <https://doi.org/10.1016/J.CRME.2008.02.013>
- Bo, L., & Capponi, A. (2018). Portfolio choice with market–credit-risk dependencies. *SIAM Journal on Control and Optimization*, 56(4), 3050–3091. <https://doi.org/10.1137/16M1084092>
- Boyaval, S., Martel, S., & Reygnier, J. (2022). Finite-volume approximation of the invariant measure of a viscous stochastic scalar conservation law. *IMA Journal of Numerical Analysis*, 42(3), 2710–2770. <https://doi.org/10.1093/IMANUM/DRAB049>
- Bueno-Guerrero, A., Moreno, M., & Navas, J. F. (2017). Malliavin Calculus for Stochastic Strings with Applications To Barrier Options and Optimal Portfolios. *SSRN Electronic Journal*. <https://doi.org/10.2139/SSRN.2935579>
- Burrage, P. M., & Burrage, K. (2003). A variable stepsize implementation for stochastic differential equations. *SIAM Journal on Scientific Computing*, 24(3), 848–864. <https://doi.org/10.1137/S1064827500376922>

- Cameron, R. H., & Martin, W. T. (1947). The Orthogonal Development of Non-Linear Functionals in Series of Fourier-Hermite Functionals. *The Annals of Mathematics*, 48(2), 385.  
<https://doi.org/10.2307/1969178>
- Castillo, E., Conejo, A. J., Pedregal, P., Garcia, R., Alguacil, N., & Allen, B. D. (2002). BUILDING AND SOLVING MATHEMATICAL PROGRAMMING MODELS IN ENGINEERING AND SCIENCE A BOOK REVIEW. In *Journal of Applied Mathematics and Stochastic Analysis*. www.gams.com.
- Chen, D., & Li, C. (2022). Closed-form expansion for option price under stochastic volatility model with concurrent jumps. *IIE Transactions*, 1–13.  
[https://doi.org/10.1080/24725854.2022.2135797/SUPPL\\_FILE/UIIE\\_A\\_2135797\\_SM9868.PDF](https://doi.org/10.1080/24725854.2022.2135797/SUPPL_FILE/UIIE_A_2135797_SM9868.PDF)
- Chen, I.-T., Chang, L.-C., & Chang, F.-J. (2018). Exploring the spatio-temporal interrelation between groundwater and surface water by using the self-organizing maps. *Journal of Hydrology*, 556, 131–142. <https://www.academia.edu/78894870>
- Cianci, R., Massabó, M., & Paladino, O. (2011). An analytical solution of the advection dispersion equation in a bounded domain and its application to laboratory experiments. *Journal of Applied Mathematics*, 2011. <https://doi.org/10.1155/2011/493014>
- Cosentino, F., Oberhauser, H., & Abate, A. (2021). *Grid-Free Computation of Probabilistic Safety with Malliavin Calculus*. <https://arxiv.org/abs/2104.14691v2>
- Cramer, H. (1970). Random Variables and Probability Distributions. *Random Variables and Probability Distributions*. <https://doi.org/10.1017/CBO9780511470936>
- Croci, M., Giles, M. B., & Farrell, P. E. (2019). Multilevel quasi Monte Carlo methods for elliptic PDEs with random field coefficients via fast white noise sampling. *ArXiv*.  
<http://arxiv.org/abs/1911.12099>
- Curtain, R. F., & Pritchard, A. J. (1977). *Functional analysis in modern applied mathematics*. 339.
- Custodio, E., Jódar, J., Herrera, C., Custodio-Ayala, J., & Medina, A. (2018). Changes in groundwater reserves and radiocarbon and chloride content due to a wet period intercalated in an arid climate sequence in a large unconfined aquifer. *Undefined*, 556, 427–437.  
<https://doi.org/10.1016/J.JHYDROL.2017.11.035>
- Dagan, G. (2002). An overview of stochastic modeling of groundwater flow and transport: From theory to applications. *Eos*, 83(53). <https://doi.org/10.1029/2002EO000421>
- Debus, P. (2013). *Application of Stochastic Volatility Models in Option Pricing*.
- Deng, Z.-Q., Singh, V. P., Asce, F., & Bengtsson, L. (2004). *Numerical Solution of Fractional Advection-Dispersion Equation*. <https://doi.org/10.1061/ASCE0733-94292004130:5422>
- Di Nunno, Giulia., Øksendal, B. K. (2011). *Advanced mathematical methods for finance*. 536.
- Di, Nunno., Øksendal, B. Proske, F. (2009). *Malliavin Calculus for Lévy Processes with Applications to Finance*. Springer Universitext, <https://doi.org/10.1007/978-3-540-78572-9>
- Di Nunno, G., Ortiz-Latorre, S., & Petersson, A. (2023). SPDE bridges with observation noise and their spatial approximation. *Stochastic Processes and Their Applications*, 158, 170–207.  
<https://doi.org/10.1016/J.SPA.2023.01.007>
- Dou, F., & Lu, Q. (2019). Partial approximate controllability for linear stochastic control systems. *SIAM Journal on Control and Optimization*, 57(2), 1209–1229.  
<https://doi.org/10.1137/18M1164640>
- Dumitrescu, R., Øksendal, B., & Sulem, A. (2018). Stochastic Control for Mean-Field Stochastic Partial Differential Equations with Jumps. *Journal of Optimization Theory and Applications*, 176(3), 559–584. <https://doi.org/10.1007/S10957-018-1243-3>
- Dunn, W. L., & Shultis, J. K. (2023). Pseudorandom Number Generators. *Exploring Monte Carlo Methods*, 55–110. <https://doi.org/10.1016/B978-0-12-819739-4.00011-1>
- Durrett, R. (2010). *Probability: theory and examples*. *Cambridge Series in Statistical and Probabilistic Mathematics*. 438.  
<http://books.google.com/books?hl=en&lr=&id=evbGTPhuvSoC&oi=fnd&pg=PR5&dq=Probability:+theory+and+examples&ots=b5d7sfbyri&sig=uy8hJbWlC1P4QgxsM89qOV8WjRE>
- Einstein, A. (1905). *ON THE ELECTRODYNAMICS OF MOVING BODIES*.
- El-Amrani, M., Seaid, M., & Zaïdi, N. L. (2012). *A new stochastic approach for advection-diffusion problems with uncertain parameters*.

- Eldred, M. S., & Burkardt, J. (2009). Comparison of non-intrusive polynomial chaos and stochastic collocation methods for uncertainty quantification. *47th AIAA Aerospace Sciences Meeting Including the New Horizons Forum and Aerospace Exposition*. <https://doi.org/10.2514/6.2009-976>
- Elsevier., Deb, M. K., Babuska, I. M., & Tinsley Oden, J. (2001). Solution of stochastic partial differential equations using Galerkin finite element techniques. *Comput. Methods Appl Mech. Engrg*, *190*, 6359–6372. [www.elsevier.com/locate/cma](http://www.elsevier.com/locate/cma)
- Elvira, V., Closas, P., & Martino, L. (2019). Gauss-Hermite quadrature for non-Gaussian inference via an importance sampling interpretation. *European Signal Processing Conference, 2019-September*. <https://doi.org/10.23919/EUSIPCO.2019.8902662>
- Engblom, S. (2009). Spectral approximation of solutions to the chemical master equation. *Journal of Computational and Applied Mathematics*, *229*(1), 208–221. <https://doi.org/10.1016/J.CAM.2008.10.029>
- Eringen, A. C. (2002). *Nonlocal continuum field theories*. Springer Science & Business Media.
- Fabbri, G., Gozzi, F., & Świąch, A. (2017). *Stochastic Optimal Control in Infinite Dimension*. *82*. <https://doi.org/10.1007/978-3-319-53067-3>
- Faria, G., & Correia-da-Silva, J. (2014). A closed-form solution for options with ambiguity about stochastic volatility. *Review of Derivatives Research* *2014 17:2*, *17*(2), 125–159. <https://doi.org/10.1007/S11147-014-9097-9>
- Farmer, W. H., & Vogel, R. M. (2016). On the deterministic and stochastic use of hydrologic models. *Water Resources Research*, *52*(7), 5619–5633. <https://doi.org/10.1002/2016WR019129>
- Fetter, C. W. (2001). *Applied Hydrogeology\_e7ce669a880a8c4c70b4214641f93a02.pdf*. 598.
- Fleming, W., & Lions, P.-L. (Eds.). (1988). *Stochastic Differential Systems, Stochastic Control Theory and Applications*. *10*. <https://doi.org/10.1007/978-1-4613-8762-6>
- Ford, L. H. (2005). Stochastic Spacetime and Brownian Motion of Test Particles. *International Journal of Theoretical Physics*, *44*(10). <https://doi.org/10.1007/s10773-005-8893-z>
- Fournié, E., Lasry, J.-M., Lebuchoux, J., Lions, P.-L., & Touzi, N. (1999). Applications of Malliavin calculus to Monte Carlo methods in finance. *Finance and Stochastics* *1999 3:4*, *3*(4), 391–412. <https://doi.org/10.1007/S007800050068>
- Frankowska, H., & Lü, Q. (2020). First and second order necessary optimality conditions for controlled stochastic evolution equations with control and state constraints. *Journal of Differential Equations*, *268*(6), 2949–3015. <https://doi.org/10.1016/J.JDE.2019.09.045>
- Frauenfelder, P., Schwab, C., & Todor, R. A. (2005). Finite elements for elliptic problems with stochastic coefficients. *Computer Methods in Applied Mechanics and Engineering*, *194*(2-5 SPEC. ISS.), 205–228. <https://doi.org/10.1016/J.CMA.2004.04.008>
- Freeze, R. A., & Cherry, J. A. (1979). Groundwater. *Groundwater*. <https://books.google.com/books/about/Groundwater.html?id=feVOAAAAMAAJ>
- Furman, A. (2008). Modeling Coupled Surface–Subsurface Flow Processes: A Review. *Vadose Zone Journal*, *7*(2), 741–756. <https://doi.org/10.2136/VZJ2007.0065>
- Gedeon A G A N, B. D. (2084). Solute transport in heterogeneous porous formations. *J. Fluid Mteh*. <https://doi.org/10.1017/S0022112084002858>
- Gelhar, L. W., Welty, C., & Rehfeldt, K. R. (1992). A critical review of data on field-scale dispersion in aquifers. *Water Resources Research*, *28*(7), 1955–1974. <https://doi.org/10.1029/92WR00607>
- Ghanem, R. (1998). Probabilistic characterization of transport in heterogeneous media. *Computer Methods in Applied Mechanics and Engineering*, *158*(3–4), 199–220. [https://doi.org/10.1016/S0045-7825\(97\)00250-8](https://doi.org/10.1016/S0045-7825(97)00250-8)
- Ghanem, R. G., & Spanos, P. D. (1991). Stochastic Finite Elements: A Spectral Approach. *Stochastic Finite Elements: A Spectral Approach*. <https://doi.org/10.1007/978-1-4612-3094-6>
- Ghoraba, S. M., Zyedan, B. A., & Rashwan, I. M. H. (2013). Solute transport modeling of the groundwater for quaternary aquifer quality management in Middle Delta, Egypt. *Alexandria Engineering Journal*, *52*(2), 197–207. <https://doi.org/10.1016/J.AEJ.2012.12.007>
- Gillespie, D. T. (1977). Exact stochastic simulation of coupled chemical reactions. *Journal of Physical Chemistry*, *81*(25), 2340–2361. [https://doi.org/10.1021/J100540A008/ASSET/J100540A008.FP.PNG\\_V03](https://doi.org/10.1021/J100540A008/ASSET/J100540A008.FP.PNG_V03)

- Ginting, V., Pereira, F., & Rahunathan, A. (2014). Rapid quantification of uncertainty in permeability and porosity of oil reservoirs for enabling predictive simulation. *Mathematics and Computers in Simulation*, 99, 139–152. <https://doi.org/10.1016/J.MATCOM.2013.04.015>
- Gjessing, H., Holden, H., Lindstr, T., Ub, J., & Zhang, T.-S. (1992). *THE WICK PRODUCT*.
- Glasserman, P. (2003). *Monte Carlo Methods in Financial Engineering*. 53. <https://doi.org/10.1007/978-0-387-21617-1>
- Gramacy, R. B., & Lee, H. K. H. (2007). Bayesian treed Gaussian process models with an application to computer modeling. *Journal of the American Statistical Association*, 103(483), 1119–1130. <https://doi.org/10.48550/arxiv.0710.4536>
- Gubner, J. A. (2020). *Gaussian Quadrature and the Eigenvalue Problem*.
- Gustafsson, O., Gustafsson, S., Manukyan, L., & Mihranyan, A. (2018). Significance of Brownian Motion for Nanoparticle and Virus Capture in Nanocellulose-Based Filter Paper. *Membranes* 2018, Vol. 8, Page 90, 8(4), 90. <https://doi.org/10.3390/MEMBRANES8040090>
- Harrison, J. M. (2011). Brownian models of performance and control. *Brownian Models of Performance and Control*, 1–208. <https://doi.org/10.1017/CBO9781139087698>
- Henning, P., & Ohlberger, M. (2009). The heterogeneous Multiscale finite element method for elliptic homogenization problems in perforated domains. *Numerische Mathematik*, 113(4), 601–629. <https://doi.org/10.1007/S00211-009-0244-4>
- Heston, S. L. (1993). A Closed-Form Solution for Options with Stochastic Volatility with Applications to Bond and Currency Options. *The Review of Financial Studies*, 6(2), 327–343. <https://doi.org/10.1093/RFS/6.2.327>
- Hida, T., & Ikeda, N. (2001). ANALYSIS ON HILBERT SPACE WITH REPRODUCING KERNEL ARISING FROM MULTIPLE WIENER INTEGRAL. *Selected Papers of Takeyuki Hida*, 142–168. [https://doi.org/10.1142/9789812794611\\_0009](https://doi.org/10.1142/9789812794611_0009)
- Higham, D. J. (2001). An Algorithmic Introduction to Numerical Simulation of Stochastic Differential Equations. *Society for Industrial and Applied Mathematics*, 43(3), 525–546. <http://www.maths.strath.ac.uk/~aas96106/algfiles.html>
- Higham, D. J. (2008). Modeling and Simulating Chemical Reactions. <https://doi.org/10.1137/060666457>, 50(2), 347–368. <https://doi.org/10.1137/060666457>
- Higham, D. J., Mao, X., & Yuan, C. (2007). Almost sure and moment exponential stability in the numerical simulation of stochastic differential equations. *SIAM Journal on Numerical Analysis*, 45(2), 592–609. <https://doi.org/10.1137/060658138>
- Holden, H. (1996). *Stochastic partial differential equations: a modeling, white noise functional approach*. 230.
- Holden, H., Lindstrøm, T., Øksendal, B., Ubøe, J., & Zhang, T. (1991). *Stochastic boundary value problems. A white noise functional approach*. <https://www.duo.uio.no/handle/10852/43486>
- Holden, H., Lindstrøm, T., Øksendal, B., Ubøe, J., & Zhang, T. S. (1993). Stochastic boundary value problems: a white noise functional approach. *Probability Theory and Related Fields*, 95(3), 391–419. <https://doi.org/10.1007/BF01192171>
- Holden, H., Øksendal, B., Ubøe, J., & Zhang, T. (1996). *Stochastic Partial Differential Equations*. <https://doi.org/10.1007/978-1-4684-9215-6>
- Holden, H., Øksendal, B., Ubøe, J., & Zhang, T. (2010). *Stochastic Partial Differential Equations*. Springer New York. <https://doi.org/10.1007/978-0-387-89488-1>
- Hu, B. X., Wu, J., & He, C. (2004). On stochastic modeling of groundwater flow and solute transport in multi-scale heterogeneous formations. *Computational and Applied Mathematics*, 23(3), 121–151. [www.scielo.br/cam](http://www.scielo.br/cam)
- Huschto, T., & Sager, S. (2013). Stochastic optimal control in the perspective of the Wiener chaos. *2013 European Control Conference, ECC 2013*, 3059–3064. <https://doi.org/10.23919/ECC.2013.6669220>
- Hu, Y., Nualart, D., Sun, X., Xie, Y., Hu, Y., Nualart, D., Sun, X., & Xie, Y. (2019). Smoothness of density for stochastic differential equations with Markovian switching. *Discrete and Continuous Dynamical Systems - B*, 24(8), 3615–3631. <https://doi.org/10.3934/DCDSB.2018307>

- Hu, Y., Qian, Z., & Zhang, Z. (2012). *Gradient estimates for porous medium and fast diffusion equations by martingale method*. <http://arxiv.org/abs/1206.1394>
- Hu, Y., & Yan, J. (2009). *Wick Calculus For Nonlinear Gaussian Functionals*. <http://arxiv.org/abs/0901.4911>
- Istvan Gyongy, B., & Nualart, D. (1999). ON THE STOCHASTIC BURGERS' EQUATION IN THE REAL LINE. *The Annals of Probability* (Vol. 27, Issue 2).
- ITO, K. (1951). Multiple Wiener Integral. <https://doi.org/10.2969/Jmsj/00310157>, 3(1), 157–169.
- Jacka, S. D., & Oksendal, B. (1987). Stochastic Differential Equations: An Introduction with Applications. *Journal of the American Statistical Association*, 82(399), 948. <https://doi.org/10.2307/2288814>
- Jansons, K. M., & Lythe, G. D. (2003). Exponential timestepping with boundary test for stochastic differential equations. *SIAM Journal on Scientific Computing*, 24(5), 1809–1822. <https://doi.org/10.1137/S1064827501399535>
- Kadison, R. V., & Ringrose, J. R. (1992). Fundamentals of the Theory of Operator Algebras. *Fundamentals of the Theory of Operator Algebras*. <https://doi.org/10.1007/978-1-4612-2968-1>
- Kaintura, A., Dhaene, T., & Spina, D. (2018). Review of Polynomial Chaos-Based Methods for Uncertainty Quantification in Modern Integrated Circuits. *Electronics*, 7(3), 30. <https://doi.org/10.3390/electronics7030030>
- Kallianpur, G., & Sundar, P. (2014). Stochastic Analysis and Diffusion Processes. *Stochastic Analysis and Diffusion Processes*. <https://doi.org/10.1093/ACPROF:OSO/9780199657063.001.0001>
- Kamrani, M. (2016). Numerical solution of stochastic partial differential equations using a collocation method. *ZAMM - Journal of Applied Mathematics and Mechanics / Zeitschrift Für Angewandte Mathematik Und Mechanik*, 96(1), 106–120. <https://doi.org/10.1002/zamm.201400080>
- Kashyap, D., Sharma, P. K., & Subrahmanyam, P. (2011). Stochastic modelling of groundwater contamination around an ash slurry holding dyke. *ISH Journal of Hydraulic Engineering*, 17(1), 58–70. <https://doi.org/10.1080/09715010.2011.10515033>
- Keese, A. (2003). *A Review of Recent Developments in the Numerical Solution of Stochastic Partial Differential Equations (Stochastic Finite Elements)*. <https://doi.org/10.24355/DBBS.084-200511080100-583>
- Kim, K. B., Kwon, H. H., & Han, D. (2018). Exploration of warm-up period in conceptual hydrological modelling. *Journal of Hydrology*, 556, 194–210. <https://doi.org/10.1016/J.JHYDROL.2017.11.015>
- Kim, K. K. K., Shen, D. E., Nagy, Z. K., & Braatz, R. D. (2013). Wiener's Polynomial Chaos for the Analysis and Control of Nonlinear Dynamical Systems with Probabilistic Uncertainties [Historical Perspectives]. *Undefined*, 33(5), 58–67. <https://doi.org/10.1109/MCS.2013.2270410>
- Kloeden, P. E., & Neuenkirch, A. (2007). The Pathwise Convergence of Approximation Schemes for Stochastic Differential Equations. *LMS Journal of Computation and Mathematics*, 10, 235–253. <https://doi.org/10.1112/S146115700001388>
- Kloeden, P. E., & Platen, E. (1992). Numerical Solution of Stochastic Differential Equations. *Numerical Solution of Stochastic Differential Equations*. <https://doi.org/10.1007/978-3-662-12616-5>
- Kohatsu-Higa, A., & Montero, M. (2001). *An application of Malliavin Calculus to Finance*. <https://arxiv.org/abs/cond-mat/0111563v1>
- Konda, U., Singla, P., Singh, T., & Scott, P. D. (2011). State uncertainty propagation in the presence of parametric uncertainty and additive white noise. *Journal of Dynamic Systems, Measurement and Control, Transactions of the ASME*, 133(5). <https://doi.org/10.1115/1.4004072/466578>
- Koonin, E. v. (2007). The cosmological model of eternal inflation and the transition from chance to biological evolution in the history of life. *Biology Direct*, 2, 15. <https://doi.org/10.1186/1745-6150-2-15>
- Kosarwal, R., Kulasiri, D., & Samarasinghe, S. (2020). Novel domain expansion methods to improve the computational efficiency of the Chemical Master Equation solution for large biological networks. *BMC Bioinformatics*, 21(1), 1–42. <https://doi.org/10.1186/S12859-020-03668-2/TABLES/8>
- Kroese, D. P., Taimre, T., & Botev, Z. I. (2011). Handbook of Monte Carlo Methods. *Handbook of Monte Carlo Methods*, 1–752. <https://doi.org/10.1002/9781118014967>

- Kulasiri, Don. (2015). *Non-fickian solute transport in porous media. Part of the book series: Advances in Geophysical and Environmental Mechanics and Mathematics, Springer Nature.*
- LaBolle, E. M., Quastel, J., Fogg, G. E., & Gravner, J. (2000). Diffusion processes in composite porous media and their numerical integration by random walks: Generalized stochastic differential equations with discontinuous coefficients. *Water Resources Research*, 36(3), 651–662. <https://doi.org/10.1029/1999WR900224>
- Lai, Y., & Yao, H. (2016). SIMULATION OF MULTI-ASSET OPTION GREEKS UNDER A SPECIAL LÉVY MODEL BY MALLIAVIN CALCULUS. *ANZIAM J*, 57, 280–298. <https://doi.org/10.1017/S1446181115000292>
- Lalley, S. P. (2012). *Notes on the Itô Calculus 1 Continuous-Time Processes: Progressive Measurability 1.1 Progressive Measurability.*
- Lanconelli, A. (2022). *Using Malliavin calculus to solve a chemical diffusion master equation.* <http://arxiv.org/abs/2203.14676>
- Le Matre, O. P., Reagan, M. T., Najm, H. N., Ghanem, R. G., & Knio, O. M. (2002). A stochastic projection method for fluid flow. II. Random process. *Journal of Computational Physics*, 181(1), 9–44. <https://doi.org/10.1006/jcph.2002.7104>
- Lemke, L. D., Barrack, W. A., Abriola, L. M., & Goovaerts, P. (2004). Matching Solute Breakthrough with Deterministic and Stochastic Aquifer Models. *Groundwater*, 42(6), 920–939. <https://doi.org/10.1111/J.1745-6584.2004.T01-10-X>
- Lemons, D. S., Gythiel, A., Lemons, D. S., & Gythiel, A. (1997). Paul Langevin's 1908 paper "On the Theory of Brownian Motion" ["Sur la théorie du mouvement brownien," C. R. Acad. Sci. (Paris) 146, 530-533 (1908)]. *AmJPh*, 65(11), 1079–1081. <https://doi.org/10.1119/1.18725>
- Levajković, T. L., Pilipović, S. P., & Seleši, D. (2015). CHAOS EXPANSION METHODS IN MALLIAVIN CALCULUS: A SURVEY OF RECENT RESULTS. *Novi Sad J. Math*, 45(1), 45–103.
- Li, J. B., Huang, G. H., Chakma, A., Zeng, G. M., & Liu, L. (2003). Integrated fuzzy-stochastic modeling of petroleum contamination in subsurface. *Energy Sources*, 25(6), 547–563. <https://doi.org/10.1080/00908310390195615>
- Lisei, H. (2011). *Stochastic Schrödinger equation driven by cylindrical Wiener process and fractional Brownian motion.* Retrieved December 11, 2022, from [https://www.academia.edu/18704527/Stochastic\\_Schr%C3%B6dinger\\_equation\\_driven\\_by\\_cylindrical\\_Wiener\\_process\\_and\\_fractional\\_Brownian\\_motion](https://www.academia.edu/18704527/Stochastic_Schr%C3%B6dinger_equation_driven_by_cylindrical_Wiener_process_and_fractional_Brownian_motion)
- Li, S. -G., & McLaughlin, D. (1991). A nonstationary spectral method for solving stochastic groundwater problems: Unconditional analysis. *Water Resources Research*, 27(7), 1589–1605. <https://doi.org/10.1029/91WR00881>
- Liu, K., Chen, J., Zhang, J., & Tan, X. (2022). Application of Malliavin Calculus in Mean-Variance Hedging Strategy. *Mathematical Problems in Engineering*, 2022. <https://doi.org/10.1155/2022/3096866>
- Liu, W., Kou, C. K. L., Park, K. H., & Lee, H. K. (2021). Solving the inverse problem of time independent Fokker–Planck equation with a self supervised neural network method. *Scientific Reports 2021 11:1*, 11(1), 1–11. <https://doi.org/10.1038/s41598-021-94712-5>
- Li, X., Nair, P. B., Zhang, Z., Gao, L., & Gao, C. (2014). Aircraft Robust Trajectory Optimization Using Nonintrusive Polynomial Chaos. <https://doi.org/10.2514/1.C032474>, 51(5), 1592–1603. <https://doi.org/10.2514/1.C032474>
- Li, Y. P., Huang, G. H., Nie, S. L., & Liu, L. (2008). Inexact multistage stochastic integer programming for water resources management under uncertainty. *Journal of Environmental Management*, 88, 93–107. <https://doi.org/10.1016/j.jenvman.2007.01.056>
- Løkka, A., Øksendal, B., & Proske, F. (2004). Stochastic partial differential equations driven by Lévy space-time white noise. *Annals of Applied Probability*, 14(3), 1506–1528. <https://doi.org/10.1214/105051604000000413>
- Lototsky, S., Mikulevicius, R., & Rozovskii, B. L. (1997). Nonlinear filtering revisited: A spectral approach. *SIAM Journal on Control and Optimization*, 35(2), 435–461. <https://doi.org/10.1137/S0363012993248918>
- Lototsky, S. v., & Rozovskii, B. L. (2006). *From Stochastic Calculus to Mathematical Finance: The Shiryaev Festschrift.* 433–507.

- Lund, Diderik., Øksendal, B. K. (Bernt K., & Universitetet i Oslo. Sosialøkonomisk institutt. Senter for anvendt forskning. (1991). *Stochastic models and option values : applications to resources, environment, and investment problems*. 301.
- Lunz, D., Batt, G., Ruess, J., & Bonnans, J. F. (2021). Beyond the chemical master equation: Stochastic chemical kinetics coupled with auxiliary processes. *PLoS Computational Biology*, 17(7). <https://doi.org/10.1371/JOURNAL.PCBI.1009214>
- Lü, Q., & Zhang, X. (2021). *Mathematical Control Theory for Stochastic Partial Differential Equations*. 101. <https://doi.org/10.1007/978-3-030-82331-3>
- Lü, Q., Zhang, X., Lü, Q., & Zhang, X. (2022). A concise introduction to control theory for stochastic partial differential equations. *Mathematical Control and Related Fields*, 12(4), 847–954. <https://doi.org/10.3934/MCRF.2021020>
- Mackevičius, Vigirdas. (2011). *Introduction to stochastic analysis: integrals and differential equations*. 276.
- Ma, D. L., & Braatz, R. D. (2001). Worst-Case Analysis of Finite-Time Control Policies. *IEEE TRANSACTIONS ON CONTROL SYSTEMS TECHNOLOGY*, 9(5).
- Ma, J., Zhang, G., Hayat, T., & Ren, G. (2019). Model electrical activity of neuron under electric field. *Nonlinear Dynamics*, 95(2), 1585–1598. <https://doi.org/10.1007/s11071-018-4646-7>
- Malliavin, P., Malliavin, & Paul. (1978). Proceedings of the International Symposium on Stochastic Differential Equations, Kyoto, 1976. In *Proceedings of the International Symposium on Stochastic Differential Equations, Kyoto, 1976*. Wiley and Sons.
- Manthey, R., & Mittmann, K. (2007). On the qualitative behaviour of the solution to a stochastic partial functional - differential equation arising in population dynamics. <https://doi.org/10.1080/17442509908834190>, 66(1–2), 153–166.
- Marelli, S., & Sudret, B. (2014). *UQLab: A Framework for Uncertainty Quantification in Matlab*.
- Márquez-Carreras, D., Mellouk, M., & Sarrà, M. (2001). On stochastic partial differential equations with spatially correlated noise: smoothness of the law. *Stochastic Processes and Their Applications*, 93(2), 269–284. <https://ideas.repec.org/a/eee/spapps/v93y2001i2p269-284.html>
- Mata, A. S. da. (2020). Complex Networks: a Mini-review. *Brazilian Journal of Physics*, 50(5), 658–672. <https://doi.org/10.1007/S13538-020-00772-9/FIGURES/15>
- Matthies, H. G., Brenner, C. E., Bucher, C. G., & Soares, C. G. (1997). Uncertainties in probabilistic numerical analysis of structures and solids - Stochastic finite elements. *Structural Safety*, 19(3), 283–336. [https://doi.org/10.1016/S0167-4730\(97\)00013-1](https://doi.org/10.1016/S0167-4730(97)00013-1)
- Matthies, H. G., & Keese, A. (2005). Galerkin methods for linear and nonlinear elliptic stochastic partial differential equations. *Computer Methods in Applied Mechanics and Engineering*, 194(12–16), 1295–1331. <https://doi.org/10.1016/J.CMA.2004.05.027>
- McComas, D. J., Bzowski, M., Dayeh, M. A., -, al, Yao, Y., Sun, Y., Liang -, X., Mariani, A., Nugrahani, E. H., & Lesmana, D. C. (2016). Numerical solution for option pricing with stochastic volatility model. *IOP Conference Series: Earth and Environmental Science*, 31(1), 012024. <https://doi.org/10.1088/1755-1315/31/1/012024>
- Medved, A., Davis, R., & Vasquez, P. A. (2020). Understanding Fluid Dynamics from Langevin and Fokker–Planck Equations. *Fluids 2020, Vol. 5, Page 40*, 5(1), 40. <https://doi.org/10.3390/FLUIDS5010040>
- Meyer, M. (2000). *Continuous Stochastic Calculus with Applications to Finance*. <https://doi.org/10.1201/9781420035599>
- Michta, M. (2004). On weak solutions to stochastic differential inclusions driven by semimartingales. *Stochastic Analysis and Applications*, 22(5), 1341–1361. <https://doi.org/10.1081/SAP-200026471>
- Millet, A., & Morien, P. L. (2000). On a stochastic wave equation in two space dimensions: regularity of the solution and its density. *Stochastic Processes and Their Applications*, 86(1), 141–162. [https://doi.org/10.1016/S0304-4149\(99\)00090-3](https://doi.org/10.1016/S0304-4149(99)00090-3)
- Munsky, B., & Khammash, M. (2007). A multiple time interval finite state projection algorithm for the solution to the chemical master equation. *Journal of Computational Physics*, 226(1), 818–835. <https://doi.org/10.1016/J.JCP.2007.05.016>

- Musiela, M., & Zariphopoulou, T. (2009). *Stochastic partial differential equations and portfolio choice*.
- Najm, H. N. (2008). Uncertainty Quantification and Polynomial Chaos Techniques in Computational Fluid Dynamics. *Http://Dx.Doi.Org/10.1146/Annurev.Fluid.010908.165248*, 41, 35–52. <https://doi.org/10.1146/ANNUREV.FLUID.010908.165248>
- Nobile, F., Tempone, R., & Webster, C. G. (2008). A Sparse Grid Stochastic Collocation Method for Partial Differential Equations with Random Input Data. *Https://Doi.Org/10.1137/060663660*, 46(5), 2309–2345. <https://doi.org/10.1137/060663660>
- Nualart, D., & Saussereau, B. (2009). *Malliavin calculus for stochastic differential equations driven by a fractional Brownian motion*. 119(2), 391–409. <https://doi.org/10.1016/j.spa.2008.02.016>
- Ohsumi, A. (2019). An interpretation of the Schrödinger equation in quantum mechanics from the control-theoretic point of view. *Automatica*, 99, 181–187. <https://doi.org/10.1016/J.AUTOMATICA.2018.10.033>
- Øksendal, B. (2006). Optimal Control of Stochastic Partial Differential Equations. *Http://Dx.Doi.Org/10.1081/SAP-200044467*, 23(1), 165–179. <https://doi.org/10.1081/SAP-200044467>
- Øksendal, B. K. (Bernt K., & Sulem, A. (2007). *Applied stochastic control of jump diffusions*. 257. [https://books.google.com/books/about/Applied\\_Stochastic\\_Control\\_of\\_Jump\\_Diffu.html?id=ALHJxprw4ksC](https://books.google.com/books/about/Applied_Stochastic_Control_of_Jump_Diffu.html?id=ALHJxprw4ksC)
- Paganin, D. M., & Morgan, K. S. (2019). X-ray Fokker–Planck equation for paraxial imaging. *Scientific Reports 2019 9:1*, 9(1), 1–18. <https://doi.org/10.1038/s41598-019-52284-5>
- Pang, L., & Hunt, B. (2001). Solutions and verification of a scale-dependent dispersion model. *Journal of Contaminant Hydrology*, 53(1–2), 21–39. [https://doi.org/10.1016/S0169-7722\(01\)00134-6](https://doi.org/10.1016/S0169-7722(01)00134-6)
- Petrou, E. (2008). *Malliavin Calculus in Lévy spaces and Applications to Finance*. Retrieved September 3, 2023, from <http://www.math.washington.edu/~ejpecp/>
- Pettersson, P., Iaccarino, G., & Nordström, J. (2014). A stochastic Galerkin method for the Euler equations with Roe variable transformation. *Journal of Computational Physics*, 257, 481–500. <https://doi.org/10.1016/J.JCP.2013.10.011>
- Pütz, M., Pollack, M., Hasse, C., & Oevermann, M. (2022). A Gauss/anti-Gauss quadrature method of moments applied to population balance equations with turbulence-induced nonlinear phase-space diffusion. *Journal of Computational Physics*, 466, 111363. <https://doi.org/10.1016/J.JCP.2022.111363>
- Reverberi, A. Pietro, Chiarioni, A., Vegliò, F., & Del Borghi, A. (2008). Fluctuating fast chemical reactions in a batch process modelled by stochastic differential equations. *Journal of Cleaner Production*, 16(2), 192–197. <https://doi.org/10.1016/J.JCLEPRO.2006.09.003>
- Rippin, D. W. T. (1983). Simulation of single- and multiproduct batch chemical plants for optimal design and operation. *Computers & Chemical Engineering*, 7(3), 137–156. [https://doi.org/10.1016/0098-1354\(83\)85016-9](https://doi.org/10.1016/0098-1354(83)85016-9)
- Schoutens, Wim. (2003). *Lévy processes in finance : pricing financial derivatives*. 170. <https://www.wiley.com/en-us/L%26eacute%3Bvy+Processes+in+Finance%3A+Pricing+Financial+Derivatives-p-9780470851562>
- Serrano, S. E., & Unny, T. E. (1987). Stochastic Partial Differential Equations in Hydrology. *Advances in the Statistical Sciences: Stochastic Hydrology*, 113–130. [https://doi.org/10.1007/978-94-009-4792-4\\_7](https://doi.org/10.1007/978-94-009-4792-4_7)
- S., H., & S., T. (2006). Application of polynomial chaos in stability and control. *Automatica (Journal of IFAC)*, 42(5), 789–795. <https://doi.org/10.1016/J.AUTOMATICA.2006.01.010>
- Sidje, R. B., & Vo, H. D. (2015). Solving the chemical master equation by a fast adaptive finite state projection based on the stochastic simulation algorithm. *Mathematical Biosciences*, 269, 10–16. <https://doi.org/10.1016/J.MBS.2015.08.010>
- Siopacha, M., & Teichmann, J. (2011). Weak and strong Taylor methods for numerical solutions of stochastic differential equations. *Quantitative Finance*, 11(4), 517–528. <https://doi.org/10.1080/14697680903493573>

- Soheili, A. R., & Namjoo, M. (2007). Strong runge-kutta method with order one for numerical solution of itô stochastic differential equations. *Applied Mathematics Research Express*, 2007. <https://doi.org/10.1093/AMRX/ABM003>
- Soini, V., & Lorentzen, S. (2019). Option prices and implied volatility in the crude oil market. *Energy Economics*, 83, 515–539. <https://doi.org/10.1016/J.ENERCO.2019.07.011>
- Solé, J. L., Utzet, F., & Vives, J. (2007). Canonical Lévy process and Malliavin calculus. *Stochastic Processes and Their Applications*, 117(2), 165–187. <https://doi.org/10.1016/J.SPA.2006.06.006>
- Srinivasan, B., Bonvin, D., Visser, E., & Palanki, S. (2002). *Dynamic optimization of batch processes II. Role of measurements in handling uncertainty*.
- Srivastava, R., Sharma, P. K., & Brusseau, M. L. (2002). Spatial moments for reactive transport in heterogeneous porous media. *Journal of Hydrologic Engineering*, 7(4), 336–341. [https://doi.org/10.1061/\(ASCE\)1084-0699\(2002\)7:4\(336\)](https://doi.org/10.1061/(ASCE)1084-0699(2002)7:4(336))
- Stochastic Calculus of Variations in Mathematical Finance. (2006). *Stochastic Calculus of Variations in Mathematical Finance*. <https://doi.org/10.1007/3-540-30799-0>
- Taylor, S. J., & Princeton, O. (2005). *Asset Price Dynamics, Volatility, and Prediction*.
- Tian, T. H., & Burrage, K. (2002). Two-stage stochastic Runge-Kutta methods for stochastic differential equations. *BIT Numerical Mathematics*, 42(3), 625–643. <https://doi.org/10.1023/A:1021963316988>
- Tryoen, J., Maître, O. Le, Ndjinga, M., & Ern, A. (2010). Intrusive Galerkin methods with upwinding for uncertain nonlinear hyperbolic systems. *Journal of Computational Physics*, 229(18), 6485–6511. <https://doi.org/10.1016/J.JCP.2010.05.007>
- Unny, T. E. (1989). Stochastic partial differential equations in groundwater hydrology. *Stochastic Hydrology and Hydraulics* 1989 3:2, 3(2), 135–153. <https://doi.org/10.1007/BF01544077>
- van der Vaart, A. W., & Wellner, J. A. (1996). *Donsker Theorems*. 127–133. [https://doi.org/10.1007/978-1-4757-2545-2\\_17](https://doi.org/10.1007/978-1-4757-2545-2_17)
- Velasco, S. (1985). On the Brownian motion of a harmonically bound particle and the theory of a Wiener process. *European Journal of Physics*, 6(4), 259. <https://doi.org/10.1088/0143-0807/6/4/009>
- Venturi, D., Wan, X., Mikulevicius, R., Rozovskii, B. L., & Karniadakis, G. E. (2013). Wick–Malliavin approximation to nonlinear stochastic partial differential equations: analysis and simulations. *Proceedings of the Royal Society A: Mathematical, Physical and Engineering Sciences*, 469(2158), 20130001. <https://doi.org/10.1098/rspa.2013.0001>
- Villegas, M., Augustin, F., Gilg, A., Hmadi, A., & Wever, U. (2012). Application of the Polynomial Chaos Expansion to the simulation of chemical reactors with uncertainties. *Mathematics and Computers in Simulation*, 82(5), 805–817. <https://doi.org/10.1016/J.MATCOM.2011.12.001>
- Walsh, J. B. (2006). An introduction to stochastic partial differential equations. *École d'Été de Probabilités de Saint Flour XIV - 1984*, 265–439. <https://doi.org/10.1007/BFB0074920>
- Wan, X., & Karniadakis, G. E. (2006). Multi-Element Generalized Polynomial Chaos for Arbitrary Probability Measures. <https://doi.org/10.1137/050627630>, 28(3), 901–928. <https://doi.org/10.1137/050627630>
- Wattanatorn, W., & Sombultawee, K. (2021). The Stochastic Volatility Option Pricing Model: Evidence from a Highly Volatile Market. *The Journal of Asian Finance, Economics and Business*, 8(2), 685–695. <https://doi.org/10.13106/JAFEB.2021.VOL8.NO2.0685>
- Wick, G. C. (1950). The Evaluation of the Collision Matrix. *Physical Review*, 80(2), 268. <https://doi.org/10.1103/PhysRev.80.268>
- Wiener, N. (1938). The Homogeneous Chaos. *American Journal of Mathematics*, 60(4), 897. <https://doi.org/10.2307/2371268>
- Wu, J.-L., & Yang, W. (2012). *On Stochastic Differential Equations and a Generalised Burgers Equation*. 425–435. [https://doi.org/10.1142/9789814383585\\_0021](https://doi.org/10.1142/9789814383585_0021)
- Xiu, D. (2007). Efficient Collocational Approach for Parametric Uncertainty Analysis. *COMMUNICATIONS IN COMPUTATIONAL PHYSICS*, 2(2), 293–309.
- Xiu, D. (2009). Fast Numerical Methods for Stochastic Computations: A Review. *COMMUNICATIONS IN COMPUTATIONAL PHYSICS*, 5(4), 242–272. <http://www.global-sci.com/>

- Xiu, D. (2010). Numerical methods for stochastic computations: A spectral method approach. *Numerical Methods for Stochastic Computations: A Spectral Method Approach*.
- Xiu, D., & Karniadakis, G. E. (2003). Modeling uncertainty in flow simulations via generalized polynomial chaos. [https://doi.org/10.1016/S0021-9991\(03\)00092-5](https://doi.org/10.1016/S0021-9991(03)00092-5)
- Xiu, D., & Karniadakis, G. E. (2006). The Wiener--Askey Polynomial Chaos for Stochastic Differential Equations. <Http://Dx.Doi.Org/10.1137/S1064827501387826>, 24(2), 619–644. <https://doi.org/10.1137/S1064827501387826>
- Xiu, D., Lucor, D., Su, C. H., & Karniadakis, G. E. (2002). Stochastic modeling of flow-structure interactions using generalized polynomial chaos. *Journal of Fluids Engineering, Transactions of the ASME*, 124(1), 51–59. <https://doi.org/10.1115/1.1436089>
- Xiu, D., & Shen, J. (2008). Efficient stochastic Galerkin methods for random diffusion equations. <https://doi.org/10.1016/j.jcp.2008.09.008>
- Yadav, R. R., & Roy, J. (2018). Solute transport with periodic input point source in one-dimensional heterogeneous porous media. *International Journal of Engineering, Science and Technology*, 10(2), 50–63. <https://doi.org/10.4314/ijest.v10i2.6>
- Yidana, S. M., Addai, M. O., Asiedu, D. K., & Banoeng-Yakubo, B. (2016). Stochastic groundwater modeling of a sedimentary aquifer: evaluation of the impacts of abstraction scenarios under conditions of reduced recharge. *Arabian Journal of Geosciences*, 9(17). <https://doi.org/10.1007/S12517-016-2718-X>
- Yoshioka, H., Unami, K., & Kawachi, T. (2011). Stochastic process model for solute transport and the associated transport equation. <https://doi.org/10.1016/j.apm.2011.09.011>
- Yuan, C., & Mao, X. (2004). Stability in distribution of numerical solutions for stochastic differential equations. *Stochastic Analysis and Applications*, 22(5), 1133–1150. <https://doi.org/10.1081/SAP-200026423>
- Zhang, D., Lu, L., Guo, L., & Karniadakis, G. E. (2018). Quantifying total uncertainty in physics-informed neural networks for solving forward and inverse stochastic problems. <https://doi.org/10.1016/j.jcp.2019.07.048>
- Zhang, J. E., & Shu, J. (2003). Pricing S&P 500 index options with Heston's model. *IEEE/IAFE Conference on Computational Intelligence for Financial Engineering, Proceedings (CIFER), 2003-January*, 85–92. <https://doi.org/10.1109/CIFER.2003.1196246>
- Zhang, Z., & Karniadakis, G. E. (2017). Numerical Methods for Stochastic Partial Differential Equations with White Noise. 196. <https://doi.org/10.1007/978-3-319-57511-7>
- Zhang, Z., Tretyakov, M. V., Rozovskii, B., & Karniadakis, G. E. (2015). Wiener Chaos Versus Stochastic Collocation Methods for Linear Advection-Diffusion-Reaction Equations with Multiplicative White Noise. <Http://Dx.Doi.Org/10.1137/130932156>, 53(1), 153–183. <https://doi.org/10.1137/130932156>
- Zhong, H., & Cass, T. (2017). Malliavin calculus applied to Monte Carlo methods in mathematical finance.
- Zhou, T., & Tang, T. (2012). Galerkin methods for stochastic hyperbolic problems using bi-orthogonal polynomials. *Journal of Scientific Computing*, 51(2), 274–292. <https://doi.org/10.1007/s10915-011-9508-0>
- Zhou, X. Y. (2006). On the Necessary Conditions of Optimal Controls for Stochastic Partial Differential Equations. <Https://Doi.Org/10.1137/0331068>, 31(6), 1462–1478. <https://doi.org/10.1137/0331068>